Rational design of insect cell-based vaccine production

Bridging metabolomics with mathematical tools to study virus-host interactions

Francisca Monteiro

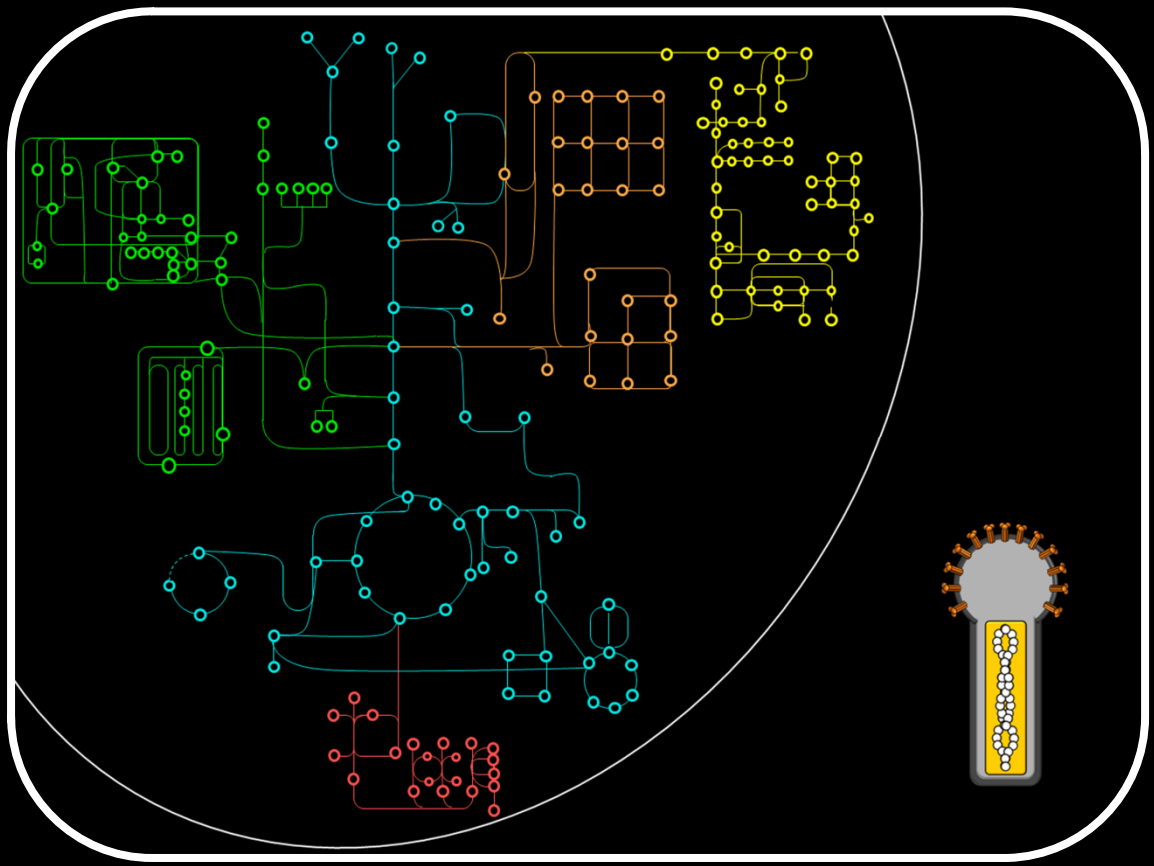

Dissertation presented to obtain the Ph.D degree in Engineering and Technology Sciences-Biotechnology

Instituto de Tecnologia Química e Biológica António Xavier | Universidade Nova de Lisboa

Oeiras,
September, 2015

INSTITUTO DE TECNOLOGIA QUÍMICA E BIOLÓGICA ANTÓNIO XAVIER /UNL

Knowledge Creation

ITQB-UNL | Av. da República, 2780-157 Oeiras, Portugal
Tel (+351) 214 469 100 | Fax (+351) 214 411 277

www.itqb.unl.pt

Rational design of insect cell-based vaccine production

Bridging metabolomics with mathematical tools to study virus-host interactions

Francisca Sarreira Simões Horta Monteiro

Dissertation presented to obtain the Ph.D degree in Engineering and Technology Sciences-Biotechnology

Instituto de Tecnologia Química e Biológica António Xavier | Universidade Nova de Lisboa

Oeiras, September, 2015

INSTITUTO
DE TECNOLOGIA
QUÍMICA E BIOLÓGICA
ANTÓNIO XAVIER /UNL

Knowledge Creation

RATIONAL DESIGN OF INSECT CELL-BASED VACCINE PRODUCTION

Bridging metabolomics with mathematical tools to study virus-host interactions

Francisca Sarreira Simões Horta Monteiro

Dissertation presented to obtain a Ph.D. degree in Engineering and Technology Sciences, Biotechnology

Instituto de Tecnologia Química e Biológica António Xavier, Universidade Nova de Lisboa

Supervisor: Paula Marques Alves

Co-supervisor: Vicente Bernal Sanchez

Oeiras, September, 2015

With the financial support from FCT, under contract SFRH / BD / 70139 / 2010

FCT Fundação para a Ciência e a Tecnologia
MINISTÉRIO DA EDUCAÇÃO E CIÊNCIA

Rational design of insect cell-based vaccine production

Bridging metabolomics with mathematical tools to study virus-host interactions

By Francisca Monteiro

First edition: August 2015

Cover: Combined figure of a diagram of a metabolic network of cellular metabolism and a baculovirus particle.

ITQB-UNL/iBET Animal Cell Technology Unit

Instituto de Tecnologia Química e Biológica/

Instituto de Biologia Experimental e Tecnológica

Av. da República EAN, 2780-157 Oeiras, Portugal

http://tca.itqb.unl.pt

http://www.itqb.unl.pt

http://www.ibet.pt

Printed in Portugal

Supervisors:

Dr. Paula Marques Alves, Invited Associate Professor at Faculdade de Ciências e Tecnologia, UNL, Caparica, Portugal, Principal Investigator at ITQB-UNL, Director of Animal Cell Technology Unit, ITQB-UNL, Oeiras, Portugal, , CEO of IBET (Supervisor).

Dr. Vicente Bernal, Scientist, Biology Area - New Energies - Technology Center, Repsol S.A, previously Researcher at Departamento de Bioquímica y Biología Molecular B e Inmunología, Universidad de Murcia, Murcia, Spain (Co-supervisor).

Jury:

Dr. Otto-Wilhelm Merten, Head of the Applied Vectorology and Innovation group of Généthon, Généthon, Évry, France

Dra. Isabel Rocha, Assistant Professor at Department of Biological Engineering, Universidade do Minho, Braga, Portugal, Researcher at Institute for Biotechnology and Bioengineering, Center of Biological Engineering, Universidade do Minho, Braga, Portugal.

Dr. Guilherme Ferreira, Assistant Professor with Aggregation at Universidade do Algarve, Faro, Portugal, Principal Investigator at Biosensors and Bioengineering laboratory, Universidade do Algarve, Faro, Portugal, and Director of Center for Biomedical Research.

Prof. Manuel J. T. Carrondo, Professor of Chemical and Biochemical Engineering at Faculdade de Ciências e Tecnologia, UNL, Caparica, Portugal, Head of the Engineering Cellular Applications Laboratory from Animal Cell Technology Unit, ITQB-UNL, Oeiras, Portugal, Vice-President of IBET.

Foreword

The present thesis dissertation is the result of four years of research at the Animal Cell Technology Unit of ITQB-UNL/iBET, Oeiras, Portugal, under the supervision of Dr. Paula Marques Alves and Dr. Vicente Bernal.

This PhD thesis aimed at improving insect cell-based bioprocesses *via* baculovirus expression for the production of complex biopharmaceuticals, using metabolomics and fluxomics tools to extend the knowledge on the physiology and metabolic requirements of insect cells.

Acknowledgments

I would like to express my gratitude to all the people that contributed directly or indirectly to this thesis. Also, to the hosting institutions, iBET and ITQB, for the excellent working conditions.

To my supervisor, Dr. Paula M. Alves, for giving me the opportunity to join the animal cell technology unit (ACTU) and the scientific support invaluable for the work herein presented. For the vote of confidence that enabled me to grow as scientist, for pushing me forward and promoting my independence. For teaching me that a PhD journey goes beyond science, placing me in confrontation with my own beliefs, which undoubtedly promoted my development as an individual.

To my co-supervisor, Dr. Vicente Bernal, for the guidance and scientific support throughout these years. For his truly scientific soul and devoted mentoring that always inspired me, his critical insights and for broadening my scientific perspectives. For welcoming me at University of Murcia, for his friendship and for making me feel a peer.

To Prof. Manuel Carrondo for truly being an entrepreneur and founding iBET, an institute in which I have the privilege to work. For the example of determination and motivation in fighting for his own beliefs, and for teaching me to always reach out for the best.

To Prof. Manuel Cánovas, for welcoming me at his lab in Universidad de Murcia. For making me feel a member, for his scientific advices and for the working conditions provided.

To Dr. Imre Berger for accepting me in his lab at EMBL Grenoble. For the excellent working conditions provided and the scientific enthusiasm in our discussions. Also, to Maxime Chaillet for all the help, technical support and good will during my staying.

To the financial support provided by Fundação para a Ciência e Tecnologia (SFRH/BD/70139/2010) and by European Commission, through the *FP7* project ComplexInc.

To all my colleagues of the animal cell technology unit, past and present, for the good working environment, inspirational discussions and great times shared throughout this years. In particular, to Marcos Sousa for the support in bioprocess operations, Dr. Cristina Peixoto for the help and assistance in the downstream work, to Nuno Carinhas and António Roldão, for the bright full insights and wise advices in the modeling work.

To my colleagues of the insect cell task force, João and Mafalda, for sharing with me the hurdles and joys of working with such amazing cell lines. To Ana Sofia, Carina, Daniel S., Marta S., Tiago D., Fabiana and Hugo for the support and making my daily life in the lab happier. To Sofia Rebelo, for her truly and honest companionship, kindness and support.

À minha colega e amiga Filipa, companheira de tantas e todas as horas. Agradeço-te por seres quem és, pelo teu entusiasmo contagiante, pelas longas conversas e acesas trocas de ideias. Há pessoas que entram na nossa vida e que, por a enriquecerem tremendamente, não as devemos deixar sair. Tu és uma dessas pessoas!

Aos meus companheiros e amigos de luta Paulo, Zeca, Dimi e Alex. O equilibrio comanda a vida, e a minha sem qualquer um de vós seria inevitalvelmente sensaborona. Em especial ao Paulo, por reunires em ti tantos bocadinhos bons de felicidade: passados, presentes e, sem qualquer dúvida, futuros.

Aos meus amigos Catarina, Grilo, Sofia, Mafalda e Raquel, pelo companheirismo e amizade, pelas gargalhadas e momentos únicos que tanto me enriquecem.

Às minhas amigas Ivette e Laura, mulheres incríveis, cuja força e coragem extraordinárias são inspiradoras. Obrigada por partilharem comigo a vossa jornada.

Aos meus anjos em vida, Filipa e Rita. A amizade incondicional é um privilégio raro de alcançar, pelo que sou uma afortunada em ter-vos comigo.

À minha família, turbilhão e Norte da minha vida. Às minhas madrinhas e avós Maria do Céu e Clara, verdadeiras forças da Natureza que me completam e constituem. Aos meus avôs Sebastião e José, meus pilares de força e abrigo.

À minha mãe, pequeno génio provido de amor e apoio incondicionais, ao meu pai, espírito livre e génio criativo de tremenda sensibilidade. Aos meus queridos irmãos Ruizinho e Madalena, eternos companheiros e cúmplices, mesmo na ausência de palavras. Trago em mim um pedaço de todos vós!

Ao meu marido Luís Benjamim das Almas Bacalhau. Por teres em ti todos os sonhos do mundo, e desejares partilhá-los comigo. Obrigada pela tua devoção, alegria constante e ingenuidade enternecedora. Sem o teu apoio entusiasta esta etapa teria sido indiscutivelmente mais solitária.

À memória do meu avô Sebastião,

Ao meu avô José

"A suposição de que a identidade de uma pessoa transcende, em grandeza e importância, tudo o que ela possa fazer ou produzir é um elemento indispensável da dignidade humana."

Hannah Arendt, in 'A Condição Humana'

Abstract

The increasing demand of baculovirus- based biopharmaceuticals raises the interest in developing high-titer production processes. Baculovirus infection boosts the host biosynthetic activity towards the production of viral components and the recombinant protein of interest, hyper-productive phenotypes being the result of a successful adaptation of the cellular network to that scenario. Thus, the comprehensive knowledge of the host cell metabolism, mainly in the post-infection phase, can provide clues on the metabolic adaptations that occur and, ultimately, aid bioprocess engineers in developing rational and targeted optimization strategies.

This PhD work aimed at improving insect cell-based bioprocesses *via* baculovirus expression for the production of complex biopharmaceuticals, ranging from recombinant proteins to multiprotein complexes as novel vaccine candidates, and baculovirus vectors with improved titers and quality. A thorough metabolic analysis and characterization of the IC-BEVS system was attained to support the rational bioprocess optimization, having present the physiological determinants that contribute to productivity, as well as the target requirements for enhanced product quality.

In **Chapter II**, the combined analysis of enzyme activities with metabolic fluxes retrieved noteworthy insights on the metabolism of Sf9 cells, with the identification of possible limiting steps of metabolic activity. Additionally, as a consequence of baculovirus infection, key enzymes controlling the flux via anaplerotic reactions were identified has being greatly activated. High Five cells were analyzed by MFA (**Chapter III**); the cellular metabolic efficiency was identified to be directly correlated with the culture media used, which impacted the level of by-products accumulation throughout culture time. In addition, oxidative metabolism was hampered in High Five cells, which correlates with the carbon overflow towards lactate and alanine production. A comparative fluxome analysis of Sf9 and High Five cells metabolism was performed to have a quantitative overview of the cellular fluxome dynamics that

followed growth and infection (**Chapter IV**). A high dependence of amino acid metabolism and anaplerosis was observed in High Five cells, to counteract the lower channeling of glucose to the TCA cycle. After baculovirus infection, the metabolic activity was rearranged, and the channeling of glucose towards pyruvate formation and further oxidation at the TCA cycle was much more efficient. The strong correlation observed between the metabolic state of both host cells with baculovirus infection highlights the capacity of this virus to act as a metabolic engineer, re-directing the cellular fluxome to support viral replication and virions production.

Although meaningful insights were provided by the fluxome description of Sf9 and High Five cells, is difficult to perceive if the changes in the metabolic fluxes are related to lower enzymatic activities of key regulatory enzymes, or even with perturbations on the intracellular metabolite pools. In this regard, extra and intracellular metabolite quantification was pursued to directly visualize the main compensatory events that occurred on the host cell metabolism (**Chapter V**). Infection impact was considerably higher in High Five cells, with a myriad of metabolic pathways being hijacked to support massive production of heterologous proteins and viral particles. Specifically, amino acid metabolism, redox homeostasis, glutathione and taurine metabolism, and nucleosides biosynthetic pathways were highlighted as being regulated upon baculovirus infection. This information was then applied to design tailored supplementation schemes to boost IC-BEVS production yields of three targets with increasing complexity: recombinant influenza neuraminidase (rNeur); enveloped influenza VLPs (Inf-VLP) and the baculovirus itself (BV) (**Chapter VI**). Higher rNeur yields were achieved when supplementing High Five cultures with cholesterol; for Sf9 cells, GSH, antioxidants combined with polyamines, and cholesterol yielded the best outputs during InfVLPs and infectious BVs production. The fine tuning of the MOI, along with the enhancement of redox and cholesterol metabolism, yielded an improvement of the systems' specific productivity up to 6 fold. Summing-up, for the IC-BEVS, the maintenance of redox homeostasis,

coupled with an enhanced cholesterol metabolism, are key parameters that should be considered when developing and implementing highly productive bioprocesses.

The scarcity of fundamental knowledge on the baculovirus-host cell interaction is a major drawback for the improvement of bioprocesses through Metabolic Engineering. Virus-based bioprocesses are highly dependent on the proper infection of the producer cell, as well as efficient viral replicative cycle and expression of the heterologous genes. This thesis contributed to extend that landscape, by enlarging the knowledge on the physiology and metabolic requirements of insect cells for the production of high-demanding recombinant products.

Resumo

A crescente procura por biofármacos produzidos pelo sistema de expressão baculovirus-célula de insecto torna clara a necessidade de desenvolver processos de produção altamente eficientes e produtivos. Após a infecção pelo baculovirus, a capacidade biosintética da célula hospedeira é levada ao limite com o objectivo de produzir não só os vários componentes virais como também a proteína recombinante de interesse. Os estados celulares considerados hiper productivos reflectem o sucesso da adpatação da célula hospedeira ao cenário de infecção. Assim sendo, o estudo do metabolismo celular, principalmente no cenário pós-infecção, poderá fornecer pistas acerca das adaptações metabólicas que ocorrem durante este processo e, em última instância, contribuir para o desenvolvimento e implementação de estratégias de optimização do bioprocesso e engenharia metabólica.

Esta tese de doutoramento teve como objectivo optimizar o sistema de expressão baculovirus-célula de insecto para produção de biofármacos complexos, desde proteínas recombinantes a partículas semelhantes a vírus que podem ser usadas como vacinas e vectores virais, em maior quantidade e de qualidade superior. De modo a optimizar este processo de expressão de uma forma racional, procedeu-se à analise do metabolismo celular, dando especial atenção aos determinantes fisiológicos e requisitos bioquímicos do produto alvo que contribuem para uma maior productividade e qualidade do mesmo.

No **Capítulo II**, a análise combinada dos fluxos metabólicos e actividades enzimáticas revelou dados importantes acerca da actividade metabólica das células de insecto Sf9, como por exemplo a identificação das vias metabólicas potencialmente limitantes. Mais ainda, foi observado um aumento na actividade de enzimas de vias anapleróticas como consequência da infecção viral. Procedeu-se igualmente à análise dos fluxos metabólicos nas células High Five (**Capítulo III**), tendo-se observado que a eficiência metabólica destas células está directamente correlacionada com o meio de cultura usado, o qual influencia os níveis de produção de sub-produtos do metabolismo celular ao longo da cultura. Mais ainda, foi

observado que o metabolismo oxidativo das células High Five se encontra limitado, levando à produção e acumulação excessiva de lactato e alanina. O metabolismo das duas células de insecto mais utilizadas pela indústria, Sf9 e High Five, foi analisado e comparado através da análise quantitativa dos fluxos metabólicos (**Capítulo IV**). Os resultados obtidos indicam que as células High Five estão altamente dependentes da actividade anaplerótica e do metabolismo amino acídico como forma de contrabalançar o reduzido direccionamento de glucose para o ciclo dos ácidos tricarboxílicos (ATC). Após a infecção com baculovirus, a actividade metabólica da célula sofre um rearranjo significativo, tornando o direccionamneto de glucose para formação de piruvato e subsequente incorporação no ciclo dos ACT muito mais eficiente. Todos estes estudos sugerem que o baculovirus tem um papel activo na reorganização da actividade metabólica das células hospedeiras, actuando ele próprio como um engenheiro metabólico que controla e direciona a actividade energética celular para suportar a sua própria replicação e progenia.

Apesar da análise do fluxoma das células Sf9 e High Five ter gerado conhecimento aprofundado acerca da dinâmica do metabolismo celular antes e após infecção com baculovirus, não foi possível aferir se as alterações nos fluxos metabólicos advêm de diferenças nas actividades das enzimas que regulam essas vias, ou até mesmo de flutuações na quantidade e disponibilidade dos metabolitos que actuam como substratos. De modo a responder a esta questão, procedeu-se à quantificação dos metabolitos extra e intracelulares como forma de visualizar diretamente quais os eventos compensatórios que ocorrem no metabolismo das células Sf9 e High Five durante o crescimento celular e após infecção com baculovirus (**Capítulo V**). O impacto da infecção foi significativamente mais elevado nas células High Five, com um elevado número de vias metabólicas a serem recrutadas/redireccionadas para suportar a replicação viral e produção da proteína recombinante de interesse. Entre as mais essenciais podemos incluir as vias metabólicas que pertencem ao metabolismo de amino ácidos, glutationo, biotina, taurina, resposta ao stress oxidativo e percursores da síntese de ácidos nucleicos. Esta informação foi depois

usada para desenhar estratégias de suplementação de meios de cultura com o objectivo de intensificar as vias identificadas por análise metabolómica e, subsequentemente, potenciar a expressão de três produtos com elevado grau de complexidade: i) proteína recombinante neuraminidase (rNeur), ii) partículas envelopadas semelhantes a vírus compostas por proteínas de Influenza (Inf-VLPs), e iii) baculovirus (BV) (**Capítulo VI**). Relativamente às células High Five, a adição de colesterol ao meio de cultura promoveu um aumento na produção de rNeur por célula. No caso das células Sf9, a adição de glutationo, antioxidantes, poliaminas e colesterol resultou no aumento da produção de Inf-VLPs e de BVs por célula. Conjugando a multiplicidade de infecção (MOI) com a intensificação do metabolismo do colesterol e resposta ao stress oxidativo conseguiu-se um aumento de 6 vezes na produção por células no caso células Sf9. Em suma, a manutenção do equilíbrio das reacções de oxidação-redução e um metabolismo do colesterol mais eficiente são parametros chave que devem ser considerados aquando do desenvolvimento e implementação de bioprocessos altamente produtivos baseados no sistema baculoviurs-célula de insecto.

O desenvolvimento de estratégias de optimização por engenharia metabólica é limitado pelo pouco conhecimento dos processos chave que regulam a interacção do baculovirus com a célula hospedeira. O sucesso de bioprocessos baseados em vírus é extraordinariamente dependente da relação estabelecida entre o vírus e a célula, bem como da eficiência do ciclo replicativo viral e expressão dos genes heterólogos. Esta tese contribuíu para uma melhor compreensão do cénario de infecção em células de insecto, proporcionando um conhecimento abrangente da fisiologia celular e dos determinantes metabólicos envolvidos na produção de biofármacos complexos.

Thesis publications

Published:

1. Bernal V, **Monteiro F**, Carinhas N, Ambrósio R, Alves PM (2010). An integrated analysis of enzyme activities, cofactor pools and metabolic fluxes in baculovirus-infected Spodoptera frugiperda Sf9 cells. *Journal of Biotechnology* Nov;150(3):332-42.

2. **Monteiro, F.**, Carinhas, N., Carrondo, M. J. T., Bernal, V., and Alves, P. M. (2012). Toward system-level understanding of baculovirus-host cell interactions: from molecular fundamental studies to large-scale proteomics approaches. *Frontiers in Microbiology* 3, 391.
3. **Monteiro F**, Bernal V, Saelens X, Lozano AB, Bernal C, Sevilla A, Carrondo MJ, Alves PM (2014). Metabolic profiling of insect cell lines: Unveiling cell line determinants behind system's productivity. *Biotechnology and Bioengineering* Apr;111(4):816-28

Submitted:

4. **Monteiro F**, Bernal V, Chaillet M, Berger I and Alves PM, Tackling bottlenecks in the IC-BEVS: Enhancing enveloped viral particles production by targeted supplementation design, (*in revision*);

In preparation:

5. **Monteiro F**, Bernal V and Alves PM, Metabolic fluxes of cultured High Five cells: the impact of culture media and baculovirus infection, (*in preparation*)
6. **Monteiro F**, Bernal V and Alves PM, Fluxome analysis of the IC-BEVS: The role of host cell line physiology in systems productivity, (*in preparation*)

Other publications in the scope of virus production:

7. Real G, **Monteiro F**, Burger C, Alves PM (2011). Improvement of lentiviral transfer vectors using cis-acting regulatory elements for increased gene expression, Appl Microbiol Biotechnology; Sep 91(6):1571-91

List of contents

Chapter I

INTRODUCTION

Part of this chapter is adapted from the manuscript:

Monteiro, F., Carinhas, N., Carrondo, M. J. T., Bernal, V., and Alves, P. M. (2012). Toward system-level understanding of baculovirus-host cell interactions: from molecular fundamental studies to large-scale proteomics approaches. *Frontiers in Microbiology* 3, 391.

Contents

1. Baculovirus: valuable expression vectors and therapeutic viruses

1.1 Baculovirus biology and life cycle: from *in vivo* to *in vitro* cultures

Baculoviruses (BVs) are rod-shaped viruses with double-stranded DNA genomes. They infect arthropods, mainly insects, a feature that encouraged their usage as ecologically friendly biopesticides (Miller, 1997). Later on, BVs started to be exploited as viral vectors for eukaryotic protein expression, which quickened the pace of their characterization at the cellular and molecular levels (Possee, 1993). The best-studied member of this family, *Autographa californica* multicapsid nucleopolyhedrovirus (*Ac*MNPV), encodes for 150 genes and its genome has been completely sequenced.

Baculoviruses have a biphasic replication cycle in the insect host, involving the formation of two types of virions, produced in different phases of the infection process: the occlusion-derived virions (ODVs), adapted for stability outside the insect host, and the budded virions (BdVs), non-occluded and responsible for the systemic, cell to cell dissemination of the virus within the insect. Infection starts when insect larvae ingest the occlusion bodies (Keddie et al., 1989). When facing the alkaline conditions in the insect midgut, the occlusion body dissolves and the ODVs are released (Wang and Granados, 1997). The replicative cycle begins when ODVs infect the midgut columnar epithelial cells *via* the PIF complex, which mediate virion-specific binding to receptors located at the membrane of midgut epithelial cells (Horton and Burand, 1993; Kikhno et al., 2002). Afterwards, viral entry occurs through membrane fusion of the virion envelope with the cellular microvilli, followed by the release of the nucleocapsids into the cytoplasm. Nucleocapsids then migrate to the nucleus in a process that involves actin polymerization (Ohkawa et al., 2010). Once having reached the nucleus, the host cell RNA polymerase-dependent transcription of viral immediate-early/early genes initiates (0–6 h post-infection, hpi). This set of genes encodes mainly for transactivators essential for viral gene expression and subversion of host cell activity (Passarelli and Miller, 1993). The transition from early to late phase is marked by the onset of viral DNA replication (6–18 hpi) and the activity of a virus-encoded RNA polymerase (Grula et al., 1981). Viral

DNA replication occurs together with the expression of viral components necessary for the assembly of new nucleocapsids. The newly assembled nucleocapsids are transported from the nucleus to the plasma membrane for budding through GP64-enriched areas, originating the budded viruses (BdVs; Passarelli, 2012). BdVs are non-occluded virions surrounded by a plasma membrane-derived envelope containing GP64 as a major structural protein (Washburn et al., 2003). BdVs are required for secondary infection: once released, they are transported through the hemolymph to infect new cells, a process which, in contrast to what is described for ODVs, is undertaken by GP64 *via* clathrin-mediated endocytosis (Blissard and Wenz, 1992; Long et al., 2006). In this regard, BdVs are the virus form responsible for viral dissemination through the host, culminating in a systemic infection. A secondary infection cycle begins with the entrance of BdVs into another cell of the insect. After entering the cell, the infection process is similar to what happens in a primary infection, with the nucleocapsids traveling to the nucleus for DNA replication and subsequent viral protein expression. The very late phase of infection (18 hpi) initiates with the expression of proteins that constitute the crystalline matrix of the ODVs, namely polyhedrin. After nucleocapsid assembly, they are enveloped by the polyhedrin matrix to constitute the ODVs. The secondary cycle ends with the extensive infection of larvae tissues and cell lysis, culminating in insect larvae death, and dissemination of ODVs to the environment, where they can remain viable for several years until being ingested by other larvae (Volkman, 1997). Summarizing, BdVs and ODVs are genetically identical but differ in their envelope compositions and tissue tropisms, and are produced at different times during infection.

The *in vitro* life cycle of baculovirus is similar to what happens *in vivo*, with a major difference that cultured cells need to be directly infected with the BVs. Since ODVs are forms resistant to environmental factors, there is no need of an occlusion matrix for *in vitro* virus survival. In fact, polyhedrin can be viewed as non-essential for baculovirus *in vitro* cell culture. Given that, recombinant baculoviruses are constructed by replacing the polyhedrin gene (*polh*) by a gene of interest under the

control of the very late *polh* promoter (Merrington et al., 1997). Besides the strong activity of *polh* promoter, that allows high productivities of the recombinant protein, it is only expressed in the very late stage of the infection cycle.

1.2 Introduction to the baculovirus-insect cell system

The first papers that illustrated the potential of using the *Ac*MNPV to produce recombinant proteins in insect cells were published 30 years ago (Pennock et al., 1984; Smith et al., 1983), a hallmark of the birth of the baculovirus expression vector system (BEVS). In the next decades, BEVS technology matured significantly as a common manufacture platform of recombinant proteins, vaccines and gene therapy vectors to address unmet medical and industrial needs worldwide (van Oers et al., 2015). Growing knowledge on baculovirus basic biology, coupled with increased know-how on insect cell bioprocessing, has contributed outstandingly to the settlement of BEVS-based operations.

The first cell line to be generically used for *Ac*MNPV propagation was the Sf21 clone (Vaughn et al., 1977), originated from the pupal ovarian tissue of the fall armyworm *Spodoptera frugiperda*. Sf9, a clonal isolate of Sf21, has progressively replaced its parent in the research and industrial fields owing to its improved growth and production characteristics. Several other cell lines exist that are derived from the lepidopteran *Trichopulsia ni*, namely Tn5 and its clonal isolate High Five, which is known to permit higher specific recombinant protein production than Sf9 cells (Drugmand et al., 2012). However, the later produce higher quantities of infectious baculovirus particles (Taticek et al., 2001), and the reasons behind this host-specific productivity phenotype remained to be addressed.

Insect cell metabolism has some notable differences from that of mammalian cells in culture. Sf9 cells do not significantly accumulate lactate and ammonia, major metabolic by-products that can hinder culture performance. A more active tricarboxilic acids (TCA) cycle, together with the presence of an efficient enzymatic recycling system for ammonia detoxification, are the primary causes for the observed

metabolic efficiency (Neermann and Wagner, 1996). However, this phenotype is not seen in High Five cell cultures, which are known to produce high levels of toxic by-products throughout culture time accompanied by intense nutrient uptake rates (Rhiel et al., 1997). Thus, metabolic regulation appears to differ between the two cell lines. When reaching out for animal therapeutics, considerations regarding the bioactivity of the recombinant product arise. Insect cells offer a eukaryotic environment for protein processing and post-translation modifications to occur, however the complexity of such processes is not at the same level as in mammalian cells. Insect cells are not able to generate complex *N*-glycanes profiles, mainly due to the lack of galactosyltranferases and sialyltransferases expression. This limitation has been tackled by the generation of insect cell lines stably expressing enzymes that mimic the synthesis of mammalian/human glycoform, offering the possibility to perform humanized glycosylation profiles (Jarvis, 2003; Tomiya et al., 2003). In addition, the baculovirus itself has been engineered to express glyco-enzymes providing an alternative way to recreate mammalian-like patterns in the BEVS (Jarvis et al., 2001; Palmberger et al., 2013).

1.3 Therapeutic and research applications of the baculovirus-insect cell system

Due to the attributes described above, a wide repertoire of recombinant products has been expressed in insect cells using the BEVS (Summers, 2006). Besides the monopolization of structural and drug discovery fields (Assenberg et al., 2013), BEVS-driven expression of recombinant targets has gained notorious attention in pharmaceutical research compelled by the recent approval of several human therapeutics, namely Cervarix® (GlaxoSmithKline Biologics); Flublok® (Protein Sciences Corporation); Glybera® (UniQure). An updated overview of the approved vaccines and therapies based on baculovirus expression technology is provided in Table 1.

Table 1. Approved vaccines and therapies based on baculovirus expression technologies

Product	Manufacturer	Product Type	Indication	Use	Year of release
Porcilis Pesti	MSD Animal Health	subunit	Classical swine fever	Pigs	1998
BAYOVAC CSF E2/Advasure	Bayer AG/Pfizer Animal Health	subunit			2001
Circumvent PCV	Intervet/Merck Animal Health	VLP			2005
CircoFLEX	Boehringer Ingelheim Vetmedica	VLP	Porcine circovirus type 2		2008
Porcilis PCV	MSD Animal Health	VLP			2009
Cervarix	GlaxoSmithKlein	VLP	Cervical cancer	Females	2007
Flublock	Protein Sciences Corporation	subunit	Influenza	Humans	2013
Provenge	Dendreon	immunotherapy	Prostate cancer	Men	2010
Glybera	UniQure	rAAV-based gene therapy	Lipoprotein lipase deficiency	Humans	2012

The ability to express multi-protein complexes promotes the exploitation of the BEVS as a production platform for virus-like particles (VLPs), a reservoir of new vaccine candidates for challenging diseases (Liu et al., 2013). Baculovirus are able to transduce different types of mammalian cells, which have empowered their study as gene therapy vectors (Airenne et al., 2013). Since they are unable to replicate and propagate within a human host, baculovirus are seen as attractive and safer alternatives to classical mammalian viruses. In addition, the concept of using the baculovirus as a vectored vaccine has been challenged (Lu et al., 2012), further evidencing the plasticity of such vectors is serving a myriad of biotechnological and therapeutic applications. The validation of these approaches still requires generating knowledge on the mechanisms governing tissue targeting, gene delivery, and host immunological responses to the engineered baculoviruses.

2. Baculovirus infection: impact on the host insect cells

In the different phases of infection, baculoviruses induce profound changes on host cell properties. For that aim, several virus-encoded proteins interact with host cell factors, altering cellular structures and normal functions, and taking control of cellular gene expression machinery for their own profit (Table 2). As a result of such alterations several effects arise: cellular cytoskeleton rearrangement, cell cycle arrest and cytomegaly, apoptosis inhibition, metabolism subversion and global shut-off of host protein synthesis. Current knowledge on the biology of the proteins involved in the regulation of each of these specific responses has been recently reviewed (Monteiro et al., 2012). Concerning the major aim of this thesis, we will focus on the baculovirus impact on the physiology of the host insect cells, emphasizing the role of metabolism towards a productive infection.

2.1 Baculovirus subversion of host cell metabolism

Viral infection claims an intensification of host cell biosynthetic activity in order to supply building blocks needed for the biogenesis of membrane lipids and for the synthesis of viral nucleic acids and proteins (Munger et al., 2010, 2006). In fact, viruses are considered as “metabolic engineers” (Maynard et al., 2010). In this regard, the success of infection is highly dependent on the metabolic state of the cells at the moment of infection, jointly with the viral manipulation of energy metabolism to fit such needs (Carinhas et al., 2011a, 2010). Despite many recent reports, the characterization of insect cells metabolic response to baculovirus infection is still at its infancy.

Baculovirus infection provokes an important metabolic burden on insect cells, causing an enhancement of the fluxes through the major catabolic pathways, namely glycolysis and tricarboxylic acid cycle (TCA) (Bernal et al., 2009) as reflected in the changes in fluxes and enzyme activities after infection (Bernal et al., 2010) (fig. 1). A concomitant increase in the oxygen uptake rate is also observed, which accounts for

Table 2. Baculovirus genes affecting host function

	Baculovirus protein/factors	Host counterparts	Function
Cellular adhesion & entry	ODV: *pifs* (P74, PIF-1 and PIF-2)	Receptors on midgut epithelial cells	Viral entry through membrane fusion;
	BV: GP-64	Receptors on cells	Viral entry by clathrin-mediated endocytosis.
Cytoskeleton remodeling	VP39, P78, VP80	F-actin	Actin cables formation for nucleocapsids transport across the cytoplasm;
	Arif-1	F-actin	Actin cables accumulation at cell borders;
	Ie-1, PE38, HE65, Ac004, Ac102, Ac152	G-actin	Drive G-actin accumulation into the nucleus;
	P78/83-C42	G-actin	Arp2/3-mediated nuclear actin polymerization;
	P10	?	Nuclear integrity;
	EXON0	β-tubulin	Nucleocapsids engagement to microtubular network and further egress;
	Ac93	?	Intranuclear microvesicles formation for virions maturation and egress;
	Bm61	?	Egress;
Cell cycle arrest	EC27	Cdc2	Cell cycle arrest at G2/M;
	EC27	Cdk6	Override cellular checkpoints to allow viral DNA replication;
Cellular stress response	*Lefs*	ATM and/or ATR	Viral DNA replication, shut off of host protein synthesis;
	PK1 ?; others	PI3K-Akt/ MAPK-ERK-JNK members	Viral DNA replication/ late gene expression and progeny production;
	P35	Effector caspases	Blockage of the apoptotic pathway;
	P49	Initiator and effector caspases	Blockage of the apoptotic pathway;
	IAPs	?	Inhibition of apoptosis, activation of ubiquitination pathway;
	?	HSP/HSC70	Viral DNA replication, virions assembly and maturation;
Metabolism	?	?	Boost in catabolic pathways to fuel infection.

a higher rate of respiration upon infection (Bernal et al., 2009; Kamen et al., 1996; Palomares et al., 2004).

Moreover, there is a drop in systems productivity when insect cells are infected with baculovirus at high cell densities, the so called “cell density effect”. Bernal et al. (2009) succeeded in deciphering the metabolic basis of such phenomenon, during which Sf9 cells undergo a progressive inhibition of central metabolism (Bernal et al., 2009). Since a successful viral infection strongly correlates with the energetic state of the cell, viral replication is impaired in high cell density cultures. Iwanaga and coworkers performed an exploratory analysis using subtractive hybridization in order to identify differentially expressed host genes following *Bm*NPV infection (Iwanaga et al., 2007). The authors paid special attention to the response of energy metabolism to infection, and reported the up-regulation of *citrate synthase* and *ATP-dependent proteasome 26S* homologous genes. Citrate synthase is the first enzyme of the TCA cycle, which plays a central role in aerobic energy production and metabolic interconversions in mitochondria (Holloszy et al., 1970).

On the other hand, the proteasome-ubiquitin pathway plays an important role during baculovirus infection as mentioned previously (Katsuma et al., 2011). Next-generation sequencing and gene enrichment analysis also showed that gene sets related to mitochondrial function were highly up-regulated during the course of *Bm*NPV infection of *Bm*5 cells (Xue et al., 2012). A recent high throughput analysis of baculovirus proteomic responses of Sf9 cells to infection with *Ac*MNPV identified two up-regulated metabolic enzymes, pyruvate dehydrogenase and aldehyde dehydrogenase (Carinhas et al., 2011b). Therefore, the up-regulation of such cellular proteins indicates that baculoviruses manipulate host energy metabolism to fuel its own replication and further envisages the importance of energy metabolism in supporting infection.

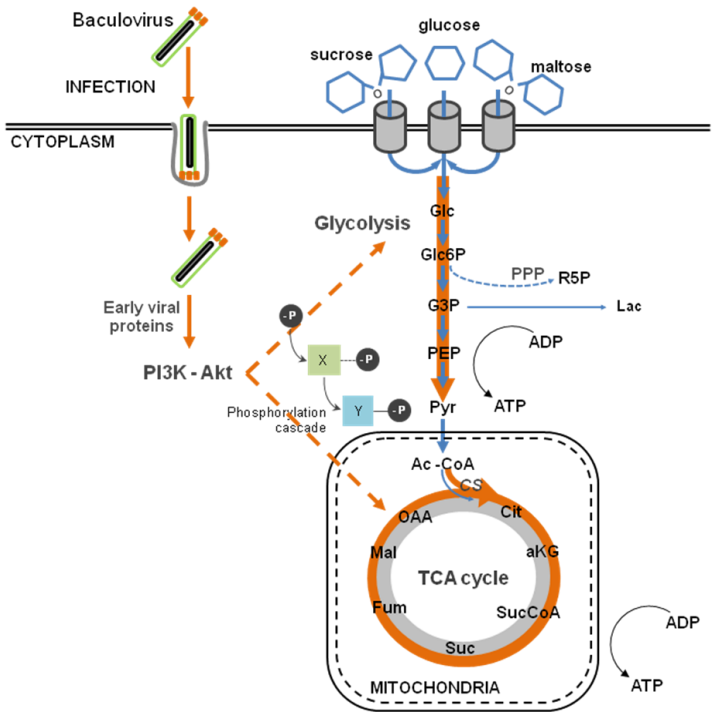

Figure 1. Baculovirus infection impact on host cell metabolism. Baculovirus infection causes an intensification of glycolytic and tricarboxylic acid cycle (TCA) fluxes, which indirectly follows the activation of the PI3K-Akt signaling pathway.

Baculovirus replication depends on the activation of PI3K-Akt signaling pathway (Xiao et al., 2009). One of the downstream targets of Akt is the adenosine 5′monophosphate (AMP)-activated kinase (AMPK), a key sensor which regulates the metabolic status of cells (Cantó et al., 2009). In fact, it is activated by an increase in the AMP:ATP ratio (*i.e.* a low energy charge) and balances energy homeostasis by up-regulating catabolic processes while inhibits anabolism. A similar regulatory mechanism is activated in other viruses (Terry et al., 2012). In addition, both *Ac*MNPV and *Bm*NPV encode nucleotide diphosphate hydrolases belonging to the Nudix family. The corresponding genes are expressed early in infection and are essential for the replication of the virus (Chen et al., 2010; Ge et al., 2007). The essentiality of this activity is intriguing, although several metabolic regulatory roles have been proposed

for nucleotides and related metabolites, which might contribute to the observed effects of infection (Tong and Denu, 2010).

2.2 Systems-level analysis of Baculovirus-Host cell interactions

As seen along the previous section, viral infection induces profound alterations on the physiology of the host cells, and the latter respond to such changes by translating a complex network of protein-protein interactions and biochemical signaling events into functional responses. Systems level knowledge about the host effectors involved in the response to virus and the functions induced by viruses is crucial to understand the molecular basis of viral pathogenesis at a whole cell/organism level.

In addition to their well proven biotechnological and biomedical potentials, the study of the molecular biology of baculovirus infection has also offered meaningful insights into conserved viral mechanisms of manipulation and subversion of the host cell (Clem, 2001; Goley et al., 2006).

Despite the advances in the so-called *omic* technologies, their application to the baculovirus-host system has been held back by the lack of sequenced host genomes, and the scarcity of curated databases. While complete genome sequences for more than 53 baculovirus are available (van Oers, 2011), currently, only two fully sequenced insect host exist, *B. mori* (Xia et al., 2004) and *S. frugiperda* (Kakumani et al., 2014). Global gene expression profiles of *S. frugiperda* and *B. mori* derived cell lines have been recorded at various time-points, following baculovirus infection (Iwanaga et al., 2007; Nobiron, 2003; Sagisaka et al., 2010; Salem et al., 2011). Also, the temporal gene expression programs of the viral genes of several members of the *Baculoviridae* family (*Ac*MNPV, *Tn*SNPV, *Bm*NPV) have been elucidated during their respective infection cycles (Iwanaga et al., 2007, 2004; van Munster et al., 2006; Yamagishi et al., 2003). Even scarcer are large scale proteomic studies. Popham *et al.* (2010) performed a proteomic analysis based on 2D-GE-MS/MS to examine the protein expression of permissive and non-permissive insect host cells (*H. zea* and *Heliothis virescens* derived cell lines, respectively) for *Ac*MNPV. The authors

identified 18 differentially expressed proteins after 24 h.p.i. in the permissive cell line, among which there were members of signal transduction pathways, protein function and homeostasis, and cell survival (Popham et al., 2010). Recently, Carinhas *et al.* (2011) applied a SILAC approach for quantitative proteomics of *Sf*9 cells during growth and early baculovirus infection, contributing with the first comparative quantitative proteomic analysis of the response of *S. frugiperda* cells to infection. The lack of an annotated genome sequence was overcome by cross-referencing to a database that included sequences of proteins from *S. frugiperda* and related insect species. The authors found new differentially expressed proteins related to energy metabolism, endoplasmatic reticulum and oxidative stress during *Ac*MNPV infection (Carinhas et al., 2011b). In particular, the up-regulation of two metabolic enzymes, PDH-E3 and ALDH, was observed, which account for an increased efficiency of the coupling of glycolysis and the TCA cycle and for the anaplerotic feeding of carboxylic acids, respectively. These observations go along with the increased metabolic fluxes of central carbon metabolism during baculovirus infection (Bernal et al., 2009), emphasizing the importance of energetic metabolism during viral infection. Concerning the cellular stress response to infection, the authors observed a decrease in the levels of the chaperone ERp57 and the polypeptide transporter SRP57. Both proteins are effectors of the untranslated-protein response (UPR), and their down-regulation envisages the baculovirus capacity in avoiding the deleterious effects of cellular stress response. Altogether, these results demonstrate that baculovirus efficient replication depends on the capacity of viral manipulation of different cellular pathways, highlighting regulatory mechanisms that are under the success of viral infections.

Systems-level knowledge of baculovirus-host interactions requires an effort from the scientific community in the direction of insect cells/host genome sequencing. Recent efforts by Nguyen *et al.* (2012) succeeded in the transcriptome sequencing of *H. zea* cell line (Nguyen et al., 2012), providing a microarray platform to investigate baculovirus-insect cell interactions. This study paved the way for a genome-scale

analysis of the differential mRNA expression of *H.zea* cells infected with *Ha*NPV, in which the authors were able to identify host genes of utmost importance in sustaining infection (Nguyen et al., 2013). These are related to energy generation pathways, transcriptional activity, translation initiation and protein processing, among others. Also, Xue *et al.* (2012) used next-generation sequencing to analyze differential gene expression following *Bm*NPV infection of *Bm*5 cell line. A gene enrichment analysis showed that gene sets enclosing cytoskeleton, transcription, translation, energy metabolism, iron metabolism, and ubiquitin-proteasome pathways are altered during the course of baculovirus infection (Xue et al., 2012). The information gathered during transcriptional analysis was then used to define the interactome network between *Bm*NPV and host proteins at a systems level, revealing direct interaction of viral proteins with cellular components, such as the proteasome, the cytoskeleton and the spliceosome (Xue et al., 2012).

Baculoviruses have developed several strategies to subvert the mechanisms of cellular defense against infection. In this fight, baculoviruses take control of cellular structures, such as the cytoskeleton, and trigger signaling responses leading to cell cycle arrest, induction of the DNA damage response, inhibition of apoptosis and intensification of energy metabolism. Although many studies concerning baculovirus molecular biology and infection process have been pursued, there is a lack of whole-system level integration of cross-platform reported data. Thus far, the application of high-throughput transcriptomic and proteomic approaches has been hampered by the current unavailability of lepidopteran genome sequences. System-level studies can provide useful insights on the dynamic host response to infection. Mapping such intricate network of interactions and, more importantly, deciphering their outcome at the cellular level, will provide a step-further in our current knowledge on the biological outcome of infection.

3. Metabolic modelling for bioprocess engineering

Rational engineering of biological systems is an inherently demanding process due to their evolved nature. Cells are complex operational units, whose function depends on the integration of different layers of information spanning from genome to metabolome. The comprehensive knowledge of the information flow is key to understand and predict cellular phenotypes. In this regard, System Biology emerges with the endeavor to organize, in a comprehensive and actionable manner, the data generated from high-throughput omic technologies. The final aim is to apply the gained knowledge for the rational design of improved bioprocesses, hosts and products that cope with industrial and manufacture needs. The successful application of Systems Biology principles for bioprocess engineering is hindered by the availability of omic tools and databases that recapitulate host cell physiological processes. Although significant advances have been made in industrial microbial systems (Sagt, 2013), this is not the case in the animal cell technology field. Lack of complete annotated genome sequences of biotechnological relevant cell lines, coupled with the higher complexity of animal cell systems, are some of the existing pitfalls. We have witnessed a joint effort of the scientific community to overcome such imposing limitations, with the recent sequencing of the genome of Chinese Hamster Ovary (CHO) cells, the most used cell line for the production of biopharmaceuticals in the animal cell technology field (Xu et al., 2011). It is thus expected raising interest that for the application of systems-level approaches in animal cell bioprocesses.

Molecular signatures can be explored at other levels of information that are more close to the phenotypic portrait. Metabolism is the functional output of the transcriptome and the proteome, being the closest layer to phenotype. Therefore, metabolic networks mirror the cellular readjustments that encompass genome to proteins, being informative of the physiological state of the cell. Metabolomics aims at the identification and simultaneous quantification of free low weight metabolite pools within a cell population at a certain time (Oliver et al., 1998). Thus, a snapshot

of the metabolic portrait of a cell is taken, which will capture the physiological moment. Several analytical approaches are available for the determination of metabolites in cell culture (Zhang et al., 2012), however no single technique is likely to capture whole systems information. Thus, the choice of the most suited technique(s) is sometimes based on prior knowledge of the physiology of the cell, to drive efforts to characterize pre-determined sets of representative metabolites. If such information is not available, non-targeted metabolomic approaches are applied, aiming at measuring the higher number possible of metabolites that will pave the way for metabolic characterization of the system (Nielsen and Oliver, 2005). The application of metabolomics for bioprocess monitoring and control has gained increasing attention, and notable reports can be found in the literature, recently reviewed in Dickson, 2014. Whichever analytical approach is used, large amounts of data are generated that will require extensive analysis and interpretation. Multivariate statistical analysis is usually employed to retrieve meaningful associations from such complex datasets. The application of pathway analysis tools, which widespread use has facilitated understanding of the underlying biology of differentially expressed genes and proteins (Khatri et al., 2012), can also be applied. Although limited by the availability of metabolic data of industrially relevant systems, we have witnessed recent efforts from the systems biology community to change this scenario (Xia et al., 2012).

Metabolic models are often used to contextualize metabolomic data within a network representative of the main metabolic cellular events. A primary metabolic modelling technique is metabolic flux analysis (MFA), which aims at the quantitative analysis of primarily carbon and nitrogen flow throughout a metabolic network, *i.e.* the cellular fluxome. By MFA, intracellular fluxes are calculated by closing balances of intracellular metabolite pools and experimentally measuring a set of consumption and/or production rates (Stephanopoulos, G et al., 1998). Exchange rates of extracellular nutrients and cellular by-products are typically determined, although intracellular flux ratios may also be determined using radiolabelled substrates. This

approach relies heavily on experimental measurements. However, flux distributions in complex metabolic networks may be hampered, *e.g.* due to the existence of parallel pathways and isozymes, metabolic cycles (including the so-called futile cycles), etc. In these cases, obtaining a mathematical solution often requires the utilization of reduced stoichiometric models. The resulting output is a comprehensive map that depicts the calculated fluxes distribution under the experimental conditions of interest. To increase flux resolution, ^{13}C labelling experiments can be conducted (Sauer 2006), although being labor-intensive and computationally demanding. MFA approaches have led the way for a better understanding of the culture system, providing a rational basis for further engineering towards improved production of biopharmaceuticals (Boghigian et al., 2010).

Although the outburst in genome sequences available have materialized in genome-scale stoichiometric models of industrial microorganisms (Blazeck and Alper, 2011; Boghigian et al., 2010), their application to mammalian systems is more recent (Selvarasu et al., 2010). Model refinement is of course important to correct inconsistencies between model predictions and experimental observations, particularly at the genome-scale level. The difficulties to embrace all cellular levels of information in a single metabolic network are obvious, however efforts have been made in including gene expression and regulatory constraints to endow liability into metabolic models (Covert et al., 2008; Min Lee et al., 2008).

4. Challenges in the baculovirus-insect cell system: the bioprocess perspective

Insect cells possess several advantages as protein expression factories. They grow in suspension without serum supplementation, are able to perform post-translational modifications and the scale-up of cultures is quite straightforward (Ikonomou et al., 2003).

However, the production potential of insect cells has been hampered by the so called “cell density effect”, *i.e.*, the drop in specific productivity when cells are infected with baculovirus at high cell concentration. As cells attain high densities, central metabolism suffers a general down-regulation (Bernal et al., 2009). Metabolic regulation appears to differ between Sf9 and High Five cell lines, which might be on the basis of their target-dependent productivity phenotype. Viral infection induces a multi-level response in the host, during which a vast number of intracellular pathways are regulated and profound metabolic changes occur. These changes are ultimately responsible for the production performance of the system. A deeper understanding of such phenomena will certainly allow for the rational design of strategies for bioprocess optimization. The genome of the majority of the insect cell lines remains unsequenced, which limits the extent to which high throughput (genome-scale) technologies can be applied. Further investment in such area is mandatory to pave the way for a systems-level overview on the IC-BEVS.

5. Scope of this thesis

The work developed during this PhD thesis aimed at studying the metabolic constraints modulating the productivity of the insect cell-baculovirus expression system (IC-BEVS) and using that knowledge to design rational strategies for improved titers and quality of BEVS-derived biopharmaceuticals.

In a first part of the work, the characterization of insect host cells physiology was performed, as well as the main metabolic adaptations that followed baculovirus infection. The collected metabolic data were contextualized in a metabolic model representative of the central carbon and nitrogen metabolism of Sf9 and High Five cells, and the fluxome was quantitatively described. Secondly, a thorough metabolomic analysis of the IC-BEVS was attained, and the acquired data was subjected to multivariate and pathway analysis. The combination of both layers of cellular information, fluxome and metabolome, enabled the identification of the metabolic readjustments occurring in the scope of baculovirus infection. The

identification of the metabolic pathways sustaining viral life cycle and, thus, productivity was achieved, and prompted the targeted design of supplementation schemes to boost the metabolic activity of Sf9 and High Five cells. At the end, an improved bioprocess for the production of enveloped viral particles was achieved, yielding an up to 6 fold improvement on the system specific yields.

This thesis substantially advances our understanding of the IC-BEVS, constituting a reference study of the application of systems biology approaches to biotechnologically relevant bioprocesses. Moreover, provides clues on the impact of baculovirus and infection on the insect host cell, adding new insights for the complex study of virus-host interactions and basic virology.

6. Author contribution

Francisca Monteiro wrote this chapter based on the refereed bibliography and by adapting the above-mentioned publication.

7. References

Airenne, K.J., Hu, Y.-C., Kost, T.A., Smith, R.H., Kotin, R.M., Ono, C., Matsuura, Y., Wang, S., Ylä-Herttuala, S., 2013. Baculovirus: an Insect-derived Vector for Diverse Gene Transfer Applications. Mol. Ther. 21, 739–749.

Assenberg, R., Wan, P.T., Geisse, S., Mayr, L.M., 2013. Advances in recombinant protein expression for use in pharmaceutical research. Curr. Opin. Struct. Biol. 23, 393–402. doi:10.1016/j.sbi.2013.03.008

Bernal, V., Carinhas, N., Yokomizo, A.Y., Carrondo, M.J.T., Alves, P.M., 2009. Cell density effect in the baculovirus-insect cells system: a quantitative analysis of energetic metabolism. Biotechnol. Bioeng. 104, 162–80.

Bernal, V., Monteiro, F., Carinhas, N., Ambrósio, R., Alves, P.M., 2010. An integrated analysis of enzyme activities, cofactor pools and metabolic fluxes in baculovirus-infected Spodoptera frugiperda Sf9 cells. J. Biotechnol. 150, 332–42.

Blazeck, J., Alper, H., 2011. Systems metabolic engineering: Genome-scale models and beyond. Biotechnol. J. 5, 647–659.

Boghigian, B.A., Seth, G., Kiss, R., Pfeifer, B.A., 2010. Metabolic flux analysis and pharmaceutical production. Metab. Eng. 12, 81–95.

Cantó, C., Gerhart-Hines, Z., Feige, J.N., Lagouge, M., Noriega, L., Milne, J.C., Elliott, P.J., Puigserver, P., Auwerx, J., 2009. AMPK regulates energy expenditure by modulating NAD+ metabolism and SIRT1 activity. Nature 458, 1056–60.

Carinhas, N., Bernal, V., Monteiro, F., Carrondo, M.J.T., Oliveira, R., Alves, P.M., 2010. Improving baculovirus production at high cell density through manipulation of energy metabolism. Metab. Eng. 12, 39–52.

Carinhas, N., Bernal, V., Teixeira, A.P., Carrondo, M.J., Alves, P.M., Oliveira, R., 2011a. Hybrid metabolic flux analysis: combining stoichiometric and statistical constraints to model the formation of complex recombinant products. BMC Syst. Biol. 5, 34.

Carinhas, N., Robitaille, A.M., Moes, S., Carrondo, M.J.T., Jenoe, P., Oliveira, R., Alves, P.M., 2011b. Quantitative proteomics of Spodoptera frugiperda cells during growth and baculovirus infection. PLoS One 6, e26444.

Chen, H., Li, G., Huang, G., Chen, K., Yao, Q., 2010. Characterization of ORF29 of Bombyx mori nucleopolyhedrovirus. Acta Virol. 275–280.

Clem, R.J., 2001. Baculoviruses and apoptosis: the good, the bad, and the ugly. Cell Death Differ. 8, 137–43.

Covert, M.W., Xiao, N., Chen, T.J., Karr, J.R., 2008. Integrating metabolic, transcriptional regulatory and signal transduction models in Escherichia coli. Bioinformatics 24, 2044–2050.

Dickson, A.J., 2014. Enhancement of production of protein biopharmaceuticals by mammalian cell cultures: the metabolomics perspective. Curr. Opin. Biotechnol. 30C, 73–79. doi:10.1016/j.copbio.2014.06.004

Drugmand, J.-C., Schneider, Y.-J., Agathos, S.N., 2012. Insect cells as factories for biomanufacturing. Biotechnol. Adv. 30, 1140–57. doi:10.1016/j.biotechadv.2011.09.014

Ge, J., Wei, Z., Huang, Y., Yin, J., Zhou, Z., Zhong, J., 2007. AcMNPV ORF38 protein has the activity of ADP-ribose pyrophosphatase and is important for virus replication. Virology 361, 204–11.

Goley, E.D., Ohkawa, T., Mancuso, J., Woodruff, J.B., D'Alessio, J. a, Cande, W.Z., Volkman, L.E., Welch, M.D., 2006. Dynamic nuclear actin assembly by Arp2/3 complex and a baculovirus WASP-like protein. Science 314, 464–7.

Holloszy, J.O., Oscai, L.B., Don, I.J., Molé, P.A., 1970. Mitochondrial citric acid cycle and related enzymes: adaptive response to exercise. Biochem. Biophys. Res. Commun. 40, 1368–73.

Ikonomou, L., Schneider, Y.-J., Agathos, S.N., 2003. Insect cell culture for industrial production of recombinant proteins. Appl. Microbiol. Biotechnol. 62, 1–20.

Iwanaga, M., Shimada, T., Kobayashi, M., Kang, W., 2007. Identification of differentially expressed host genes in Bombyx mori nucleopolyhedrovirus infected cells by using subtractive hybridization. Appl. Entomol. Zool. 42, 151–159.

Iwanaga, M., Takaya, K., Katsuma, S., Ote, M., Tanaka, S., Kamita, S.G., Kang, W., Shimada, T., Kobayashi, M., 2004. Expression profiling of baculovirus genes in permissive and nonpermissive cell lines. Biochem. Biophys. Res. Commun. 323, 599–614.

Jarvis, D.L., 2003. Developing baculovirus-insect cell expression systems for humanized recombinant glycoprotein production. Virology.

Jarvis, D.L., Howe, D., Aumiller, J.J., 2001. Novel baculovirus expression vectors that provide sialylation of recombinant glycoproteins in lepidopteran insect cells. J. Virol. 75, 6223–6227.

Kakumani, P.K., Malhotra, P., Mukherjee, S.K., Bhatnagar, R.K., 2014. A draft genome assembly of the army worm, Spodoptera frugiperda. Genomics 104, 134–43. doi:10.1016/j.ygeno.2014.06.005

Kamen, a a, Bédard, C., Tom, R., Perret, S., Jardin, B., 1996. On-line monitoring of respiration in recombinant-baculovirus infected and uninfected insect cell bioreactor cultures. Biotechnol. Bioeng. 50, 36–48.

Katsuma, S., Tsuchida, A., Matsuda-Imai, N., Kang, W., Shimada, T., 2011. Role of the ubiquitin-proteasome system in Bombyx mori nucleopolyhedrovirus infection. J. Gen. Virol. 92, 699–705.

Khatri, P., Sirota, M., Butte, A.J., 2012. Ten years of pathway analysis: Current approaches and outstanding challenges. PLoS Comput. Biol.

Liu, F., Wu, X., Li, L., Liu, Z., Wang, Z., 2013. Use of baculovirus expression system for generation of virus-like particles: successes and challenges. Protein Expr. Purif. 90, 104–16. doi:10.1016/j.pep.2013.05.009

Lu, H., Chen, Y., Liu, H., 2012. Baculovirus as a vaccine vector. Bioengineered 271–274.

Maynard, N.D., Gutschow, M. V, Birch, E.W., Covert, M.W., 2010. The virus as metabolic engineer. Biotechnol. J. 5, 686–94.

Merrington, C.L., Bailey, M.J., Possee, R.D., 1997. Manipulation of baculovirus vectors. Mol. Biotechnol. 8, 283–97.

Miller, L., 1997. The Baculoviruses. Springer.

Min Lee, J., Gianchandani, E.P., Eddy, J.A., Papin, J.A., 2008. Dynamic analysis of integrated signaling, metabolic, and regulatory networks. PLoS Comput. Biol. 4.

Monteiro, F., Carinhas, N., Carrondo, M.J.T., Bernal, V., Alves, P.M., 2012. Toward system-level understanding of baculovirus-host cell interactions: from molecular fundamental studies to large-scale proteomics approaches. Front. Microbiol. 3, 391.

Munger, J., Bajad, S.U., Coller, H. a, Shenk, T., Rabinowitz, J.D., 2006. Dynamics of the cellular metabolome during human cytomegalovirus infection. PLoS Pathog. 2, e132.

Munger, J., Bennett, B.D., Parikh, A., Feng, X., Rabitz, H.A., Shenk, T., Rabinowitz, J.D., 2010. Systems-level metabolic flux profiling identifies fatty acid synthesis as a target for antiviral therapy. Nat. Biotechnol. 26, 1179–1186.

Neermann, J., Wagner, R., 1996. Comparative analysis of glucose and glutamine metabolism in transformed mammalian cell lines, insect and primary liver cells. J. Cell. Physiol. 166, 152–69.

Nguyen, Q., Chan, L.C.L., Nielsen, L.K., Reid, S., 2013. Genome scale analysis of differential mRNA expression of Helicoverpa zea insect cells infected with a H. armigera baculovirus. Virology 1–13. doi:10.1016/j.virol.2013.06.004

Nguyen, Q., Palfreyman, R.W., Chan, L.C.L., Reid, S., Nielsen, L.K., 2012. Transcriptome Sequencing of and Microarray Development for a Helicoverpa zea Cell Line to Investigate In Vitro Insect Cell-Baculovirus Interactions. PLoS One 7, e36324.

Nielsen, J., Oliver, S., 2005. The next wave in metabolome analysis. Trends Biotechnol.

Nobiron, I., 2003. Autographa californica nucleopolyhedrovirus infection of Spodoptera frugiperda cells: a global analysis of host gene regulation during infection, using a differential display approach. J. Gen. Virol. 84, 3029–3039.

Oliver, S.G., Winson, M.K., Kell, D.B., Baganz, F., 1998. Systematic functional analysis of the yeast genome. Trends Biotechnol. 16, 373–378. doi:10.1016/S0167-7799(98)01214-1

Palmberger, D., Klausberger, M., Grabherr, R., 2013. MultiBac turns sweet. Bioengineered 4, 78–83.

, O.T., 2004. Utilization of oxygen uptake rate to assess the role of glucose and glutamine in the metabolism of infected insect cell cultures. Biochem. Eng. J. 19, 87–93.

Pennock, G.D., Shoemaker, C., Miller, L.K., 1984. Strong and regulated expression of Escherichia coli beta-galactosidase in insect cells with a baculovirus vector. Mol. Cell. Biol. 4, 399–406.

Popham, H.J.R., Grasela, J.J., Goodman, C.L., McIntosh, A.H., 2010. Baculovirus infection influences host protein expression in two established insect cell lines. J. Insect Physiol. 56, 1237–45.

Possee, R.D., 1993. Baculovirus expression vectors — A laboratory manual. Trends Biotechnol. 11, 267–268.

Rhiel, M., Mitchell-Logean, C.M., Murhammer, D.W., 1997. Comparison of Trichoplusia ni BTI-Tn-5B1-4 (high five) and Spodoptera frugiperda Sf-9 insect cell line metabolism in suspension cultures. Biotechnol. Bioeng. 55, 909–920.

Sagisaka, A., Fujita, K., Nakamura, Y., Ishibashi, J., Noda, H., Imanishi, S., Mita, K., Yamakawa, M., Tanaka, H., 2010. Genome-wide analysis of host gene expression in the silkworm cells infected with Bombyx mori nucleopolyhedrovirus. Virus Res. 147, 166–75.

Sagt, C.M.J., 2013. Systems metabolic engineering in an industrial setting. Appl. Microbiol. Biotechnol. 97, 2319–2326. doi:10.1007/s00253-013-4738-8

Salem, T.Z., Zhang, F., Xie, Y., Thiem, S.M., 2011. Comprehensive analysis of host gene expression in Autographa californica nucleopolyhedrovirus-infected Spodoptera frugiperda cells. Virology 412, 167–78.

Selvarasu, S., Karimi, I. a, Ghim, G.-H., Lee, D.-Y., 2010. Genome-scale modeling and in silico analysis of mouse cell metabolic network. Mol. Biosyst. 6, 152–61.

Smith, G.E., Summers, M.D., Fraser, M.J., 1983. Production of human beta interferon in insect cells infected with a baculovirus expression vector. Mol. Cell. Biol. 3, 2156–2165.

Stephanopoulos, G, Aristidou, A.A., Nielsen, J., 1998. Metabolic Engineering. Principles and Methodologies. Academic Press, New York.

Summers, M.D., 2006. Milestones Leading to the Genetic Engineering of Baculoviruses as Expression Vector Systems and Viral Pesticides. Adv. Virus Res.

Taticek, R.A., Choi, C., Phan, S.E., Palomares, L.A., Shuler, M.L., 2001. Comparison of growth and recombinant protein expression in two different insect cell lines in attached and suspension culture. Biotechnol. Prog. 17, 676–84.

Terry, L.J., Vastag, L., Rabinowitz, J.D., Shenk, T., 2012. Human kinome profiling identifies a requirement for AMP-activated protein kinase during human cytomegalovirus infection. Proc. Natl. Acad. Sci. U. S. A. 109, 3071–6.

Tomiya, N., Betenbaugh, M.J., Lee, Y.C., 2003. Humanization of lepidopteran insect-cell-produced glycoproteins. Acc. Chem. Res. 36, 613–620.

Tong, L., Denu, J.M., 2010. Function and metabolism of sirtuin metabolite o-Acetyl-ADP-Ribose. Biochim. Biophys. Acta 1804, 1617–1625.

Van Munster, M., Willis, L.G., Elias, M., Erlandson, M. a, Brousseau, R., Theilmann, D. a, Masson, L., 2006. Analysis of the temporal expression of Trichoplusia ni single nucleopolyhedrovirus genes following transfection of BT1-Tn-5B1-4 cells. Virology 354, 154–66.

Van Oers, M.M., 2011. Opportunities and challenges for the baculovirus expression system. J. Invertebr. Pathol. 107 Suppl, S3–15.

Van Oers, M.M., Pijlman, G.P., Vlak, J.M., 2015. Thirty years of baculovirus-insect cell protein expression: From dark horse to mainstream technology. J. Gen. Virol. 96, 6–23. doi:10.1099/vir.0.067108-0

Vaughn, J.L., Goodwin, R.H., Tompkins, G.J., McCawley, P., 1977. The establishment of two cell lines from the insect Spodoptera frugiperda (Lepidoptera; Noctuidae). In Vitro 13, 213–217.

Xia, J., Mandal, R., Sinelnikov, I. V, Broadhurst, D., Wishart, D.S., 2012. MetaboAnalyst 2.0--a comprehensive server for metabolomic data analysis. Nucleic Acids Res. 40, 1–7.

Xia, Q., Zhou, Z., Lu, C., Cheng, D., Dai, F., Li, B., Zhao, P., Zha, X., Cheng, T., Chai, C., Pan, G., Xu, J., Liu, C., Lin, Y., Qian, J., Hou, Y., Wu, Z., Li, G., Pan, M., Li, C., Shen, Y., Lan, X., Yuan, L., Li, T., Xu, H., Yang, G., Wan, Y., Zhu, Y., Yu, M., Shen, W., Wu, D., Xiang, Z., Yu, J., Wang, J., Li, R., Shi, J., Li, H., Li, G., Su, J., Wang, X., Li, G., Zhang, Z., Wu, Q., Li, J., Zhang, Q., Wei, N., Xu, J., Sun, H., Dong, L., Liu, D., Zhao, S., Zhao, X., Meng, Q., Lan, F., Huang, X., Li, Y., Fang, L., Li, C., Li, D., Sun, Y., Zhang, Z., Yang, Z., Huang, Y., Xi, Y., Qi, Q., He, D., Huang, H., Zhang, X., Wang, Z., Li, W., Cao, Y., Yu, Y., Yu, H., Li, J., Ye, J., Chen, H., Zhou, Y., Liu, B., Wang, J., Ye, J., Ji, H., Li, S., Ni, P., Zhang, J., Zhang, Y., Zheng, H., Mao, B., Wang, W., Ye, C., Li, S., Wang, J., Wong, G.K.-S., Yang, H., 2004. A draft sequence for the genome of the domesticated silkworm (Bombyx mori). Science (80-.). 306, 1937–40.

Xiao, W., Yang, Y., Weng, Q., Lin, T., Yuan, M., Yang, K., Pang, Y., 2009. The role of the PI3K-Akt signal transduction pathway in Autographa californica multiple nucleopolyhedrovirus infection of Spodoptera frugiperda cells. Virology 391, 83–9.

Xu, X., Nagarajan, H., Lewis, N.E., Pan, S., Cai, Z., Liu, X., Chen, W., Xie, M., Wang, W., Hammond, S., Andersen, M.R., Neff, N., Passarelli, B., Koh, W., Fan, H.C., Wang, J., Gui, Y., Lee, K.H., Betenbaugh, M.J., Quake, S.R., Famili, I., Palsson, B.O., Wang, J., 2011. The genomic sequence of the Chinese hamster ovary (CHO)-K1 cell line. Nat. Biotechnol. 29, 735–741. doi:10.1038/nbt.1932

Xue, J., Qiao, N., Zhang, W., Cheng, R.-L., Zhang, X.-Q., Bao, Y.-Y., Xu, Y.-P., Gu, L.-Z., Han, J.-D.J., Zhang, C.-X., 2012. Dynamic Interactions between Bombyx mori Nucleopolyhedrovirus and Its Host Cells Revealed by Transcriptome Analysis. J. Virol. 86, 7345–7359.

Yamagishi, J., Isobe, R., Takebuchi, T., Bando, H., 2003. DNA microarrays of baculovirus genomes: differential expression of viral genes in two susceptible insect cell lines. Arch. Virol. 148, 587–97.

Zhang, A., Sun, H., Wang, P., Han, Y., Wang, X., 2012. Modern analytical techniques in metabolomics analysis. Analyst.

Chapter II

ANALYSIS OF ENZYME ACTIVITIES, COFACTOR POOLS AND METABOLIC FLUXES IN BACULOVIRUS-INFECTED INSECT CELLS

This chapter was adapted from the manuscript:

Bernal V, **Monteiro F**, Carinhas N, Ambrósio R, Alves PM (2010). An integrated analysis of enzyme activities, cofactor pools and metabolic fluxes in baculovirus-infected Spodoptera frugiperda Sf9 cells. *Journal of Biotechnology* Nov;150(3):332-42.

Abstract

The scarcity of fundamental knowledge on the baculovirus-host cell interaction is a major drawback for the improvement of bioprocesses through Metabolic Engineering. After the first hours post-infection, the virus takes over the control of cellular machinery, leading to the repression of host gene expression and imposing a high metabolic burden to insect cells. Nevertheless, there is a lack of detailed data on the metabolic responses to infection, which are ultimately responsible for system productivity performance. In this work, a further insight into the central metabolism of Sf9 cells is achieved by a combined analysis of enzyme activities, cellular cofactors (ATP and $NAD(P)^{(+)}$/NAD(P)H) and metabolic fluxes. Hexokinase and isocitrate dehydrogenase were identified as feasible limiting steps of metabolism; carbon and nitrogen metabolism enzymes were differentially regulated during batch cultures. Moreover, alterations occurring after infection demonstrated the importance of maintaining the energetic state of the cells for baculovirus replication, since ATP accumulated in a MOI-dependent way, and the glutamate dehydrogenase anaplerotic pathway was greatly activated. Altogether, cellular de-energization and stress responses are relevant factors in the metabolic burden imposed by infection. The implications for the improvement of bioprocess performance are discussed.

Contents

1. Introduction

Over the last decade, the Baculovirus Expression Vector System (BEVS) has gained increasing interest for the production of recombinant proteins, virus like particles (VLPs) and gene therapy vectors (Palomares et al., 2006). With such relevant applications, the need for new fundamental studies allowing an in depth understanding of the main constraints of this system is evident and novel strategies for bioprocess improvement are now available (Carinhas et al., 2010; Kim et al., 2007).

The combined analysis of different levels of metabolism regulation (gene transcription, proteome, enzyme activities, metabolome and fluxome) has been successfully applied to characterize and improve microbial processes (Bernal et al., 2007; Shimizu, 2009). However, the application of these methodologies to animal cell based bioprocesses has been much less, especially in the case of insect cells. Neermann and Wagner (1996) performed an in-depth analysis of the more relevant differences between insect and mammalian cell lines, including enzymes of central metabolism. Since then, some authors have analyzed the effect of culture conditions on metabolic (Altamirano et al., 2001; Bonarius et al., 1998; Henry et al., 2005; Sidorenko et al., 2008), enzyme activities (Vriezen and Van Dijken, 1998a; Vriezen and van Dijken, 1998b; Yallop et al., 2003), proteome (Stansfield et al., 2007; Vester et al., 2009), gene expression (Charaniya et al., 2009; Lee et al., 2007) or even a combination of various of these (Kantardjieff et al., 2010; Munger et al., 2008; Vriezen and van Dijken, 1998a) in cell lines relevant for bioprocesses. Despite the great economic impact of animal cells derived products, very limited success in the implementation of Metabolic Engineering strategies has been reported so far, if compared to microbial processes. Efforts have focused on the engineering of cell cycle, apoptosis, energy metabolism and protein glycosylation/secretion pathways (Irani et al., 1999; Jones et al., 2005; O'Callaghan and James, 2008; Peng and Fussenegger, 2009; Vives et al., 2003).

In vitro determined enzyme activities are an indicator of the maximum feasible in vivo fluxes through pathways. It is generally recognized that enzyme activities exceed fluxes, meaning that control of metabolic pathways is mostly exerted by the metabolites and cofactors involved (Janke et al., 2010; Vriezen and van Dijken, 1998a). However, changes in enzyme activities in response to environmental conditions determine altered metabolic states and novel flux distributions. The extent of the effects will depend on the degree of control exerted by that enzyme on the pathway.

Systems Biology approaches have been recently applied to understand virus–host cell interactions (Munger et al., 2008; Peng et al., 2009; Ritter et al., 2010). Viruses are efficient in their use of cell resources for their replication, provoking significant changes in the synthesis of mRNAs and proteins, as well as the induction of complex signal transduction pathways related to anti-viral response. These effects have an impact on the morphology and metabolic state of the host cells and may even induce apoptosis (Vester et al., 2009). Baculovirus infection imparts an important metabolic burden on insect cells (Bernal et al., 2009; Palomares et al., 2006; Rhiel et al., 1997; Vieira et al., 2005). Following infection, expression of host cell genes is repressed to favor viral replication and metabolism is altered. Moreover, different responses to infection have been reported for different virus/host cell pairs which could be rearranged to improve the productivity of the system (Rohrmann, 2008; Thiem, 2009).

Recently, our group analyzed the influence of baculovirus infection on the distribution of metabolic fluxes of Sf9 cells (Bernal et al., 2009; Carinhas et al., 2010). In this work, the metabolic characterization is further extended by the analysis of enzyme activities and cofactor pools and their relation with metabolic fluxes, providing a further insight into the physiological constraints affecting the performance of the BEVS.

2. Materials and Methods

2.1 Cell line and cell culture

Spodoptera frugiperda Sf9 cells were obtained from the European Collection of Cell Cultures (no. 89070101 ECACC). Cells were cultured in serum free medium SF900II (Gibco, Glasgow, UK) at 27ºC in either 500 mL erlenmeyer flasks (Corning, NY) with 50 mL working volume, or 250 mL spinner flasks (Wheaton, Millville, NJ), with 125 mL working volume. Cell concentration was determined by haemocytometer cell counts (Brandt, Wertheim/Main, Germany) and cell viability was evaluated by trypan blue exclusion (Merck, Darmstadt, Germany).

2.2 Baculovirus and infections

Recombinant Autographa californica nucleopolyhedrovirus (AcMNPV VP39-EGFP) was kindly provided by Dr. K. Airenne (University of Kuopio, Finland), and contains VP39 fused to enhanced green fluorescent protein (Kukkonen et al., 2003). Virus amplification was performed by infection of Sf9 cells in a spinner flask at 1×10^6 cells mL^{-1}, at a multiplicity of infection (MOI) of 0.1 infectious particles (IP) $cell^{-1}$ in SF900II medium. This baculovirus stock was used for all subsequent infections.

The end point dilution method (TCID50) based on the detection of EGFP fluorescence was used for virus titration (Roldão et al., 2009). Briefly, Sf9 cells were infected with serial dilutions of baculovirus samples in a 96-well culture plate (Nunc, Roskilde, Denmark). After 7 days, the wells were inspected for green fluorescence using a fluorescence microscope (Leica DM IRB, Leica Microsystems GmbH, Wetzlar, Germany). Both positive (non diluted baculovirus stock) and negative (virus free culture media) controls were performed.

For infections, Sf9 cells were cultured either in 125 mL spinner vessels or in bioreactors (see Section 2.3). Infections were performed at the different multiplicities of infection (MOIs) and cell concentrations at infection (CCIs) indicated in the text.

2.3 Bioreaction

Metabolic studies with control and infected cells were performed in a 2 L B Braun bioreactor (Melsungen, Germany) with 1 L working volume, equipped with probes for the monitoring of temperature, pH and dissolved oxygen. To ensure that cells did not suffer oxygen limitation during the runs, dissolved oxygen concentration was kept constant at 30% saturation by controlling agitation speed (70–250 rpm), air flow (0.2–1 vvm) and supplying a mix of gases with variable proportion of nitrogen, air and/or oxygen. Temperature was controlled at 27 ºC. Reactor seed cultures were grown in spinner flasks. The reactor was inoculated at a cell density of $0.3–0.5\times10^{6}$ cells mL^{-1}.

2.4 Analytical techniques

2.4.1 Sampling

Samples were taken from the culture and viable cells were counted. For the analysis of cellular cofactors, samples consisting of $1–3\times10^{6}$ cells were collected from the culture. Cells were separated by centrifugation at 1700×g. The supernatants (used for metabolite analysis) were stored at −20 ºC. In order to quench metabolism, cell pellets (used for cofactor analysis) were rapidly frozen in liquid nitrogen and stored at −80 ºC until analyzed.

2.4.2 Metabolites

Glucose, glutamine, glutamate and lactate concentrations were analyzed using an YSI 7100 Multiparameter Bioanalytical System (Dayton, OH). Ammonia was quantified enzymatically (kit no. 1112732035; Boehringer Manheim, R-Biopharm AG, Darmstadt, Germany). For the analysis of maltose and sucrose, samples were treated with either α-glucosidase or invertase (Sigma–Aldrich, St. Louis,MO) for 3 h at 37 ºC and glucose formed was quantified as previously stated. Amino acids were determined using the AccQ-Tag HPLC method (Waters, Milford, MA).

2.4.3 ATP

Intracellular ATP was determined using the ATPlite 1 step kit from Perkin Elmer (Waltham,MA) based on firefly (Photinus pyralis) luciferase. Briefly, around 5×10^5 cells were resuspended in 100 µL of PBS and mixed with 100 µL of reagent. For complete cell lysis, the mixture was incubated in the darkness for 4 min at room temperature with vigorous agitation. Luminescence measurements were performed using a Modulus Luminometer from Turner Biosystems (Sunnyvale, CA).

2.4.4 Redox cofactors

Intracellular redox cofactors were determined using a colorimetric method (Queval and Noctor, 2007). For the selective extraction of oxidized and reduced nucleotides, the cell pellet was either resuspended in 0.2 M HCl or NaOH, respectively, and incubated at 100 ºC for 1 min. Extracts were immediately transferred to ice and neutralized. The determination of NAD^+ and NADH was performed in a mixture of 100 mM Hepes buffer (pH 7.5), 2 mM EDTA, 0.12 mM dichlorophenolindophenol, 1 mM phenazine metasulphate, 125 $U.mL^{-1}$ baker's yeast alcohol dehydrogenase (Sigma–Aldrich, St. Louis, MO). Reaction was started by addition of 7.5% absolute ethanol. The determination of $NADP^+$ and NADPH was performed in a mixture of 100 mM Hepes buffer(pH 7.5), 2 mM EDTA, 0.12 mM dichlorophenolindophenol, 1 mM phenazine metasulphate, 125 $U.mL^{-1}$ glucose-6-phosphate dehydrogenase (Sigma–Aldrich, St. Louis, MO). The reaction was started by addition of 0.5 mM glucose-6-phosphate. Calibration curves were performed for each nucleotide (response was linear in the range 0.1–12 µM).

2.5 Determination of enzyme activities

Samples containing around $1–3\times10^8$ cells were collected from the bioreactor. Cells were pelleted by centrifugation (1880×g, 15 min). The pellet was washed in 10 mL of cold phosphate buffered saline (PBS) and centrifuged again. All centrifugation steps

were performed at 4 ºC. The resulting pellet was resuspended in sonication buffer (4mM $MgCl_2$, 2mM β-mercaptoethanol, 200 mM potassium phosphate buffer (pH 7.5)) and sonicated for 1min at 10% input power in a sonicator (Branson Ultrasonics Corporation, Danbury, CT). Active/inactive 15 s sonication cycles were alternated. The resulting suspension was clarified by centrifugation (10 min, 10,000×g) and used for enzyme activity measurements.

Protein concentration in the cell extracts was determined using the Bicinchoninic Acid (BCA) Protein Assay (Pierce, Rockford, IL). Protocols used for enzyme activities determination were adapted from previous works (Hirayama and Nakamura, 2002; Neermann and Wagner, 1996; Vriezen and van Dijken, 1998a). In each case, buffer composition and pH, reagent(s) concentration and extract amount were optimized using S. frugiperda cell free-extracts. Cell extracts were diluted conveniently in order to assure the linearity of assays with protein amount. See (Bernal et al., 2010) for details on the enzyme activity protocols.

2.6 Metabolic flux analysis

A thorough description of the model and the list of reactions can be found in Bernal et al. (2009). Briefly, the model totalizes 75 reactions, with 52 internal (balanced) metabolites, defined by a 75×52 stoichiometric matrix (Fig. 1). The resultant system of equations is determined; the weighted least squares method was used to calculate the model solution (Stephanopoulos, G et al., 1998). Balanceable rates were used to calculate a consistency index, h (Wang and Stephanopoulos, 1983). All computational tasks were performed using the FluxAnalyzer software

2.7 Statistical analysis

Statistical comparison of specific yields or cofactor pools' ratios was performed using unpaired, two-tailed Student's T test. A 95% confidence level was considered to be statistically significant (Klamt et al., 2003). In order to check the consistency of the

experimental data and the metabolic network, carbon and nitrogen mass balances were performed.

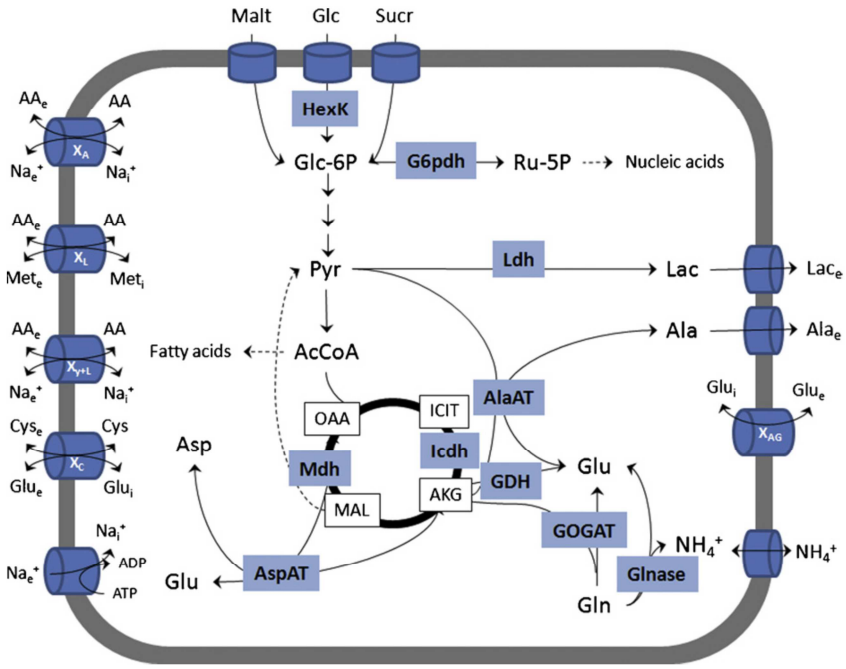

Figure 1. Metabolism of Sf9 cells. The enzyme activities determined in this work are shown in boxes and are representative of the main metabolic pathways: hexokinase (HexK), glucose-6-phosphate dehydrogenase (G6pdh), lactate dehydrogenase (Ldh), NADP+-dependent isocitrate dehydrogenase (Icdh), malate dehydrogenase (Mdh), alanine aminotransferase (AlaAT), aspartate aminotransferase (AspAT), NADH and NADPH-dependent glutamate dehydrogenases (Gdh), glutaminase (Glnase) and NADH- dependent glutamate synthase (GOGAT). Amino acids transport systems are represented by: XA (short chain amino acid transporter), XAG (anionic amino acid transporter), XL (hydrophobic amino acid transporter) Ly+L (cationic amino acid transporter) and XC (cysteine transporter). Adapted from previous works (Bernal et al., 2009; Doverskog et al., 1997; Wahl et al., 2008).

3. Results

3.1 Metabolism of Sf9 cells

To further understand the main metabolic features and flux distribution of insect cells, the dynamics of redox and energy nucleotides and 10 enzyme activities were determined along the culture in serum-free medium (Fig. 2A).

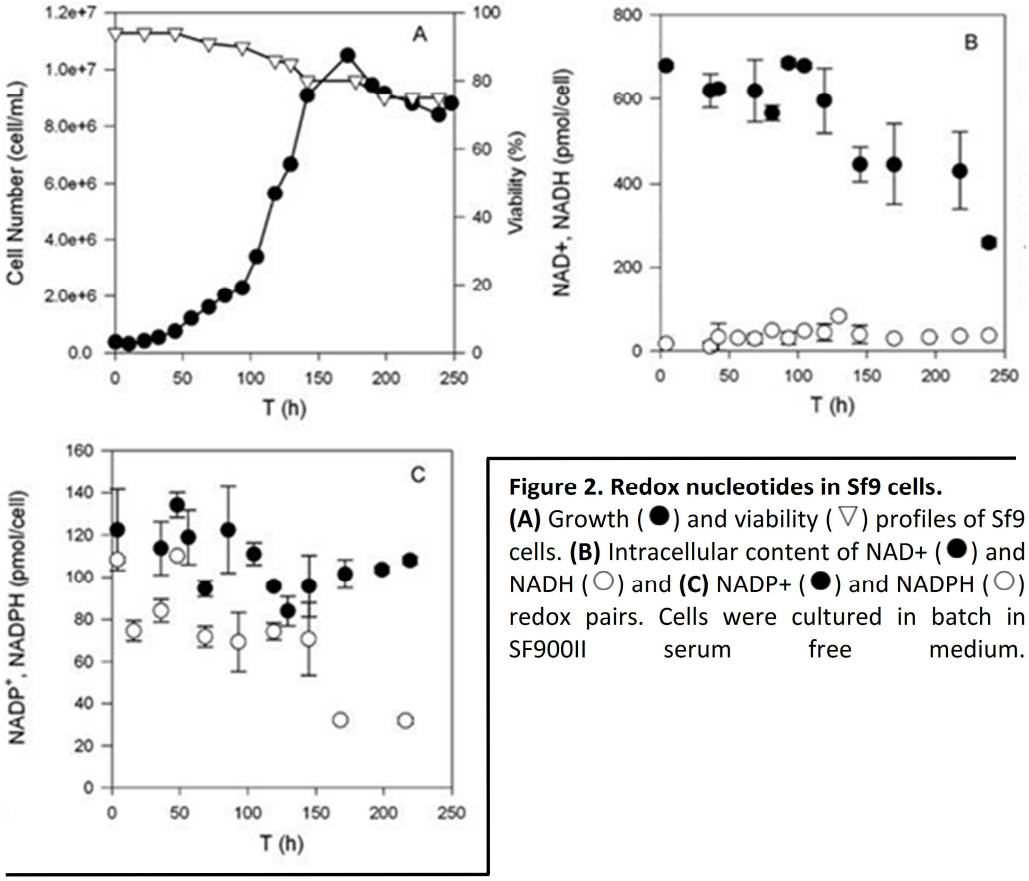

Figure 2. Redox nucleotides in Sf9 cells.
(A) Growth (●) and viability (▽) profiles of Sf9 cells. **(B)** Intracellular content of NAD+ (●) and NADH (○) and **(C)** NADP+ (●) and NADPH (○) redox pairs. Cells were cultured in batch in SF900II serum free medium.

3.1.1 Redox and energy cofactors

The redox state of Sf9 cells was characterized by the pools of the two main redox pairs (NAD^+/NADH and $NADP^+$/NADPH). Important differences were observed, in both their concentrations and profiles. The NAD(H) pool was 3- to 6-fold higher than the NADP(H) pool along the whole culture. In addition, the concentrations of NAD^+ and NADH indicated a high NAD^+/NADH ratio (Fig. 2B and C). Intracellular ATP content depended on the phase of growth: during exponential growth, the ATP content increased slightly, reaching a maximum at the onset of the stationary phase. During the cell death phase, ATP concentration decreased, indicating the decline in cellular activity and viability (Fig. 3A).

3.1.2 Enzyme activities of central metabolism pathways

Enzymes of the main metabolic pathways were selected for analysis on the basis of (i) their relevance for flux control or (ii) as markers for the pathways.

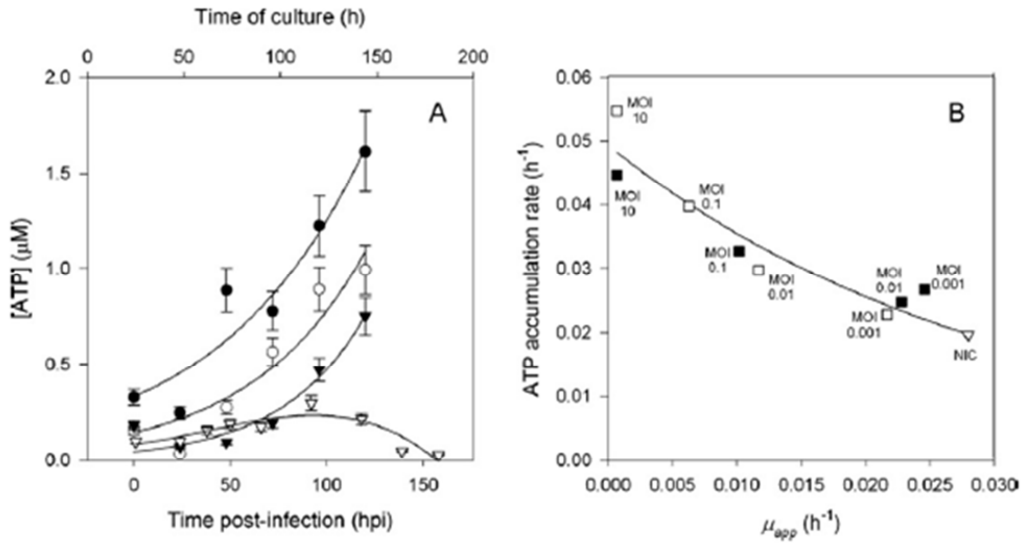

Figure 3. Effect of infection on the cellular ATP content. (A) Intracellular ATP levels in Sf9 cells infected at MOI 10 (black circles), 0.1 (white circles), 0.001 (black triangles) pfu cell^{-1}. Non-infected cells (white triangles) are shown for comparison. Infections were performed at 1×10^6 cells mL^{-1} (CCI 1) as explained in the Section 2. **(B)** Correlation between the apparent cellular growth rate (μ_{app}) and the ATP specific accumulation rate in insect cells. Data for non-infected cells (triangle) and cells infected at CCI 1 (white squares) and CCI 3 (black squares) are shown. At each CCI, infections were performed at four different MOIs (0.001, 0.01, 0.1 and 10 pfu mL^{-1}), as indicated in the figure. See the text for details.

The cytosolic isozyme is involved in the production of NADPH while mitochondrial isozymes are players in the TCA cycle (Caspi et al., 2008; Vriezen and van Dijken, 1998b). In Sf9 cells, we only detected the NADP$^+$-dependent ICDH activity, which in mammalian tissues has an important role in supplying NADPH for cholesterol and fatty acid synthesis and desaturation and for the regeneration of antioxidants, slowing oxidative damage and cellular aging processes (Jennings et al., 1994). On the other hand, activities of nitrogen metabolism enzymes (with the exception of AspAT, Fig. 4F) increased along culture, indicating the up-regulation of amino acid catabolism

(Fig. 4G–J). Low levels of GOGAT and GDH were detected during the culture. Two GDH activities with different cofactor specificities were detected. Under all conditions tested, their profiles run parallel meaning that, either (i) these are two different enzymes which are co-ordinately regulated or (ii) this is a single enzyme with broad cofactor specificity. GLNase activity is not shown due to the high variability observed. MDH and AspAT activities have to be considered apart since, besides being involved in the TCA cycle and amino acid metabolism, respectively, they are also part of the malate–aspartate shuttle. Thus, the activities analyzed correspond to the pool of both mitochondrial and cytosolic isozymes.

3.2 Metabolic burden in baculovirus infected Sf9 cells

In order to further explore the interplay of infection and cell density, Sf9 cells were infected using a recombinant baculovirus (VP39-EGFP) at several CCIs and MOIs. The uptake and production of the main metabolites was followed along infections (Table 1). The kinetics of baculovirus replication was in accordance with previous reports (Carinhas et al., 2009) (Table 2).

Table 1. Metabolism of S. frugiperda Sf9 cells during batch culture and when infected with baculovirus.

	Non-infected cells[a]	Baculovirus infected cells		
		CCI 1, MOI 5[b]	CC1 1 MOI 0.1[b]	CCI 3, MOI 0.1[b]
Glucose	-70.11	-79.2	-39.51	-26.84
Maltose	-9.53	-4.78	-18.02	-8.12
Sucrose	-10.44	-10.2	-0.71	-3.65
Lactate	-0.11	1.66	0.11	-0.61
Glutamine	-33.11	-5.64	-9.21	-5.06
Glutamate	-15.57	-1.8	-7.66	-2.59
Alanine	14.08	31.28	16.44	17.32
h^{-1}	0.027	0.01	0.009	0.006

Specific rates of production/consumption of glucose, maltose, sucrose, lactate, glutamine, glutamate, aspartate and alanine were determined for non-infected (control) cells and cells infected at two MOIs (5 and 0.1 infectious particles/cells). The rates are expressed as nmol $(10^6$ cells $h)^{-1}$. See the Section 2 for details. [a]Data refer to exponentially growing cells (cell density 1–2 × 10^6 cells mL^{-1}); [b]Rates calculated considering the data within the 0–72 hpi interval.

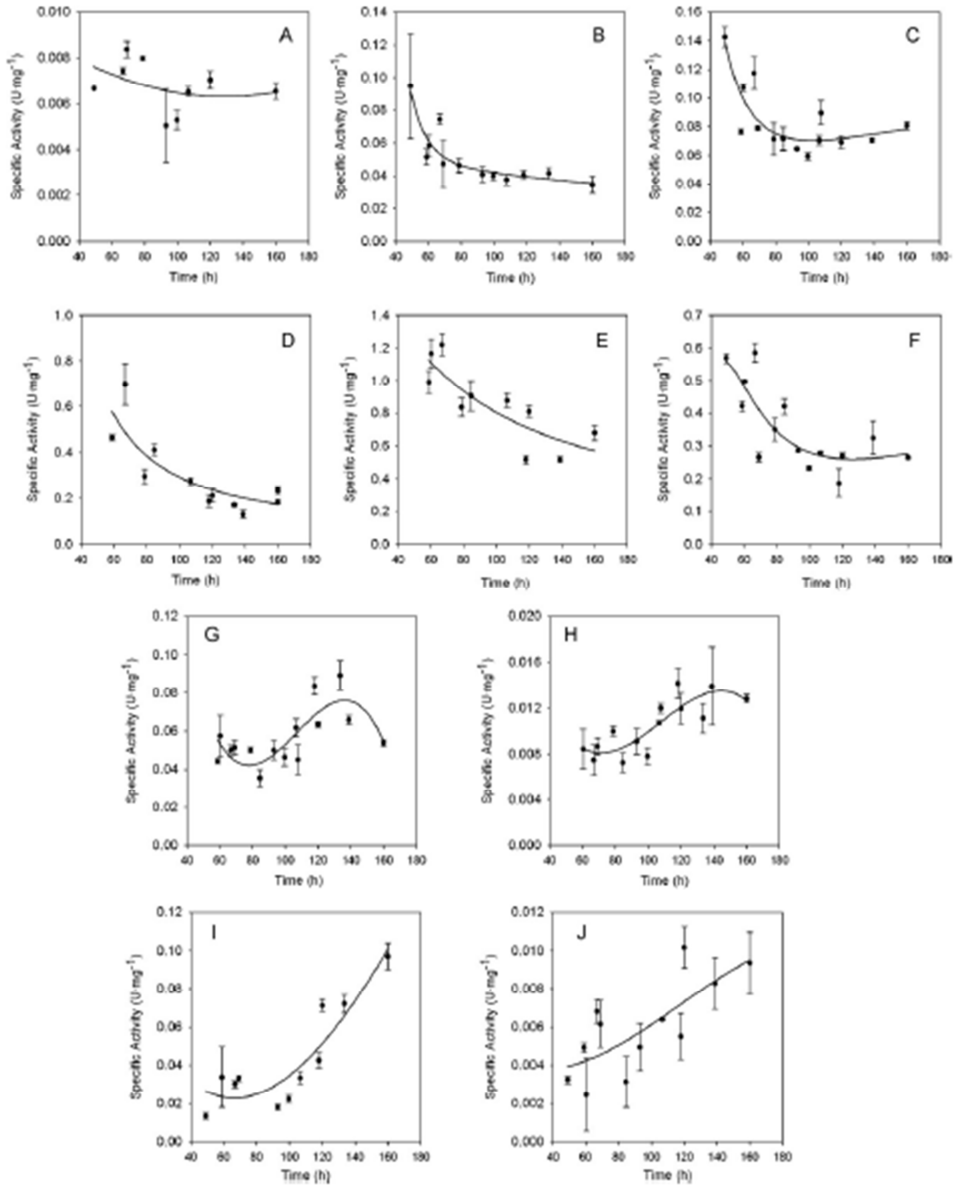

Figure 4. Enzyme activity profiles of batch-cultured Sf9 cells. (A) hexokinase, **(B)** NADP+-dependent isocitrate dehydrogenase, **(C)** glucose-6-phosphate dehydrogenase, **(D)** lactate dehydrogenase **(E)** malate dehydrogenase, **(F)** aspartate aminotransferase **(G)** alanine aminotransferase, **(H)** NADH-dependent glutamate synthase (GOGAT), **(I)** NADH- dependent glutamate dehydrogenase and (J) NADPH-dependent glutamate dehydrogenase. Experiments were performed in SF900II serum free medium in bioreactors with dissolved oxygen controlled at 30%. Samples were withdrawn from the cultures at different cell densities; enzymes were extracted and assayed as explained in Section 2. All enzyme activities are shown in U mg total protein^{-1} (equivalent to □moles of substrate (min mg total protein)$^{-1}$).

3.2.1 Redox and energy cofactors

To characterize the effect of infection on the redox and energy state of cells, several experiments were performed at different MOIs and CCIs. The redox state of the cells was affected by the strategy of infection. Intracellular NAD(H) levels increased after infection at both cell densities and specially when the infection was performed at low MOI, reaching a higher content per cell.

Table 2. Summary of baculovirus production indicators for different cell concentrations at infection (CCIs) and multiplicities of infection (MOIs).

MOI	CCI (cells.mL-1)	Virus titer (10^7 pfu.mL^{-1})	Specific yield (pfu.cell^{-1})	Virus amplification factor[a]
Low (0.1)	1 x 10^6	2.9	23	290
	3 x 10^6	2.5	8.7*	83
High (5)	1 x 10^6	6.1	45	12

[a]Ratio between the virus produced (virus titer) and the virus used at infection (CCI × MOI). Experiments were performed in a Braun B bioreactor, as explained in the Section 2. *p < 0.01 (compared to low MOI, CCI 1 × 10^6 cells mL^{-1}).

However, the NAD^+/NADH ratio, which is an indicator of the redox state of the cells, was similar to that of non-infected cells (Table 3), except when the infection was performed at CCI 3. On the other hand, both $NADP^+$ and NADPH increased after infection. The total NADP(H) content in infected cells depended on both the cell concentration at infection and the MOI used: when the infections were performed at high MOI, the total NADP(H) content and the $NADP^+$/NADPH ratios were higher.

The cellular ATP content increased steeply after infection. Several infections were performed at different MOIs (10, 0.1 and 0.001) and at two CCIs (1 and 3×10^6 cells mL^{-1}), demonstrating that the effect depended on infection kinetics, being faster at high MOIs (when all cells are synchronously infected) (Fig. 3A). A significant effect of CCI on ATP accumulation was not be observed, since it occurred at both CCIs. More likely, the steep increase in ATP cellular content was due to the arrest of cell cycle

caused by baculovirus infection and the consequent slow down in the apparent cellular division rate (Fig. 3B).

Table 3. Intracellular concentration of redox nucleotides and redox ratios of S. frugiperda Sf9 cells.

	Non-infected cells	Infected cells			
		CCI 1			CCI 3
MOI (pfu.cell^{-1})	*N.A.*	10	0.1	0.001	0.1
[NAD$^+$] (nmol.10^{-6}cell)	632±59	419±13	486±25	642±2	1337±34
[NADH] (nmol.10^{-6}cell)	42±8	29±1	41±9	53±6	52±13
Total *per cell* NAD(H) content (nmol.10^{-6}cell)	674±67	448±13	528±34	695±8	1389±67
[NAD$^+$]/[NADH]	15.6±3.8	14.7±0.4	12.0±2.3	12.1±1.2	26.5±5.6**
[NADP$^+$] (nmol.10^{-6}cell)	109±13	205±2	150±18	133±10	207±8
[NADPH] (nmol.10^{-6}cell)	72±3	169±7	162±9	147±1	151±30
Total *per cell* NADP(H) content (nmol.10^{-6}cell)	181±16	374±8	312±27	280±11	358±38
[NADP$^+$]/[NADPH]	1.5±0.2	1.2±0.0	0.9±0.1	0.9±0.1	1.4±0.2*

Experiments were performed in spinner flasks as explained in the text. For proper comparison, data for non-infected cells correspond to exponentially growing cells and for cells infected with VP39-GFP recombinant baculovirus data refer to 72 hpi. N.A.- Not Applicable. *p<0.05 (compared to MOI=0.1pfu.cell^{-1}, CCI=1×10^6 cells.mL^{-1}); **p<0.01 (compared to MOI=0.1pfu.cell^{-1}, CCI=1×10^6 cells.mL^{-1}).

3.2.2 Enzyme activities of central metabolism pathways

In order to disclose the effects of cell growth and infection on the enzyme activities of Sf9 cells, three experimental conditions were compared: low cell density (1×10^6 cells mL^{-1}) at low and high MOI (0.1 and 5 pfu cell^{-1}) and high cell density (3×10^6 cells mL^{-1}) at low MOI (0.1 pfu cell^{-1}). In Fig. 5, enzyme activities of infected cells are presented. The variability observed in the 0 hpi data are due to slight differences in the time of infection, and were especially important in the cultures infected at low cell density (1–1.5×10^6 cells mL^{-1}), since these cells were undergoing fast changes, as previously explained. In general, enzyme activities decreased upon infection; HexK and ICDH activities were similar to those of non-infected (control) cultures. More drastic changes were observed in G6PDH, LDH, MDH, AlaAT, AspAT

and GOGAT, which decreased markedly after infection below the levels in non-infected cultures (Fig. 5).

Contrary to what was observed with cell density, AlaAT and GOGAT (nitrogen metabolism enzymes) were down-regulated in infected cells, reflecting the decreased uptake of amino acids after infection (Bernal et al., 2009). More intriguing was the MOI-dependent increase observed in the GDH activities (Fig. 6). For the high MOI experiments, maximum activity levels were observed at 24 hpi, while at low MOI the peak in the activity was attained at 48 hpi or later, due to asynchronous infection. Importantly, although this observation seems to underline the relevance of amino acid metabolism in baculovirus-infected cells, the up-regulation was not followed by a significant increase in the glutamate uptake rate post-infection (Table 1).

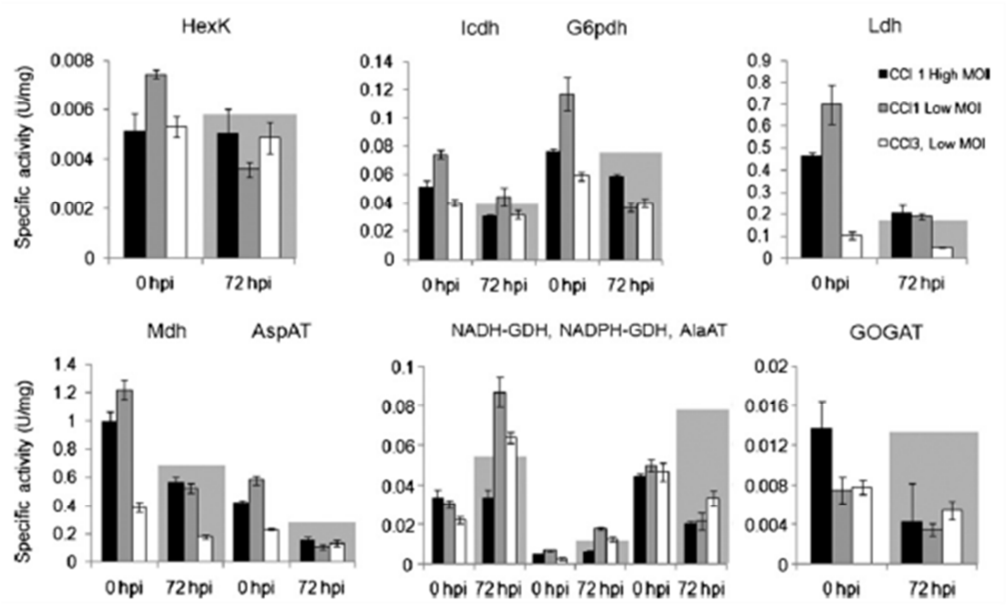

Figure 5. Effect of baculovirus infection on the enzyme activity profile of Sf9 cells. In order to assess the effect of infection on the metabolism of Sf9 cells, enzyme activities at 0 hpi (control, sample taken just before infection) and 72 hpi (once all cell population is infected and before cellular viability dropped below 80%) are shown. Cells were infected at CCI 1 with high and low MOI (5 and 0.1 pfu.cell^{-1}, respectively) and at CCI 3 with low MOI (0.1 pfu.cell^{-1}). All enzyme activities are shown in U.mg.total protein^{-1} (μmol.(min.mg.total.protein)$^{-1}$). Shaded boxes are the reference levels for each enzyme activity in non-infected cells. See the text for details.

3.3 Enzyme activities and fluxes in Sf9 cells

Enzyme activities determined under optimal in vitro conditions can be considered as the maximum possible fluxes through given metabolic pathways. All activities measured were high enough to support the metabolic fluxes estimated. In fact, almost all fluxes were much lower than the corresponding enzyme activities, both in infected and in non-infected cells (Table 4). Especially interesting is the case of LDH, which activity largely exceeded in vivo flux in both infected and non-infected cells. This enzyme is responsible for lactate formation from pyruvate, which is negligible in oxygen controlled cultures. When comparing different culture phases and/or infected/non-infected cells, the differences in the fluxes are larger than those observed on the enzymes. This indicates that flux regulation is only partially exerted

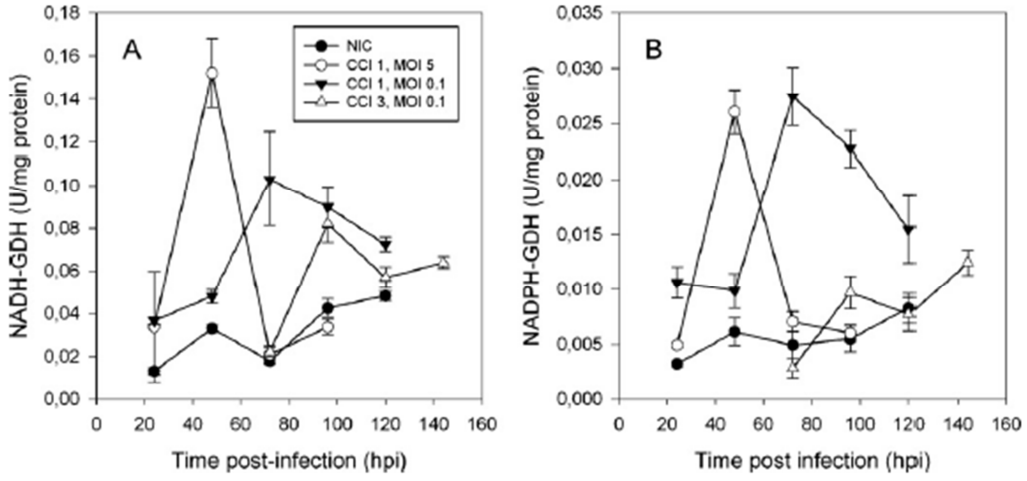

Figure 6. Effect of baculovirus infection on the (A) NADH and (B) NADPH-dependent glutamate dehydrogenase (NAD(P)H-GDH) enzyme activity profiles of Sf9 cells. Cells were infected at CCI 1 with high and low MOI and at CCI 3 with low MOI as explained in the text. Low and high MOI experiments were performed at 0.1 and 5 pfu $cell^{-1}$, respectively. Experiments were performed in SF900II serum free medium with dissolved oxygen controlled at 30%. Samples were withdrawn from the cultures at different times post-infection and enzymes were extracted and assayed as explained in the Section 2. All enzyme activities are expressed in U mg total $protein^{-1}$ (μmol (min mg total $protein)^{-1}$).

by enzyme synthesis and/or degradation, and largely occurs within the constraints of the existing set of proteins/enzymes (Stansfield et al., 2007; Vriezen and van Dijken, 1998a), through the alteration of the kinetics of individual reactions or reaction networks. This type of control is advantageous for the cells, since allows rapid responses to face changes in the environment. Similar results have been observed by other authors (Korke et al., 2004; Seow et al., 2001; Vriezen and van Dijken, 1998a). On the other hand, HexK and ICDH flux to enzyme activity ratios were close to one in non-infected cells, meaning that these are likely to be flux controlling steps, as previously proposed (Neermann and Wagner, 1996; Vriezen and van Dijken, 1998a). In baculovirus-infected Sf9 cells, HexK was the main controlling enzyme (Table 4).

Table 4. Ratios[a] between enzyme activities and estimated metabolic fluxes in control and baculovirus-infected Sf9 cells.

	Non-infected cells[b]		Baculovirus infected cells[c]		
	Low cell density	High cell density	CCI 1 MOI 5	CCI 1 MOI 0.1	CCI 3 MOI 0.1
HexK	<1	1	<1	1	1
G6PDH	63	221	233	347	471
ICDH	1	2	1	4	3
MDH	14	39	15	68	27
LDH	7570	15,295	891	24.953	838
AlaAT	5	14	4	11	14
AspAT	95	134	61	313	170
NADH-GDH[d]	16	61	990	132	101
NADPH-GDH[d]	2	7	169	28	15
NADH-GOGAT	2	8	4	12	9

To determine the influence baculovirus infection at different cell densities, the cells were infected at low and high cell concentrations and with two MOIs. See the text for detail;.[a]In order to calculate the ratios, both enzyme activities and fluxes were expressed in nmol.(10^6 cell.h)$^{-1}$. Protein content *per* 10^6 cells was determined for each condition. Enzyme activities are average values for the time intervals in which fluxes were determined; [b]Data refer to exponentially growing cells (cell density 1–2 × 10^6 cells.mL^{-1}); [c]Data refer to the 0–72 hpi interval; [d]Both NADH and NADPH-dependent reactions are referred to the total GDH flux.

4. Discussion

Reports on the integrated analysis of the metabolism of animal cell-based bioprocesses are scarce, especially in the case of insect cells. In this paper, enzyme activities, fluxes and cellular cofactors are analyzed for the first time in insect cells during batch cultures and after infection, providing useful information on the most relevant scenarios for bioprocesses and a further understanding of the alterations caused by the interplay of viral and host cell machineries. Metabolic differences between various mammalian and insect cell lines have been analyzed, including the enzymes of central metabolism (Neermann and Wagner, 1996). Enzymes have also been analyzed in bioprocess-relevant mammalian cell lines, such as myeloma (Vriezen and Van Dijken, 1998a) and Madin–Darby Canine Kidney (MDCK) cells (Ritter et al., 2010). In insect cells, nitrogen metabolism has attracted special attention (Doverskog et al., 2000; Drews et al., 2000; Ferrance et al., 1993). All these works are in close agreement with enzyme activities reported here for Sf9 cells. For certain enzymes (such as ICDH, G6PDH, AspAT and GDH) activities in mammalian and insect cells are similar. Significant differences are observed for HexK and LDH, which are 10- and 5-fold higher, respectively, in mammalian cells, which is in agreement with the higher rates of glucose consumption and lactate production(Janke et al., 2010; Neermann and Wagner, 1996). On the other hand, the 10-fold higher AlaAT activity in Sf9 cells correlates with the high alanine production rates for ammonia detoxification (Bernal et al., 2009). Historically, it has been general practice to measure enzyme activities under non-physiological conditions, since this allows attaining increased assay sensitivity (Janke et al., 2010; Vriezen and van Dijken, 1998a). A number of Systems Biology Consortia are working on the definition of standardized assays for enzyme activities determination mimicking intracellular conditions. These assays should be specifically defined for different strains/cell lines, cultivation conditions or cellular compartments. In addition, in vivo, metabolites and cofactors are bound to proteins, and enzymes are in a crowded environment, which may affect protein–protein interactions and, thereby, their activities, hindering the

extrapolation of in vitro activities to in vivo conditions (Van Eunen et al., 2010). In order to determine their relevance for the physiologic state of cells, enzyme activities were compared with the corresponding fluxes. Previous works had already reported that HexK and ICDH are flux controlling steps of the glycolysis (Janke et al., 2010; Neermann and Wagner, 1996) and the TCA cycle (Vriezen and Van Dijken, 1998a), respectively, in certain mammalian and insect cell lines. The enzyme to flux ratios determined confirm their importance in Sf9 cells (Table 4). All other enzyme activities determined were more than enough to support the fluxes calculated. Therefore, data here presented are physiologically relevant and support the robustness of the methodology to give a snapshot of the main metabolic features of a cell line in culture. Interesting features of insect cells' metabolism can be inferred from enzyme profiles. During a batch culture, nutrient concentrations change over time, therefore affecting the enzyme dynamics (Fig. 4). Results point to the lower activity of energy metabolism and a higher catabolism of amino acids as cell culture progresses, even before any nutrient reached a limiting or inhibitory concentration. This correlates with the so-called "cell density effect", which is responsible for the decreased production of baculoviruses and recombinant proteins in insect cells infected at high cell concentrations (Bernal et al., 2009; Carinhas et al., 2009). Upon infection, baculovirus machinery represses the expression of host cell genes (Palomares et al., 2006) and a decrease in the levels of many enzyme activities of central metabolism could be expected. The activities of flux-controlling HexK and ICDH remained close to those of non-infected cells, underlining their importance for maintaining the energetic state of infected insect cells (Bernal et al., 2009).The more drastic changes were observed for MDH and AspAT (involved in the TCA cycle and amino acids catabolism, respectively, and in the malate–aspartate shuttle) and G6PDH (related to NADPH production). It has to be underlined that fluxes may be underestimated, since MFA cannot identify absolute fluxes in parallel and cyclic pathways using solely extracellular metabolite balances (Carinhas et al., 2010; Maier et al., 2008). This underestimation might be especially relevant for the pentose phosphate pathway

upon up-regulation of NADPH-requiring processes (such as nucleotide synthesis and/or dealing with oxidative stress).

The most striking effect was observed in GDH, which increased during batch culture progression (Fig. 4I and J) and, especially, following infection (Fig. 6). Amino acids metabolism occurred fundamentally through the GOGAT/AlaAT pathway in rapidly growing cells, while GDH/AlaAT predominated in the stationary phase and after infection. The up-regulation of GDHs during infection might help to maintain the pool of α-ketoglutarate, an anaplerotic molecule, therefore contributing to maintain the post-infection energetic status of cells. Baculovirus replication is highly dependent on the energetic state of the cells and increases upon culture supplementation with α-ketoglutarate and pyruvate (Bernal et al., 2009; Carinhas et al., 2010), which further supports this hypothesis.

Altogether, this suggests that GDH activity might be regulated by cell growth; in fact, the cell cycle dependence of amino acid transport in animal cells has been previously reported (Bussolati et al., 1996; Doverskog et al., 1997). It has been recently reported that GDH activity is enhanced by sirtuin proteins in mammalian cells in order to increase ATP production upon nutrient starvation/ deprivation. Sirtuins are key players in signaling related to stress resistance and energy metabolism (Finkel et al., 2009; Lombard et al., 2007; Schlicker et al., 2008). Therefore, it seems likely that GDH has a conserved role in the cellular general metabolic response to stress.

Redox ratios are frequently estimated by considering equilibrium marker reactions for the different cellular compartment (Williamson et al., 1967; Zupke et al., 1995). For instance, lactate and pyruvate are frequently used to estimate the cytosolic NAD^+/NADH ratio. Cytosolic and mitochondrial NAD^+/NADH ratios are extremely different as a result of mitochondrial compartmentalization (e.g. 725 and 8 in the cytosol and mitochondria of rat liver, respectively), and the free and protein-bound nucleotide ratios differ (Williamson et al., 1967). The experimentally determined NAD^+/NADH ratios reported in this work (Table 3) are whole cell averages, not

accounting for differences between compartments nor between the protein-bound and free pools. These ratios are in good agreement with those reported previously by other authors (Queval and Noctor, 2007; Xie et al., 2009). Moreover, different redox ratios were determined in cells infected at low and high CCIs (Table 3). The effect of baculovirus infection on the redox state of cells (Wang et al., 2001) and on the productivity of the BEVS (Vieira et al., 2006) has been previously demonstrated. Our current knowledge does not allow drawing new conclusions on this effect and further research is needed to unveil the redox state changes in baculovirus infected cells.

Unlike mammalian cells, glucose is significantly metabolized through the TCA cycle in Sf9 cells, determining high ATP production rates (Bernal et al., 2009; Neermann and Wagner, 1996). Moreover, a linear relationship between ATP production and growth has been described in hybridoma (Xie and Wang, 1994), while ATP production is uncoupled from growth in infected Sf9 cells (Bernal et al., 2009; Carinhas et al., 2010). Accumulation of ATP has already been described in infected insect cells (Cruz et al., 1999; Olejnik et al., 2004). Olejnik et al. proposed ATP accumulation as a way to monitor protein production and the progress of infection. However, these authors failed to observe that ATP also accumulates in cells infected at high CCIs, despite the low productivities associated to these conditions. In this work, we have demonstrated that ATP accumulation is MOI-dependent and correlates with apparent growth rate (Fig. 3). Thus, accumulation probably occurs due to unbalanced production/consumption in cell cycle arrested cells, reflecting the de-regulation caused by infection. Infection has an important impact on the energetic state of cells (Burgener et al., 2006; Munger et al., 2008; Ritter et al., 2010). MFA based calculations suggested that ATP needs for virus synthesis do not exceed 2% of the total ATP turnover during the stationary cell growth phase (Sidorenko et al., 2008; Wahl et al., 2008). Therefore, these changes do not stem from the metabolic burden imposed by virus replication but, rather, from cytopathic effects, such as the induction of anti-viral mechanisms or the onset of virus-induced apoptosis (Ritter et al., 2010) or from the need to deal with oxidative stress related to baculovirus

infection (Vieira et al., 2006; Wang et al., 2001). A further analysis of post-infection mechanisms in the baculovirus insect cells system is needed.

5. Conclusions

The combined analysis of enzyme activities, cofactors and metabolic fluxes allowed us to determine flux controlling steps in the metabolism of insect cells. Hexokinase and isocitrate dehydrogenase activities are control points in the metabolism of Sf9 cells. Carbon and nitrogen pathways are differently regulated, and both are altered by infection. The energetic state of the cells is importantly altered following infection as a consequence of (i) growth arrest, (ii) changes in fluxes and (iii) the consequent metabolic burden imposed. These observations substantiate the importance of the different cofactors pools to define the cell state and, ultimately, bioprocess performance. Finally, this work allowed us to shed further light on the main constraints that the metabolism imposes on the performance of the BEVS.

6. Acknowledgments

This work was partially supported by the European Project BACULOGENES (FP6 LHSB-CT-2006-037541) and CLINIGENE-NoE (FP6 LSHB-CT-2004-018933). Vicente Bernal holds a post-doctoral research contract funded by the Saavedra Fajardo Program (Fundación Séneca-Murcia, Spain). Nuno Carinhas holds a PhD fellowship from Fundac¸ ão para a Ciência e a Tecnologia (FCT, Portugal) (SFRH/BD/36676/2007). The authors are thankful to A. L. Simplício (ITQB, Portugal) for her advice with HPLC analysis and to K. Airenne (University of Kuopio, Finland) for the kind gift of the recombinant baculovirus.

7. Author contribution

Francisca Monteiro participated in the experimental setup and design, performed part of the experiments, analyzed the data and wrote the chapter.

8. References

Altamirano, C., Cairó, J. J., and Gòdia, F. (2001). Decoupling cell growth and product formation in Chinese hamster ovary cells through metabolic control. *Biotechnology and Bioengineering* 76, 351–360.

Bernal, V., Carinhas, N., Yokomizo, A. Y., Carrondo, M. J. T., and Alves, P. M. (2009). Cell density effect in the baculovirus-insect cells system: a quantitative analysis of energetic metabolism. *Biotechnology and bioengineering* 104, 162–80.

Bernal, V., Monteiro, F., Carinhas, N., Ambrósio, R., and Alves, P. M. (2010). An integrated analysis of enzyme activities, cofactor pools and metabolic fluxes in baculovirus-infected Spodoptera frugiperda Sf9 cells. *Journal of biotechnology* 150, 332–42.

Bernal, V., Sevilla, Á., Cánovas, M., and Iborra, J. L. (2007). Production of L-carnitine by secondary metabolism of bacteria. *Microbial Cell Factories* 6, 31.

Bonarius, H. P., Houtman, J. H., De Gooijer, C. D., Tramper, J., and Schmid, G. (1998). Activity of glutamate dehydrogenase is increased in ammonia-stressed hybridoma cells. *Biotechnology and Bioengineering* 57, 447–453.

Burgener, A., Coombs, K., and Butler, M. (2006). Intracellular ATP and Total Adenylate Concentrations Are Critical Predictors of Reovirus Productivity From Vero Cells. *Biotechnology and Bioengineering*.

Bussolati, O., Uggeri, J., Belletti, S., Dall'Asta, V., and Gazzola, G. C. (1996). The stimulation of Na,K,Cl cotransport and of system A for neutral amino acid transport is a mechanism for cell volume increase during the cell cycle. *The FASEB journal official publication of the Federation of American Societies for Experimental Biology* 10, 920–926.

Carinhas, N., Bernal, V., Monteiro, F., Carrondo, M. J. T., Oliveira, R., and Alves, P. M. (2010). Improving baculovirus production at high cell density through manipulation of energy metabolism. *Metabolic engineering* 12, 39–52.

Carinhas, N., Bernal, V., Yokomizo, A. Y., Carrondo, M. J. T., Oliveira, R., and Alves, P. M. (2009). Baculovirus production for gene therapy: the role of cell density, multiplicity of infection and medium exchange. *Applied microbiology and biotechnology* 81, 1041–9.

Caspi, R., Foerster, H., Fulcher, C. A., Kaipa, P., Krummenacker, M., Latendresse, M., Paley, S., Rhee, S. Y., Shearer, A. G., Tissier, C., et al. (2008). The MetaCyc Database of metabolic pathways and enzymes and the BioCyc collection of Pathway/Genome Databases. *Nucleic Acids Research* 36, D623–31.

Charaniya, S., Karypis, G., and Hu, W.-S. (2009). Mining transcriptome data for function-trait relationship of hyper productivity of recombinant antibody. *Biotechnology and Bioengineering* 102, 1654–1669.

Cruz, H. J., Moreira, L., and Carrondo, M. J. T. (1999). Metabolic Shifts by Nutrient Manipulation in Continuous Cultures of BHK Cells. *Biotechnology and Bioengineering*.

Doverskog, M., Jacobsson, U., Chapman, B. E., Kuchel, P. W., and Häggström, L. (2000). Determination of NADH-dependent glutamate synthase (GOGAT) in Spodoptera frugiperda (Sf9) insect cells by a selective 1H/15N NMR in vitro assay. *Journal of biotechnology* 79, 87–97.

Doverskog, M., Ljunggren, J., Ohman, L., and Häggström, L. (1997). Physiology of cultured animal cells. *Journal of biotechnology* 59, 103–15.

Drews, M., Doverskog, M., Ohman, L., Chapman, B. E., Jacobsson, U., Kuchel, P. W., and Häggström, L. (2000). Pathways of glutamine metabolism in Spodoptera frugiperda (Sf9) insect cells: evidence for the presence of the nitrogen assimilation system, and a metabolic switch by 1H/15N NMR. *Journal of biotechnology* 78, 23–37.

Van Eunen, K., Bouwman, J., Daran-Lapujade, P., Postmus, J., Canelas, A. B., Mensonides, F. I. C., Orij, R., Tuzun, I., Van Den Brink, J., Smits, G. J., et al. (2010). Measuring enzyme activities under standardized in vivo-like conditions for systems biology. *The FEBS journal* 277, 749–760.

Ferrance, J. P., Goel, A., and Ataai, M. M. (1993). Utilization of glucose and amino acids in insect cell cultures: Quantifying the metabolic flows within the primary pathways and medium development. *Biotechnology and Bioengineering* 42, 697–707.

Finkel, T., Deng, C.-X., and Mostoslavsky, R. (2009). Recent progress in the biology and physiology of sirtuins. *Nature* 460, 587–591.

Henry, O., Perrier, M., and Kamen, A. (2005). Metabolic flux analysis of HEK-293 cells in perfusion cultures for the production of adenoviral vectors. *Metabolic Engineering* 7, 467–476.

Hirayama, C., and Nakamura, M. (2002). Regulation of glutamine metabolism during the development of Bombyx mori larvae. *Biochimica et Biophysica Acta* 1571, 131–137.

Irani, N., Wirth, M., Van Den Heuvel, J., and Wagner, R. (1999). Improvement of the primary metabolism of cell cultures by introducing a new cytoplasmic pyruvate carboxylase reaction. *Biotechnology and bioengineering* 66, 238–46.

Janke, R., Genzel, Y., Wahl, A., and Reichl, U. (2010). Measurement of key metabolic enzyme activities in mammalian cells using rapid and sensitive microplate-based assays. *Biotechnology and Bioengineering* 107, 566–581.

Jennings, G. T., Sechi, S., Stevenson, P. M., Tuckey, R. C., Parmelee, D., and McAlister-Henn, L. (1994). Cytosolic NADP(+)-dependent isocitrate dehydrogenase. Isolation of rat cDNA and study of tissue-specific and developmental expression of mRNA. *The Journal of Biological Chemistry* 269, 23128–23134.

Jones, J., Krag, S. S., and Betenbaugh, M. J. (2005). Controlling N-linked glycan site occupancy. *Biochimica et Biophysica Acta* 1726, 121–137.

Kantardjieff, A., Jacob, N. M., Yee, J. C., Epstein, E., Kok, Y.-J., Philp, R., Betenbaugh, M., and Hu, W.-S. (2010). Transcriptome and proteome analysis of Chinese hamster ovary cells under low temperature and butyrate treatment. *Journal of biotechnology* 145, 143–59.

Kim, E. J., Kramer, S. F., Hebert, C. G., Valdes, J. J., and Bentley, W. E. (2007). Metabolic Engineering of the Baculovirus- expression System via Inverse "'Shotgun'" Genomic Analysis and RNA Interference (dsRNA) Increases Product Yield and Cell Longevity. *Biotechnology and Bioengineering* 98, 645–654.

Klamt, S., Stelling, J., Ginkel, M., and Gilles, E. D. (2003). FluxAnalyzer: exploring structure, pathways, and flux distributions in metabolic networks on interactive flux maps. *Bioinformatics (Oxford, England)* 19, 261–269.

Korke, R., Gatti, M. D. L., Lau, A. L. Y., Lim, J. W. E., Seow, T. K., Chung, M. C. M., and Hu, W.-S. (2004). Large scale gene expression profiling of metabolic shift of mammalian cells in culture. *Journal of Biotechnology* 107, 1–17.

Kukkonen, S., Airenne, K., Marjomaki, V., Laitinen, O., Lehtolainen, P., Kankaanpaa, P., Mahonen, A., Raty, J., Nordlund, H., Oker-Blom, C., et al. (2003). Baculovirus capsid display: a novel tool for transduction imaging. *Molecular therapy the journal of the American Society of Gene Therapy* 8, 853–862.

Lee, Y. Y., Wong, K. T. K., Nissom, P. M., Wong, D. C. F., and Yap, M. G. S. (2007). Transcriptional profiling of batch and fed-batch protein-free 293-HEK cultures. *Metabolic Engineering* 9, 52–67.

Lombard, D. B., Alt, F. W., Cheng, H.-L., Bunkenborg, J., Streeper, R. S., Mostoslavsky, R., Kim, J., Yancopoulos, G., Valenzuela, D., Murphy, A., et al. (2007). Mammalian Sir2 Homolog SIRT3 Regulates Global Mitochondrial Lysine Acetylation. *Molecular and Cellular Biology* 27, 8807–8814.

Maier, K., Hofmann, U., Reuss, M., and Mauch, K. (2008). Identification of metabolic fluxes in hepatic cells from transient 13C-labeling experiments: Part II. Flux estimation. *Biotechnology and bioengineering* 100, 355–70.

Munger, J., Bennett, B. D., Parikh, A., Feng, X.-J., McArdle, J., Rabitz, H. A., Shenk, T., and Rabinowitz, J. D. (2008). Systems-level metabolic flux profiling identifies fatty acid synthesis as a target for antiviral therapy. *Nature Biotechnology* 26, 1179–1186.

Neermann, J., and Wagner, R. (1996). Comparative analysis of glucose and glutamine metabolism in transformed mammalian cell lines, insect and primary liver cells. *Journal of cellular physiology* 166, 152–69.

O'Callaghan, P. M., and James, D. C. (2008). Systems biotechnology of mammalian cell factories. *Briefings in functional genomics proteomics* 7, 95–110.

Olejnik, a M., Czaczyk, K., Marecik, R., Grajek, W., and Jankowski, T. (2004). Monitoring the progress of infection and recombinant protein production in insect cell cultures using intracellular ATP measurement. *Applied microbiology and biotechnology* 65, 18–24.

Palomares, L. A., Estrada-Moncada, S., and Ramirez, O. T. (2006). "Principles and applications of the insect cell-baculovirus expression vector system.," in Cell Culture Technology for Pharmaceutical and Cell Based Therapies, , eds. S. S. Ozturk and W. S. Hu (New York).

Peng, R.-W., and Fussenegger, M. (2009). Molecular engineering of exocytic vesicle traffic enhances the productivity of Chinese hamster ovary cells. *Biotechnology and Bioengineering* 102, 1170–1181.

Peng, X., Chan, E. Y., Li, Y., Diamond, D. L., Korth, M. J., and Katze, M. G. (2009). Virus-host interactions: from systems biology to translational research. *Current opinion in microbiology* 12, 432–8.

Queval, G., and Noctor, G. (2007). A plate reader method for the measurement of NAD, NADP, glutathione, and ascorbate in tissue extracts: Application to redox profiling during Arabidopsis rosette development. *Analytical Biochemistry* 363, 58–69.

Rhiel, M., Mitchell-Logean, C. M., and Murhammer, D. W. (1997). Comparison of Trichoplusia ni BTI-Tn-5B1-4 (high five) and Spodoptera frugiperda Sf-9 insect cell line metabolism in suspension cultures. *Biotechnology and Bioengineering* 55, 909–920.

Ritter, J. B., Wahl, A. S., Freund, S., Genzel, Y., and Reichl, U. (2010). Metabolic effects of influenza virus infection in cultured animal cells: Intra- and extracellular metabolite profiling. *BMC systems biology* 4, 61.

Rohrmann, G. F. (2008). *Baculovirus Molecular Biology*. Bethesda.

Roldão, A., Oliveira, R., Carrondo, M. J. T., and Alves, P. M. (2009). Error assessment in recombinant baculovirus titration: evaluation of different methods. *Journal of virological methods* 159, 69–80.

Schlicker, C., Gertz, M., Papatheodorou, P., Kachholz, B., Becker, C. F. W., and Steegborn, C. (2008). Substrates and regulation mechanisms for the human mitochondrial sirtuins Sirt3 and Sirt5. *Journal of Molecular Biology* 382, 790–801.

Seow, T. K., Korke, R., Liang, R. C., Ong, S. E., Ou, K., Wong, K., Hu, W. S., and Chung, M. C. (2001). Proteomic investigation of metabolic shift in mammalian cell culture. *Biotechnology Progress* 17, 1137–1144.

Shimizu, K. (2009). Toward systematic metabolic engineering based on the analysis of metabolic regulation by the integration of different levels of information. *Biochemical Engineering Journal* 46, 235–251.

Sidorenko, Y., Wahl, A., Dauner, M., Genzel, Y., and Reichl, U. (2008). Comparison of metabolic flux distributions for MDCK cell growth in glutamine- and pyruvate-containing media. *Biotechnology progress* 24, 311–20.

Stansfield, S. H., Allen, E. E., Dinnis, D. M., Racher, A. J., Birch, J. R., and James, D. C. (2007). Dynamic Analysis of GS-NS0 Cells Producing a Recombinant Monoclonal Antibody During Fed-Batch Culture. *Biotechnology and Bioengineering* 97, 410–424.

Stephanopoulos, G, Aristidou, A. A., and Nielsen, J. (1998). *Metabolic Engineering. Principles and Methodologies.* New York: Academic Press.

Thiem, S. M. (2009). Baculovirus genes affecting host function. *In vitro cellular & developmental biology. Animal* 45, 111–26.

Vester, D., Rapp, E., Gade, D., Genzel, Y., and Reichl, U. (2009). Quantitative analysis of cellular proteome alterations in human influenza A virus-infected mammalian cell lines. *Proteomics* 9, 3316–27.

Vieira, H. L. A., Estevao, C., Roldao, A., Peixoto, C. C., Sousa, M. F. Q., Cruz, P. E., Carrondo, M. J. T., and Alves, P. M. (2005). Triple layered rotavirus VLP production: Kinetics of vector replication, mRNA stability and recombinant protein production. *Journal of Biotechnology* 120, 72–82.

Vieira, H. L. A., Pereira, A. C. P., Carrondo, M. J. T., and Alves, P. M. (2006). Catalase effect on cell death for the improvement of recombinant protein production in baculovirus-insect cell system. *Bioprocess and Biosystems Engineering* 29, 409–414.

Vives, J., Juanola, S., Cairó, J. J., and Gòdia, F. (2003). Metabolic engineering of apoptosis in cultured animal cells: implications for the biotechnology industry. *Metabolic Engineering* 5, 124–132.

Vriezen, N., and Van Dijken, J. P. (1998a). Fluxes and enzyme activities in central metabolism of myeloma cells grown in chemostat culture. *Biotechnology and bioengineering* 59, 28–39.

Vriezen, N., and Van Dijken, J. P. (1998b). Subcellular localization of enzyme activities in chemostat-grown murine myeloma cells. *Journal of biotechnology* 61, 43–56.

Wahl, A., Sidorenko, Y., Dauner, M., Genzel, Y., and Reichl, U. (2008). Metabolic flux model for an anchorage-dependent MDCK cell line: characteristic growth phases and minimum substrate consumption flux distribution. *Biotechnology and bioengineering* 101, 135–52.

Wang, N., and Stephanopoulos, G. (1983). Application of macroscopic balances to the identification of gross measurement errors. *Biotechnology and Bioengineering* 25, 2177–208.

Wang, Y., Oberley, L. W., and Murhammer, D. W. (2001). Evidence of oxidative stress following the viral infection of two lepidopteran insect cell lines. *Free Radical Biology & Medicine* 31, 1448–1455.

Williamson, D. H., Lund, P., and Krebs, H. A. (1967). The redox state of free nicotinamide-adenine dinucleotide in the cytoplasm and mitochondria of rat liver. *The Biochemical journal* 103, 514–527.

Xie, L., and Wang, D. I. (1994). Applications of improved stoichiometric model in medium design and fed-batch cultivation of animal cells in bioreactor. *Cytotechnology* 15, 17–29.

Xie, W., Xu, A., and Yeung, E. S. (2009). Determination of NAD(+) and NADH in a single cell under hydrogen peroxide stress by capillary electrophoresis. *Analytical Chemistry* 81, 1280–1284.

Yallop, C. a, Nørby, P. L., Jensen, R., Reinbach, H., and Svendsen, I. (2003). Characterisation of G418-induced metabolic load in recombinant CHO and BHK cells: effect on the activity and expression of central metabolic enzymes. *Cytotechnology* 42, 87–99.

Zupke, C., Sinskey, A. J., and Stephanopoulos, G. (1995). Intracellular flux analysis applied to the effect of dissolved oxygen on hybridomas. *Applied Microbiology and Biotechnology* 44, 27–36.

Chapter III

METABOLIC FLUXES OF CULTURED HIGH FIVE CELLS: THE IMPACT OF CULTURE MEDIA AND BACULOVIRUS INFECTION

This chapter is based on data to be published as:

Metabolic fluxes of cultured High Five cells: the impact of culture media and baculovirus infection

Francisca Monteiro, Vicente Bernal, Paula M. Alves (*in preparation*)

Abstract

The Insect Cell-Baculovirus Expression Vector System (IC-BEVS) is widely used for the production of recombinant proteins for pre-clinical research and industrial vaccine manufacture. The combination of a tunable viral vector with the high productivities achieved in insect cells is a major driver for the success of this platform. Nonetheless, the knowledge on insect cells' physiology and their dynamics after infection is still scarce in what concerns the main physiological aspects that contribute to productivity. Metabolic Flux Analysis (MFA) is a well-established technique for the assessment of the metabolic adaptations undergone by any type of cell in culture. In the present work, the quantitative description of the energetic metabolism of High Five cells was performed during growth in different culture media and after baculovirus infection. The metabolic efficiency was directly correlated with the culture media used, since in High Five cultures performed in Insect Xpress media almost 90% of the glucose was channeled to the the TCA cycle to be oxidized, in opposition to only 60% when Sf900II media was used. The accumulation of by-products proved to be directly correlated with the specific consumption rate of carbon and nitrogen sources, thus higher for cultures in Sf900II. Following baculovirus infection in SF900II medium, the fluxes throughout the TCA cycle increased, which resulted in a boost in the energetic state of infected High Five cells, as reflected by the increase in the net ATP synthesis. The analysis of the metabolic adaptations undergone by High Five cells revealed important modulations of central carbon metabolism as a consequence of the culture media used. The strong correlation observed between the metabolic state of the cell with baculovirus infection indicates that there is room for improvement in the IC-BEVS system, paving the way for metabolic and bioprocess engineers to take part of such quest.

Contents

1. Introduction

For the past thirty years the Insect Cell-Baculovirus Expression System (IC-BEVS) has been exploited as a production platform of recombinant proteins with high value in industry and medicine (van Oers et al., 2015). Compared to other production systems, the IC-BEVS outstands given the versatility of the baculovirus vectors, combined with the robustness of insect cells in culture and the high productivities achieved (Assenberg et al., 2013). Moreover, insect cells are able to perform post-translational modifications and have a similar folding machinery to mammalian cells, which together with the efforts in tuning the baculovirus to express mammalian-like glycosylation profiles (Palmberger et al., 2013), empower the IC-BEVS as platform of choice for the production of human therapeutics. Although highly explored in industrial settings, the IC-BEVS is still poorly understood in what concerns the main physiological aspects of cultured insect cells.

Metabolism and productivity go alongside, the metabolic state of the host cell being critical to support highly productive bioprocesses. A common phenomenon to virus-based bioprocess is the so-called cell density effect, *i.e.*, the significant drop in cellular specific productivity when cells are infected at high cell densities. Insect cells are not an exception, and the probable causes for such phenomena have been a matter of extensive debate (Bhatia et al., 1996; Doverskog et al., 1997; Ikonomou et al., 2003; Palomares et al., 2006). Although no consensual explanation exists, the cell density effect has been associated with the down-regulation of central carbon metabolism, hindered metabolic activity and lower energy production (Bernal et al., 2009). Consequently, the biosynthetic processes associated with cell growth are slowed down, with a drop in mRNA levels, down-regulation of translation and protein synthesis, which culminates in humbler productivities (Carinhas et al., 2009; Huynh et al., 2013).

Trichoplusia ni derived BTI-Tn-5B1-4 (High Five) cells have been greatly exploited as production platforms of several recombinant proteins in BEVS given to their high productivities (Krammer et al., 2010; Palmberger et al., 2011; Wilde et al., 2014).

Although their widespread use, only few studies were performed to characterize the metabolism of High Five cells in culture (Bédard et al., 1993; Benslimane et al., 2005; Rhiel et al., 1997). Alanine is the main by-product of High Five metabolism, and its accumulation is directly correlated with the net consumption of glucose and glutamine from the culture media (Benslimane et al., 2005; Ikonomou et al., 2003; Rhiel et al., 1997). The production of high levels of lactate and ammonia was described in High Five cells, however this was dependent on the culture media used (Ikonomou et al., 2003; Rhiel et al., 1997). The above-mentioned studies pinpointed specific metabolic features of cultured High Five cells, and highlighted that different media compositions interfere with the metabolic activity of those hosts. However, the quantitative description of High Five cells metabolism is still lacking, thus the in-depth analysis of High Five cells metabolism in bioprocess relevant conditions is of noteworthy importance.

Metabolic models provide a global overview of the metabolic rearrangements that occur in a living cell, thus playing a major role in the contextualization and further interpretation of the physiological alterations that follow the bioprocess time-frame. The mathematical description of host cell metabolism can be achieved by Metabolic Flux Analysis (MFA), a well-established technique for the assessment of the metabolic adaptations undergone by any type of cell in culture. It makes use of stoichiometric analysis based on metabolite balancing, which retrieves the quantification of intracellular fluxes and their distribution within a network representative of the main cellular metabolic events (Stephanopoulos, G et al., 1998). The application of MFA to relevant industrial systems has retrieved noteworthy insights on host cell metabolism and production capabilities (Carinhas et al., 2013; Martínez et al., 2013; Niklas et al., 2013).

In the present work we implemented a metabolic network reflecting the main physiological peculiarities of the central pathways of carbon and nitrogen metabolism of High Five cells. MFA was performed during growth and after baculovirus infection, to give a comprehensive overview of the High Five fluxome in

both scenarios. Moreover, different culture media were used, and the effect of such distinct environments on the physiology of High Five cells was analyzed.

2. Materials and Methods

2.1 Cell lines and culture maintenance

Trichoplusia ni derived BTI-Tn-5B1-4 (High Five) was obtained from Invitrogen (Paisley, UK). The cells were maintained in serum- and protein-free Insect Xpress insect cell medium (Lonza, Basel, Switzerland) and Sf900II medium (Gibco, Glasgow, UK), and cultured in 500 mL Erlenmeyer flasks (Corning, USA) with 50 mL working volume. Cultures were kept in a humidified incubator operated at 90 rpm and at 27ºC. For maintenance, High Five cells were re-inoculated every 3-4 days at $0.3x10^6$ cells.mL^{-1}. Cell concentration was determined by hemocytometer cell counts (Brandt, Wertheinmain, Germany) and cell viability evaluated by the trypan blue exclusion method (Merck, Darmstadt, Germany).

2.2 Virus handling and viral stock preparation

The recombinant *Autographa californica* nucleopolyhedrovirus BvGCN4-NA1, kindly provided by Dr. Xavier Saelens (Ghent University, Belgium), contains an inserted gene encoding a secreted form of influenza N1 type neuraminidase under the control of the polyhedrin promoter (Deroo et al., 1996). BvGCN4-NA1 was used as the expression vector of recombinant Neuraminidase (rNeur) throughout the work. BvGCN4-NA1 was amplified by infecting Sf9 cells at $1x10^6$ cells.mL^{-1} with a MOI of 0.1 IP.$cell^{-1}$ (IP-Infectious baculovirus particles) in 500 mL Erlenmeyer flasks (Corning, USA).

2.3 Cell culture and Infections

Growth and infection studies were performed in 100 mL Erlenmeyer flasks (Corning, USA) with a working volume of 10 mL. High Five cells were inoculated at 0.4

x 10^6 cells.mL^{-1} and infected once they reached 1x10^6 cells.mL^{-1}. Two MOIs were used, namely 0.1, and 5 IP.cell^{-1}. Cultures were sampled every 12 to 24 hours to check for cell concentration, viability and metabolites quantification. Samples for the productivity assays were withdrawn at 48 hours post-infection (hpi).

2.4 Baculovirus titration

Baculovirus infectious particles titration was performed following the MTT assay as previously described in Roldão *et al*. (2009).

2.5 Quantification of Recombinant Neuraminidase

Recombinant Neuraminidase was quantified by a fluorimetric activity assay measuring the release of 4-methylumbelliferone (4-MU), as described in Deroo *et al.* (1996). rNeuraminidase activity assays were performed in culture supernatant samples. One unit was defined as the amount of enzyme that releases 1 µmol of 4-MU *per* minute.

2.6 Cell dry weight quantification

High Five cells were harvested at exponential growth phase and at 48 hpi in baculovirus infected cultures. Viable cell samples containing 10 x 10^6 cells were pelleted by centrifugation (300 xg, 10 minutes), and the cellular pellets were washed with phosphate buffer saline (PBS) buffer. The pellets were subsequently dried at 100ºC *O/N* and weighted in an analytical balance. The measurements were performed in triplicates.

2.7 Metabolite Analytical Methods

Glucose and lactate concentrations were determined using an YSI 7100 Multiparameter Bioanalytical System (YSI Life Sciencies, Dayton, OH). Ammonia was quantified enzymatically using a UV based kit (No. AK00091; NZYTech, Lisbon,

Portugal). Amino acids were determined by HPLC after derivatization using the AccQ-Tag Method (Waters, Milford, MA).

2.8 Metabolic Flux Analysis

2.8.1 Metabolic Network

The model describing the metabolic network of Sf9 cells (Bernal et al. 2009) was adapted to reflect the central carbon metabolism of High Five cells. Briefly, the model contains the main reactions of glycolysis, pentose phosphate pathway (PPP), tricarboxylic acids (TCA) cycle, amino acids metabolism and transport, energy production pathways, and biomass synthesis. Contrary to Sf9 cells, High Five cells do not possess NADH-dependent glutamate synthase (GOGAT) activity, thus this reaction was withdrawn from the model. Moreover, since we were not able to detect sucrose and maltose consumption in Insect Xpress media, the respective reactions of sucrose and maltose metabolism were not considered in the metabolic network. A complete list of the metabolic reactions considered in the model can be found in Appendix I (Table I-1).

In order to fit the model to High Five cells, the biomass and protein synthesis equations were calculated considering the cells dry weight during exponential growth and after baculovirus infection. Additionally, for the analysis of baculovirus infected cultures, the reactions of baculovirus and recombinant neuraminidase synthesis were also included (Appendix I, Table I-2). The detailed description of the biomass equations is provided in Appendix I (Tables I-3, I-4 and I-5).

2.8.2 Flux calculations

Two models were generated to consider High Five cells metabolism during growth and after baculovirus infection, respectively. The growth model totalizes 68 reactions with 50 internal (balanced) metabolites, defined by a 68 x 50 stoichiometric matrix. The infection model considers 73 reactions with 56 internal (balanced)

metabolites, described by a 73 x 56 stoichiometric matrix. The rank of the resulting stoichiometric matrices is 47 and 53, thus the number of degrees of freedom of the systems is 21 and 20, respectively. The balances of urea, mevalonate, ADP and ATP could not be closed since these metabolites participate in other reactions not considered in both metabolic networks. From the extracellular profiling, 23 and 25 exchange fluxes were experimentally determined, including the uptake/production rates of nutrients, cellular growth rate, baculovirus synthesis and rNeur formation, respectively. Also, the intracellular synthesis of lactate from pyruvate was set equal to the net lactate production rate. The resultant system of equations is over-determined, meaning that it is possible to compute all unknown rates, and redundant, with 3 redundant measurements. The system was solved by the weighted least squares method (Stephanopoulos, G et al., 1998). Overall, the carbon and nitrogen balances closed to an average of 94% and 90% in growth cultures, and 85% and 87% in infected cultures, respectively. Balanceable rates, which arise from system redundancy, were used to calculate the consistency index *h* (Wang and Stephanopoulos, 1983). Comparison of *h* with the χ^2 test function allows the evaluation of the consistency of the experimental data with the assumed biochemistry and the pseudo steady-state assumption. All computational tasks were performed using the FluxAnalyzer software (Ginkel et al., 2003).

3. Results

3.1 Growth profiles and productivity of High Five cells

High Five cells were cultured in Insect Xpress and Sf900II media, as detailed in the Materials and Methods section Their growth profile was monitored throughout culture time (Fig. 1). Cellular growth rate was 0.04 h^{-1} and 0.03 h^{-1} (Table 1) and the maximum cell density achieved was 5 x 10^6 cells.mL^{-1} and 4 x 10^6 cells.mL^{-1}, in cultures performed in Insect Xpress and Sf900II media, respectively (Fig. 1). The specific productivity of High Five cells was assessed in baculovirus infected cultures.

The titers of rNeur and baculovirus IPs were 2 to 3 times higher in cultures infected with the highest MOI (Fig. 2).

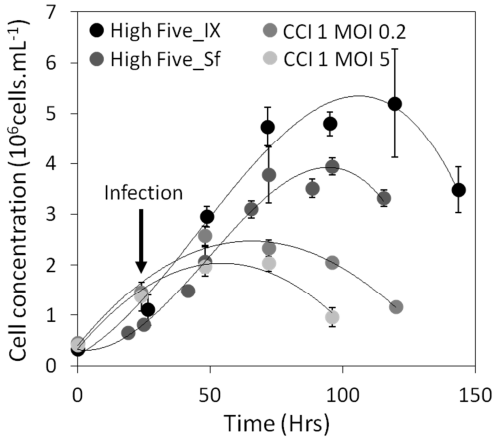

Figure 1. Growth profile of High Five cells during growth and after baculovirus infection. Cells were cultured in Insect Xpress (IX) and Sf900II (Sf) media; infections were performed at low and high MOI (0.2 and 5 IP.cell^{-1}, respectively), as explained in the Materials and Methods section. Error bars indicate the standard deviation of three independent biological replicates (n=3).

3.2 Metabolic features of growing and baculovirus infected High Five cells

The cellular specific rates of nutrient consumption and by-products formation were assessed throughout culture time. For growth experiments, the specific consumption and production rates were calculated considering two culture phases, early-mid and late exponential phases. For infected cultures, a single phase post-infection, from 0 to 48 hpi, was considered (Table 1).

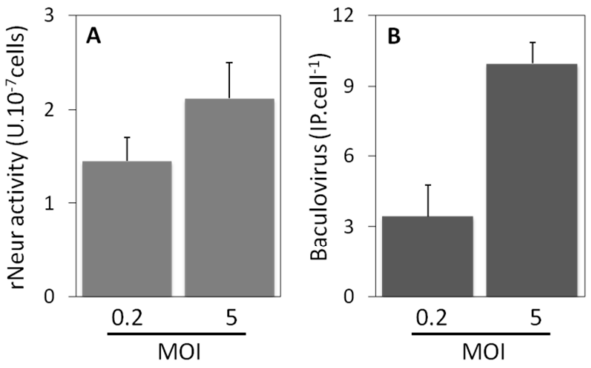

Figure 2. Specific yields of rNeuraminidase (A) and infectious baculovirus (B) in High Five cells. High Five cells were cultured in Sf900II media, and infected at MOI of 0.2 and 5 IP.mL^{-1} once they reached a cellular concentration of 1x10^6 cells.mL^{-1}. The quantification of rNeur and baculovirus IPs were performed in supernatant samples of infected cultures at 48 hpi, as detailed in the Materials and Methods section. Standard error reflects the standard deviation of the mean average of three independent biological replicates (n=3).

Although the specific uptake rate of glucose was similar in both culture media, the lactate production rate was 5 to 10 times higher in Sf900II cultures (Table 1).

Table 1. Specific consumption and production rates of High Five cells in different culture media after baculovirus infection

	High Five					
	Growth				Infection	
	Insect Xpress		Sf900II			
	Early-mid Exponential	Late Exponential	Early-mid Exponential	Late Exponential	CCI 1 MOI 0.2	CCI 1 MOI 5
	Rate ± SE	Rate ± SE	Rate ± SE	Rate ± SE	Rate ± SE	Rate ± SE
μ (h-1)	0.04 ± 0.0	0.01 ± 0.00	0.03 ± 0.00	0.01 ± 0.00	*N.A.*	*N.A.*
Glucose	-110.8 ± 3.5	-77.0 ± 9.5	-114.5 ± 5.2	-99.5 ± 6.5	-143.3 ± 5.4	-167.3 ± 23.2
Lactate	11 ± 0.6	2.5 ± 1.0	54.3 ± 10.0	28.4 ± 1.5	24.1 ± 2.7	86.1 ± 18.3
Aspartate	-35.1 ± 1.2	-10.1 ± 1.2	-4.0 ± 0.7	-5.6 ± 1.3	-24.0 ± 4.8	-22.7 ± 3.6
Glutamate	-28 ± 1.8	-5.9 ± 1.5	-26.0 ± 2.1	-11.4 ± 2.0	-8.7 ± 1.4	-40.2 ± 5.3
Serine	15.2 ± 2.6	2.4 ± 1.9	-6.0 ± 0.5	-4.8 ± 1.0	-3.2 ± 2.8	-21.1 ± 7.4
Asparagine	-94.7 ± 0.2	-12.6 ± 2.7	-126.9 ± 3.7	-40.4 ± 2.4	-80.2 ± 4.3	-116.9 ± 7.2
Glycine	-7.2 ± 0.9	0.9 ± 0.0	-9.7 ± 1.0	-4.4 ± 0.1	-5.2 ± 1.2	-3.1 ± 0.9
Glutamine	-31.5 ± 1.6	-10.3 ± 2.0	-47.9 ± 5.2	-24.7 ± 1.7	-59.4 ± 6.2	-73.0 ± 4.4
Histidine	-3.9 ± 1.2	-0.9 ± 0.2	-3.4 ± 0.6	-2.1 ± 0.2	-2.2 ± 0.4	-9.4 ± 0.0
Threonine	-7.4 ± 1.1	-2.7 ± 0.5	-2.8 ± 0.2	-4.2 ± 0.6	-8.4 ± 1.2	-16.6 ± 4.9
Arginine	-13.4 ± 0.4	-5.3 ± 0.4	-25.3 ± 5.5	-6.4 ± 0.9	-8.5 ± 0.6	-18.3 ± 6.3
Alanine	79 ± 17.1	14.8 ± 0.3	148.0 ± 7.1	16.0 ± 3.9	83.2 ± 8.3	107.1 ± 21.4
Proline	-13.3 ± 3.9	-3.7 ± 0.2	-11.5 ± 3.5	-3.7 ± 0.6	-13.3 ± 2.9	-20.5 ± 5.9
Tyrosine	-3.9 ± 0.7	-1.7 ± 0.3	-4.4 ± 0.8	-2.8 ± 0.2	-4.2 ± 1.0	-8.7 ± 2.9
Cysteine	*N.D.*	*N.D.*	*N.D.*	*N.D.*	-4.4 ± 0.3	-12.6 ± 3.8
Valine	-11.3 ± 4	-2.9 ± 0.1	-12.7 ± 3.3	-6.0 ± 0.5	-9.4 ± 2.2	-21.7 ± 6.2
Methionine	-12.4 ± 3.5	-0.9 ± 0.0	-5.5 ± 0.9	-5.1 ± 0.9	-6.9 ± 2.0	-22.5 ± 0.9
Isoleucine	-16.3 ± 1.2	-1.6 ± 0.1	-6.2 ± 1.3	-4.4 ± 0.3	-8.7 ± 2.1	-25.2 ± 1.2
Leucine	-11.4 ± 1.3	-4.4 ± 0.2	-12.0 ± 1.6	-7.9 ± 0.7	-13.4 ± 1.1	-23.9 ± 7.5
Lysine	-12.1 ± 3.6	-3.5 ± 0.1	-13.0 ± 2.6	-6.6 ± 0.8	-10.2 ± 1.6	-20.8 ± 5.3
Phenylalanine	-17 ± 2.9	-1.0 ± 0.1	-4.3 ± 1.2	-3.6 ± 0.4	-6.3 ± 1.9	-23.4 ± 1.4
Ammonia	102.4 ± 9.6	15.6 ± 0.4	132.1 ± 16.8	66.1 ± 7.4	81.4 ± 5.5	143.8 ± 9.1

Cultures were performed as described in the Materials and Methods section. Two culture phases were considered in growth cultures, early-to-mid and late exponential phases; a single phase after infection was considered (0-48 hpi); negative values indicate nutrient consumption. Rates are expressed in nmol.(10^6.cells.h)$^{-1}$; SE- Standard deviation of two independent replicates for Insect Xpress cultures, and three independent biological replicates for cultures performed in Sf900II media during growth and infection. N.D.- Not Determined, N.A.- Not Applicable.

Asparagine was the most consumed amino acid, being exhausted from the culture media after 72 to 96 hours in Insect Xpress and Sf900II cultures, respectively. Additionally, in cultures performed in Insect Xpress media, aspartate was highly consumed, which specific uptake rate was up to 9 times superior than in cultures

performed in Sf900II (Table 1). Comparing early-mid and late exponential phases, a net decrease in the consumption of glucose and amino acids was observed (6 and 2-fold in cultures performed in Insect Xpress and Sf900II, respectively) (Table 1).

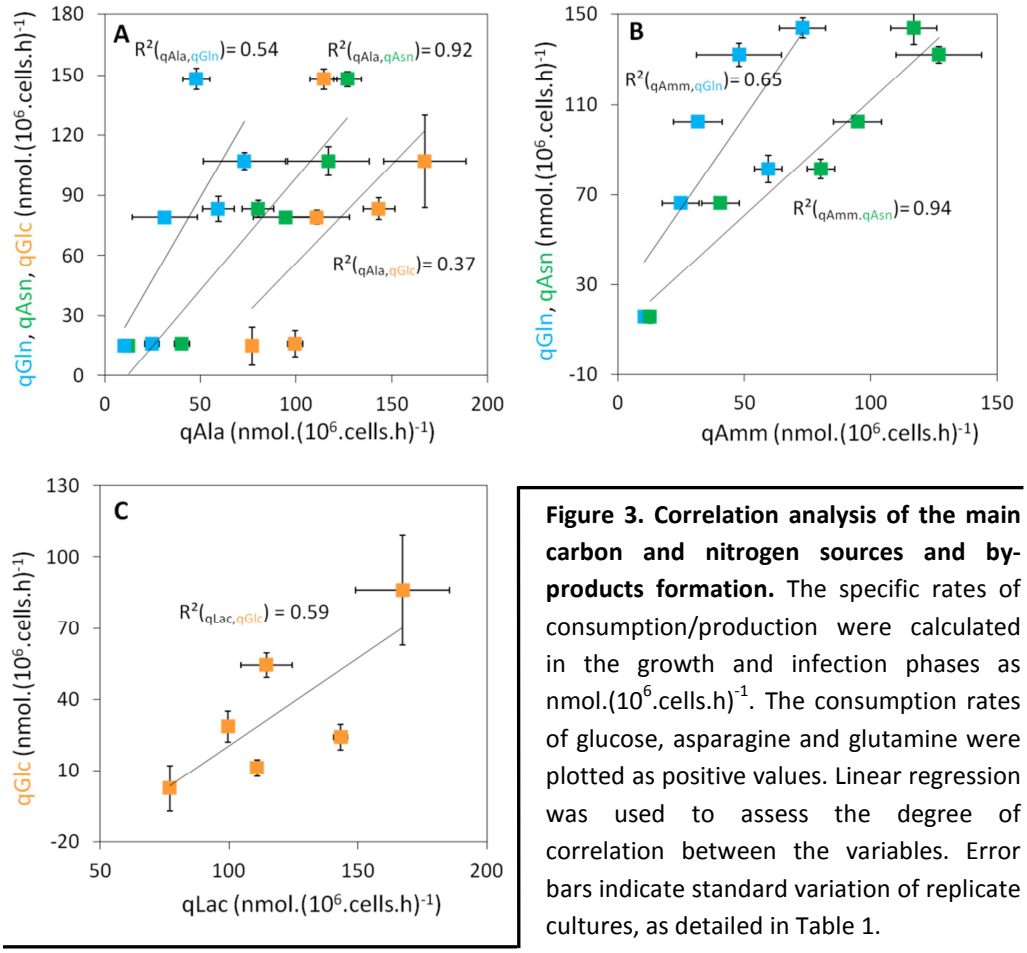

Figure 3. Correlation analysis of the main carbon and nitrogen sources and by-products formation. The specific rates of consumption/production were calculated in the growth and infection phases as nmol.(10^6.cells.h)$^{-1}$. The consumption rates of glucose, asparagine and glutamine were plotted as positive values. Linear regression was used to assess the degree of correlation between the variables. Error bars indicate standard variation of replicate cultures, as detailed in Table 1.

After baculovirus infection at high MOI, a 3-fold increase in the rate of amino acids consumption was observed. However, the production of alanine and ammonia was reduced after infection, suggesting that the higher uptake rates of carbon and nitrogen sources may be supporting biosynthesis (Table 1).

The consumption of the main carbon (glucose) and nitrogen (asparagine and glutamine) sources was correlated with the accumulation of the major nitrogen metabolism by-products (alanine, lactate and ammonia) (Fig. 3). The main by-product

of High Five cells was alanine, both in growing as well as in baculovirus infected cultures (Table 1). The production of alanine and ammonia followed a direct correlation with the consumption of asparagine (Fig. 3A and B, respectively). Accumulation of lactate was not directly correlated to the specific consumption of glucose (Fig. 3C).

3.3 Metabolic fluxes quantification in growing and baculovirus infected High Five cells

Metabolic flux analysis was performed to characterize High Five cells metabolism during growth in two different culture media, and after baculovirus infection. For the calculation of metabolic fluxes, culture time was divided in early-mid (phase I) and late (phase II) exponential phases for growth cultures, and from 0 to 48 hpi in infected cultures (Fig. 4 and 5, respectively). In all scenarios, the consistency index *h* was below the χ^2 value within a 95% confidence interval. This condition indicates that the model is well-posed and that no gross measurements are being propagated in the measured fluxes.

3.3.1 Impact of the culture media on High Five cells metabolism

The pentose phosphate pathway (PPP) activity, represented by the flux of glucose-6-phosphate, was directly proportional to the cellular growth rate, being higher at early-mid exponential phase (Fig.4A). The fluxes of the glycolytic pathway were similar between High Five cultures performed in Insect Xpress and Sf900II media (Fig. 4A). The main differences were observed regarding the lactate dehydrogenase (LDH) and alanine aminotransferase (AlaAT) fluxes, which were 5 and 2 fold higher in Sf900II cultures, respectively (Fig. 4A); this is in accordance with the higher levels of lactate and alanine also produced in such cultures (Table 1).

The fluxes throughout the TCA cycle were 2 fold higher in cultures performed in Insect Xpress media, mainly at early-mid exponential phase (Fig. 4B). This reflects the

lower production of alanine and lactate, thus the pyruvate can be more efficiently channeled into the TCA cycle. In fact, the ratio between the fluxes of citrate synthase (CS) and pyruvate dehydrogenase (PDH), an indicator of the efficiency of the channeling of the consumed glucose in the TCA cycle, was 0.9 in cultures performed in Insect Xpress medium, and only 0.6 in Sf900II cultures (Fig. 4B).

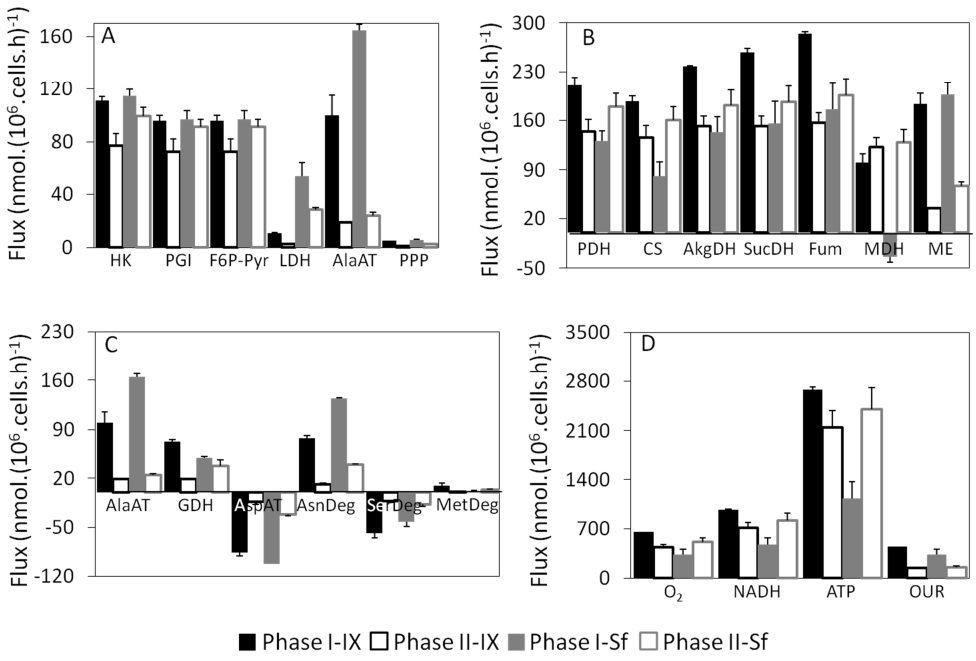

Figure 4. Fluxome of High Five cells during growth in different culture media. Two culture phases were considered, early-to-mid (phase I) and late (phase II) exponential phases, as detailed in the Materials and Methods section. Flux calculations were performed using the FluxAnalyzer software, and are expressed as nmol.(10^6.cells.h)$^{-1}$. Error bars indicate the standard variation of two independent cultures in Insect Xpress (IX), and three independent cultures for Sf900II (Sf) cultured cells.

Regarding amino acids metabolism, the fluxes through aspartate aminotransferase (AspAT) and asparagine degradation pathways are in accordance with the levels of aspartate and asparagine consumption, being higher at early-mid exponential phase (Fig. 4C and Table 1). When looking closer at the anaplerotic reactions, major differences arise in cultures performed in Insect Xpress and Sf900II media. More specifically, the flux through malate dehydrogenase (MDH) occurs in

the reverse direction in early-mid exponential Sf900II cultures, and the replenishing of the oxaloacetate (OAA) pool is ensured by the high flux of AspAT (Fig. 4B and C).

The increase in cell density resulted in a down-regulation of the fluxes through carbon and nitrogen metabolism, regardless of the culture media used (Fig. 4). This was translated in a decrease in the cell specific growth rate of 0.01 h^{-1}, 3 to 4 fold lower than in early-mid exponential cultures (Table 1). The net ATP synthesis reflected the metabolic activity in the conditions analyzed, being higher at early-mid exponential phase in Insect Xpress cultures and at late exponential phase in Sf900II cultures (Fig. 4D). This is in accordance to the higher net flux throughout the TCA cycle in these two conditions, the major energy generating hub of cellular metabolism. In accordance, the oxygen consumption and NADH recycling followed this same trend (Fig. 4D).

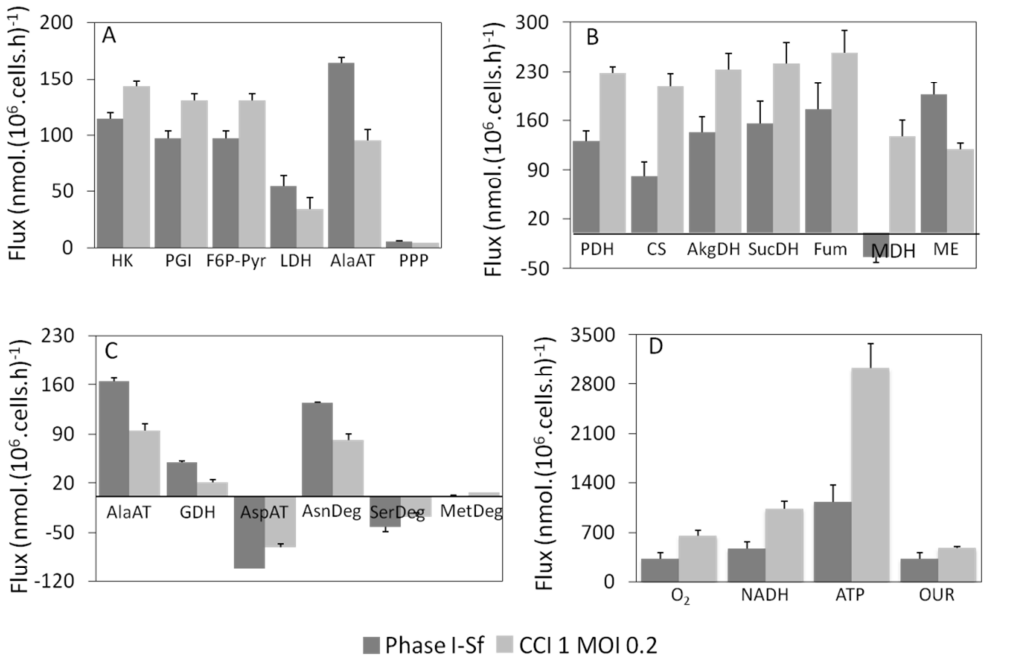

Figure 5. Fluxome of High Five cells after baculovirus infection. Infection was performed with a MOI 0f 0.2 IPs.cell^{-1}, and a single phase post-infection was considered, as detailed in the Materials and Methods section. The fluxome data of early-mid exponential (phase I) cultures performed in Sf900II (Sf) media was plotted for comparison. Fluxes were calculated using the FluxAnalyzer software, and are expressed as nmol.(10^6.cells.h)$^{-1}$. Error bars indicate the standard variation of three independent biological replicates.

3.3.2 Impact of baculovirus infection on High Five cells metabolism

The fluxes of the glycolytic pathway were 30% higher in baculovirus infected cultures when compared to the non-infected control of Sf900II High Five cultures at early-mid exponential phase (Fig. 5A). Additionally, the production of lactate and alanine decreased following infection (Table 1), as denoted by the 2-fold decrease in the fluxes of LDH and AlaAT at low MOI. As a consequence, 90% of the pyruvate was channeled into the TCA cycle, which resulted in a net increase of up to 4 fold of the fluxes throughout the cycle (Fig. 5B). We observed a decrease of 1.5 to 2.5 fold in the fluxes of amino acids catabolism (Fig. 5C), which is in accordance to the lower uptake rates of the majority of the amino acids in infected cultures at low MOI (Table 1).

The ATP net synthesis flux reflected the metabolic activity during glycolysis and TCA cycle, being 3 times higher in infected cultures (Fig. 5D).

4. Discussion

The productivity phenotype of High Five cells was previously analyzed in close comparison with other insect cell lines (Krammer et al., 2010; Palmberger et al., 2011; Taticek et al., 2001). Although highly explored as production platforms, the metabolism of High Five cells has not been fully characterized yet, especially the alterations and cellular adaptations to an infection scenario.

In this work, a comprehensive network describing carbon and nitrogen metabolism in High Five cells sheds light on the interplay of cell culture media and baculovirus infection on the metabolic status of the cells.

One of the most remarkable characteristics of *Spodoptera frugiperda* Sf9 cells metabolism is the efficient channeling of glucose for further oxidation in the TCA cycle, thus hindering the production and accumulation of significant amounts of lactate in the culture media (Drugmand et al., 2012; Ikonomou et al., 2003). In High Five cells cultures, the metabolic efficiency was importantly affected by the culture media used. In cultures performed in Insect Xpress almost 90% of the glucose was

channeled to the TCA cycle to be oxidized, in opposition to only 60% in Sf900II cultures. The media composition is similar; however they differ in the quantities of the glucose provided, as well as in the quantities of particular amino acids such as glutamine and asparagine, all more abundant in the Sf900II medium. Although unregulated nutrient uptake may be blamed by the metabolic overflow phenotype observed, it should be noticed that glucose uptake rate was essentially the same in both media. Since the formation of by-products was directly correlated with the net consumption of asparagine, for instance, the higher specific uptake rates will result in higher amounts of alanine and ammonia produced. A close correlation between major carbon and nitrogen sources and alanine production was observed both in infected and non-infected cells. Therefore, this suggests that metabolic overflow in High Five cells is a consequence of deregulated and fast consumption of amino acids, alanine being the major overflow metabolite. In fact, alanine is described as the major by-product derived from insect cells metabolic activity (Ikonomou et al., 2003). High Five cells produce considerable levels of ammonia, which is linked to the absence of an ammonia recycling and detoxification system like that found in other insect cell lines, such as in the case of Sf9 cells (Doverskog et al., 2000). However, alanine overflow limits the toxic effects of excess nitrogen secretion, since it is by far less toxic than ammonia.

The increase in cell density was followed by a down-regulation of the metabolic activity, with the decrease in the overall fluxome of growing High Five cells. The reduced flux activity had consequences on the energetic state in the sense that lower ATP levels were generated. Moreover, this observation was independent of the cell culture media used, and not directly linked with the exhaustion of specific nutrients from both media. As a consequence, the cellular growth rate was markedly reduced, which is in accordance to the characteristic phenotype of high cell density insect cell cultures (Bernal et al., 2009).

Baculovirus infection resulted in metabolic rearrangements, as illustrated by the changes in the overall fluxome of High Five cells. The net flux of the TCA cycle

increased, accompanied by the decrease in AlaAT and LDH fluxes. The incorporation of glucose into the TCA cycle increased, as indicated by the higher flux through CS, a determining step for the channeling of carbon skeletons. Moreover, MDH flux was considerably higher following baculovirus infection, which contributes to a direct feeding of oxaloacetate to the cycle. Altogether, these alterations culminated in a boost in the energetic state of baculovirus infected High Five cells, as reflected by the increase in the ATP net synthesis rate. Thus, this is by far a more favorable scenario to support the efficient replication of the virus, *i.e.*, more energy is available to sustain the high biosynthetic demand. Reports in the literature have already shown the ability of viruses to manipulate and subvert host metabolic pathways for their own profit, generating a more amenable environment to support their replicative cycle (reviewed in Maynard et al., 2010). Baculovirus are no exception, and similar to what happens in Sf9 cells (Bernal et al., 2010), the results point to the manipulation of central carbon and nitrogen metabolism in baculovirus-infected High Five cells.

The analysis of the metabolic adaptations undergone by High Five cells revealed important modulations of central carbon metabolism as a consequence of cell density and baculovirus infection. The metabolism of the cell line was affected by the choice of the growth medium. Unbalanced medium composition affects the metabolic efficiency of cells. As shown in this chapter, MFA is a valuable technique to assess the effect of environmental conditions on the metabolic state of cells.

5. Author contribution

Francisca Monteiro conceived the experimental set-up and design, performed the experiments, analyzed the data and wrote the chapter.

6. References

Assenberg, R., Wan, P.T., Geisse, S., Mayr, L.M., 2013. Advances in recombinant protein expression for use in pharmaceutical research. Curr. Opin. Struct. Biol. 23, 393–402. doi:10.1016/j.sbi.2013.03.008

Bédard, C., Tom, R., Kamen, A., 1993. Growth, nutrient consumption, and end-product accumulation in Sf-9 and BTI-EAA insect cell cultures: insights into growth limitation and metabolism. Biotechnol. Prog. 9, 615–24.

Benslimane, C., Elias, C.B., Hawari, J., Kamen, A., 2005. Insights into the central metabolism of Spodoptera frugiperda (Sf-9) and Trichoplusia ni BTI-Tn-5B1-4 (Tn-5) insect cells by radiolabeling studies. Biotechnol. Prog. 21, 78–86.

Bernal, V., Carinhas, N., Yokomizo, A.Y., Carrondo, M.J.T., Alves, P.M., 2009. Cell density effect in the baculovirus-insect cells system: a quantitative analysis of energetic metabolism. Biotechnol. Bioeng. 104, 162–80.

Bernal, V., Monteiro, F., Carinhas, N., Ambrósio, R., Alves, P.M., 2010. An integrated analysis of enzyme activities, cofactor pools and metabolic fluxes in baculovirus-infected Spodoptera frugiperda Sf9 cells. J. Biotechnol. 150, 332–42.

Bhatia, R., Jesionowski, G., Ferrance, J., Ataai, M.M., 1996. Insect cell physiology. Cytotechnology. doi:10.1007/BF00350387

Carinhas, N., Bernal, V., Yokomizo, A.Y., Carrondo, M.J.T., Oliveira, R., Alves, P.M., 2009. Baculovirus production for gene therapy: the role of cell density, multiplicity of infection and medium exchange. Appl. Microbiol. Biotechnol. 81, 1041–9.

Carinhas, N., Duarte, T.M., Barreiro, L.C., Carrondo, M.J.T., Alves, P.M., Teixeira, A.P., 2013. Metabolic signatures of GS-CHO cell clones associated with butyrate treatment and culture phase transition. Biotechnol. Bioeng. 110, 3244–3257. doi:10.1002/bit.24983

Deroo, T., Jou, W.M., Fiers, W., 1996. Recombinant neuraminidase vaccine protects against lethal influenza. Vaccine 14, 561–9.

Doverskog, M., Jacobsson, U., Chapman, B.E., Kuchel, P.W., Häggström, L., 2000. Determination of NADH-dependent glutamate synthase (GOGAT) in Spodoptera frugiperda (Sf9) insect cells by a selective 1H/15N NMR in vitro assay. J. Biotechnol. 79, 87–97.

Doverskog, M., Ljunggren, J., Ohman, L., Häggström, L., 1997. Physiology of cultured animal cells. J. Biotechnol. 59, 103–15.

Drugmand, J.-C., Schneider, Y.-J., Agathos, S.N., 2012. Insect cells as factories for biomanufacturing. Biotechnol. Adv. 30, 1140–57. doi:10.1016/j.biotechadv.2011.09.014

Ginkel, M., Dieter, E., Klamt, S., 2003. FluxAnalyzer: exploring structure, pathways, and flux distributions in metabolic networks on interactive flux maps. Bioinformatics 19, 261–269.

Huynh, H.T., Tran, T.T.B., Chan, L.C.L., Nielsen, L.K., Reid, S., 2013. Decline in baculovirus-expressed recombinant protein production with increasing cell density is

strongly correlated to impairment of virus replication and mRNA expression. Appl. Microbiol. Biotechnol. 97, 5245–57. doi:10.1007/s00253-013-4835-8

Ikonomou, L., Schneider, Y.-J., Agathos, S.N., 2003. Insect cell culture for industrial production of recombinant proteins. Appl. Microbiol. Biotechnol. 62, 1–20.

Krammer, F., Schinko, T., Palmberger, D., Tauer, C., Messner, P., Grabherr, R., 2010. Trichoplusia ni cells (High Five) are highly efficient for the production of influenza A virus-like particles: a comparison of two insect cell lines as production platforms for influenza vaccines. Mol. Biotechnol. 45, 226–34.

Martínez, V.S., Dietmair, S., Quek, L.-E., Hodson, M.P., Gray, P., Nielsen, L.K., 2013. Flux balance analysis of CHO cells before and after a metabolic switch from lactate production to consumption. Biotechnol. Bioeng. 110, 660–6. doi:10.1002/bit.24728

Maynard, N.D., Gutschow, M. V, Birch, E.W., Covert, M.W., 2010. The virus as metabolic engineer. Biotechnol. J. 5, 686–94.

Niklas, J., Priesnitz, C., Rose, T., Sandig, V., Heinzle, E., 2013. Metabolism and metabolic burden by α1-antitrypsin production in human AGE1.HN cells. Metab. Eng. 16, 103–114.

Palmberger, D., Klausberger, M., Grabherr, R., 2013. MultiBac turns sweet. Bioengineered 4, 78–83.

Palmberger, D., Rendić, D., Tauber, P., Krammer, F., Wilson, I.B.H., Grabherr, R., 2011. Insect cells for antibody production: evaluation of an efficient alternative. J. Biotechnol. 153, 160–6.

Palomares, L.A., Estrada-Moncada, S., Ramirez, O.T., 2006. Principles and applications of the insect cell-baculovirus expression vector system., in: Ozturk, S.S., Hu, W.S. (Eds.), Cell Culture Technology for Pharmaceutical and Cell Based Therapies. New York.

Rhiel, M., Mitchell-Logean, C.M., Murhammer, D.W., 1997. Comparison of Trichoplusia ni BTI-Tn-5B1-4 (high five) and Spodoptera frugiperda Sf-9 insect cell line metabolism in suspension cultures. Biotechnol. Bioeng. 55, 909–920.

Roldão, A., Oliveira, R., Carrondo, M.J.T., Alves, P.M., 2009. Error assessment in recombinant baculovirus titration: evaluation of different methods. J. Virol. Methods 159, 69–80.

Stephanopoulos, G, Aristidou, A.A., Nielsen, J., 1998. Metabolic Engineering. Principles and Methodologies. Academic Press, New York.

Taticek, R.A., Choi, C., Phan, S.E., Palomares, L.A., Shuler, M.L., 2001. Comparison of growth and recombinant protein expression in two different insect cell lines in attached and suspension culture. Biotechnol. Prog. 17, 676–84.

Van Oers, M.M., Pijlman, G.P., Vlak, J.M., 2015. Thirty years of baculovirus-insect cell protein expression: From dark horse to mainstream technology. J. Gen. Virol. 96, 6–23. doi:10.1099/vir.0.067108-0

Wang, N., Stephanopoulos, G., 1983. Application of macroscopic balances to the identification of gross measurement errors. Biotechnol. Bioeng. 25, 2177–208.

Wilde, M., Klausberger, M., Palmberger, D., Ernst, W., Grabherr, R., 2014. Tnao38, high five and Sf9--evaluation of host-virus interactions in three different insect cell lines: baculovirus production and recombinant protein expression. Biotechnol. Lett. 36, 743–9. doi:10.1007/s10529-013-1429-6

Chapter IV

FLUXOME ANALYSIS OF THE IC-BEVS: THE ROLE OF HOST CELL PHYSIOLOGY IN SYSTEMS PRODUCTIVITY

This chapter is based on data to be published as:

Fluxome analysis of the IC-BEVS: The role of host cell physiology in systems productivity

Francisca Monteiro, Vicente Bernal, Paula M. Alves (*in preparation*)

Abstract

The Insect Cell-Baculovirus Expression System (IC-BEVS) has a major track record for the production of recombinant proteins, vaccines and vectors for gene therapy. Although its widespread use, the physiological aspects that contribute to productivity are still to be disclosed. Virus-based bioprocesses are dependent on the proper infection of the producer cell, as well as efficient viral replicative cycle and expression of the heterologous genes. Knowledge of the host cell metabolism, mainly in the post-infection phase, can provide clues on the metabolic adaptations that occur and, ultimately, aid bioprocess engineers in developing rational optimization strategies.

In the present work, the metabolic features of the two main insect host cell lines, Sf9 and High Five, were analyzed in culture and after baculovirus infection in SF900II medium. The gathered data were contextualized in a metabolic network representative of central carbon and nitrogen metabolism. Metabolic Flux Analysis (MFA) was performed to have a quantitative overview of the cellular fluxome dynamics that followed infection. In addition, the main carbon sources that contributed most to flux activity were identified. Oxidative metabolism was hampered in High Five cells, leading to high accumulation of by-products, mainly lactate and alanine, a scenario not observed for Sf9 cells. Additionally, the high dependence of amino acid metabolism and anaplerosis observed in the High Five cell line indicated that the cells are able to re-adjust and combine different catabolic pathways to ensure proper metabolic activity and energy generation. However, after baculovirus infection, the metabolic activity suffered a rearrangement, and the channeling of glucose towards pyruvate formation and further oxidation at the TCA cycle was much more efficient. The strong correlation observed between the metabolic state of both host cells with baculovirus infection highlights the capacity of this virus to act as a metabolic engineer, re-directing the cellular fluxome to support viral replication and virions production. These results pave the way to deepen our knowledge on the relationship between a host cell and the virus, contributing to the disclosure of the metabolic determinants that contribute to productivity.

Contents

1. Introduction

The high protein expression levels achieved in the Insect Cell-Baculovirus Expression System (IC-BEVS), coupled with the tunable properties of baculoviral vectors, have contributed to the popularity of this system in the Animal Cell Technology field. As a consequence, in the past two decades, insect cells have been exploited as production factories of a myriad of biopharmaceuticals with high biotechnological and biomedical impact. Examples include several human therapeutics already in the market, namely Cervarix® (GlaxoSmithKline Biologics); Flublok® (Protein Sciences Corporation); Glybera® (UniQure) (Cox and Hollister, 2009; Lowy and Schiller, 2006; Moran, 2012). Although highly explored in industrial settings, the IC-BEVS is still poorly understood in what concerns the main physiological aspects that contribute to productivity.

Metabolism is the downstream indicator of the physiological processes that occur in a living cell, being the functional output of the tight regulation between the transcriptome and the proteome. Host cell metabolism and productivity are directly correlated, and several works have shown the impact that environmental and culture conditions have on the metabolic portrait of a cell line, and how it affects its productive phenotype (Chong et al., 2012; Dean and Reddy, 2013; Dietmair et al., 2012; Khoo and Al-Rubeai, 2009; Niklas et al., 2013). Additionally, infection of cells with a virus greatly affects several physiological processes, especially metabolism. Viruses tale advantage of the host cell biosynthetic machinery for their own profit, and several studies have highlighted the capacity of viruses in manipulating host physiological processes, either to ensure a proper environment for progeny generation, or for survival (reviewed in Maynard et al., 2010). Virus-based bioprocesses are highly dependent on the proper infection of the producer cell, as well as efficient viral replicative cycle and expression of the heterologous genes. Thus, the comprehensive knowledge of the host cell metabolism, mainly in the post-infection phase, can provide clues on the metabolic adaptations that occur and,

ultimately, aid bioprocess engineers in developing rational and targeted optimization strategies.

Two host cell lines have been explored as the main production platforms in BEVS, *Spodoptera frugiperda* Sf9 cells and *Trichoplusia ni* derived BTI-Tn-5B1-4 (High Five) cells. It is recognized that Sf9 cells are a better host for the production of infectious baculovirus vectors, while High Five are preferred for high level expression of recombinant proteins (Krammer et al., 2010; Taticek et al., 2001; Wilde et al., 2014). Previous works dedicated to the metabolic analysis of both cell lines have evidenced major differences between the carbon and nitrogen metabolism. Alanine is the main by-product of Sf9 and High Five cells metabolism, and its accumulation follows the net consumption of glucose and glutamine from the culture media (Benslimane et al., 2005; Ikonomou et al., 2003; Rhiel et al., 1997). High Five cells have a mammalian-like metabolism, with high levels of lactate and ammonia accumulation throughout culture time, however this phenotype was dependent on the culture media (Ikonomou et al., 2003; Rhiel et al., 1997). Sf9 cells have a highly efficient oxidative metabolism, with the channeling of glucose towards pyruvate formation and further incorporation of this carbon source in the TCA cycle (Bernal et al., 2010, 2009). Moreover, the low levels of ammonia produced by Sf9 cells are related with the presence of a detoxification and recycling mechanism driven by glutamate synthase (GOGAT) activity (Doverskog et al., 2000). Although key metabolic features of Sf9 and High Five cells have been identified, the interpretation of the observed extracellular fluxes in the frame of a metabolic network is still lacking for High Five cells. The quantitative description of the host cell metabolism can provide meaningful insights on the operation of key metabolic pathways that support energy generating processes and, thus, biosynthesis. Moreover, since IC-BEVS productivity is determined by the crosstalk established between the host cell and the baculovirus, the in-depth analysis of the post-infection scenario becomes mandatory.

The quantitative assessment of cellular metabolism can be pursued by the stoichiometric analysis of the reactions operating in a network representative of the

main cellular metabolic events. The quantification of the distribution of intracellular fluxes within a metabolic network becomes possible through metabolite balancing, and a quantitative description of the cellular fluxome can be achieved. In this regard, Metabolic Flux Analysis (MFA) is such an enabling technique, and has the capability to identify the main metabolic adaptations undergone by cells in culture (Stephanopoulos, G et al., 1998). Its widespread use has shed light on the main metabolic events that characterize disease-related phenotypes (Duckwall et al., 2013), cellular adaptation to stressful and infection conditions (Munger et al., 2010), and predictive metabolic markers (Sauer and Zamboni, 2008). Moreover, MFA-based characterization of industrial relevant systems retrieves noteworthy outputs in what concerns host cell line productive capabilities, as well as cellular behavior under bioprocess stringent conditions (Carinhas et al., 2013; Martinez et al., 2010; Niklas et al., 2013).

The application of MFA to baculovirus-infected Sf9 cells was previously done by our group to address the post-infection adaptations in Sf9 cellular metabolism (Bernal et al., 2009). Furthermore, the combination of MFA with the quantification of enzyme activities culminated with the identification of the key cellular metabolic control points (Bernal et al., 2010).

In this work we applied MFA to quantify the fluxome distribution shifts in response to infection in High Five cells. MFA was performed during growth and after baculovirus infection, to yield a comprehensive overview of the High Five cells fluxome in both scenarios. Moreover, the quantification of Sf9 cells fluxome allowed to have a comparative analysis between both host cell lines. The main implications of baculovirus infection in host cell metabolism are discussed, and the correlation with the productivity phenotypes is highlighted.

2. Materials and Methods

2.1 Cell lines and culture maintenance

Spodoptera frugiperda derived Sf9 cell line was obtained from the European Collection of Cell Cultures (No. 89070101, ECCAC) and *Trichoplusia ni* derived BTI-Tn-5B1-4 (High Five) cells were obtained from Invitrogen (Paisley, UK). Both cell lines were maintained in serum- and protein-free Sf900II insect cell medium (Gibco, Glasgow, UK) and cultured in 500 mL Erlenmeyer flasks (Corning, USA) with 50 mL working volume. Cultures were kept in a humidified incubator operated at 90 rpm and at 27ºC. Sf9 and High Five cells were re-inoculated every 3-4 days at $0.45x10^5$ cells.mL^{-1} and 0.3×10^5 cells.mL^{-1}, respectively. Cell concentration was determined by hemocytometer cell counts (Brandt, Wertheinmain, Germany) and cell viability evaluated by trypan blue exclusion method (Merck, Darmstadt, Germany).

2.2 Virus handling and viral stock preparation

The recombinant *Autographa californica* nucleopolyhedrovirus BvGCN4-NA1, kindly provided by Dr. Xavier Saelens (Ghent University, Belgium), contains an inserted gene encoding a secreted form of influenza N1 type neuraminidase under the control of the polyhedrin promoter (Deroo et al., 1996). BvGCN4-NA1 was used as the expression vector of recombinant Neuraminidase (rNeur) throughout this work. BvGCN4-NA1 was amplified by infecting Sf9 cells at $1x10^6$ cells.mL^{-1} at a multiplicity of infection (MOI) of 0.1 IP.cell-^{1} (IP-Infectious baculovirus particles). Infected cultures were kept at 27ºC in 500 mL Erlenmeyer flasks (Corning, New York, USA), agitated at 90 rpm. The viral stock was titrated as indicated and stored at 4ºC until further use.

2.3 Cell culture and Infections

Growth and infection studies were performed in 100 mL Erlenmeyer flasks (Corning, USA) with a working volume of 10 mL. Sf9 and High Five cells were

inoculated at 0.5 and 0.4 x 10^6 cells.mL^{-1}, respectively, and infected once they reached a cell concentration at infection (CCI) of 1x10^6 cells.mL^{-1}, as indicated in the results section. Two MOIs were used, namely 0.2, and 5 IP.cell^{-1}. Cultures were sampled every 12 to 24 hours to monitor cell concentration and viability, and for the quantification of metabolites. Samples for the productivity assays were withdrawn every 24 hours post-infection (hpi).

2.4 Quantification of infectious and total baculovirus particles

Titration of baculovirus infectious particles (IPs) was performed following the MTT assay as described in Roldão *et al*. (2009).

The concentration of total baculovirus particles (TPs) was measured using Nanosight NS500 (Nanosight Ltd., Salisbury, UK), making use of the Nanoparticle Tracking Analysis (NTA) functionality. This method enables the visualization, analysis and quantification of particles in liquid suspensions, through the relation of the rate of Brownian motion to particle size. To take into account the Nanosight sensitivity, the culture supernatant samples were diluted to a concentration of 1 to 9 x 10^8 total particles (TP) per mL in phosphate buffer saline (PBS). Since we are analyzing culture supernatants that have also cellular debris, exosomes, and other soluble factors that can interfere with the accuracy of the measurements, appropriate controls were performed (supernatant of non-infected cultures at the correspondent cell densities). The measurements were performed at least in triplicates with a typical standard deviation (SD) below 20%.

2.5 Quantification of Recombinant Neuraminidase

Recombinant Neuraminidase was quantified by a fluorimetric activity assay measuring the release of 4-methylumberlliferone (4-MU), as described in Deroo et al (1996). rNeuraminidase activity assay was performed in culture supernatant samples. One unit was defined as the amount of enzyme that releases 1 µmol of 4-MU per minute.

2.6 Cell dry weight quantification

Sf9 and High Five cells were harvested in the mid-exponential growth phase of non-infected cultures and at 48 hpi in baculovirus infected cultures. Samples containing 10 x 10^6 viable cells were pelleted by centrifugation (300 xg, 10 minutes), and washed with phosphate buffered saline (PBS) buffer. The pellets were dried *O/N.* at 100ºC and weighted in an analytical balance. The measurements were performed in triplicates.

2.7 Analytical methods for metabolite quantification

Glucose and lactate concentrations were determined using an YSI 7100 Multiparameter Bioanalytical System (YSI Life Sciences, Dayton, OH). Ammonia was quantified enzymatically using a UV based kit (No. AK00091; NZYTech, Lisbon, Portugal). Amino acids were determined by HPLC after derivatization using the AccQ-Tag Method (Waters, Milford, MA).

2.8 Metabolic Flux Analysis

2.8.1 Metabolic Network

The model describing the metabolic network of High Five cells is described in the previous chapter (Chapter II). For Sf9 cells, the model described in Bernal et al. (2009) was adapted. Briefly, the model contains the main reactions of glycolysis, pentose phosphate pathway (PPP), tricarboxylic acids (TCA) cycle, transport and metabolism of amino acids, energy production, and biomass synthesis. A complete list of the metabolic reaction considered in the model can be found in Appendix I (Table I-1).

The biomass and protein synthesis equations of the Sf9 and High Five cells were calculated considering the dry weight of each cell line during exponential growth and after baculovirus infection. Additionally, for the analysis of baculovirus infected cultures, the reactions of baculovirus and recombinant neuraminidase synthesis were

also included (Appendix I, Table I-2). The detailed description of the biomass equations is provided in Appendix I (Tables I-3, I-4 and I-5).

2.8.2 Flux calculations

Altogether, four metabolic models were generated in order to consider Sf9 and High Five cells metabolism during growth and after baculovirus infection, respectively. For Sf9 cells, the growth model totalizes 69 reactions with 50 internal (balanced) metabolites, defined by a 69 x 50 stoichiometric matrix. The infection model considers 74 reactions with 56 internal (balanced) metabolites, described by a 74 x 56 stoichiometric matrix. The rank of the resulting stoichiometric matrices is 48 and 54, respectively, thus the number of degrees of freedom of the systems is 21 and 20, respectively. For High Five cells, the growth model totalizes 68 reactions with 50 internal (balanced) metabolites, defined by a 68 x 50 stoichiometric matrix. The infection model considers 73 reactions with 56 internal (balanced) metabolites, described by a 73 x 56 stoichiometric matrix. The rank of the resulting stoichiometric matrices is 47 and 53, thus the number of degrees of freedom of the systems is 21 and 20, respectively.

In all four metabolic models, the balances of urea, mevalonate, ADP and ATP could not be closed since these metabolites participate in other reactions not considered in the metabolic networks. From the extracellular metabolites profiling, 23 and 25 exchange fluxes were experimentally determined in non-infected and infected cultures, respectively, including the uptake/production rates of nutrients, cellular growth rate, baculovirus synthesis and rNeur formation. Also, the intracellular synthesis of lactate from pyruvate was set equal to the respective extracellular measured rates. The resultant system of equations is over-determined, meaning that it is possible to compute all unknown rates, and redundant, with 2 redundant measurements in the case of the Sf9, and 3 for High Five metabolic models. The systems of linear equations were solved by the weighted least squares method (Stephanopoulos, G et al., 1998).

The carbon and nitrogen balances closed to an average of 94% and 93% in growth cultures, and 85% and 78% in High Five infected cultures, respectively. For Sf9 cells, the carbon and nitrogen balances closed to an average of 78% and 63% in growth cultures, and 75% and 52% in infected cultures, respectively. Balanceable rates, which arise from system redundancy, were used to calculate the consistency index *h* (Wang and Stephanopoulos, 1983). Comparison of *h* with the χ^2 test function allows the evaluation of the consistency of the experimental data with the assumed biochemistry and the pseudo steady-state assumption. All computational tasks were performed using the FluxAnalyzer software (Ginkel et al., 2003).

2.9 Statistical Analysis

Hypothesis testing on the comparison between intracellular fluxes was performed using Student's t-test. A 95% confidence interval was considered to be statistically significant

3. Results

3.1 Metabolic profile of cultured Sf9 and High Five cells

Sf9 and High Five cells were cultured in Sf900II insect cell medium and their growth profiles were followed throughout culture time (Fig. 1). The cellular specific growth rate was slightly higher for High Five in comparison with Sf9 cells (0.033 and 0.027 h^{-1}, respectively) (Table 1), although the maximum viable cell concentration reached by Sf9 cells was higher (1x and $4x10^6$ cells.mL^{-1}, respectively) (Fig. 1).

The extracellular metabolites profiles were assessed by quantifying the consumption of the main carbon and nitrogen sources from samples throughout culture time. The specific rates of nutrient consumption and by-products formation were calculated at exponential phase and are detailed in Table 1. High Five cells showed higher net consumption of all the nutrients present in the culture media, which is in agreement with their higher size. Regarding amino acid consumption,

High Five cells preferably consume asparagine, which specific consumption rate was 60 times higher than in Sf9 cells. In the latter, the most consumed amino acid was glutamine, with a specific uptake rate of 18.7 nmol.(10^6.cells.h)$^{-1}$ (Table 1). Alanine was the main by-product of both High Five and Sf9 metabolism, with a 10-fold higher specific rate in High Five cells, which is in agreement with the higher rates of glucose and amino acids consumption observed. Low levels of ammonia accumulation were observed in Sf9 cultures, whereas High Five cells produced almost 30 times more ammonia (Table 1).

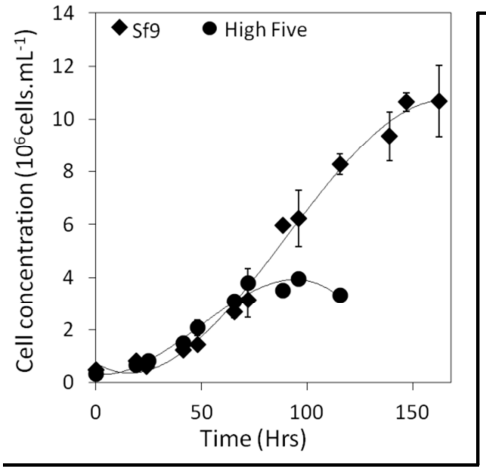

Figure 1. Growth profile of Sf9 and High Five cells. Cells were cultured in Sf900II media, as explained in the Materials and Methods section. Error bars indicate the standard error of three independent replicates (n=3).

3.2 Fluxome distribution of cultured Sf9 and High Five cells

Metabolic flux analysis was performed to characterize and compare Sf9 and High Five cells metabolism during growth. For the calculation of metabolic fluxes, a single early-to-mid exponential phase was considered (Fig. 2). The consistency index *h* was below the χ^2 value within a 95% confidence interval. This condition indicates that the model is well-posed and that no gross measurements are being propagated in the measured fluxes.

High Five and Sf9 cells have different cell sizes, with High Five cells having in average 30 to 50% higher cellular volume than Sf9 cells, thus the absolute fluxes reflect this differences. The calculated fluxes were normalized by the specific glucose uptake rate of each cell line calculated in the same culture phase (early-to-mid

exponential). Comparison of normalized fluxes will allow better discerning the differences between the metabolism of both cell lines. The absolute values of the cellular fluxes are provided in Table III-1 (Appendix III).

Table 1. Specific growth, consumption and production rates of High Five and Sf9 cells

	High Five	Sf9
	Rate ± SE	Rate ± SE
μ (h^{-1})	0.033 ± 0.002	0.027 ± 0.001
Glucose	-114.5 ± 5.2	-58.6 ± 3.9
Lactate	54.3 ± 10.0	2.1 ± 0.5
Aspartate	-4.0 ± 0.7	-2.9 ± 0.3
Glutamate	-26.0 ± 2.1	-7.7 ± 0.7
Serine	-6.0 ± 0.5	-7.8 ± 1.8
Asparagine	-126.9 ± 3.7	-2.4 ± 0.0
Glycine	-9.7 ± 1.0	-3.3 ± 0.0
Glutamine	-47.9 ± 5.2	-18.7 ± 1.7
Histidine	-3.4 ± 0.6	-1.4 ± 0.0
Threonine	-2.8 ± 0.2	-4.1 ± 0.8
Arginine	-25.3 ± 5.5	-5.9 ± 1.8
Alanine	148.0 ± 7.1	15.4 ± 1.8
Proline	-11.5 ± 3.5	-4.5 ± 1.4
Tyrosine	-4.4 ± 0.8	-1.7 ± 0.0
Cysteine	*N.D.*	-2.5 ± 0.2
Valine	-12.7 ± 3.3	-5.5 ± 1.4
Methionine	-5.5 ± 0.9	-2.4 ± 0.0
Isoleucine	-6.2 ± 1.3	-4.5 ± 1.2
Leucine	-12.0 ± 1.6	-6.5 ± 1.0
Lysine	-13.0 ± 2.6	-4.7 ± 0.1
Phenylalanine	-4.3 ± 1.2	-2.1 ± 0.0
Ammonia	132.1 ± 16.8	5.1 ± 0.2

Cultures were performed in SF900II as described in Materials and Methods. A single exponential growth phase was considered; negative values denote nutrient consumption. Cultures were performed in three independent triplicates. Consumption and production rates are expressed in nmol.(10^6.cells.h)$^{-1}$ as the mean average value of the replicates (n=3). N.D.- Not Determined.

The glycolytic fluxes were similar in both cell lines, however the incorporation of glucose to the TCA cycle for further oxidation was significantly different (Fig. 1). More specifically, the citrate synthase (CS) flux was significantly higher in the Sf9 cell line, which accounted for the incorporation of 74% of the glucose in the TCA cycle, in

opposition to the 36% observed for High Five cells. This low activity of the TCA cycle led to the overflow of the excess of pyruvate produced. The alanine aminotransferase (AlaAT) and lactate dehydrogenase (LDH) fluxes were significantly higher in High Five cells, and are in accordance with the high rates of alanine and lactate production observed for this cell line (Table 1).

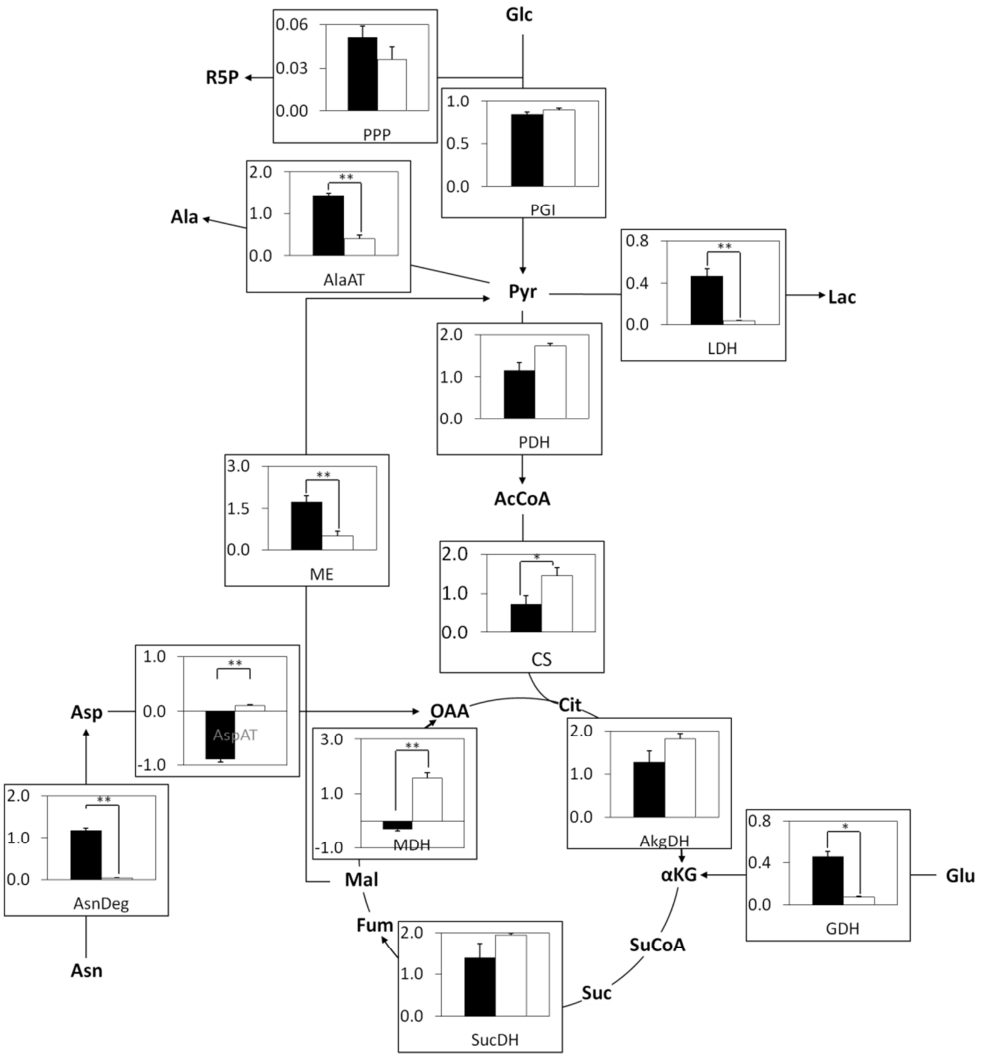

Figure 2. Fluxome distribution of High Five and Sf9 cells during growth. High Five (black bars) and Sf9 (white bars) were cultured in Sf900II media as detailed in the Materials and Methods section. Fluxes were calculated using the FluxAnalyzer software, and normalized by the glucose specific uptake rate. The data presented corresponds to the exponential phase of three independent cultures (n=3). * $p<0.05$; ** $p<0.01$.

Amino acid catabolism provided the entry of carbon backbones to the TCA cycle, especially in the case of High Five cells, ensuring the activity of the TCA cycle and energy generation (Fig 1). Two main entry points were observed, at the α-ketoglutarate (αKG) and oxaloacetate (OAA) levels, through the activities of glutamate dehydrogenase (GDH) and aspartate aminotransferase (AspAT), respectively. Moreover, the aspartate pool was also ensured by asparagine metabolism in High Five cells, which followed the high levels of asparagine consumption observed in this cell line (Table 1). The anaplerotic flux through malic enzyme (ME) was significantly higher in High Five cells, with a 3.4 fold increase with respect to Sf9 cells (Fig. 1). Moreover, the ME flux activity was 2-fold higher than the flux through malate dehydrogenase (MDH) in the High Five cell line, which led to the channeling of malate towards the formation of pyruvate. This scenario is a consequence of the high rate of incorporation of amino acids to the TCA cycle, anaplerotic fluxes thus avoiding the accumulation of TCA cycle intermediates in the cell.

3.3 Metabolic partitioning at the pyruvate and α-ketoglutarate nodes in cultured Sf9 and High Five cells

Metabolic partitioning coefficients were calculated to give an extended overview of the metabolic constraints operating at key nodes of central carbon and nitrogen metabolism (pyruvate and α-ketoglutarate nodes, respectively) (Fig. 3A and B). A detailed description of the metabolic partitioning coefficients calculations is provided in Appendix II.

The interpretation of partitioning coefficients at key metabolic nodes allows to quantitatively understand differences in the activity of the TCA cycle, amino acids metabolism, anaplerosis and metabolic overflow, underlining the relative importance of these pathways in each cell line. At the pyruvate node, the main differences between Sf9 and High Five cells reflected the high LDH and AlaAT fluxes, thus the partitioning coefficients of lactate and alanine were 9 and 3 fold higher in High Five

cells (Fig. 3A and B, respectively). In addition, given to the high rate of malic enzyme in High Five cells (Fig. 2), the partitioning coefficient of malate was considerably higher in this cell line, contributing to the replenishing of the pyruvate pool (Fig. 3B).

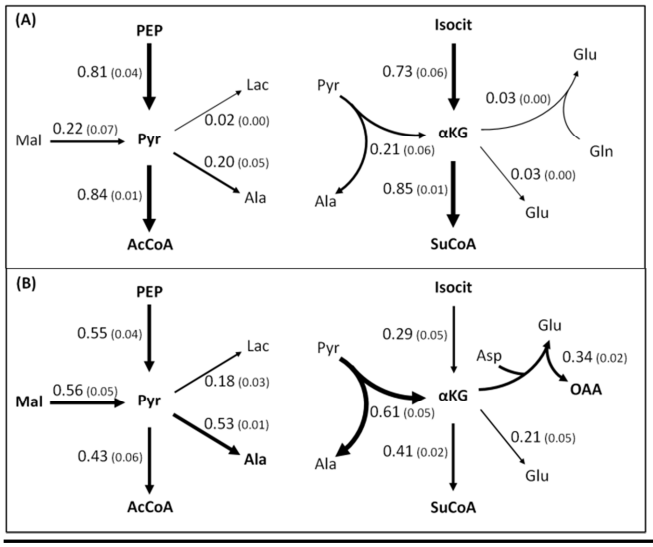

Figure 3. Metabolic partitioning at the pyruvate and α-ketoglutarate nodes of Sf9 (A) and High Five (B) cells during growth. Metabolic partitioning coefficients were calculated as explained in the text (Appendix II).
Arrow thickness is representative of the net flow of each reaction. Standard error, in brackets, corresponds to three independent cultures (n=3).

The partitioning of the α-ketoglutarate node of Sf9 cells reflected the high activity of the TCA cycle dependent on the glucose oxidation (Fig 3A). In High Five cells, the node partitioning reflects the dependence of amino acid metabolism for the functioning of the TCA cycle, with high partitioning coefficient of pyruvate from AlaAT activity, and OAA production via AspAT (Fig. 3B).

3.4 Contribution of sugars and amino acids carbon skeletons to the TCA cycle in Sf9 and High Five cells

In order to evaluate the contribution of carbon sources for the metabolic activity of both cell lines, the relative weight of glucose and amino acids incorporation to the TCA cycle was determined (Fig. 4A). A clear difference between cell lines was observed. In Sf9 cells, the pathway depended mostly on the contribution of glucose, which incorporation represented 80% of the carbon flux into the cycle, in comparison to a contribution of only 30% in the case of High Five cells. In the later, the carbon backbones from amino acids were incorporated to a greater extent to the TCA cycle

(70%), which correlates with the high dependence on amino acid metabolism observed in this cell line as described in the previous section.

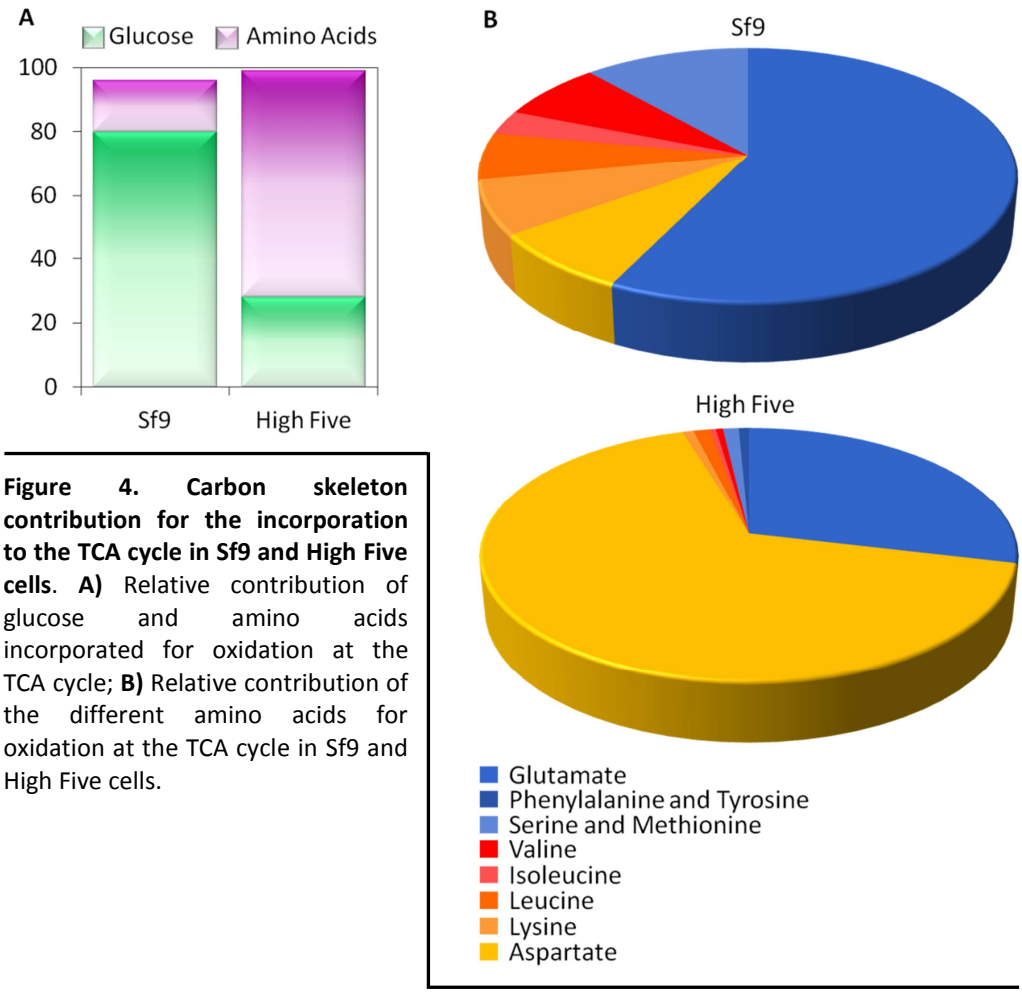

Figure 4. Carbon skeleton contribution for the incorporation to the TCA cycle in Sf9 and High Five cells. **A)** Relative contribution of glucose and amino acids incorporated for oxidation at the TCA cycle; **B)** Relative contribution of the different amino acids for oxidation at the TCA cycle in Sf9 and High Five cells.

Additionally, the particular contribution of the individual amino acids for the TCA cycle activity was assessed (Fig. 4B). In Sf9 cells, the amino acids that were highly incorporated to the TCA cycle were glutamate (57%), serine and methionine (12%). For High Five cells the picture was quite different, with the TCA cycle activity being highly dependent mainly of the oxidation of aspartate (67%) and glutamate (29%) (Fig 4B).

3.5 Productivity and metabolic profiles of baculovirus infected Sf9 and High Five cells

Sf9 and High Five cells were grown until they reached a concentration of $1x10^6$cells.mL^{-1} and infected at MOI of 0.2 and 5 IP.mL^{-1}, as detailed in the Materials and Methods section. The growth profiles of infected cultures were followed throughout culture time (Fig. 5), and the cellular specific productivities of rNeuraminidase (rNeur), infectious (IPs) and total (TPs) baculovirus particles were determined after 48 hpi (Table 2).

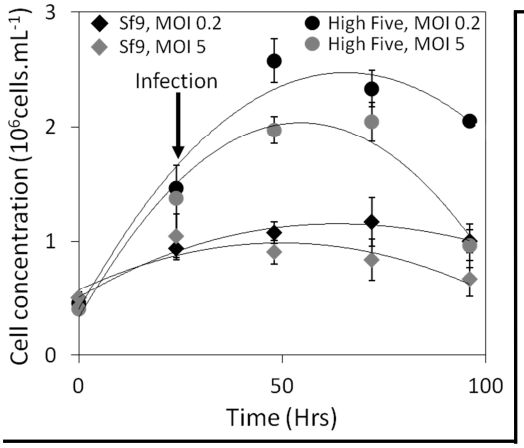

Figure 5. Growth profile of Sf9 and High Five cells after baculovirus infection. Cells were cultured in Sf900II media, as explained in the Materials and Methods section. Error bars indicate the standard deviation of three independent replicates (n=3).

Better productivity yields were observed in High Five cells for the production of rNeur and TPs, namely 2 to 3 fold higher, regardless of the MOI used. On the other hand, Sf9 cells produced higher levels of IPs, achieving up to 3 fold higher specific viral titers than High Five cells (Table 2).

Table 2. Specific productivities of Sf9 and High Five cells

	rNeur (U.10^{-6}cells)		BvGCN4 (10^1 IP.cell^{-1})		BvGCN4 (10^4 TP.cell^{-1})	
MOI	Sf9	High Five	Sf9	High Five	Sf9	High Five
0.2	0.07 ± 0.00	0.14 ± 0.03	3.22 ± 6.24	0.34 ± 0.13	N.D.	
5	0.12 ± 0.02	0.21 ± 0.04	4.28 ± 6.70	0.99 ± 0.90	0.67 ± 0.11	1.89 ± 1.30

Sf9 and High Five cells were cultured in Sf900II media, and infected with MOIs of 0.2 and 5 IP.cell^{-1} once they reached a cellular concentration of $1x10^6$ cells.mL^{-1}. The quantification of rNeur, baculovirus IPs and TPs were performed in supernatant samples of infected cultures at 48 hpi, as detailed in the Materials and Methods section. SE- standard deviation of the mean average of three independent replicates (n=3).

The specific nutrient consumption and by-product production rates were calculated considering a single phase post-infection (0-48 hpi), and are detailed in Table 3.

Table 3. Specific consumption and production rates of High Five and Sf9 cells after baculovirus infection

	Hi5		Sf9	
	CCI 1		CCI 1	
	MOI 0.2	MOI 5	MOI 0.2	MOI 5
	Rate ± SE	Rate ± SE	Rate ± SE	Rate ± SE
Glucose	-143.3 ± 5.4	-167.3 ± 23.2	-54.8 ± 5.1	-97.0 ± 29.3
Lactate	24.1 ± 2.7	86.1 ± 18.3	0.6 ± 0.3	3.2 ± 0.9
Aspartate	-24.0 ± 4.8	-22.7 ± 3.6	-13.4 ± 2.3	-40.8 ± 2.0
Glutamate	-8.7 ± 1.4	-40.2 ± 5.3	-7.1 ± 1.3	-53.3 ± 15.0
Serine	-3.2 ± 2.8	-21.1 ± 7.4	-10.6 ± 2.7	-10.1 ± 1.4
Asparagine	-80.2 ± 4.3	-116.9 ± 7.2	-5.7 ± 1.7	-20.1 ± 8.0
Glycine	-5.2 ± 1.2	-3.1 ± 0.9	-4.3 ± 0.7	-13.2 ± 2.3
Glutamine	-59.4 ± 6.2	-73.0 ± 4.4	-18.6 ± 2.5	-28.7 ± 6.5
Histidine	-2.2 ± 0.4	-9.4 ± 0.0	-2.2 ± 0.5	-5.6 ± 0.8
Threonine	-8.4 ± 1.2	-16.6 ± 4.9	-1.6 ± 0.3	-11.9 ± 1.0
Arginine	-8.5 ± 0.6	-18.3 ± 6.3	-3.1 ± 0.1	-15.9 ± 1.3
Alanine	83.2 ± 8.3	107.1 ± 21.4	34.3 ± 4.4	22.6 ± 7.8
Proline	-13.3 ± 2.9	-20.5 ± 5.9	-3.3 ± 0.8	-13.6 ± 2.6
Tyrosine	-4.2 ± 1.0	-8.7 ± 2.9	-1.6 ± 0.1	-5.2 ± 0.1
Cysteine	-4.4 ± 0.3	-12.6 ± 3.8	-6.8 ± 0.6	-5.1 ± 0.0
Valine	-9.4 ± 2.2	-21.7 ± 6.2	-4.5 ± 0.7	-18.1 ± 3.0
Methionine	-6.9 ± 2.0	-22.5 ± 0.9	-6.1 ± 0.6	-22.6 ± 1.1
Isoleucine	-8.7 ± 2.1	-25.2 ± 1.2	-5.7 ± 1.1	-20.7 ± 4.0
Leucine	-13.4 ± 1.1	-23.9 ± 7.5	-4.6 ± 0.4	-9.1 ± 0.5
Lysine	-10.2 ± 1.6	-20.8 ± 5.3	-4.8 ± 0.5	-17.3 ± 2.3
Phenylalanine	-6.3 ± 1.9	-23.4 ± 1.4	-5.9 ± 1.0	-20.9 ± 3.6
Ammonia	81.4 ± 5.5	143.8 ± 9.1	9.0 ± 1.4	44.8 ± 9.5

Cultures were performed as described in Materials and Methods. A single phase after infection was considered (0-48 hpi); negative values indicate nutrient consumption. Consumption and production rates are expressed in nmol.(10^6.cells.h)$^{-1}$ as the mean average value of three independent replicates (n=3). Standard error (SE) describes the standard deviation of the three independent culture replicates performed. N.D. stands for Not Determined.

The impact of baculovirus infection in both cell lines metabolism is evident, with a net increase in the uptake rates proportional to the MOI used (Tables 3 and 1,

respectively). In High Five cells, the main nitrogen source consumed was also asparagine, as already described for non-infected cultures. For Sf9 cells, although glutamine was highly consumed after baculovirus infection, glutamate became the major nitrogen source consumed, especially in cultures infected at high MOI, with a 7-fold increase in the specific uptake rate.

3.6 Fluxome distribution of baculovirus infected Sf9 and High Five cells

Metabolic flux analysis was performed to characterize and compare the impact of baculovirus infection on the metabolism of Sf9 and High Five cells. For the calculation of metabolic fluxes, a single post-infection phase (0-48 hpi) was considered (Fig. 6). The consistency index *h* was below the χ^2 value within a 95% confidence interval for the cultures infected at low MOI. At high MOI we still observed significant consumption of nutrients, while the cellular growth rate was 0 or even negative as a consequence of cell lysis resulted from viral infection. Thus, we could not obtain consistency in this set of cultures, which means that the pseudo steady-state hypothesis was not applicable. We chose to proceed to the analysis of Sf9 and High Five cultures infected at low MOI's (0.2 IP.mL^{-1}). Similarly to non-infected Sf9 and High Five cells, the normalization of the calculated fluxes was performed by the specific glucose uptake rate of each cell line calculated in the same culture phase (0-48 hpi). The absolute values of the cellular fluxes are provided Table III-2 (Appendix III).

In High Five cells, baculovirus infection resulted in a decrease in the AspAT and LDH flux activity in comparison to non-infected cultures (Fig. 6 and 2, respectively). This observation is in accordance with the lower levels of alanine and lactate produced in High Five infected cultures at low MOI (Table 3). As a consequence, the flux through PDH and the glucose incorporation in the TCA cycle was higher in High Five cells after baculovirus infection (Fig. 6 and 2, respectively). Moreover, ME flux decreased approximately 2 fold after baculovirus infection, accompanied by an up-regulation of 4-fold of the MDH activity (Table III-2). Besides this, the fluxes

throughout the TCA cycle were significantly higher in Sf9 cells in comparison to the High Five counterpart (Fig. 6).

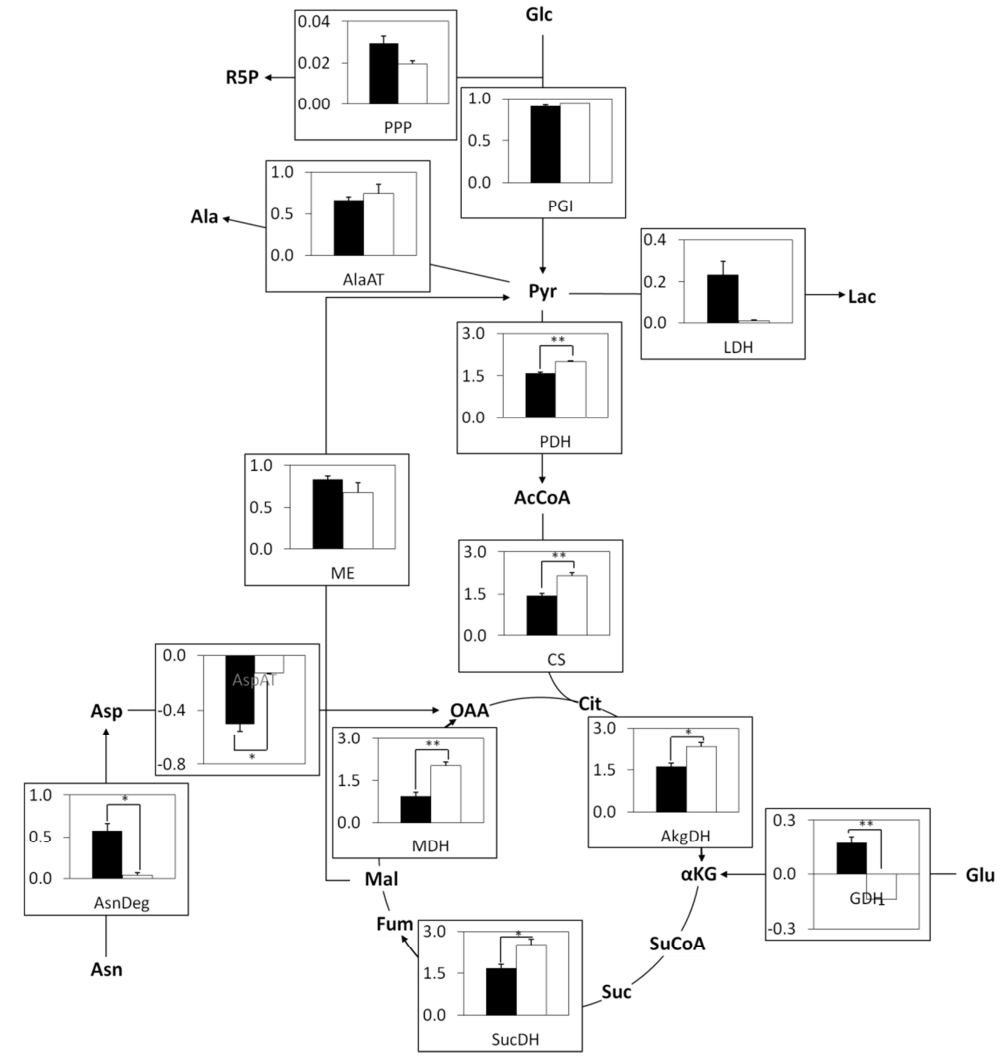

Figure 6. Fluxome distribution of High Five and Sf9 cells after baculovirus infection. High Five (black bars) and Sf9 (white bars) were cultured in Sf900II media and infected with an MOI of 0.2 IP.cell^{-1}, as detailed in the Materials and Methods section. Fluxes were calculated using the FluxAnalyzer software, and normalized by the glucose specific uptake rate. The data presented correspond to three independent cultures (n=3). * $p<0.05$; ** $p<0.01$.

Although the contribution of amino acid catabolism for the energetic metabolism of High Five cells was notorious in non-infected cultures (Fig. 2), the dependence of

such carbon sources after baculovirus infection was lower. In detail, the fluxes of AspAT, GDH and Asparagine degradation reactions were up to 2 fold lower in baculovirus infected High Five cultures (Fig. 6).

Altogether, this means that the activity of the TCA cycle in High Five cells increased after baculovirus infection, and this increase at the expense of amino acid catabolism but due to increased glucose oxidation.

3.7 Metabolic partitioning at the pyruvate and α-ketoglutarate nodes in baculovirus infected Sf9 and High Five cells

The metabolic partitioning coefficients of Sf9 and High Five infected cultures were calculated using the absolute flux values (Table III-2) as inputs.

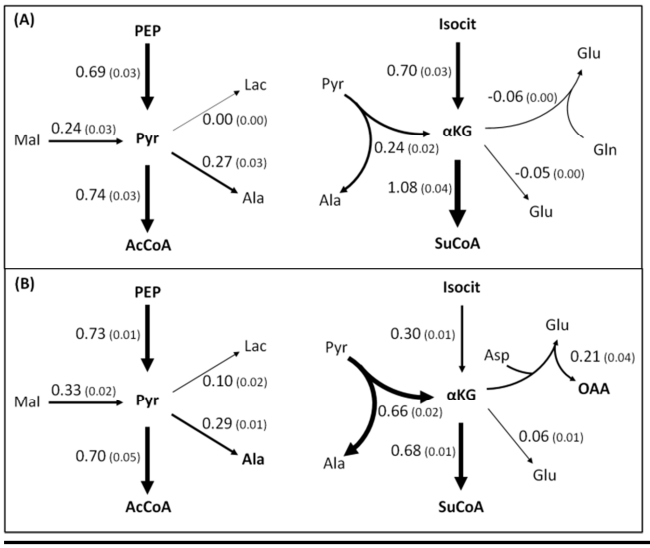

Figure7. Metabolic partitioning at the pyruvate and α-ketoglutarate nodes of Sf9 (A) and High Five (B) cells after baculovirus infection. Cells were infected with MOI of 0.2 IP.cell^{-1}, as detailed above. Partitioning coefficients were calculated as explained in the text (Appendix II). Arrow thickness is representative of the net flow of each reaction. Standard error, in brackets, corresponds to three independent cultures (n=3).

After baculovirus infection, the calculated partitioning coefficients at the pyruvate node were very similar between Sf9 and High Five cells (Fig. 7A and B, respectively). The channeling of 70% of the pyruvate to acetyl-CoA formation in High Five cells was correlated with the lower activity of the AlaAT and LDH, combined with a significant decrease of the anaplerotic flux through ME, as detailed in the previous section. The partitioning of the α-ketoglutarate node of Sf9 cells resembled the high TCA cycle activity (Fig 7A). In High Five cells, the node partitioning reflected the

dependence of amino acid metabolism for the functioning of the TCA cycle, together with the enhanced pyruvate channeling in the TCA cycle (Fig. 7B).

4. Discussion

Productivity is a consequence of the biosynthetic capacity of a host cell, which is ultimately connected to the metabolic state that precludes the production time-frame. When considering virus-based bioprocesses, the virus counterpart needs to be taken into account. In such systems, the relationship that is established between the virus and the host is of paramount importance in dictating the bioprocess outcome and productivity.

It is widely known that High Five cells are better producers of recombinant proteins, and Sf9 cells are more suitable hosts for the production of baculoviral infectious particles (Krammer et al., 2010; Palmberger et al., 2011; Taticek et al., 2001). The reasons behind such cell and target specific productivity phenotypes are still to be disclosed. Both Sf9 and High Five cell lines are susceptible to baculovirus infection, and can sustain the viral replicative cycle towards the generation of newly formed functional virions (Chen et al., 2013; Yamagishi et al., 2003). Thus, no obvious limitations are operating at the molecular level that can constraint virus replication in both cellular systems. Since metabolism and productivity go alongside, a closer look on the main metabolic adaptations that occur in a post-infection scenario can provide clues on cell specific alterations that follow baculovirus infection. In the present study, the application of MFA to the IC-BEVS system was performed to better understand the effect of baculovirus infection on the metabolic status of Sf9 and High Five cells, and how this can affect cellular productivity. A close comparison of the fluxome of both cell lines was attained, and the host-derived adaptations to the infection scenario are discussed.

In comparison to Sf9, High Five cells produced higher amounts of lactate and ammonia throughout culture time. High Five cells were described to have an impaired channeling of the glucose in the TCA cycle, and this can be attributed to a

low activity of the pyruvate dehydrogenase (Neermann and Wagner, 1996). The heterologous expression of pyruvate carboxylase improved glucose oxidation *via* the TCA cycle by 2 fold (Benslimane et al., 2005), but failed at decreasing lactate overflow significantly. Pyruvate carboxylase is an anaplerotic enzyme, replenishing the TCA cycle with intermediates drained by the cell to support the biosynthesis of amino acids. In this work we have assessed that High Five cells catabolize amino acids in order to fulfill this anaplerotic activity, as seen by the high net consumption rates of amino acids and the increased intracellular fluxes of amino acids catabolism. This allowed an increased energy production, and compensates for the limited capacity of High Five cells to drive the consumed glucose to the TCA cycle. Additionally, the contribution of the carbon derived from amino acid sources to the overall TCA cycle activity was significantly higher in High Five cells, with aspartate and glutamate being the main contributors to the net flux throughout the TCA cycle. These two amino acids are derived from asparagine and glutamine, respectively, which are preferentially consumed by High Five cells (Benslimane et al., 2005; Rhiel et al., 1997). Anaplerosis plays a major role in this scenario, with the replenishing of TCA cycle intermediates derived from amino acid catabolism as carbon sinks to be fully oxidized. In fact, the role of anaplerosis in contributing to the TCA cycle, the central energy metabolism pathway, has been documented and recognized (reviewed in Owen et al., 2002).

Baculovirus infection resulted in metabolic rearrangements in Sf9 and High five cells, as illustrated by the changes in the overall fluxome. The net flux of the TCA cycle increased in both cell lines, and to a larger extent in High Five cells. In detail, the fluxes through citrate synthase (CS) and malate dehydrogenase (MDH) suffered the most significant increase, followed by the remaining enzymes of the TCA cycle. Citrate synthase (CS) is a determining step for the channeling of carbon skeletons, together with acetyl-CoA, in the TCA cycle. Thus, higher fluxes of CS will contribute to a higher activity of the cycle, continuously replenishing the cycle with citrate for further oxidation and energy generation. In addition, the higher flux of MDH

indicates that the whole cycle is active and contributing for energy generation. This is the result of the lower contribution of anaplerosis to the activity of the TCA cycle in infected cells. In fact, when amino acid carbon backbones are oxidized in the TCA cycle, only a part of the cycle is used, leading to a partial increase in the fluxes. Metabolism is the result of the fine-tuning of a combination of metabolic reactions that readjust their activity in a dynamic fashion is response to the demand of energy to support biosynthesis. In a post-infection scenario, the energetic needs increase substantially to support the synthesis of the viral components and heterologous gene expression. Thus, it is of no surprise that baculovirus have evolved in the sense to manipulate host cell metabolism to produce higher amounts of ATP to fuel their own needs.

The shift in anaplerotic and amino acid catabolic fluxes observed after baculovirus infection were cell line dependent. The higher activity of the TCA cycle in High Five cells was followed by a decrease in the flux through the anaplerotic reactions (GDH and AspAT), which was coincident with lower amino acid catabolic fluxes. In Sf9 cells the opposite situation was observed, and a higher dependence on the amino acid metabolism to support the high activity of the TCA cycle. Moreover, the nodal analysis at the pyruvate branching point revealed an identical metabolic rearrangement in both cell lines, characterized by similar anaplerotic flux and by-products formation. Although the fluxome rearrangements in both cell lines were different, the final output achieved was very similar in terms of flux partitioning at the pyruvate and α-ketoglutarate nodes, suggesting similar metabolic responses to baculovirus infection.

The net ATP synthesis was always higher in Sf9 cells, either in growth and in baculovirus infected cultures. This was a consequence of the high TCA cycle activity observed in this cell line, a mirror of a very efficient metabolism that characterizes the Sf9 cell line (Bernal et al., 2009). The baculovirus life cycle culminates with the production of newly formed virions that comprise infectious and defective non-infectious particles. By analyzing the infectious to total particles ratio, one can have

an indication of the viral stock quality, which can be affected by the bioprocess performance. While productivity is a consequence of the overall host biosynthetic capacity, product quality is a much more difficult variable to control and predict. Baculovirus stock quality can be influenced by the metabolic state of the producer cell, as productivity and cellular metabolism are correlated processes (Aucoin et al., 2010; Carinhas et al., 2010, 2009). Thus, the increased viral infectivity observed for the virus produced in Sf9 cells might be a result of metabolic state of the producer cell line. However, the cell line itself is determinant for the completion of successful infection cycles, Sf9 cells being more compliant with the baculovirus life cycle progression and particles maturation.

The analysis of the metabolic adaptations undergone by Sf9 and High Five cells performed in this work revealed important differences between central carbon and nitrogen metabolism in both cell lines, especially following baculovirus infection. The strong correlation between the metabolic state of both host cells and baculovirus infection highlights the capacity of these viruses to act as a metabolic engineer, re-directing the cellular fluxome to support viral replication and virions production. MFA is a valuable technique to provide clues on the fluctuations and adaptations of the metabolic portrait of a cell to an external driving force. However, it lacks the capability to discriminate between cause and consequence, for instance if the observed flux alterations are related to lower intracellular substrate pool availability, or even transcriptional, post-transcriptional or post-translational regulation effects, which are known to be effected by virus infection. The combination with other techniques for metabolic inspection, such as metabolomics, is encouraged, and can offer the possibility to identify metabolic constraints and targets for further directed bioprocess optimization.

5. Author contribution

Francisca Monteiro conceived the experimental set-up and design, performed the experiments, analyzed the data and wrote the chapter.

6. References

Aucoin, M.G., Mena, J.A., Kamen, 2010. Bioprocessing of baculovirus vectors: a review. Curr. Gene Ther. 10, 174–186.

Benslimane, C., Elias, C.B., Hawari, J., Kamen, A., 2005. Insights into the central metabolism of Spodoptera frugiperda (Sf-9) and Trichoplusia ni BTI-Tn-5B1-4 (Tn-5) insect cells by radiolabeling studies. Biotechnol. Prog. 21, 78–86.

Bernal, V., Carinhas, N., Yokomizo, A.Y., Carrondo, M.J.T., Alves, P.M., 2009. Cell density effect in the baculovirus-insect cells system: a quantitative analysis of energetic metabolism. Biotechnol. Bioeng. 104, 162–80.

Bernal, V., Monteiro, F., Carinhas, N., Ambrósio, R., Alves, P.M., 2010. An integrated analysis of enzyme activities, cofactor pools and metabolic fluxes in baculovirus-infected Spodoptera frugiperda Sf9 cells. J. Biotechnol. 150, 332–42.

Carinhas, N., Bernal, V., Monteiro, F., Carrondo, M.J.T., Oliveira, R., Alves, P.M., 2010. Improving baculovirus production at high cell density through manipulation of energy metabolism. Metab. Eng. 12, 39–52.

Carinhas, N., Bernal, V., Yokomizo, A.Y., Carrondo, M.J.T., Oliveira, R., Alves, P.M., 2009. Baculovirus production for gene therapy: the role of cell density, multiplicity of infection and medium exchange. Appl. Microbiol. Biotechnol. 81, 1041–9.

Carinhas, N., Duarte, T.M., Barreiro, L.C., Carrondo, M.J.T., Alves, P.M., Teixeira, A.P., 2013. Metabolic signatures of GS-CHO cell clones associated with butyrate treatment and culture phase transition. Biotechnol. Bioeng. 110, 3244–3257. doi:10.1002/bit.24983

Chen, Y.-R., Zhong, S., Fei, Z., Hashimoto, Y., Xiang, J.Z., Zhang, S., Blissard, G.W., 2013. The Transcriptome of the Baculovirus Autographa californica Multiple Nucleopolyhedrovirus in Trichoplusia ni Cells. J. Virol. 87, 6391–6405. doi:10.1128/JVI.00194-13

Chong, W.P.K., Thng, S.H., Hiu, A.P., Lee, D.-Y., Chan, E.C.Y., Ho, Y.S., 2012. LC-MS-based metabolic characterization of high monoclonal antibody-producing Chinese hamster ovary cells. Biotechnol. Bioeng. 109, 3103–11.

Cox, M.M.J., Hollister, J.R., 2009. FluBlok, a next generation influenza vaccine manufactured in insect cells. Biologicals 37, 182–9.

Dean, J., Reddy, P., 2013. Metabolic analysis of antibody producing CHO cells in fed batch production. Biotechnol. Bioeng. 1–42.

Deroo, T., Jou, W.M., Fiers, W., 1996. Recombinant neuraminidase vaccine protects against lethal influenza. Vaccine 14, 561–9.

Dietmair, S., Hodson, M.P., Quek, L.-E., Timmins, N.E., Gray, P., Nielsen, L.K., 2012. A multi-omics analysis of recombinant protein production in Hek293 cells. PLoS One 7, e43394.

Doverskog, M., Jacobsson, U., Chapman, B.E., Kuchel, P.W., Häggström, L., 2000. Determination of NADH-dependent glutamate synthase (GOGAT) in Spodoptera frugiperda (Sf9) insect cells by a selective 1H/15N NMR in vitro assay. J. Biotechnol. 79, 87–97.

Duckwall, C.S., Murphy, T.A., Young, J.D., 2013. Mapping cancer cell metabolism with(13)C flux analysis: Recent progress and future challenges. J. Carcinog. 12, 13. doi:10.4103/1477-3163.115422

Ginkel, M., Dieter, E., Klamt, S., 2003. FluxAnalyzer: exploring structure, pathways, and flux distributions in metabolic networks on interactive flux maps. Bioinformatics 19, 261–269.

Ikonomou, L., Schneider, Y.-J., Agathos, S.N., 2003. Insect cell culture for industrial production of recombinant proteins. Appl. Microbiol. Biotechnol. 62, 1–20.

Khoo, S.H.G., Al-Rubeai, M., 2009. Metabolic characterization of a hyper-productive state in an antibody producing NS0 myeloma cell line. Metab. Eng. 11, 199–211.

Krammer, F., Schinko, T., Palmberger, D., Tauer, C., Messner, P., Grabherr, R., 2010. Trichoplusia ni cells (High Five) are highly efficient for the production of influenza A virus-like particles: a comparison of two insect cell lines as production platforms for influenza vaccines. Mol. Biotechnol. 45, 226–34.

Lowy, D.R., Schiller, J.T., 2006. Prophylactic human papillomavirus vaccines. J. Clin. Invest. 116, 1167–1173.

Martinez, V., Gerdtzen, Z.P., Andrews, B.A., Asenjo, J.A., 2010. Viral vectors for the treatment of alcoholism: use of metabolic flux analysis for cell cultivation and vector production. Metab. Eng. 12, 129–37. doi:10.1016/j.ymben.2009.09.003

Maynard, N.D., Gutschow, M. V, Birch, E.W., Covert, M.W., 2010. The virus as metabolic engineer. Biotechnol. J. 5, 686–94.

Moran, N., 2012. First gene therapy nears landmark European market authorization. Nat. Biotechnol. 30, 807–9. doi:10.1038/nbt0912-807

Munger, J., Bajad, S.U., Coller, H. a, Shenk, T., Rabinowitz, J.D., 2006. Dynamics of the cellular metabolome during human cytomegalovirus infection. PLoS Pathog. 2, e132.

Munger, J., Bennett, B.D., Parikh, A., Feng, X., Rabitz, H.A., Shenk, T., Rabinowitz, J.D., 2010. Systems-level metabolic flux profiling identifies fatty acid synthesis as a target for antiviral therapy. Nat. Biotechnol. 26, 1179–1186.

Neermann, J., Wagner, R., 1996. Comparative analysis of glucose and glutamine metabolism in transformed mammalian cell lines, insect and primary liver cells. J. Cell. Physiol. 166, 152–69.

Niklas, J., Priesnitz, C., Rose, T., Sandig, V., Heinzle, E., 2013. Metabolism and metabolic burden by α1-antitrypsin production in human AGE1.HN cells. Metab. Eng. 16, 103–114.

Owen, O.E., Kalhan, S.C., Hanson, R.W., 2002. The key role of anaplerosis and cataplerosis for citric acid cycle function. J. Biol. Chem. 277, 30409–30412. doi:10.1074/jbc.R200006200

Palmberger, D., Rendić, D., Tauber, P., Krammer, F., Wilson, I.B.H., Grabherr, R., 2011. Insect cells for antibody production: evaluation of an efficient alternative. J. Biotechnol. 153, 160–6.

Rhiel, M., Mitchell-Logean, C.M., Murhammer, D.W., 1997. Comparison of Trichoplusia ni BTI-Tn-5B1-4 (high five) and Spodoptera frugiperda Sf-9 insect cell line metabolism in suspension cultures. Biotechnol. Bioeng. 55, 909–920.

Roldão, A., Oliveira, R., Carrondo, M.J.T., Alves, P.M., 2009. Error assessment in recombinant baculovirus titration: evaluation of different methods. J. Virol. Methods 159, 69–80.

Sauer, U., Zamboni, N., 2008. From biomarkers to integrated network responses. Nat. Biotechnol. 26, 1090–1092. doi:10.1038/nbt1008-1090

Stephanopoulos, G, Aristidou, A.A., Nielsen, J., 1998. Metabolic Engineering. Principles and Methodologies. Academic Press, New York.

Taticek, R.A., Choi, C., Phan, S.E., Palomares, L.A., Shuler, M.L., 2001. Comparison of growth and recombinant protein expression in two different insect cell lines in attached and suspension culture. Biotechnol. Prog. 17, 676–84.

Wang, N., Stephanopoulos, G., 1983. Application of macroscopic balances to the identification of gross measurement errors. Biotechnol. Bioeng. 25, 2177–208.

Wilde, M., Klausberger, M., Palmberger, D., Ernst, W., Grabherr, R., 2014. Tnao38, high five and Sf9--evaluation of host-virus interactions in three different insect cell lines: baculovirus production and recombinant protein expression. Biotechnol. Lett. 36, 743–9. doi:10.1007/s10529-013-1429-6

Yamagishi, J., Isobe, R., Takebuchi, T., Bando, H., 2003. DNA microarrays of baculovirus genomes: differential expression of viral genes in two susceptible insect cell lines. Arch. Virol. 148, 587–97.

Yu, Y., Clippinger, A.J., Alwine, J.C., 2011. Viral effects on metabolism: Changes in glucose and glutamine utilization during human cytomegalovirus infection. Trends Microbiol. 19, 360–367. doi:10.1016/j.tim.2011.04.002

Chapter V

METABOLIC PATHWAY ANALYSIS OF INSECT CELL LINES FOR THE IDENTIFICATION OF PRODUCTIVITY TRAITS

This chapter is adapted from:

Monteiro F, Bernal V, Saelens X, Lozano AB, Bernal C, Sevilla A, Carrondo MJ, Alves PM (2014). Metabolic profiling of insect cell lines: Unveiling cell line determinants behind system's productivity. *Biotechnology and Bioengineering* Apr;111(4):816-28

Abstract

Baculovirus infection boosts the host biosynthetic activity towards the production of viral components and the recombinant protein of interest, hyper-productive phenotypes being the result of a successful adaptation of the cellular network to that scenario. *Spodoptera frugiperda* derived Sf9 and *Trichoplusia ni* derived High Five cell lines have a major track record for the production of recombinant proteins, with High Five cells presenting higher productivities. A metabolic profiling of the two insect cell lines was pursued to underpin specific cellular traits behind productive phenotypes. Multivariate analysis identified cell-line dependent metabolic signatures linked to productivity. Pathway analysis highlighted cellular pathways of paramount importance in supporting infection and protein production. Moreover, better producer phenotypes proved to be correlated with the capacity of cells to shift their metabolism in favor of energy-generating pathways to fuel biosynthesis, a scenario observed in the High Five cell line. Metabolomic profiling allowed us to identify metabolic pathways involved in infection and recombinant protein production, which can be selected as targets for further improvement of the system.

Contents

1. Introduction

The Insect-Cell Baculovirus Expression Vector System (IC-BEVS) is a well-known tool for the production of recombinant proteins (Drugmand et al., 2011). It has shown a high potential for vaccine production, being the production platform for FDA approved human papilloma virus (HPV) and influenza vaccines (Cervarix^{R}, GlaxoSmithKline Biologicals; Flublok^{R}, Protein Sciences Corporation, respectively) (Lowy and Schiller, 2006; Cox and Hollister, 2009). Notwithstanding their powerful production potential, the knowledge on insect cells' physiology and their dynamics after infection is still scarce. Viruses can be understood as metabolic engineers, subverting cellular resources towards optimal replication and progeny generation (Maynard et al., 2010). The success of the IC-BEVS is directly linked with the metabolic state of cells at the moment of infection, along with the virus capacity of redirecting host metabolism to fulfil the increased biosynthetic demands (Bernal et al., 2009; Carinhas et al., 2010). In fact, metabolism can be viewed as the downstream indicator of the intricate regulatory network that governs cellular performance. A profound knowledge of the metabolic cellular state is of paramount importance for the rational design of cell engineering and optimization strategies towards more productive states.

Metabolomics aims at the identification and simultaneous quantification of free low molecular weight metabolite pools, enabling the monitoring of the physiological state of a biological system. Given the correlation between cellular metabolic and physiologic states with productivity, it is easy to understand the relevance of a detailed and comprehensive view of cellular metabolism. Several works have focused on elucidating the correlation between the metabolic portrait of cells and systems productivity (Niklas et al., 2013; Dean and Reddy, 2013; Khoo and Al-Rubeai, 2009; Dietmair et al., 2012b; Chong et al., 2012). Metabolomic studies of mAb producing CHO cell lines linked higher amounts of redox cofactors and sugar precursors pools with better producer phenotypes (Chong et al., 2012). Khoo and Al-Rubeai characterized a hyper-productive state in NS0 antibody producing cell line, and

related increasing lipid, fatty acid metabolism and ascorbate formation as a metabolic adaptation to support protein production (Khoo and Al-Rubeai, 2009). Profiling intra and extracellular metabolites of MDCK cells during influenza infection (Ritter et al., 2010) correlated the impact of infection with the viral life cycle; such time dependences represent an opportunity to fine tune metabolism at time points critical for bioprocess improvement.

Despite the foreseen positive impact, metabolomics has been modestly used in bioprocess development, control and optimization. To the best of our knowledge, an extensive metabolomic characterization of the IC-BEVS systems has never been reported. A focus on hyper-productive states will enable a better understanding of the traits behind phenotype, which can be further used to guide cell engineering. With this aim a thorough characterization was conducted of two insect cell lines with a major track record in the biotechnology industry for virus and recombinant protein production: the *Spodoptera frugiperda* derived Sf9 and *Trichoplusia ni* derived High Five cell lines. Although taxonomically related, they present significantly different productivities, with High Five cells yielding more recombinant proteins regardless of their complexity. A deep metabolic analysis of both cell lines in the context of recombinant production *via* BEVS was pursued, in order to identify specific pathways related to productivity.

2. Materials and Methods

2.1 Cell Line and Cell Culture

Spodoptera frugiperda Sf9 and *Trichoplusia ni* derived BTI-Tn-5B1-4 (High Five) cell lines were obtained from the European Collection of Cell Cultures (No. 89070101, ECACC) and Invitrogen (Paisley, UK), respectively. Cells were routinely cultured in 500 mL Erlenmeyer flasks with 50 mL (working volume) at 27ºC with an agitation rate of 90 rpm, of serum-free SF900II medium (Gibco, Glasgow, UK) for Sf9 cells and Insect Xpress (Lonza, Basel, Switzerland) for High Five. For recombinant protein production exploratory studies, cells were cultured in 15 mL (working volume) in 100 mL shake

flasks. Cell concentration was determined by haemocytometer cell counts (Brandt, Wertheinmain, Germany) and cell viability was evaluated by trypan blue exclusion dye (Merck, Darmstadt, Germany).

2.2 Viruses and Infections

Recombinant *Autographa californica* nucleopolyhedrovirus, containing an inserted gene encoding green fluorescent protein (GFP) under the control of the polyhedrin promoter (BvGFP), was kindly provided by Dr. Monique M. van Oers (Laboratory of Virology, Wageningen University, The Netherlands). Recombinant *Autographa californica* nucleopolyhedrovirus BvtGCN4-NAs contained an inserted gene encoding a secreted form of recombinant influenza N1 type neuraminidase under the control of the polyhedrin promoter. Virus amplification was performed by infection of Sf9 cells at $1x10^6$ cells/mL, at a multiplicity of infection (MOI) of 0.1 pfu/cell in SF900II medium in a spinner flask (Wheaton, Millville, NJ). The amplified viral stocks were stored in culture medium at 4ºC in the dark for a maximum period of 2 to 3 weeks and used for subsequent experiments. Sf9 and High Five cells infection was performed either at a high (5) or a low (0.1) MOI, as indicated in the text. Cell concentrations at infection (CCI) of 1 and 3 x 10^6 cells/mL, were tested to identify the best conditions for protein production. For metabolomic studies, Sf9 and High Five cells were cultured in 500 mL erlenmeyer flasks and infections performed at a MOI of 5 pfu/cell when cells reached 1 x 10^6 cells/mL.

2.3 Baculovirus Titration

Baculovirus titration assays were performed using Sf9 cells. For BvGFP titration, the End Point Dilution method ($TCID_{50}$) based on the detection of GFP fluorescence was used, whereas for BvtGCN4-NAs titration, the MTT method was applied, as described elsewhere (Carinhas et al., 2009; Roldão et al., 2009). Briefly, 100 µl of $0.5x10^6$ cells/mL of Sf9 cells were seeded in 96-weel plates (Nunc, Roskilde, Denmark) and infected with serial dilutions of baculovirus samples. Both positive

(non diluted baculovirus stock) and negative (virus free culture media) controls were performed. For the $TCID_{50}$ method, plates were incubated during 7 days at 27ºC, and the wells were inspected for green fluorescence using a fluorescence microscope (Leica DM IRB, Leica Microsystems GmbH, Wetzlar, Germany). For the MTT assay, plates were incubated during 6 days at 27ºC, after which 0.5 mg/mL of thiazolyl blue tetrazolium bromide (Sigma–Aldrich, St. Louis, USA) were added. After removing the supernatant, the formazan crystals were solubilized with dimethyl sulfoxide (Sigma–Aldrich, St. Louis, USA) and the absorbance (570/690 nm wavelength) was measured using a SPECTRAmax™ microplate reader (Molecular Devices Corporation, Sunnyvale, USA).

The collected data were analyzed using Prism 4 for Windows (Graph-Pad Software Inc., La Jolla, USA) for the tissue culture lethal dose 50 ($TCLD_{50}$) determinations. The conversion of $TCLD_{50}$ to viral titers (pfu/ml) was carried out using the mathematical regressions reported in (Roldão et al., 2009).

2.4 Analytical Methods for extracellular metabolite analysis

Glucose, glutamine, glutamate and lactate concentrations were routinely determined using an YSI 7100 Multiparameter Bioanalytical System (YSI Life Sciences, Dayton, OH). For the analysis of maltose and sucrose, these were enzymatically hydrolyzed and the resulting glucose was measured using the YSI 7100 system. Ammonia was quantified enzymatically using a UV based kit (No. AK00091; NZYTech, Lisbon, Portugal). Amino acids were determined by HPLC after derivatization using the AccQ-Tag Method (Waters, Milford, MA).

2.5 Recombinant protein quantification

GFP quantification was performed with a commercial ELISA kit (No. ab117992, Abcam, Cambridge,UK). The extracellular fraction was measured from culture supernatants. The intracellular fraction was recovered after sonication of cells (Bernal et al., 2010). Briefly, the cellular pellet was resuspended in sonication buffer

(4 mM $MgCl_2$, 2 mM β-mercaptoethanol, 200 mM potassium phosphate buffer (pH 7.5)) and sonicated for 1 min at 10% input power in a sonicator (Branson Ultrasonics Corporation, Danbury, CT). Active/inactive 15 s sonication cycles were alternated. The resulting suspension was clarified by centrifugation (10 min, 10,000×g) and used for quantification. Recombinant neuraminidase (rNeur) was quantified by a fluorimetric-based activity assay, measuring the release of 4-methylumbelliferone (4-MU), as described in Deroo et al., (1996). One unit was defined as that amount of enzyme which releases 1 µmol of 4-MU per min.

2.6 Metabolomic analysis

The metabolomic analysis work-flow comprised four sequential steps: *(i)* Quenching; *(ii)* Extraction; *(iii)* Metabolite analysis and *(iv)* Quality control. A fully detailed protocol is provided in Appendix IV. LC-MS experiments were performed on a 1200 series HPLC instrument (Agilent Technologies; California, USA) coupled to an Agilent 6120 single quadrupole mass spectrometer with orthogonal ESI source. The separation was performed using two different methods based on the chemical classes of the analyzed metabolites. For amino acids and co-enzymes the method previously described in (Preinerstorfer et al., 2010) was applied, using a ZIC-HILIC stationary phase, 150 mm x 4.6 mm internal diameter, and 5 µm particle size, provided with a guard column, 20 x 2.1 mm, 5 µm (Merck SeQuant, Marl, Germany). The mass spectrometer was operated in the positive ESI mode. For organic acids, an Aminex-HPX-87H cation exchange column, 300 x 7.8 mm internal diameter and 9 µm particle size (BioRad Labs, Hercules, USA) was used. The mass spectrometer was operated in the negative ESI mode. The utilized diagnostic ions, their relative intensities, as well as the SIM mode for the m/z of each compound are summarized in Table IV-1. Data were acquired using the Agilent Chemstation software package, and EasyLCMS was used for automated quantification (Fructuoso et al., 2012).

2.7 Statistical analysis

Normalized concentrations of intracellular metabolites (nmol·10^{-6}cells) were uploaded to http://metaboanalyst.ca, an online program for the analysis of metabolomic data (Xia et al., 2009, 2012). The detected remaining missing values (4.1%) were replaced by the half of the minimum positive value in the original uploaded file. The resultant data were normalized by sum and $\log_2$ transformed before advancing to statistical analysis. Multivariate analysis was performed with the purpose of identifying metabolites whose concentrations were significantly different between both cell lines, before and after infection, thus with discriminative potential. Unsupervised principal component analysis (PCA) and supervised partial least squares-discriminant analysis (PLS-DA) were applied. Metabolites with a variance of importance (VIP) scores above 1 were selected as being significantly different between cell lines.

2.8 Pathway Analysis

Pathway analysis was performed using http://metaboanalyst.ca as well, enabling the combination of pathway enrichment analysis with topology analysis (Xia et al., 2009, 2012). The primary goal of such analysis was the identification of the most relevant pathways involved in baculovirus infection and to correlate these with recombinant protein production. Pathway enrichment analysis is a quantitative tool that uses the metabolites concentration values as input, being highly sensitive to identify subtle but consistent changes among compounds involved in the same biological pathway. Pathway topology analysis takes into consideration the network structure of biological pathways, since changes in more important positions of the network will trigger a more severe impact on the pathway than changes occurring in marginal or relatively isolated positions. The pathway library from *Drosophila melanogaster* was used for pathway analysis, one of the reference pathway libraries provided by http://metaboanalyst.ca. The pathway enrichment method used was

Globaltest (Hulsegge et al., 2009), and the node importance measure for topological analysis was relative betweenness centrality.

3. Results

3.1 Growth profiles and recombinant protein production

Specific productivities of Sf9 and High Five cell lines for GFP and recombinant neuraminidase (rNeur) were assessed. To evaluate the impact of culture conditions, namely cell concentration at infection (CCI), multiplicity of infection (MOI) and time of harvest (TOH), recombinant proteins were quantified from intracellular fractions and supernatant samples.

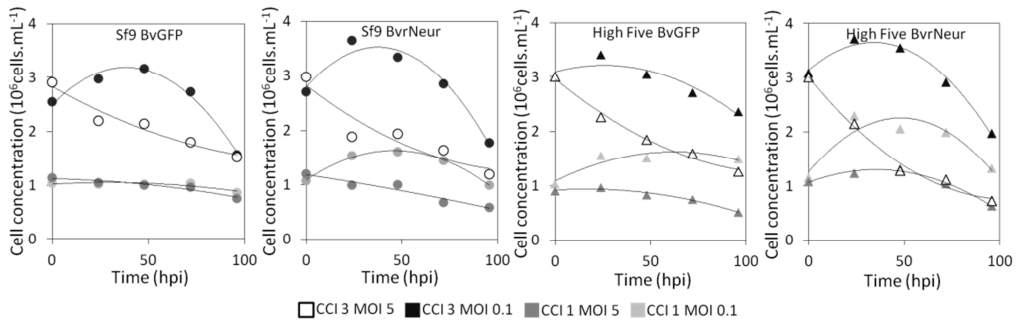

Figure 1. Sf9 and High Five growth profiles during GFP (A, C) and rNeuraminidase (B, D) production, respectively. Infections were performed at a CCI of 1 and CCI 3x106 cells.mL^{-1} with an MOI of 0.1 and 5 IP.cell^{-1}, as indicated above.

Similar growth profiles were obtained for both cell lines independently of the protein expressed (Fig. 1). Higher titers were achieved for CCI 1 and MOI 5 the best TOH being 96 hours post-infection (hpi), at a cellular viability of approximately 60%. Better production yields were observed for High Five (Fig. 2A and B), namely seven fold higher specific productivity for GFP (total, extra- and intracellular) and two times higher for rNeur.

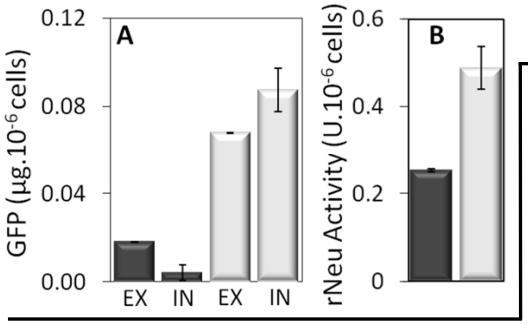

Figure 2. Specific productivities of Sf9 and High Five cell lines for GFP (A) and rNeuraminidase (B). Extracellular GFP (Ext) was quantified in culture supernatant samples and intracellular GFP (Int) after sonication and recovery of the intracellular extract. rNeuraminidase activity was assessed from supernatant samples, as described in the Materials and Methods section. Infections were performed at CCI of $1x10^6$cells.mL^{-1} and MOI of 5 IP.cell^{-1}. The data shown corresponds to 96 hpi. Cultures were run in triplicates; error bars indicate standard deviations of replicate measurements.

To evaluate if the culture medium composition affects cell line productivity, we compared rNeur production in Sf9 grown in Insect Xpress and High Five cells grown in Sf900II. Specific productivities were similar for each cell line regardless of culture media used for all the parameters and conditions tested (Fig. 3).

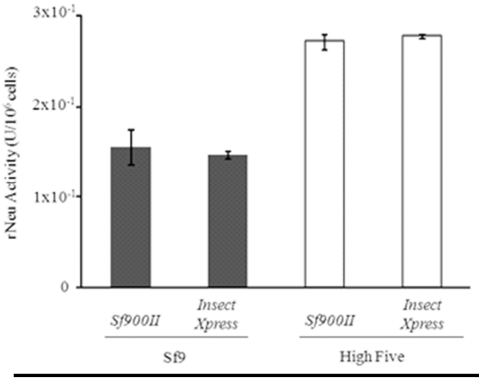

Figure 3. Effect of culture medium composition in Sf9 and High Five specific productivities of rNeuraminidase. Cultures were performed in two different commercial media, Sf900II and Insect Xpress. rNeuraminidase activity was quantified in supernatant samples, as described in the Materials and Methods section. Infections were performed at CCI of $1x10^6$cells.mL^{-1} and MOI of 5 IP.mL^{-1}. The data shown corresponds to samples collected at 96 hpi.

3.2 Exo-metabolome analysis of insect cell lines

The rates of nutrient consumption and by-products accumulation were profiled throughout the culture. The major carbon source consumed by Sf9 cells was glucose, and consumption of alternative sugar sources (maltose and sucrose) was also detected, although at much lower rates (Table 1). In the case of High Five cells, only glucose consumption was detected, although the medium also has sucrose and maltose in its composition. As for the amino acids uptake rates, the specific consumption rate of glutamine, glutamate, asparagine and aspartate, major

substrates for energy-generating cellular processes, both cell lines have similar net (total) consumptions (88 nmol.(10^6cells.h)$^{-1}$). Alanine is a major by-product for both cell lines, with higher production rates for High Five cells. Low levels of ammonia accumulation were seen for Sf9 cells, whereas cultures of High Five cells accumulated 10 to 20-fold more ammonia.

Table 1. Specific growth, consumption or production rates of Sf9 and High Five cells during growth and after baculovirus infection.

	Sf9			High Five		
	Growth	**GFP**	**rNeur**	**Growth**	**GFP**	**rNeur**
	Rate ± SE	**Rate ± SE**	**Rate ± SE**	**Rate ± SE**	**Rate ± SE**	**Rate ± SE**
μ (hr^{-1})	0.02±0.004	*N.A.*	*N.A.*	0.03±0.002	*N.A.*	*N.A.*
Glucose	-48.9±0.7	-41.1±1.4	-47.2±6.8	-91.6±7.0	-134.0±7.2	-148.0±3.4
Lactate	2.3±0.8	8.7±2.1	6.2±2.1	6.9±0.9	8.9±0.4	13.8±0.2
Maltose	-8.5±0.0	-8.4±3.6	-10.6±1.6	*N.A.*	*N.A.*	*N.A.*
Sucrose	-4.2±0.0	-12.3±2.8	-9.7±0.0	*N.A.*	*N.A.*	*N.A.*
Ammonia	4.5±0.8	4.8±1.3	5.2±0.03	56.1±10.4	94.1±8.5	65.2±21.6
Aspartate	-22.9±0.9	-23.8±2.0	-20.6±0.2	-15.5±4.7	-12.2±6.5	-12.7±2.8
Glutamate	-15.3±4.9	-41.1±9.4	-30.0±0.7	-23.8±10.8	-24.9±0.0	-25.7±5.1
Serine	-12.4±2.7	-9.9±5.3	-4.5±0.7	5.0±1.8	21.8±5.4	12.0±8.1
Asparagine	-13.6±7.9	-24.1±8.5	-10.8±6.8	-30.7±10.9	-96.5±14.9	-72.7±44.1
Glycine	-7.0±7.0	-10.2±4.9	-8.6±1.6	-3.3±1.2	-1.1±2.6	-1.3±2.8
Glutamine	-36.1±0.0	-25.6±11.8	-21.3±4.7	-18.1±3.3	-27.1±0.9	-41.2±12.5
Histidine	-3.7±4.0	-3.3±2.4	-2.5±0.3	-1.3±0.6	-0.8±0.7	-1.9±0.9
Threonine	-6.4±2.4	-8.0±2.7	-6.4±0.8	-3.2±1.0	-0.4±2.5	-8.2±0.8
Arginine	-9.4±7.1	-12.0±4.7	-8.8±1.2	-7.3±2.1	-6.0±2.6	-7.7±1.4
Alanine	11.9±7.3	10.6±3.4	17.8±2.6	37.0±11.3	83.0±11.2	75.2±18.5
Proline	-9.0±5.5	-6.9±7.2	-5.6±2.8	-4.9±3.6	-8.4±3.0	-7.6±1.5
Tyrosine	-5.5±4.7	-4.2±0.7	-2.9±0.3	-2.3±0.3	-5.1±3.0	-3.0±0.0
Valine	-9.3±4.5	-14.5±4.6	-8.5±0.6	-3.2±1.9	-4.8±1.3	-6.1±2.4
Metionine	-10.1±9.8	-17.2±4.2	-11.0±4.2	-6.0±4.5	-8.2±2.0	-7.5±0.8
Isoleucine	-7.2±4.8	-16.7±3.8	-10.1±1.0	-5.7±0.0	-4.9±3.3	-6.6±0.9
Leucine	-8.5±3.3	-8.3±1.8	-6.9±1.0	-5.3±1.6	-4.2±2.2	-13.3±1.2
Lysine	-5.8±6.3	-11.1±1.4	-11.1±3.7	-4.6±3.5	-3.0±2.3	-9.0±1.7
Phenylalanine	-11.4±0.0	-14.7±8.4	-12.0±3.5	-2.4±0.0	-5.3±0.0	-5.1±0.8

Cultures were performed as described in Materials and Methods Section. For uninfected cells, the phase concerning exponential growth was considered. For infected cells a single phase after infection (0-72 hpi) was assessed. Rates are expressed as nmol.(10^6cells.h)$^{-1}$.

Regarding the impact of infection on nutrient uptake rates, a distinct behavior was observed between cell lines. The major differences concerning infected and non-

infected (*i.e.* growing) Sf9 cells are related to sucrose and glutamate consumption rates, which increased two to three fold following infection with recombinant baculovirus. All other uptake/production rates varied minimally, *i.e*., between no change and a maximum decrease of 30%. In infected High Five cells the major impact was observed for asparagine consumption, which increased three-fold. With the exception of alanine, glycine, arginine, methionine and isoleucine, the later two increasing 30%, the remaining amino acids showed a two-fold increase in specific uptake rate.

3.3 Endo-metabolome analysis of insect cell lines

Samples from Sf9 and High Five cultures were collected for intracellular metabolite analysis at three time points, corresponding to the early and mid-exponential phases (Fig. 4A and C). For infected cultures, samples were withdrawn at four time points that correlate to the onset of the different steps of the viral infection cycle: immediate early, early, late and very late gene expression (Fig. 4B and D). A total of 63 intracellular metabolites were quantified by LC-MS (Table 2).

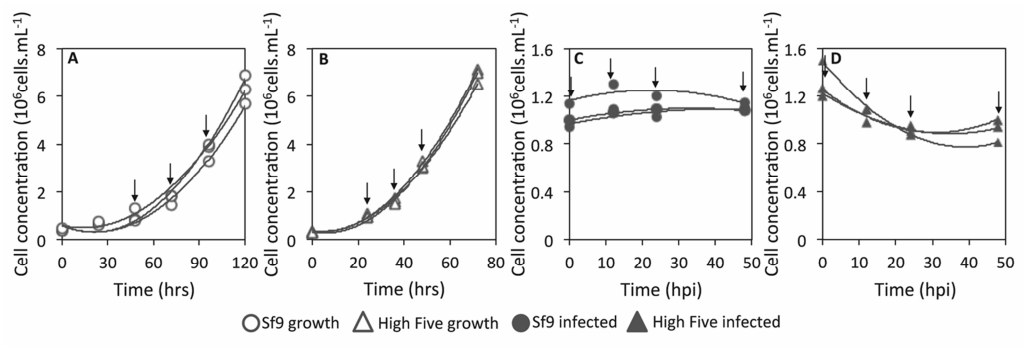

Figure 4. Growth profiles of Sf9 and High Five cells of three independent experiments. Samples for metabolomic experiments of uninfected cultures were withdrawn from initial and mid-exponential phases of culture growth (**A, C**). Samples of infected cultures were taken at key time points of baculovirus life cycle (**B, D**). Infections were performed at a CCI of $1x10^6$ cells.mL^{-1} with an MOI of 5 IP.$cell^{-1}$. Arrows indicate sampling time points.

Metabolite profiles of growing and infected cells were analyzed using multivariate analysis. Both principal component analysis (PCA) and projection to

latent structures – discriminant analysis (PLS-DA) of all samples resulted in clearly separated clusters for each cell line (Fig. 5).

Table 2. List of intracellular metabolites analysed by LC-MS and their respective KEGG ID.

Metabolite name	KEGG ID	Metabolite name	KEGG ID
L-Phenylalanine	C00079	Flavin Mononucleotide	C00061
L-Tryptophan	C00078	NADH	C00004
L-Isoleucine	C00407	Taurine	C00245
Uridine 5'-monophosphate	C00105	Acetyl-CoA	C00024
Biotin	C00120	L-Alanine	C00041
Citicoline	C00307	Coenzyme A	C00010
Cytidine triphosphate	C00063	5-Thymidylic acid	C00364
L-Leucine	C00123	Glutathione	C00051
Citrulline	C00327	L-Glutamine	C00064
Inosinic acid	C00130	Adenosine monophosphate	C00020
Uridine 5'-diphosphate	C00015	NAD	C00003
Adenosine triphosphate	C00002	L-Glutamic acid	C00025
L-Carnitine	C00318	ADP	C00008
Uridine triphosphate	C00075	Thiamine monophosphate	C01081
Cytidine monophosphate	C00055	L-Asparagine	C00152
CDP	C00112	S-Adenosylhomocysteine	C00021
Oxidized glutathione	C00127	Xanthylic acid	C00655
L-Aspartic acid	C00049	L-Proline	C00148
L-Cystine	C00491	L-Arginine	C00062
Glycine	C00037	L-Lysine	C00047
L-Homoserine	C00263	Ornithine	C00077
L-Threonine	C00188	S-Adenosylmethionine	C00019
Hydroxyproline	C01157	L-Serine	C00065
L-Histidine	C00135	Oxoglutaric acid	C00026
Dihydrofolic acid	C00415	Citric acid	C00158
Thymine	C00178	Dihydroxyacetone phosphate	C00111
Thymidine	C00214	Fructose 1,6-bisphosphate	C00354
Hypoxanthine	C00262	Fumaric acid	C00122
L-Tyrosine	C00082	L-Lactic acid	C00186
Homocysteine	C05330	Malic acid	C00149
L-Valine	C00183	Pyruvic acid	C00022
		Succinic acid	C00042

CDP = Cytidine diphosphate; NADH = Nicotinamide adenine dinucleotide reduced; NAD = Nicotinamide adenine dinucleotide; ADP = Adenosine diphosphate.

A total of 10 metabolites were selected by PLS-DA analysis as having a major discriminant weight, with a variable importance/influence to projection (VIP) score > 1 (Table 3). Almost half (4 in 10) of the metabolites identified using PLS-DA comprised nucleotides and their intermediates, more specifically intermediates of the pyrimidine metabolism. With the exception of hypoxanthine and cystine, all were more abundant in High Five cells (Table 3). CMP and CDP nucleotides were present at concentrations ranging from 3 to 4 nmol.10^{-6} cell in High Five cells; however, they were not detected in Sf9 cells meaning that specific concentrations are low thus escaping the detection limit of LC-MS, or their interconversion is so fast that they do not accumulate intracellularly. When analyzing CDP intracellular concentrations after

infection of Sf9 cells, accumulation at low levels (0.3 nmol.10^{-6} cells) was detected at 24 hpi (data not shown).

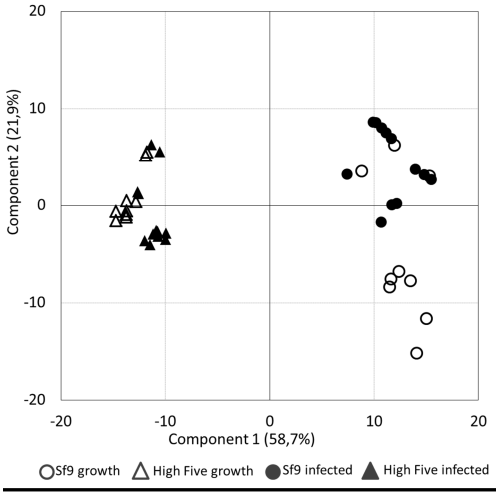

Figure 5. Multivariate analysis of intracellular metabolite concentrations. Projection to latent structures discriminant analysis (PLS-DA) score plot of the first two components of Sf9 and High Five (cells. Filled symbols indicate infected cultures.

Redox balancers and osmolytes accumulation followed a similar trend between cell lines. Taurine was only consistently detected in High Five cells. The GSH/GSSG pool was significantly higher (43-fold) in High Five cells. Also, the S-adenosylmethionine pool (SAM), the major metabolic methylating agent, was significantly higher in the High Five cell line.

Table 3. Metabolites contributing most to discrimination between Sf9 and High Five cell lines according to Projection to latent structures discriminant analysis (PLS-DA) and corresponding fold changes (FC) and relative statistical significance.

	VIP scores	FC	$\log_2$ (FC)	p value	-log p value
CMP	4.3	442	9	2.7E-24	23.6
Taurine	3.7	172	7	1.3E-23	22.9
CDP	2.8	53	6	2.4E-09	8.6
Biotin	2.9	33	5	1.6E-18	17.8
GSSG	1.3	33	5	3.3E-06	5.5
S-Adenosylmethionine	1.1	14	4	9.0E-09	8.0
Thymine	1.1	12	4	2.7E-15	14.6
GSH	1.1	10	3	7.9E-08	7.1
Hypoxanthine	1	0.18	-2	1.1E-05	4.9
L-Cystine	1.3	0.13	-3	8.2E-05	4.1

3.4 Metabolic pathway analysis

In order to disclose the impact of baculovirus infection towards recombinant protein production, PCA of infected versus non-infected Sf9 and High Five cell lines were performed (Fig. 6A and B).

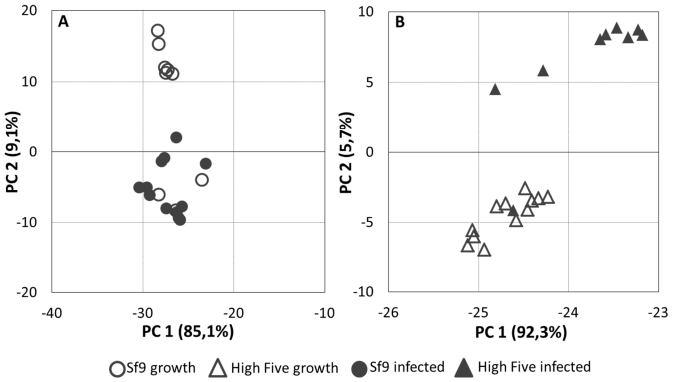

Figure 6. Principal Component analysis (PCA) of intracellular metabolite concentrations of baculovirus infected insect cells. Score plot of the first two principal components of Sf9 (**A**) and High Five (**B**) cells. PCA discriminates infected (●; ▲) from non-infected (○; △) cells, respectively.

Discriminant analysis was unable to totally separate samples from infected and non-infected cultures. This can be related to mild perturbations in intracellular metabolite pools during infection. Therefore, we performed metabolic pathway analysis (MPA) in order to disclose subtle but meaningful alterations in the host cell metabolism. This enabled us to highlight pathways being recruited during infection and protein production. A total of 44 metabolic pathways were identified in Sf9 cells as being altered during infection, but only 19 of them were selected as having statistical significance (Holms adjusted p value (Hp value)<0,05 and FDR<0,003) (Table IV-2, Appendix IV). Half of the routes (10 in 19) were related to amino acids metabolism, either for degradation towards feeding other pathways (*e.g.* TCA cycle), or biosynthesis as product building blocks (Fig. 7A).

Pathway impact is calculated from topology analysis using relative betweenness centrality measures to estimate the importance of node metabolites. The metabolic routes selected with high relevance to sustain infection and recombinant protein production encompass biosynthesis of branched-chain and aromatic amino acids,

together with histidine, glutamine and glutamate metabolism (pathway impact (PI) = 1) (Fig. 7B).

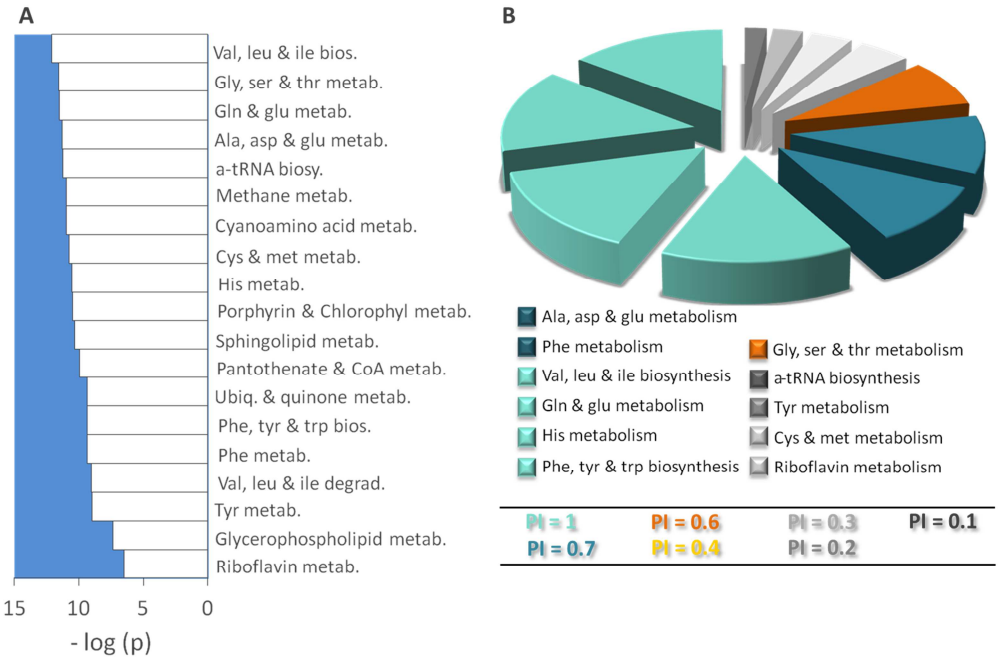

Figure 7. **Metabolic Pathway Analysis of differential intracellular metabolite pools after baculovirus infection of Sf9 cells.** (**A**) Statistical significance and **(B)** Impact level of relevant and significant (p<0,05 and FDR<0,003) metabolic pathways identified using the *Drosophila melanogaster* reference metabolome as the background set. PI-Pathway impact.

Regarding the High Five cell line, MPA identified a total of 45 metabolic routes, but only 31 were statistically significant (Hp value<0,05 and FDR<0,005) (Fig. 8A, Table IV-3, Appendix IV). Biological functions included amino acids metabolism, TCA cycle, glycolysis, glutathione and nicotinamide metabolism, and lipid metabolism. The pathway most affected by infection was biotin metabolism; glutathione, taurine and hypotaurin metabolism also had a considerable impact (PI=0,5) (Figure 8B). The pathways of utmost importance in supporting infection and heterologous protein expression in both cell lines are represented in Figure 9.

Taken together, metabolic pathway analysis underlined conserved patterns regarding viral manipulation of host cell metabolism during infection. However the

extent of such alterations is cell line dependent, which may help to explain the differences in productivities observed.

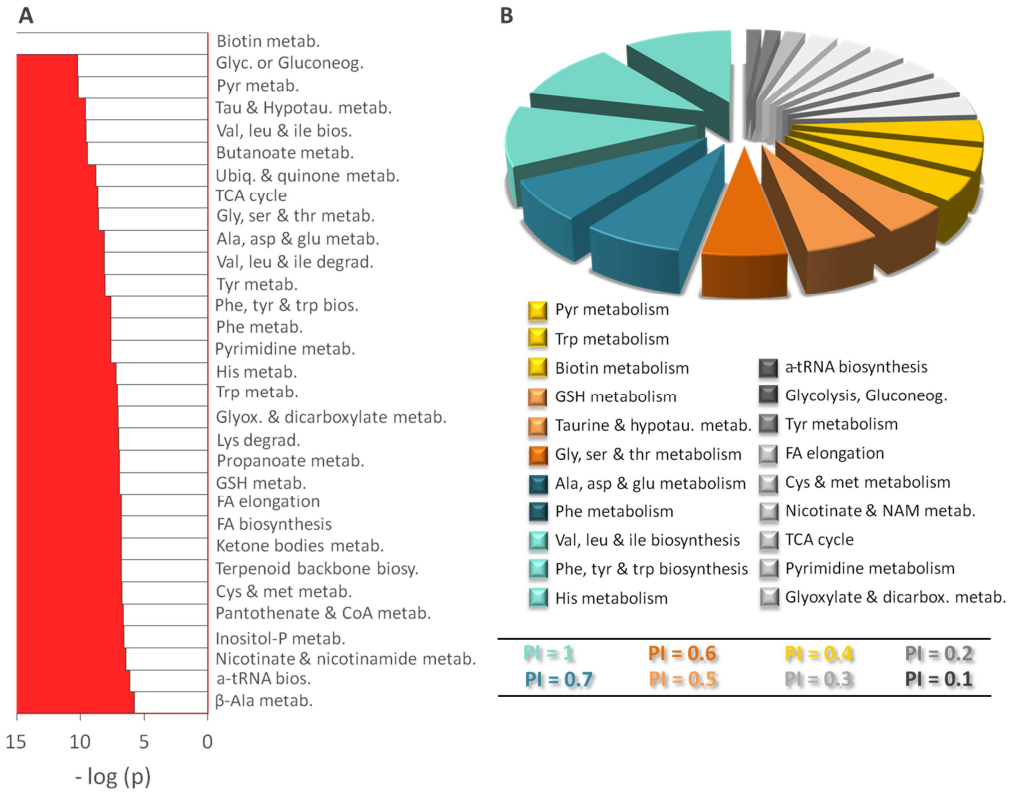

Figure 8. Metabolic Pathway Analysis of differential intracellular metabolite pools after baculovirus infection of High Five cells. (A) Statistical significance and **(B)** Impact level of relevant and significant (p<0,05 and FDR<0,005) metabolic pathways identified using the *Drosophila melanogaster* reference metabolome as the background set. PI-Pathway impact.

4. Discussion

The present study investigated the metabolic differences between two industrially relevant insect cell lines, aiming at identifying metabolic traits related to productivity for further guidance in the rational design of better producer phenotypes. To date, the majority of insect cell studies have focused on the analysis of the system “enviromics”, using the extracellular environment to get an insight of what is happening inside cells (Bernal et al., 2009; Carinhas et al., 2010; Benslimane et al., 2005). Although these strategies permit an overview of cell metabolism, a

deeper study is required to obtain an accurate perspective about cellular physiology and its dynamics.

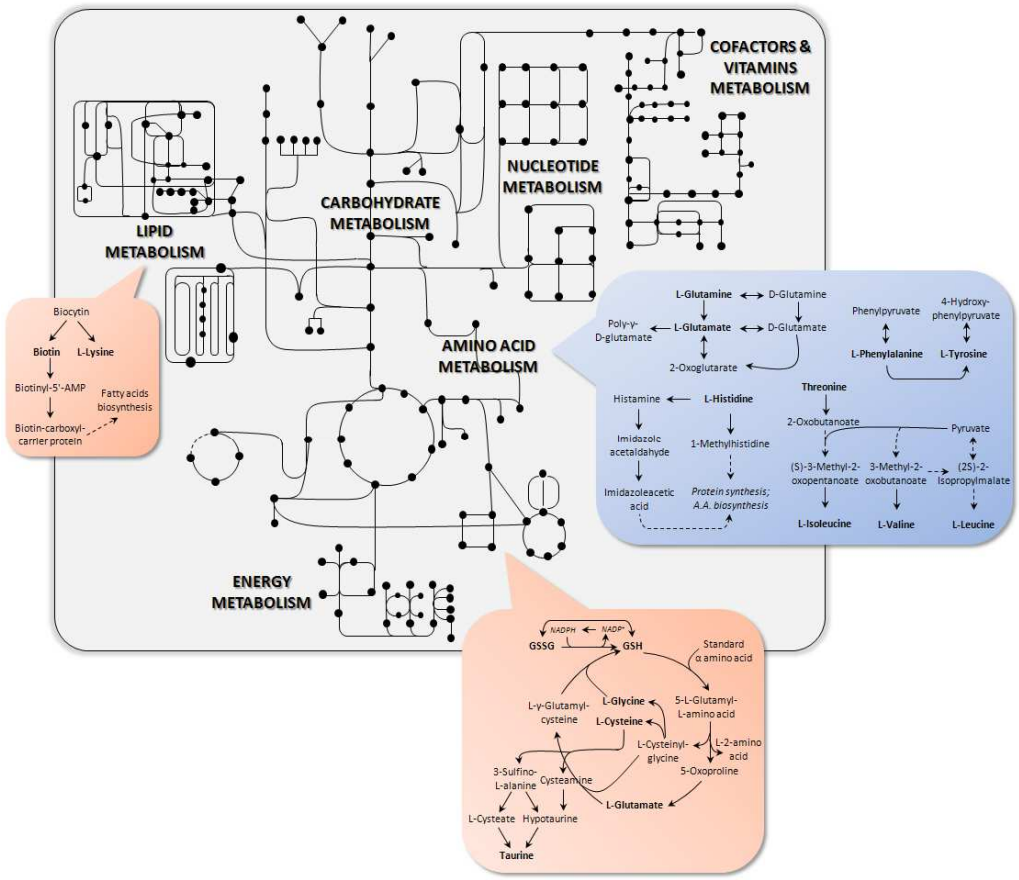

Figure 9. **Metabolic pathways of utmost importance in supporting baculovirus infection and recombinant protein production in insect cells.** In blue are depicted the pathways highlighted for both Sf9 and High Five cells and in orange pathways recruited only in High Five cells.

Protein production assays showed that, regardless of infection strategies and protein complexity, High Five cells outperformed, with specific productivities consistently higher than Sf9 cells. Several reports in the literature have shown that the High Five cell line is a better host when dealing with recombinant protein production (Taticek et al., 2001; Drugmand et al., 2011).

Extracellular metabolite profiling revealed cell line specific signatures regarding by-products accumulation and particular amino acid uptake rates. High Five cells

produced high levels of lactate, ammonia and alanine, a behavior that, with the exception of alanine, is not shown by Sf9 cells, at least in such an extent. Previous work by Benslimane et al., (2005) showed that High Five cells have a low pyruvate carboxylase (PC) activity. However, overexpression of PC did not succeed in diminishing lactate accumulation. In fact, what is limiting the metabolization of pyruvate towards entrance in the TCA cycle is most probably the pyruvate dehydrogenase complex (Icard and Lincet, 2012; Marín-Hernandez et al., 2009). Doverskog et al. (2000) realized that Sf9 cells, but not High Five, possess a system of ammonia recycling and detoxification guided by a glutamate synthase (GOGAT) (Doverskog et al., 2000). In this way, they are able to re-use the nitrogen assimilated in glutamine and glutamate *via* glutamine synthetase (GS), by reductive transfer of the amide nitrogen of glutamine to 2-oxoglutarate *via* GOGAT (Suzuki and Knaff, 2005). This enzyme is absent in mammalian cells and, in insect cells, it was only proven to be present in *S. frugiperda* derived cell lines. The total consumption of the major amino acids involved in the support of energy-generating cellular processes (glutamate, glutamine, aspartate and asparagine) was equal in both cell lines. However, when looking in detail to the individual consumption rates, each cell line presents an individual pattern. As previously described, glutamine is consumed at a larger extent by Sf9 cells, and asparagine is preferably consumed by High Five cells (Rhiel et al., 1997; Benslimane et al., 2005). Moreover, this is not a consequence of the availability of each of the amino acids in culture media, since they are provided in similar concentrations to both cell lines.

Concerning their metabolic portrait, major differences emerged regarding redox homeostasis, osmotic shock regulatory pathways and pyrimidine metabolism. GSH and GSSG intracellular pools were significantly higher in High Five cells. Glutathione metabolism is associated with the removal of reactive oxygen species (ROS) (O'Donovan and Fernandes, 2000) and protein folding and assembly, reducing the disulfide bonds formed within cytoplasmic proteins (Dalle-Donne et al., 2009). Also, taurine, a semi-essential sulfur-containing amino acid known as a membrane

stabilizer, osmoregulator and antioxidant (Huxtable, 1992), was only detected in High Five cells. Cellular energy generation and oxidative stress are correlated processes. Actually, mitochondrial respiration is a major cellular source of ROS (Turrens, 2003), and it is postulated that high recombinant protein producers experience increased aerobic metabolism that would result in greater ROS generation. Sf9 and High Five cell lines are equipped with a myriad of antioxidant enzymes (manganese dismutase, copper-zinc dismutase, ascorbate peroxidase, glutathione reductases, dehydroascorbate reductases, etc..) that act in concert to deal with the increased levels of oxidative stress that occur as a result of baculovirus infection (Wang et al., 2001b, 2001a). Although manganese dismutase and ascorbate peroxidase remained active following infection in both cell lines, the specific activities (U/mg protein) were higher in High Five cells. Moreover, this cell line has an extra enzyme responsible for dealing with ROS generation, catalase, which activity was not detected in the Sf9 cells (Wang et al., 2001b).

Altogether, the above-mentioned traits indicate that High Five cells are better suited to cope with proteotoxic stress that can further justify the higher protein production yields. Multivariate analysis also identified pyrimidine metabolism intermediates, such as CMP, CDP and thymine, as being present in superior concentrations in High Five cells. Pyrimidine synthesis is directly linked to cellular growth rate, and several authors could relate pyrimidine nucleotides content in CHO cells with growth rate and culture phase (Chen et al., 2012; Dietmair et al., 2012a). Thus, the nucleotides content can account for the differences in growth rate observed between High Five and Sf9 cell lines.

When looking for the pathways with highest importance in sustaining infection towards recombinant protein production, similar trends appeared in both cell lines, suggesting the presence of conserved mechanisms in host cell metabolism towards a productive state. More specifically, the metabolism of branched-chain (BCAA) and aromatic amino acids (AAA) is of utmost importance, and coincides with the amino acid uptake rates increased after infection. BCAA metabolism yields acyl-CoA

derivatives that can be fed into the TCA cycle or fatty acid oxidation (Voet and Voet, 1995), meaning that it can support the energetic demand imposed by infection. In an animal cell, protein synthesis consumes 20-25% of total cellular energy (Schmidt, 1999), a requirement that is substantially increased when dealing with heterologous protein production. Dietmar et al (2012) found that, despite higher amino acid uptake and downregulation of BCAA degradation pathways, the majority of intracellular amino acid concentrations were lower in HEK293 producer cultures, which could be related to a higher utilization of amino acids for recombinant protein production (Dietmair et al., 2012b). Nguyen et al (2012) showed that, upon infection, transcript levels of BCAA and AAA degradation enzymes were down-regulated in a *Helicoverpa zea* cell line (Nguyen et al., 2012). However, when analyzing the expression levels of several enzymes of the tRNA charging pathway, they were up-regulated with a 1.2 to 2.6 fold increase. A similar behavior may occur upon baculovirus infection in our insect cell lines. In fact, aminoacyl t-RNA biosynthesis pathway is being regulated during infection in both cell lines, further supporting an increased biosynthetic activity.

Pathway impact analysis showed that, in the Sf9 cells, 85% of the identified metabolic routes were related to amino acid metabolism; however, in the High Five cells they only accounted for 48%, indicating that infection impact is much more extensive in the latter. Both cell lines are susceptible to baculovirus infection, and have been extensively used as hosts for viral propagation and amplification. They both accommodate high expression levels of viral and recombinant protein genes, however present distinct phenotypes regarding protein productivities and infectious viral titers. High Five cells are better recombinant protein producers, and Sf9 cells yield more infectious virus (Wang et al., 1992; Krammer et al., 2010). Analyzing the data herein presented, it seems that upon infection High Five cells devote a significant quota of cellular resources to sustain the demand for the biosynthesis of viral components and recombinant protein. Moreover, a decay in the majority of the intracellular metabolite pools identified was observed after infection. For the Sf9

infected cells, only a small percentage of intracellular pools diminished, a scenario that is reflected in the pathway analysis, identifying a smaller number of pathways as being hired by the virus. Metabolically speaking, Sf9 cells are less affected by infection due to a reduced burden inherent to extensive protein synthesis. This behavior suggests that High Five cells re-orient their metabolism towards hyper-production of viral and recombinant proteins to such an extent that they can no longer support the productive assembly and maturation of infectious virus.

Previous work by Wang and coworkers revealed that insect cells experience an increased oxidative stress provoked by baculovirus infection (Wang et al., 2001b). Moreover, the ability to deal with increased dissolved oxygen concentrations is cell line dependent and is somehow related to productivity (Saarinen and Murhammer, 2003). In fact, by over-expressing manganese superoxide dismutase the oxidative damage was significantly decreased in baculovirus infected High Five cells (Wang et al., 2004). Our results emphasize that redox homeostasis is of extreme importance in assisting cellular performance and productivity, thus a critical point for systems engineering. Any boost in productivity will certainly go along with an increased burden on the energetic capacity of the cell. To circumvent the later, media optimization strategies can be applied, with a special focus on nutrients and/or pathways that are known to be highly connective to systems productivity. The specific metabolic routes selected during MPA constitute the targets for optimization, and feeding strategies are being designed on the basis of the gained knowledge.

This work focused on the metabolic characterization of two commercial insect cell lines, Sf9 and High Five, which have achieved great popularity in the biotechnological field. Clonal selection and lab to lab variability of insect cell lines may influence several parameters, such as productivity, fluxes and metabolite pools (Jarman-Smith et al., 2002, 2004). Moreover, differences in cell size can hinder the productivity phenotype, since it is a direct function of the cell productive volume (Bédard et al., 1993; Taticek et al., 2001). Although we have analyzed cellular volume

during both growth and infection, we observe that the impact of the differences in volume is minor. Specifically, the differences that we point out during our exo-metabolome analysis as being significant between cell lines are maintained. Likewise, our endo-metabolome analysis gave similar outputs, which indicates that the differences that we observe are physiological relevant and meaningful.

The extensive metabolic characterization pursued in this work helped us gaining insights concerning specific cellular traits connective with the productive phenotype. Moreover, the results herein presented pave the way in deepening our knowledge on the IC-BEVS, highlighting the importance of the host cell physiology on the system's performance and outcome.

5. Conclusions

The present study links the metabolic portrait of two insect cell lines with their productivity phenotype. An in depth-metabolomic analysis of Sf9 and High Five cell lines in the context of baculovirus infection gave significantly distinct outputs that mirror cell line-dependent productivity. Infection impact is considerably higher in High Five cells, with a myriad of metabolic pathways being hijacked to support massive production. This cell line proved to be able to re-orient its metabolic activity towards the increased biosynthetic activity, a behavior that seems to be on the basis of its higher productive phenotype.

The "metabolomic decomposition" of the IC-BEVS pursued in this work not only identified traits leveraging productivity, but also specific pathways of utmost importance to support it.

6. Acknowledgments

This work was supported by *PTDC/EBB-EBI/103359/2008, FP7/HEALTH.2011.1.1-1/279039*, MICINN (Spain)/FEDER-EU BIO2011-29233-C02-01, MINECO (Spain) BIO2012-38103, Fundación Séneca (Murcia, Spain) 08660/PI/08 and 12031/PI/09

projects. Francisca Monteiro acknowledges FCT for her PhD fellowship grant (SFRH/BD/7013/2010), Vicente Bernal acknowledges a postdoctoral contract from Universidad de Murcia (Programa Propio), Angel Sevilla a post-doctoral contract from MICINN (Juan de la Cierva program) and Inbionova Biotech S.L. C.B acknowledges the FPU fellowships from MICINN (Spain). The authors are thankful to Prof. Cánovas (University of Murcia, Spain) for allowing us to perform part of this research in his laboratory, to Dr. Monique van Oers (University of Wageningen, Netherlands) for the kind gift of the recombinant GFP-expressing baculovirus, and to Ana Filipa Rodrigues for fruitful discussions during the preparation of this manuscript. The authors declare that there are no conflicts of interest.

7. Author contribution

Francisca Monteiro conceived the experimental set-up and design, performed part of the experiments, analyzed the data and wrote the chapter.

8. References

Bédard, C., Tom, R., and Kamen, A. (1993). Growth, nutrient consumption, and end-product accumulation in Sf-9 and BTI-EAA insect cell cultures: insights into growth limitation and metabolism. *Biotechnology progress* 9, 615–24.

Benslimane, C., Elias, C. B., Hawari, J., and Kamen, A. (2005). Insights into the central metabolism of Spodoptera frugiperda (Sf-9) and Trichoplusia ni BTI-Tn-5B1-4 (Tn-5) insect cells by radiolabeling studies. *Biotechnology Progress* 21, 78–86.

Bernal, V., Carinhas, N., Yokomizo, A. Y., Carrondo, M. J. T., and Alves, P. M. (2009). Cell density effect in the baculovirus-insect cells system: a quantitative analysis of energetic metabolism. *Biotechnology and bioengineering* 104, 162–80.

Bernal, V., Monteiro, F., Carinhas, N., Ambrósio, R., and Alves, P. M. (2010). An integrated analysis of enzyme activities, cofactor pools and metabolic fluxes in baculovirus-infected Spodoptera frugiperda Sf9 cells. *Journal of biotechnology* 150, 332–42.

Carinhas, N., Bernal, V., Monteiro, F., Carrondo, M. J. T., Oliveira, R., and Alves, P. M. (2010). Improving baculovirus production at high cell density through manipulation of energy metabolism. *Metabolic engineering* 12, 39–52.

Carinhas, N., Bernal, V., Yokomizo, A. Y., Carrondo, M. J. T., Oliveira, R., and Alves, P. M. (2009). Baculovirus production for gene therapy: the role of cell density, multiplicity of infection and medium exchange. *Applied microbiology and biotechnology* 81, 1041–9.

Chen, F., Fan, L., Wang, J., Zhou, Y., Ye, Z., Zhao, L., and Tan, W.-S. (2012). Insight into the roles of hypoxanthine and thymidine [corrected] on cultivating antibody-producing CHO cells: cell growth, antibody production and long-term stability. *Applied microbiology and biotechnology* 93, 169–78.

Chong, W. P. K., Thng, S. H., Hiu, A. P., Lee, D.-Y., Chan, E. C. Y., and Ho, Y. S. (2012). LC-MS-based metabolic characterization of high monoclonal antibody-producing Chinese hamster ovary cells. *Biotechnology and bioengineering* 109, 3103–11.

Cox, M. M. J., and Hollister, J. R. (2009). FluBlok, a next generation influenza vaccine manufactured in insect cells. *Biologicals : journal of the International Association of Biological Standardization* 37, 182–9.

Dalle-Donne, I., Rossi, R., Colombo, G., Giustarini, D., and Milzani, A. (2009). Protein S-glutathionylation: a regulatory device from bacteria to humans. *Trends in Biochemical Sciences* 34, 85–96.

Dean, J., and Reddy, P. (2013). Metabolic analysis of antibody producing CHO cells in fed batch production. *Biotechnology and bioengineering*, 1–42.

Deroo, T., Jou, W. M., and Fiers, W. (1996). Recombinant neuraminidase vaccine protects against lethal influenza. *Vaccine* 14, 561–9.

Dietmair, S., Hodson, M. P., Quek, L.-E., Timmins, N. E., Chrysanthopoulos, P., John, S. S., Gray, P., and Nielsen, L. K. (2012a). Metabolite profiling of CHO cells with different growth characteristics. *Biotechnology and bioengineering* 109, 1404–1414.

Dietmair, S., Hodson, M. P., Quek, L.-E., Timmins, N. E., Gray, P., and Nielsen, L. K. (2012b). A multi-omics analysis of recombinant protein production in Hek293 cells. *PloS one* 7, e43394.

Doverskog, M., Jacobsson, U., Chapman, B. E., Kuchel, P. W., and Häggström, L. (2000). Determination of NADH-dependent glutamate synthase (GOGAT) in Spodoptera frugiperda (Sf9) insect cells by a selective 1H/15N NMR in vitro assay. *Journal of biotechnology* 79, 87–97.

Drugmand, J.-C., Schneider, Y.-J., and Agathos, S. (2011). Insect cells as factories for biomanufacturing. *Biotechnology advances*.

Fructuoso, S., Sevilla, A., Bernal, C., Lozano, A. B., Iborra, J. L., and Cánovas, M. (2012). EasyLCMS: an asynchronous web application for the automated quantification of LC-MS data. *BMC research notes* 5, 428.

Hulsegge, I., Kommadath, A., and Smits, M. a (2009). Globaltest and GOEAST: two different approaches for Gene Ontology analysis. *BMC proceedings* 3 Suppl 4, S10.

Huxtable, R. J. (1992). Physiological actions of taurine. *Physiological Reviews* 72, 101–163.

Icard, P., and Lincet, H. (2012). A global view of the biochemical pathways involved in the regulation of the metabolism of cancer cells. *Biochimica et biophysica acta* 1826, 423–33.

Jarman-Smith, R. F., Armstrong, S. J., Mannix, C. J., and Al-Rubeai, M. (2002). Chromosome instability in Spodoptera frugiperda Sf-9 cell line. *Biotechnology progress* 18, 623–8.

Jarman-Smith, R. F., Mannix, C., and Al-Rubeai, M. (2004). Characterisation of Tetraploid and Diploid Clones of Spodoptera frugiperda Cell Line. *Cytotechnology* 44, 15–25.

Khoo, S. H. G., and Al-Rubeai, M. (2009). Metabolic characterization of a hyper-productive state in an antibody producing NS0 myeloma cell line. *Metabolic engineering* 11, 199–211.

Krammer, F., Schinko, T., Palmberger, D., Tauer, C., Messner, P., and Grabherr, R. (2010). Trichoplusia ni cells (High Five) are highly efficient for the production of influenza A virus-like particles: a comparison of two insect cell lines as production platforms for influenza vaccines. *Molecular biotechnology* 45, 226–34.

Lowy, D. R., and Schiller, J. T. (2006). Prophylactic human papillomavirus vaccines. *Journal of Clinical Investigation* 116, 1167–1173.

Marín-Hernandez, A., Gallardo-Pérez, J., Ralph, S., Rodrígues-Enríquez, S., and Moreno-Sánchez, R. (2009). HIF-1alpha modulates energy metabolism in cancer cells by inducing over-expression of specific glycolytic isoforms. *Mini-reviews in Medicinal Chemistry* 9, 1084–101.

Maynard, N. D., Gutschow, M. V, Birch, E. W., and Covert, M. W. (2010). The virus as metabolic engineer. *Biotechnology journal* 5, 686–94.

Nguyen, Q., Palfreyman, R. W., Chan, L. C. L., Reid, S., and Nielsen, L. K. (2012). Transcriptome Sequencing of and Microarray Development for a Helicoverpa zea Cell Line to Investigate In Vitro Insect Cell-Baculovirus Interactions. *PloS one* 7, e36324.

Niklas, J., Priesnitz, C., Rose, T., Sandig, V., and Heinzle, E. (2013). Metabolism and metabolic burden by α1-antitrypsin production in human AGE1.HN cells.pdf. *Metabolic engineering*.

O'Donovan, D. J., and Fernandes, C. J. (2000). Mitochondrial glutathione and oxidative stress: implications for pulmonary oxygen toxicity in premature infants. *Molecular Genetics and Metabolism* 71, 352–358.

Palmberger, D., Rendić, D., Tauber, P., Krammer, F., Wilson, I. B. H., and Grabherr, R. (2011). Insect cells for antibody production: evaluation of an efficient alternative. *Journal of biotechnology* 153, 160–6.

Preinerstorfer, B., Schiesel, S., Lämmerhofer, M., and Lindner, W. (2010). Metabolic profiling of intracellular metabolites in fermentation broths from beta-lactam antibiotics production by liquid chromatography-tandem mass spectrometry methods. *Journal of chromatography. A* 1217, 312–28.

Rhiel, M., Mitchell-Logean, C. M., and Murhammer, D. W. (1997). Comparison of Trichoplusia ni BTI-Tn-5B1-4 (high five) and Spodoptera frugiperda Sf-9 insect cell line metabolism in suspension cultures. *Biotechnology and Bioengineering* 55, 909–920.

Ritter, J. B., Wahl, A. S., Freund, S., Genzel, Y., and Reichl, U. (2010). Metabolic effects of influenza virus infection in cultured animal cells: Intra- and extracellular metabolite profiling. *BMC systems biology* 4, 61.

Roldão, A., Oliveira, R., Carrondo, M. J. T., and Alves, P. M. (2009). Error assessment in recombinant baculovirus titration: evaluation of different methods. *Journal of virological methods* 159, 69–80.

Saarinen, M. a, and Murhammer, D. W. (2003). The response of virally infected insect cells to dissolved oxygen concentration: recombinant protein production and oxidative damage. *Biotechnology and bioengineering* 81, 106–14.

Schmidt, E. V (1999). The role of c-myc in cellular growth control. *Oncogene* 18, 2988–2996.

Selvarasu, S., Ho, Y. S., Chong, W. P. K., Wong, N. S. C., Yusufi, F. N. K., Lee, Y. Y., Yap, M. G. S., and Lee, D.-Y. (2012). Combined in silico modeling and metabolomics analysis to characterize fed-batch CHO cell culture. *Biotechnology and bioengineering* 109, 1415–29.

Suzuki, A., and Knaff, D. B. (2005). Glutamate synthase: structural, mechanistic and regulatory properties, and role in the amino acid metabolism. *Photosynthesis Research* 83, 191–217.

Taticek, R. a, Choi, C., Phan, S. E., Palomares, L. a, and Shuler, M. L. (2001). Comparison of growth and recombinant protein expression in two different insect cell lines in attached and suspension culture. *Biotechnology progress* 17, 676–84.

Turrens, J. F. (2003). Mitochondrial formation of reactive oxygen species. *The Journal of Physiology* 552, 335–344.

Voet, D., and Voet, J. G. (1995). *Biochemistry*. Second. , ed. J. & S. Wiley New York: Jonh Wiley & Sons, Inc.

Wang, P., Granados, R. R., and Shuler, M. L. (1992). Studies on serum-free culture of insect cells for virus propagation and recombinant protein production. *Journal of invertebrate pathology* 59, 46–53.

Wang, Y., Oberley, L. W., Howe, D., Jarvis, D. L., Chauhan, G., and Murhammer, D. W. (2004). Effect of expression of manganese superoxide dismutase in baculovirus-infected insect cells. *Applied Biochemistry And Biotechnology* 119, 181–193.

Wang, Y., Oberley, L. W., and Murhammer, D. W. (2001a). Antioxidant defense systems of two lipidopteran insect cell lines. *Free radical biology & medicine* 30, 1254–62.

Wang, Y., Oberley, L. W., and Murhammer, D. W. (2001b). Evidence of oxidative stress following the viral infection of two lepidopteran insect cell lines. *Free Radical Biology & Medicine* 31, 1448–1455.

Xia, J., Mandal, R., Sinelnikov, I. V, Broadhurst, D., and Wishart, D. S. (2012). MetaboAnalyst 2.0--a comprehensive server for metabolomic data analysis. *Nucleic Acids Research* 40, 1–7.

Xia, J., Psychogios, N., Young, N., and Wishart, D. S. (2009). MetaboAnalyst: a web server for metabolomic data analysis and interpretation. *Nucleic Acids Research* 37, W652–W660.

Chapter VI

TACKLING BOTTLENECKS IN IC-BEVS: ENHANCING PRODUCTIVITY BY TARGETED SUPPLEMENTATION DESIGN

This chapter is based on data to be published as:

Tackling bottlenecks in IC-BEVS: Enhancing enveloped viral particles production by targeted supplementation design

Francisca Monteiro, Vicente Bernal, Maxime Chaillet, Imre Berge rand Paula M. Alves (*under revision*)

Abstract

The increasing demand of Insect Cell-Baculovirus Expression Vector System (IC-BEVS) based biopharmaceuticals raises the interest in developing high-titer production processes. Previously, we addressed the impact of the baculovirus infection on the physiology of High Five and Sf9 host cell lines, stressing out key cellular features that support higher productivities. This information was applied to design tailored supplementation schemes to boost IC-BEVS production yields of three targets with increasing complexity: recombinant influenza neuraminidase (rNeur); enveloped influenza VLPs (Inf-VLP) and the baculovirus itself (BV). Higher rNeur productivities were achieved when supplementing High Five cultures with cholesterol. For Sf9 cells, GSH, antioxidants combined with polyamines and cholesterol yielded the best outputs during Inf-VLPs and infectious BVs production. The results also show that the viral load influence the cellular responsiveness to the supplements, with lower MOIs retrieving higher improvements of IC-BEVS specific productivity. The careful selection of the MOI in a batch infection process, along with the supplementation of culture medium with compounds altering cellular redox state and cholesterol, yielded an improvement of the systems' specific productivity up to 6 fold. The correlation between systems productivity, host cell line and target product was extensively analyzed. The resulting implications for the development of rational strategies for increased productivity are discussed.

Contents

1. Introduction

The Insect Cell-Baculovirus Expression Vector System (IC-BEVS) is a powerful tool for the production of recombinant proteins, virus like particles (VLPs) and vectors for gene therapy (reviewed in Van Oers et al., 2014; Liu et al., 2013; Airenne et al., 2013). Being the production platform of several human therapeutics already in the market, namely Cervarix® (GlaxoSmithKline Biologics); Flublok® (Protein Sciences Corporation); Glybera® (UniQure) (Lowy and Schiller, 2006; Cox and Hollister, 2009; Moran, 2012), the IC-BEVS is placed on the frontline of both pharmaceutical and biotechnological fields. Moreover, as the market of IC-BEVS based biopharmaceuticals develops (Ylä-Herttuala, 2012; Lu et al., 2012), the interest in developing high-titer production processes is expected to rise. Although progress has been made in tuning the baculovirus to accommodate the expression of more challenging targets (Bieniossek et al., 2012; Palmberger et al., 2013), only a minor focus has been pointed into the insect host cell. We still experience a significant lack of knowledge on insect cells' physiology and their dynamics after infection, which hampers the rational design of optimization plans.

Growing knowledge about the physiological requirements that sustain biosynthesis turns possible the manipulation and improvement of cell-based bioprocesses (Lim et al., 2010). While a significant amount of resources has been devoted to boost production of recombinant proteins, a limited amount of studies have dealt with the constraints of producing more complex biopharmaceuticals, such as virus like particles (VLPs) and enveloped viral vectors (Rodrigues et al., 2014). Virus-based bioprocesses depend on the interaction established between the virus and the host cell line of choice. By studying such interaction, the cellular pathways required to sustain infection and productivity can be identified, and this information applied in the development of strategies aimed to improve bioprocess performance. Although a limited number of studies have dealt with the interpretation of viral-host interactions for bioprocess applications, some noteworthy examples can be found in

the literature (Henry et al., 2005; Ferreira et al., 2005; Martinez et al., 2010; Rodrigues et al., 2013).

Molecular biology studies have provided exciting discoveries on baculovirus–host interactions (reviewed in Monteiro et al., 2012). However, the biological constraints that govern baculovirus infection in the biotechnological context are poorly understood. The analysis of cell culture parameters and media components influencing productivity has turned possible the implementation of high cell density bioprocesses with increased and sustained production of recombinant proteins *via* BEVS (Bédard et al., 1997; Chan et al., 1998; Chiou et al., 2000). The combination of metabolic flux analysis with the rational design of a feeding strategy led to the improvement of baculovirus yields (6- to 7-fold) in high cell density cultures (Carinhas et al., 2010). Also, the on-line monitoring of the oxygen uptake rate (OUR) in baculovirus infected insect cells led to the design of feeding strategies able to boost up to 13 times the recombinant protein yields (Palomares et al., 2004). Although meaningful, this approaches relied on the interpretation of the culture environment and empirical knowledge as decision makers to drive bioprocess optimization. Notwithstanding, the application of metabolic and bioprocess engineering strategies to the IC-BEVS shows potential and attractiveness, and can profit from a deeper analysis of the system.

It is well established that Sf9 cells are a preferred host for the production of functional baculovirus vectors and High Five for the expression of recombinant proteins (Taticek et al., 2001; Wilde et al., 2014). Previously, we addressed the comparison of the metabolome of Sf9 and High Five host cell lines during the production of a recombinant protein *via* baculovirus expression (Monteiro et al., 2014). An *in silico* based pathway analysis identified which were the metabolic routes of utmost importance in sustaining productivity in both cell lines (Monteiro et al., 2014), selected as targets for further improvement of the system. The maintenance of anti-oxidant defenses and redox homeostasis driven by glutathione seemed to be pivotal to support increased biosynthesis, as also observed in other production

systems (Orellana et al., 2015). The replenishing of nucleic acids precursors is also key is assisting virus-based bioprocesses, and their combination with polyamines have given valuable improvements on the production of enveloped viruses (Rodrigues et al., 2013). In addition, membrane stabilizers and co-factors of lipid metabolism were identified as being correlated with productivity, such as taurine and biotin. The importance of lipid and cholesterol metabolism has been recognized for the production of enveloped viral particles in mammalian culture systems (Chan et al., 2010), and should also be investigated in the IC-BEVS.

In the present work, we designed culture supplementation schemes aiming to reinforce the metabolic pathways previously identified as being related to IC-BEVS productivity. The selected supplements were evaluated for the production of three target products with increasing complexity: recombinant influenza neuraminidase (rNeur); enveloped influenza VLPs (Inf VLPs) and the baculovirus itself (BV). An orthogonal screening of culture conditions was performed, in order to identify the best culture setting leading to maximal productivity in the two host cell lines, Sf9 and High Five. In addition, a special focus on the characteristics of the target product was pursued, and the implementation of an optimized bioprocess for the production of enveloped viral particles was implemented.

2. Materials and methods

2.1 Cell lines and culture maintenance

Spodoptera frugiperda derived Sf9 cell line was obtained from the European Collection of Cell Cultures (No. 89070101, ECCAC) and *Trichoplusia ni* derived BTI-Tn-5B1-4 (High Five) obtained from Invitrogen (Paisley, UK). The cells were maintained in serum- and protein-free Sf900II insect cell medium (Gibco, Glasgow, UK). Cells were cultured in 500 mL Erlenmeyer flasks (Corning, USA) with 50 mL working volume. Cultures were kept in a humidified incubator operated at 90 rpm and at 27ºC. For maintenance, Sf9 and High Five cells were re-inoculated every 3-4 days at $0.45x10^5$ cells.mL^{-1} and 0.3×10^5 cells.mL^{-1}, respectively. Cell concentration was determined by

hemocytometer cell counts (Brandt, Wertheinmain, Germany) and cell viability evaluated by the trypan blue exclusion method (Merck, Darmstadt, Germany).

2.2 Baculoviruses and viral stock preparation

The recombinant *Autographa californica* nucleopolyhedrovirus BvGCN4-NA1, kindly provided by Dr. Xavier Saelens (Ghent University, Belgium), contains an inserted gene encoding a secreted form of influenza N1 type neuraminidase under the control of the polyhedrin promoter (Deroo et al., 1996). BvGCN4-NA1 was used as the expression vector for recombinant Neuraminidase (rNeur) throughout the work. The recombinant *Autographa californica* nucleopolyhedrovirus BvHA5M1 is a dual baculovirus, encoding two influenza genes: Hemagglutinin type 5 (HA5), under the control of the polyhedrin promoter, and matrix protein 1 (M1), under the control of the p10 promoter. BvHA5M1 was used throughout the work as the expression vector of the multimeric influenza enveloped VLPs (Inf-VLPs).

BvGCN4-NA1 was amplified by infecting Sf9 cells at $1x10^6$cells.mL^{-1} with a MOI of 0.1 IP.$cell^{-1}$ in 1 L Erlenmeyers (Corning, USA). BvHA5M1 was amplified by infecting Sf9 cells at $1x10^6$cells.mL^{-1} with a MOI of 0.01 IP.$cell^{-1}$ in a 10 L bioreactor (ED10, Sartorius AG, Goettingen, Germany). In order to have a highly concentrated final viral stock, a polyethylene glycol (PEG)-based concentration process was applied. Briefly, virus-containing culture supernatant was mixed with 8.5% (v/v) of a sterile PEG solution, previously prepared in phosphate buffer saline (PBS), and incubated overnight at 4ºC. Afterwards, the mixture was centrifuged at 3200xg for 30 min at 4ºC, and the collected precipitate containing the baculovirus was resuspended in 0.5 M sucrose. Care was taken in evaluating the stability and infectivity of the viral preparations after the concentration process (data not shown). The concentrated viral stocks were aliquoted and kept at -80ºC until further use.

2.3 Baculovirus titration and total particles quantification

Baculovirus infectious particles titration was performed following the MTT assay as previously described in Roldão et al. (2009).

The concentration of total baculovirus particles was measured using Nanosight NS500 (Nanosight Ltd., Salisbury, UK), making use of the Nanoparticle Tracking Analysis (NTA) functionality. The quantification of the baculovirus samples in culture supernatants was done taking into account the Nanosight sensitivity, *i.e.*, diluting the samples to a concentration of 1 to $9x10^8$ total particles (TP) per mL in phosphate buffer saline (PBS). The average size of purified Inf-VLPs samples and baculovirus was characterized for the determination of the gates for both particles quantification (data not shown). To exclude the effect of cellular debris, exosomes, and other soluble factors that can interfere with the accuracy of the measurements, appropriate controls were performed (supernatant of non-infected cultures at the correspondent cell densities). The measurements were performed at least in triplicates with a typical standard deviation (SD) below 20%.

2.4 Supplements preparation

The culture supplements tested are listed in Table 1. The supplements concentration was set taking into account the manufacturer instructions and preliminary assays of their impact in the specific productivity and cellular viability of both Sf9 and High Five cells (data not shown).

Supplements were prepared in Sf900II insect culture media (Gibco), and stored at -20 or 4ºC according to the manufacturer instructions. Cholesterol supplementation was performed in combination with 0.4 $mg.L^{-1}$ albumin (112018010, Merck Millipore, Billerica, MA, USA) as a carrier.

Table 1. Composition of culture medium supplements

Supplement	Abbreviation	Supplement final concentration	Supplier	Reference
Antioxidants	AOx	1 X	Sigma (Steinheim, Germany)	A1345
Biotin	Bio	10 µM	Sigma	B4639
Cholesterol	Chol	1 X	Gibco (Glasgow, UK)	12531-018
Lipids	Lip	1 X	Gibco	11905-031
Nucleosides	Nucl	1 X	Merck Millipore	ES-008-D
Polyamines	Poly	1 X	Sigma	P8483
Reduced glutathione	GSH	1 mM	Sigma	G1404
Taurine	Tau	10 mM	Sigma	T8691

Supplements were prepared or added to the final desired concentration to Sf900II insect culture media (Gibco), and stored at -20 or 4ºC according to the manufacturer instructions.

2.5 Cell growth, infection and production studies

In the present work, three culture settings were used as detailed in the schematic representation (Fig. 1). Firstly, we exploited the screening potential of the Ambr culture system (TAP Biosystems, Cambridge, UK) to define the best host for the production of the three different targets analyzed in combination with defined medium supplements. Sf9 and High Five cells were inoculated at 0.5 and $0.4x10^6$ cells.mL^{-1}, respectively. The bioreactors were displayed in two independent culture stations operated at 1400 rpm and kept at a constant temperature of 27ºC. Dissolved oxygen (DO) and pH were monitored throughout the culture time. Critical values that could compromise cellular performance were not reached during cultures. Infections were performed once the cell density reached approximately $1x10^6$ cells.mL^{-1} with MOIs 0.2, 1 and 5 IP.cell^{-1}.

An extensive screening was further on pursued to disclose specific requirements of each target in their better producing host cell line. This study was performed in 100 mL Erlenmeyer flasks (Corning, USA) with a working volume of 10 mL. Similarly to the Ambr cultures, Sf9 and High Five cells were inoculated at 0.5 and $0.4x10^6$ cells.mL^{-1}, respectively, and infected with the same set of MOIs at $1x10^6$ cells.mL^{-1}. High Five

cells were infected with BvGCN4-NA1 expressing rNeur and Sf9 with BvHA5M1 expressing influenza VLPs. In order to evaluate if synergistic effects of a combined supplementation strategy would occur, the combination of culture supplements was performed at this same scale, fixing the MOI at 0.2 IP.cell^{-1} of BvHA5M1 in Sf9 cells.

Finally, the best culture condition yielding the highest increase in the specific productivity of enveloped viral particles (Inf-VLPs and baculovirus) was implemented in a 0.5 L stirred tank bioreactor (BIOSTAT® QPlus, Sartorius AG, Goettingen, Germany). DO was set to 30% of air saturation and controlled by sequential N_2-stirring-O_2 cascade mode with 0.01 vvm gas flow rate. Temperature was set to 27ºC and the operation was performed within a stirring range of 90-180 rpm. Sf9 cells were inoculated at 0.5x10^6 cells.mL^{-1} and infected with an MOI of 0.2 IP.cell^{-1} of the BvHA5M1, 24 hours after inoculation when cell concentration reached approximately 1x10^6 cells.mL^{-1}.

For all culture settings, supplements were added twice, at inoculation and infection times, and their final concentrations are detailed in Table 1. In all cultures, the appropriate controls were performed, *i.e.*, non-supplemented cultures infected with the same set of MOIs. During the screening in Erlenmeyer flasks, controls were performed at least in duplicate, and in triplicate for the infections performed at a MOI of 0.2 IP.cell^{-1}. Cultures were sampled every 24 hours to check for cell concentration and viability. In the productivity assays, samples were collected at 48 hours post-infection (hpi), the time after which the expression from the polyhedrin and p10 promoters reaches its maximum. Moreover, in this specific timing, cellular viability was kept above 70% to avoid contamination of cell lysis products that could lead to the misinterpretation of the results. In the bioreactor cultures, the productivity was assessed throughout the timeline of the entire process (up to 96 hpi) to have a detailed overview of process kinetics.

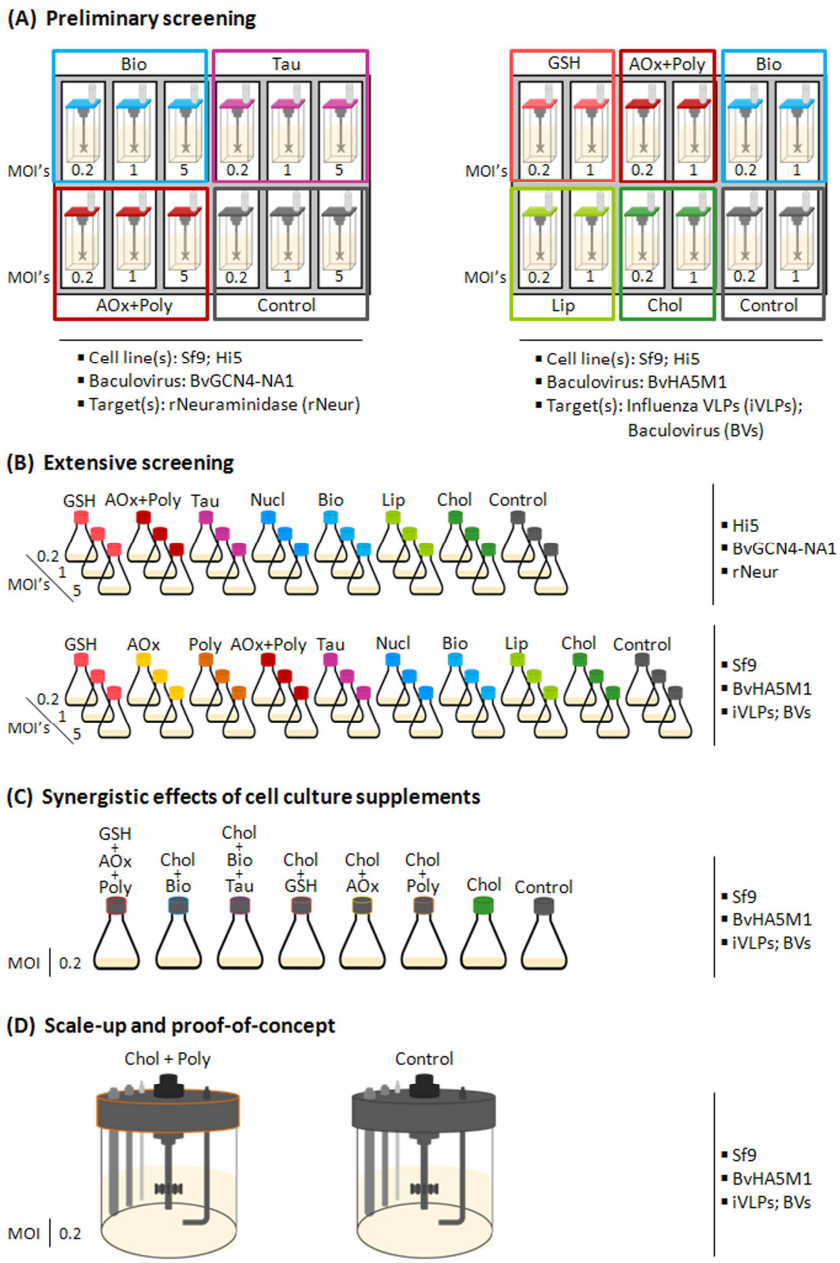

Figure 1. Schematic representation of the experimental workflow. The preliminary screening of culture supplements **(A)** was performed in the TAP Ambr system, the extensive screening **(B)** and the analysis of the synergistic effects **(C)** were performed in Erlenmeyers and the scale-up **(D)** in 0.5 L stirred tank bioreactors. Cell lines used, as well as the baculovirus and target products analyzed are indicated. The culture conditions are shown at the right side of the figure, including the MOIs used and the supplements added to cultures. Abbreviations: GSH, reduced glutathione; AOx, antioxidants; Poly, polyamines; Tau, taurine; Nucl, nucleosides; Bio, biotin; Lip, lipids; Chol, cholesterol.

2.6 Quantification of Recombinant Neuraminidase

Recombinant Neuraminidase (rNeur) was quantified by a fluorimetric enzyme activity assay measuring the release of 4-methylumberlliferone (4-MU), as described in Deroo et al (1996). The rNeuraminidase activity assay was performed in culture supernatant samples. One unit (U) was defined as the amount of enzyme that releases 1 µmol of 4-MU *per* minute.

2.7 Influenza VLPs quantification

The quantification of the influenza VLPs (Inf-VLPs) was performed through a solid phase sandwich ELISA (SEK002, Sino Biological Inc., Beijing, China) specific for the hemagglutinin (HA) displayed on the surface of the particles. The assay was performed according to the instructions of the manufacturer. The assay proved to be sensitive enough to quantify HA in supernatant samples.

2.8 Stability assays in supplemented media

Culture supernatants containing each target product (rNeur or BVs) were incubated with the supplements at the same concentration added to the cultures for production studies. Stability assays were performed at 27ºC during 48 hours, the time during which the production studies were performed. Afterwards, the respective analytical methods were performed to measure either rNeur activity or BVs infectious titers, as explained above. Appropriate controls were performed, subjected to the same incubation time in non-supplemented media.

2.9 Statistical analysis

Hypothesis testing was performed using Student's t-test. A 95% confidence interval was considered to be statistically significant.

3. Results

3.1 Media manipulation strategies affect cell growth without compromising cell viability and product stability

The growth rate of Sf9 and High Five cells was assessed in supplemented cultures, and the results are detailed in Table 2. We observed that supplements influence specific growth rate, mainly GSH, antioxidants, polyamines and cholesterol, and this negative effect is cell line dependent.

To discriminate if product titers were affected by stabilization/destabilization effects of supplements, we assessed their impact on product stability. rNeur and BVs were quantified after incubation with the tested supplements, as explained in the Materials and Methods section. These two targets were selected since their quantification is based on functional assays (enzyme activity assay for rNeur, and infection assay for the BVs). Thus, any possible loss in stability would be immediately translated into a decrease in product functionality, easily identified by the analytical methods applied. None of the supplements tested had a negative effect on the stability of rNeur and infectious BVs (Appendix V, Supplementary Figs. V-1 and V-2, respectively). Together, these results show that any possible effects observed by the supplements tested should be related with their impact on the specific productivities of Sf9 and High Five cells, rather than alteration of product stability.

3.2 Host cell line influences systems' responsiveness to the supplementation strategy in a target product-dependent manner

To investigate the influence of the host cell on IC-BEVS productivity, the production of rNeur, Inf-VLPs and BVs was evaluated in Sf9 and High Five cell lines (Table 2, Figs. 2 and 3). The results obtained show that Sf9 cells produce more infectious baculovirus vectors and High Five cells higher levels of recombinant protein, which is in accordance with previous reports (reviewed in Drugmand et al., 2012).

	High Five						Sf9							
Supplement	μ[a]	PDT[b]	MOI	Cell density at harvest[c]	rNeur Volumetric titer[d]	rNeur Yield[e]	μ[a]	PDT[b]	MOI	Cell density at harvest[c]	Inf-VLP Volumetric titer[f]	Inf-VLP Yield[g]	BVs Volumetric titer[h]	BVs Yield[i]
GSH	0.033**±0.001	15±1	0.2	1.9	0.42±0.03	0.23±0.02	0.012**±0.001	44**±2	0.2	0.91	0.56±0.02	0.63±0.03	3.32±0.00	3.70±0.00
			1	1.8	0.52±0.05	0.27±0.03			1	0.95	1.01±0.10	1.13±0.11	4.44±0.21	4.97±0.24
			5	1.5	0.57±0.06	0.36±0.04			5	0.79	3.85±0.53	4.39±0.60	7.39±0.54	8.43±0.62
Antioxidants	N.D.		0.2	N.D.			0.008**±0.002	51**±2	0.2	0.73	0.59±0.02	0.76±0.03	2.67±0.05	3.47±0.07
			1						1	0.73	1.13±0.11	1.42±0.14	6.35±2.31	7.97±2.90
			5						5	0.94	5.11±0.70	5.72±0.78	7.52±1.28	8.42±1.43
Polyamines	N.D.		0.2	N.D.			0.006*±0.002	96±24	0.2	0.6	0.57±0.02	0.86±0.04	3.65±0.44	5.50±0.66
			1						1	0.65	1.37±0.14	1.64±0.16	2.90±0.47	3.48±0.56
			5						5	0.55	4.48±0.61	7.77±1.06	7.67±1.19	13.29±2.06
Antioxidants + Polyamines	0.040±0.001	17*±0	0.2	2.0	0.50±0.02	0.26±0.01	0.012±0.003	38**±1	0.2	0.81	0.52±0.02	0.51±0.02	4.80±0.13	4.71±0.13
			1	1.7	0.53±0.05	0.29±0.03			1	0.99	1.01±0.10	1.04±0.10	4.48±0.50	4.65±0.52
			5	1.6	0.54±0.05	0.31±0.03			5	0.89	4.47±0.61	4.49±0.61	16.99±0.15	17.05±0.15
Taurine	0.040±0.01	18*±0	0.2	1.8	0.34±0.02	0.18±0.01	0.018±0.004	38±6	0.2	1.05	0.66±0.03	0.65±0.03	3.78±0.62	3.72±0.61
			1	1.5	0.38±0.02	0.24±0.01			1	1.1	2.89±0.29	2.34±0.23	4.68±1.98	3.80±1.60
			5	1.3	0.46±0.03	0.29±0.02			5	1.08	5.39±0.74	5.33±0.73	6.28±1.34	6.21±1.32
Nucleosides	0.046±0.001	19±1	0.2	1.9	0.38±0.03	0.22±0.02	0.024±0.003	24±3	0.2	1.05	0.50±0.02	0.46±0.02	2.38±0.12	2.20±0.11
			1	2.0	0.49±0.04	0.26±0.02			1	0.92	2.34±0.23	2.27±0.23	5.82±0.61	5.63±0.42
			5	1.6	0.43±0.03	0.26±0.02			5	1.04	5.28±0.72	5.27±0.72	8.42±1.08	8.39±1.07
Biotin	0.036±0.003	18**±0	0.2	2.0	0.40±0.02	0.21±0.01	0.013±0.003	47±7	0.2	0.98	0.60±0.03	0.59±0.02	2.50±0.47	2.44±0.46
			1	1.7	0.42±0.03	0.26±0.02			1	0.96	2.67±0.27	2.46±0.25	5.89±0.11	5.44±0.11
			5	1.6	0.46±0.03	0.28±0.02			5	0.93	5.74±0.79	5.76±0.79	6.51±0.46	6.53±0.46
Lipids	0.040±0.003	14**±0	0.2	2.3	0.48±0.04	0.24±0.02	0.020±0.002	26±2	0.2	1.11	0.45±0.02	0.41±0.02	3.57±0.14	3.25±0.12
			1	1.8	0.48±0.03	0.26±0.02			1	1.18	2.08±0.21	1.62±0.16	5.52±0.50	4.30±0.39
			5	1.7	0.50±0.04	0.31±0.02			5	1.07	4.02±0.55	3.73±0.51	6.36±1.73	5.91±1.61
Cholesterol	0.042±0.001	13**±0	0.2	1.9	0.63±0.04	0.34±0.02	-0.004±0.000	N.A.	0.2	0.33	0.53±0.02	1.67±0.07	4.35±2.60	8.29±1.64
			1	1.6	0.64±0.04	0.36±0.02			1	0.32	2.86±0.29	7.95±0.79	2.18±0.61	6.06±1.69
			5	1.3	0.65±0.04	0.42±0.02			5	0.24	12.16±1.67	28.73±3.94	4.37±0.64	10.33±1.52
Control	0.041±0.001	16±0	0.2	2.1	0.37±0.03	0.19±0.01	0.022±0.001	23±1	0.2	1.1	0.45±0.06	0.40±0.1	1.98±0.75	1.78±0.09
			1	2.0	0.42±0.03	0.21±0.02			1	1.0	0.99±0.53	1.52±0.6	2.90±0.49	2.89±0.14
			5	2.0	0.48±0.05	0.25±0.02			5	1.0	4.38±0.59	4.52±0.4	6.12±0.62	5.69±0.19

Units - [a]μ - Specific growth rate (h^{-1}); [b]PDT - Population doubling time (h); [c]10^6cells.ml^{-1}; [d]U.mL^{-1}; [e]U.10^{-6}cells; [f]ngHA.mL^{-1}; [g]ngHA.10^{-6}cells; [h]10^6IPs.mL^{-1}; [i]IPs.$cell^{-1}$. The growth rate and PDT were calculated in the exponential phase of cellular growth after an incubation period of 24 hours with the indicated supplements. Values are shown as average ± SD (n=3). For infected cultures, samples were collected at 48 hpi and analyzed for the production of rNeur, Inf-VLPs and infectious BVs (IP). *p value<0.05; **p value<0.01.

To address the impact of targeted environmental manipulations on IC-BEVS productivity, we conducted a preliminary screening of cell culture supplements added to Sf9 and High Five cells cultured in the Ambr culture system. The production of rNeur, Inf-VLPs and BVs was assessed under different MOIs (0.2, 1 and 5 IP.cell^{-1}), and the three targets were quantified in supernatant samples from infected cultures at 48 hpi. Cultures infected at lower MOIs reach maximal productivity later than high MOI infections. The main aim of the work was to evaluate if the selected supplements could improve productivity, either by enhancing cellular production or increasing the volumetric titers by promoting cellular growth. Thus, the tested supplements exert their effect on the producer cell from the beginning of infection, and this effect can be noticed at 48 hpi. The supplements tested are listed in Table 1, and the results summarized in Appendix V, Supplementary Figures V-3 and V-4 for Sf9 and High Five cells, respectively.

Overall, we obtained higher increases in the specific yields of rNeur in High Five supplemented cultures (Supplementary Fig. V-4A) and only modest increases in the specific yields of enveloped viral particles (Supplementary Fig. V-4B and V-4C). Cholesterol was an exception, since it improved the specific yields of Inf-VLPs by 8–fold (Supplementary Fig. V-4C). In opposition, we obtained negligible improvements in the specific yields of rNeur in Sf9 supplemented cultures (Supplementary Fig. V-3A), however for enveloped viral particles (Inf-VLPs and BVs) we achieved up to 4-fold increase (Supplementary Fig. V-3B and V-3C). Although cholesterol supplementation resulted in higher specific yields of enveloped viral particles, this was not the case for the final volumetric titers. This effect was more pronounced in the Sf9 cell line (Supplementary Fig. V-4C), and reflects the arrest in cell growth after cholesterol supplementation (Table 2).

Our data evidence the host dependent productivity phenotype, with High Five cells being better producers of recombinant proteins and Sf9 cells yielding higher quantities of infectious baculovirus. This host-target related phenotype is also maintained in supplemented cultures, and the better producer hosts for each target

respond with higher improvements accordingly. Thus, since the most interesting results were obtained for High Five when producing rNeur and Sf9 when producing enveloped viral particles (both Inf-VLPs and BVs) we decided to further analyze these two study cases.

3.3 Extended media manipulation strategies evidence host specific requirements to assist productivity in a target-oriented perspective

High Five cells were supplemented with seven culture additives (Table 1), and their impact on the production of rNeur was assessed (Table 2 and Fig. 2).

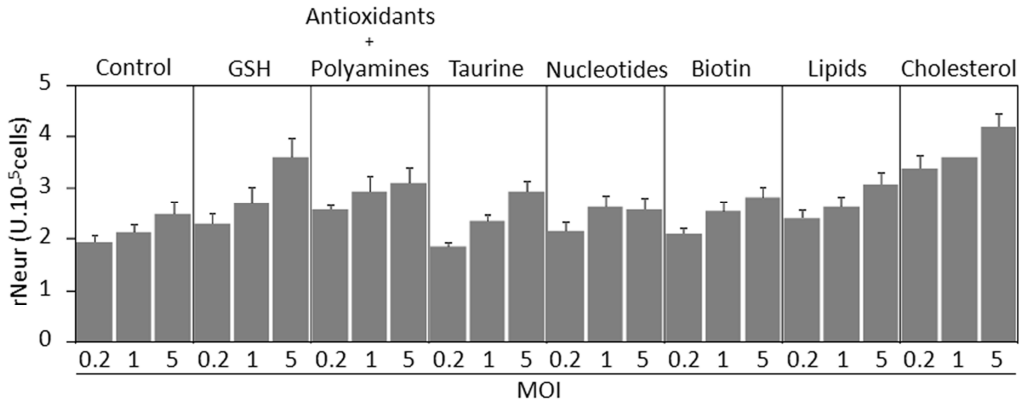

Figure 2. Extensive screening of cell culture supplements for target-oriented bioprocess optimization in High Five cells. Recombinant neuraminidase titer was assessed by a enzyme activity assay in supernatant samples. The results are reported as specific yield of rNeur Units per 10^5 cells. Cultures were performed in Erlenmeyer flasks, as described in the Materials and Methods section. Infections were performed at CCI of $1x10^6$ cells.mL^{-1} varying the MOI as indicated in the bottom axes. The data shown correspond to 48 hpi; error bars correspond to the standard deviation of three replicates.

The culture supplement contributing the highest improvement on the specific yields of rNeur (180%) was cholesterol. The fold-changes in specific productivity observed with taurine and biotin supplementations did not coincide precisely with the ones obtained previously (Supplementary Fig. V-4). Important to be noticed are the differences Ambr vessel *vs* Erlenmeyer flasks, mainly regarding stirring *vs* orbital agitation, respectively. The agitation mode can impact cellular behavior and

productivity (Hu et al., 2011), as well as product integrity and stability (Bai et al., 2012). The culture system could also influence insect cell performance, as a consequence of shear stress provoked by the high stirring agitation in the Ambr vessels (1400 rpm), or at the product level.

The effects of the supplementation strategies on the specific product yields of Sf9 cells are summarized in Table 2 and Figure 3. Nine different supplements (Table 1) were evaluated during the production of BVs (Fig. 3A) and Inf-VLPs (Fig. 3B).

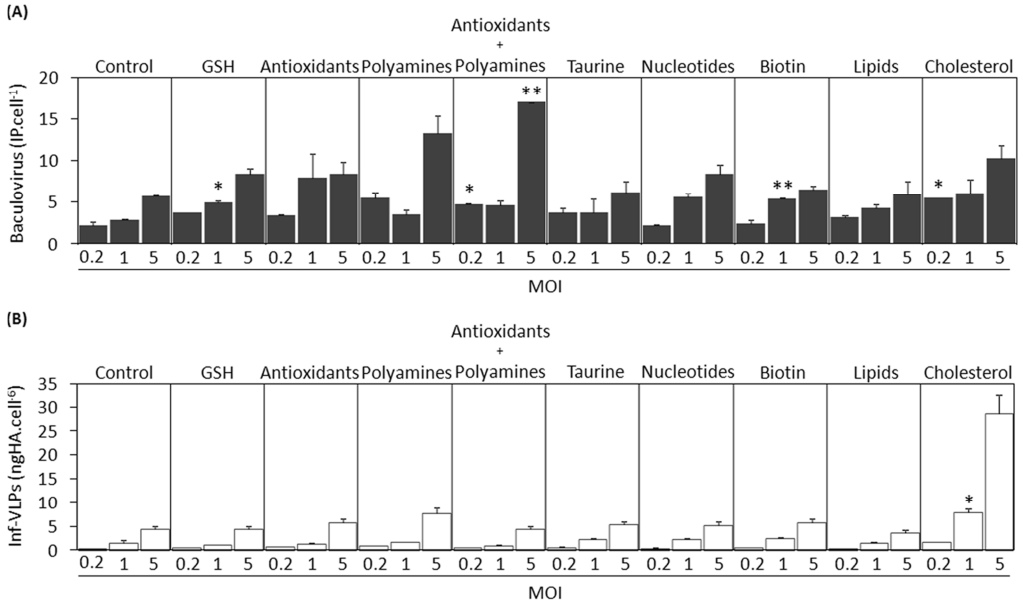

Figure 3. Extensive screening of cell culture supplements for target-oriented bioprocess optimization in Sf9 cells. (A) Infectious baculovirus (BVs), and **(B)** Influenza VLPs (Inf-VLPs). The results are reported as specific yield of baculovirus infectious particles (IPs) and ng of Inf-VLPs on a per cell basis. Cultures were performed in Erlenmeyer flasks, as described in the Materials and Methods section. Infections were performed at a CCI of $1x10^6$ cells.mL^{-1} and varying the MOI as indicated in the bottom axes. The data shown correspond to 48 hpi; error bars correspond to the standard deviation of two replicates for supplemented cultures. Control cultures were performed in triplicates for MOI 0.2 and in duplicates for MOI 1 and 5. *p value<0.05; **p value<0.01.

A correlation between supplement effect and MOI was evident, with the highest improvements obtained in general when cells were infected with low or medium MOIs. The best results were obtained in cultures supplemented with antioxidants combined with polyamines and cholesterol alone, where a 3 and 7-fold

improvements were achieved in the production of BVs and Inf-VLPs on a per cell basis, respectively (Fig.3A and B). Since the quantification of Inf-VLPs is based on the detection of hemagglutinin (HA) displayed on the surface of the particles in supernatant samples, cross-contamination with baculovirus harboring HA can occur. Although the Inf-VLPs titers could be overestimated, the degree of contamination from the baculovirus particles should be the same in all the samples. In this regard, the relative contribution from baculovirus HA is similar in all the analyzed samples, and the changes observed are representative of the increase in Inf-VLPs population. Overall, higher improvements on the production of enveloped VLPs could be obtained in Sf9 cells infected at lower MOIs, although some exceptions were observed. Thus, we decided to further analyze Sf9 as the host cell to produce enveloped viral particles.

3.4 Media manipulation strategies improve productivity and final product quality of enveloped viral particles in Sf9 cells

Virus replication results in the formation of new and fully functional viral particles (infectious particles, IPs) and non-infectious particles. To evaluate if supplementation strategies could increase the viral stock quality, we assessed the ratio of infectious particles (IPs) to total particles (TPs) during baculovirus production in Sf9 cells. With the exception of nucleosides and biotin, all the added supplements increased the specific yields of IPs (Fig. 4, bottom panel). Polyamines and cholesterol yielded proportional improvements of both TPs and IPs, resulting in similar TPs/IPs ratios (Fig. 4, upper panel). More importantly, GSH, antioxidants combined with polyamines, taurine and lipids supplementation resulted in the increase of IPs levels without altering TPs formation (Fig. 4, bottom panel). These supplements had a positive impact on final stock quality, as demonstrated by the decrease in the TPs/IPs ratio (Fig. 4, upper panel). The results suggest that, in addition to productivity, the final product quality is enhanced.

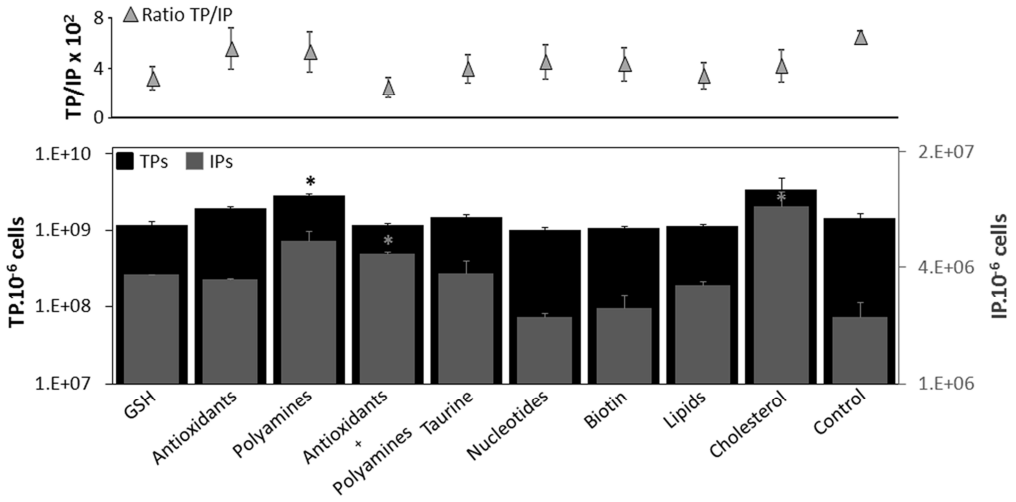

Figure 4. Effect of cell culture supplements on infectious virus titers and viral stock quality. Bottom panel: Specific yields of total (black bars) and infectious (light grey bars) viral particles produced in Sf9 cells. The left axis represents the quantification of baculovirus TPs, and the left axis the quantification of baculovirus IPs. Upper panel: Total to infectious particles content ratio (TP/IP). Cultures were performed in Erlenmeyer flasks, as described in the Materials and Methods section. Infections were performed at a CCI of $1x10^6$ cells.mL^{-1} with an MOI of 0.2. The data shown correspond to 48 hpi; error bars indicate standard deviations of two replicates and three in the case of the control. *p value<0.05.

3.5 Combinations of supplements have synergistic and antagonistic effects in assisting enveloped viral particles production in Sf9 cells

The supplementation strategies that conferred the best results were combined and their impact on the specific productivity of Sf9 cells were evaluated. Infections were performed at low MOI and the production of BVs and Inf-VLPs was assessed (Fig. 5). The combination of cholesterol with polyamines resulted in an 8-fold improvement in the specific yields of BVs, twice the value obtained by the addition of cholesterol alone, while the production of Inf-VLPs was equal. The combination of GSH with cholesterol resulted in a drop of Inf-VLPs production, in contrast to the effect observed when the supplements were added independently (Fig. 3B).

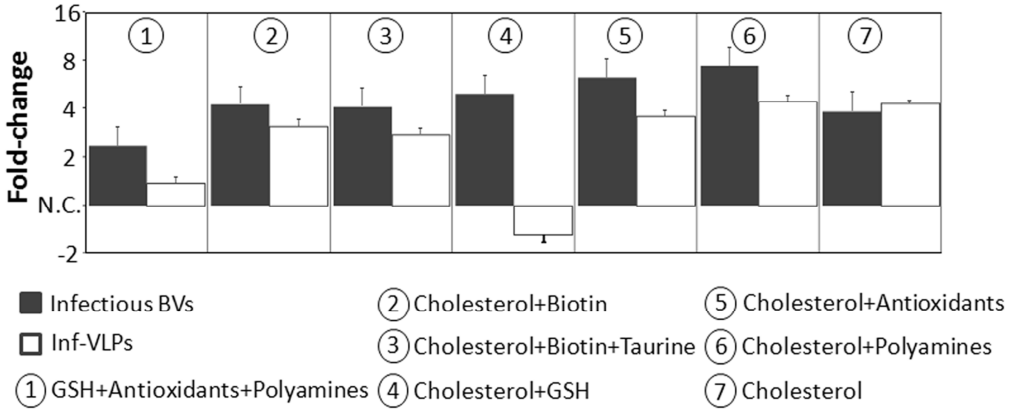

Figure 5. Synergistic and antagonistic effect of cell culture supplements on the specific yields of enveloped viral particles produced in Sf9 cells. Grey bars correspond to infectious baculovirus, BVs, titers and white bars to Influenza VLPs, Inf-VLPs, specific yields. The results are illustrated as fold-change on the specific yield of supplemented *versus* control cultures (non-supplemented). Cultures were performed in Erlenmeyer flasks, as described in the M&M section. Infections were performed at a CCI of $1x10^6$ cells.mL^{-1} with an MOI of 0.2. The data corresponds to 48 hpi; error bars correspond to 30% of inter-assay variability for infectious BVs and 10% for Inf-VLPs quantification. Control cultures were performed in triplicates. N.C. stands for - No change observed.

3.6 Implementation of an optimal bioprocess for the production of enveloped viral particles in Sf9 cells *via* BEVS

To validate the results obtained with cholesterol and polyamines supplementation during enveloped viral particles production, we scaled the system to 0.5 L stirred-tank bioreactors.

Table 3. Summary of the effect of the supplementation strategy in bioreactor cultures on the final product quality

	Supplemented culture (Cholesterol+Polyamines)					Control culture (non-supplemented)				
Time (hpi)	3	24	48	72	96	3	24	48	72	96
T.P. (10^2.$cell^{-1}$)	0.8±0.1	1.6±0.2	3±0.3	2.8±0.28	4±0.4	1.9±0.2	2.6±0.3	4.4±0.4	5.2±0.5	8.6±0.7
I.P. (10^{-1}.$cell^{-1}$)	0.8±0.2	1.3±0.4	3.2±1	5.5±2	6.9±2	1.0±0.3	0.8±0.2	1.0±0.3	1.6±0.5	1.6±0.5
Ratio T.P./I.P.	1090	1283	939	508	572	1885	3237	4383	3221	5325
Amplification factor	7	18	69	128	124	10	7	8	21	26

The amplification factor was calculated as the ratio between the volumetric productivity and the number of infectious baculovirus per mL at the time of infection (volumetric productivity/(CCI×MOI)).

Consistent with the previous experiments, the combination of both supplements increased the production of infectious BVs (Fig. 6A) and Inf-VLPs (Fig.6B). The ratio between TPs and IPs was assessed along culture time (Table 3), being lower in the supplemented cultures. In accordance, the virus amplification factor was enhanced by 6 fold.

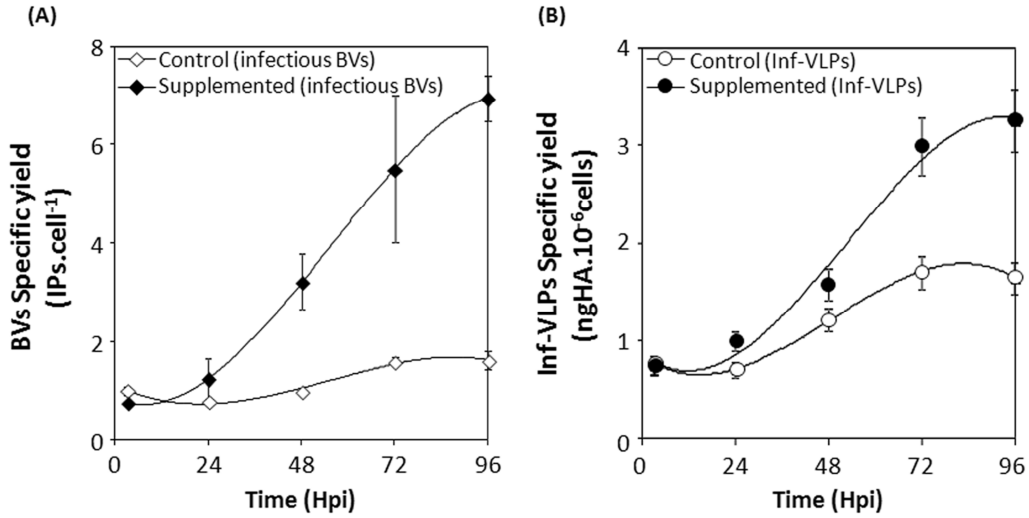

Figure 6. Up-scale and proof-of-concept of the best culture condition for target-oriented bioprocess optimization in Sf9 cells. (A) Specific yields of infectious baculovirus in control (◇) and supplemented cultures (◆); **(B)** Specific yields of Influenza VLPs in control (○) and supplemented (●) cultures**.** The results show the bioprocess timeline after infection. Cultures were performed in Biostat bioreactors, as described in the Materials and Methods section. Infections were performed at a CCI of $1x10^6$ cells.mL^{-1} with an MOI of 0.2. The supplementation scheme comprised the addition of a combination of polyamines and cholesterol at inoculation and infection, as described in the M&M section. Error bars correspond to the variability of technical replicates.

4. Discussion

Several works have been dedicated to IC-BEVS bioprocess optimization, focused in developing fed-batch strategies to improve the production of recombinant proteins (Nguyen et al., 1993; Yang et al., 1996; Taticek and Shuler, 1997; Chan et al., 1998; Palomares et al., 2004) or viral vectors (Mena et al., 2010; Liu et al., 2010; Carinhas et al., 2010). Even though the IC-BEVS is generically used for the production of VLPs (Liu et al., 2013), and efforts have been made in understanding which are the

process parameters that contribute for better VLP yields (Maranga et al., 2002; Cruz et al., 1998; Vieira et al., 2005; Pillay et al., 2009; Palomares et al., 2012), until now there are not reports dealing with the metabolic constraints of producing such targets.

Previously, the exo and endometabolome of Sf9 and High Five cells were extensively characterized after baculovirus infection (Monteiro et al., 2014). By contextualizing the acquired data in a pathway analysis framework, we identified the metabolic pathways recruited during infection, and addressed the relative importance of each metabolic pathway in supporting the BV replicative cycle. Such analysis retrieved redox homeostasis, GSH and taurine metabolism, and nucleosides biosynthesis as pathways recruited to sustain infection and, thus, correlated with productivity. In the present work, we analyze the impact of cell culture supplements intended to boost the previously identified pathways on IC-BEVS productivity. In this regard, we aimed to enhance the cellular performance by alleviating the metabolic constraints that can be limiting productivity of three model target products: soluble recombinant proteins (rNeur), enveloped VLPs (Inf-VLPs) and baculoviruses. Moreover, since the production of all the mentioned targets depends greatly on proper membrane fitness, lipid-based supplements were also considered.

The importance of cholesterol and lipids in sustaining enveloped viral particles productivity was relevant, reflected by up to 7-fold improvements of the specific yields (Fig. 3A and B). Insect cells have deficient lipid metabolism, reflected by a limited capacity of fatty acid synthesis and are unable to produce cholesterol (Drugmand et al., 2012). As a consequence, when insect cells are subjected to lipid deprivation cell degeneration occurs, and the production of baculovirus is impaired (Goodwin, 1991). Supplementation with lipid components can not only influence host cell metabolism, by assisting lipid overproduction imposed during infection and production of enveloped viral particles, but also influence membrane biogenesis and homeostasis. Similarly to wild-type virus, the budding of influenza-derived VLPs from the host cell occurs preferentially at lipid rafts (Chen et al., 2007), *i.e.,* bioactive

domains in the plasma membrane enriched in cholesterol and sphingolipids (Simons and Ikonen, 1997). Evidences suggest that baculovirus budding is not restricted to such domains (Zhang et al., 2003), however, the importance of lipidic cytosolic vesicles trafficking during the baculovirus infection cycle was demonstrated (Long et al., 2006; Yuan et al., 2011). Together, our observations highlight the importance of proper membrane fitness to enable correct folding of proteins that intimately interact with membrane lipids, and the budding of the viral particles thus produced. In fact, the manipulation of lipid metabolism culminated with meaningful outputs in several other producer systems (Chen et al., 2010; Rodrigues et al., 2009; Mitta et al., 2005; Cervera et al., 2013). Cholesterol has an important role in membrane fluidity and rigidity, being invaluable for membrane biogenesis and functionality (Bloch, 1983). It can also act in the stabilization of the envelope of the viral particles produced or aid in the maturation and budding processes (Chan et al., 2010). Moreover, cholesterol is fundamental for the folding and stability of viral capsids and envelopes, and a major contributor for the infectivity of several enveloped viruses (Carmo et al., 2006; Desplanques et al., 2010; Aizaki et al., 2008; Campbell et al., 2002). Taken together, the importance of cholesterol in cellular metabolism and viral particles formation is remarkable, and goes in line with the improved baculovirus stock quality and flu-VLPs yields obtained.

In addition to cholesterol and lipid supplementation, better specific yields were achieved when supplementing High Five and Sf9 cultures with GSH and antioxidants combined with polyamines (Fig. 2 and 3). Among several roles in a living cell, GSH is involved in reactive oxygen species (ROS) detoxification and protein folding (Chakravarthi et al., 2006). It was previously demonstrated that oxidative stress occurs as a consequence of baculovirus infection in lepidopteran cell lines (Wang et al., 2001). Prevention of such deleterious effects would result in superior cellular performance and, as a consequence, productivity. In fact, the overexpression of the antioxidant enzyme manganese superoxide dismutase improved significantly cell viability while preventing lipid and protein oxidation in baculovirus infected High Five

cells (Wang et al., 2004). Besides aiding in nucleic acids stabilization and transcription modulation, polyamines are able to improve membrane rigidity, as well as preventing lipid peroxidation given their antioxidant properties (Wallace et al., 2003). Thus, it seems likely that the joint action of polyamines and antioxidants contribute to the observed improvements on enveloped viral particles production. In fact, others already described the positive effect of polyamines on the production of enveloped virus (Rodrigues et al., 2013; Raina et al., 1981). Overall, our results indicate that redox homeostasis in invaluable to ensure maximum cellular performance in IC-BEVS and, thus, productivity.

In addition to improved infectious BVs titers, the supplements enhanced the quality of the virus produced by reducing the accumulation of non-infective particles. Lipid supplements, cholesterol, GSH and antioxidants combined with polyamines specifically improved the production of infectious BVs, without altering the number of total particles produced (Fig. 4). Baculovirus stock quality can be influenced by the metabolic state of the producer cell, as productivity and cellular metabolism are correlated (Carinhas et al., 2009, 2010; Aucoin et al., 2010). Thus, we can postulate that the increased viral infectivity in the above mentioned conditions might be a result of the metabolic state of the producer cell being more compliant with the BV life cycle progression. Although the recommended practices of baculovirus stock management were followed, such as viral amplification at low MOIs and maintenance of the virus working stock at low passage number, the virus titers obtained were low (Lesch et al., 2011). The recombinant construct expressed can influence the baculovirus stock titer, either by promoting instability of the viral DNA or by being cytotoxic, for instance. We have seen that by simply expressing constructs of different variants of influenza hemagglutinin, the generated viral stocks have significantly different titers, with 10 to 100 fold differences in infectious particles production (data not shown). Thus, a correlation between the expressed construct and the baculovirus titer appears to occur, and further work should be performed to disclose this effect.

The results suggest that lower MOIs enable the highest improvements on product specific yields after supplementation (Figs. 2 and 3). Baculovirus critically impacts host cell homeostasis, overthrowing the cellular biosynthetic machinery for its own profit (Monteiro et al., 2012). Consistently, higher viral loads have a detrimental effect on the capacity of the host cell to cope with environmental manipulations. Lower MOIs were shown to enable the successful improvement of systems' performance in fed-batch cultures, as opposed to high MOIs (Mena et al., 2010; Bédard and Kamen, 1994; Nguyen et al., 1993). The implications for bioprocess development are obvious, since lower MOIs mean a weaker dependence on high titer baculovirus stock preparations. In addition, not only the specific productivities can be improved, but also volumetric titers can also be increased since cellular growth occurs at least for a period of 24 hours after infection.

The combined action of polyamines and cholesterol resulted in remarkable improvements on the specific productivity of infectious BVs in Sf9 cells (Figs. 5 and 6). Although the majority of the combination strategies resulted in higher product titers, this does not necessarily reflect the sum of the effect of each supplement added in an individual scheme. Actually, the supplementation of GSH combined with cholesterol resulted in detrimental effects on the production of Inf-VLPs (Fig. 5). Metabolism is an intricate network of pathways that operate in a tight balance within each other. It is plausible to speculate that boosting different metabolic pathways may result in metabolic rearrangements leading to unpredicted outputs, as a consequence of additive, augmentative or non-additive effects (Seth et al., 2007). Our data illustrate these three scenarios and compellingly underscore the relevance of metabolic engineering efforts to optimize the IC-BEVS.

Productivity is a multifactorial attribute that fluctuates in response to genetic and environmental forces. Identification of the traits that influence systems' performance can empower us to develop cells with superior phenotypes, produce products with higher quality and implement more robust bioprocesses. For the IC-BEVS, the maintenance of redox homeostasis, coupled with an enhanced cholesterol

metabolism, are key parameters that should be considered when developing and implementing highly productive bioprocesses. The work herein presented merges fundamentals with applied research, which culminated in the implementation of an IC-BEVS bioprocess that delivers higher quality and quantity of the desired product.

5. Acknowledgments

This work was supported by *FP7/HEALTH.2011.1.1-1/279039* project. Francisca Monteiro acknowledges FCT for her PhD fellowship grant (SFRH/BD/7013/2010).

6. Author contribution

Francisca Monteiro conceived the experimental set-up and design, performed part of the experiments, analyzed the data and wrote the chapter.

7. References

Airenne, K. J., Hu, Y.-C., Kost, T. A., Smith, R. H., Kotin, R. M., Ono, C., Matsuura, Y., Wang, S., and Ylä-Herttuala, S. (2013). Baculovirus: an Insect-derived Vector for Diverse Gene Transfer Applications. *Mol. Ther.* 21, 739–749.

Aizaki, H., Morikawa, K., Fukasawa, M., Hara, H., Inoue, Y., Tani, H., Saito, K., Nishijima, M., Hanada, K., Matsuura, Y., et al. (2008). Critical role of virion-associated cholesterol and sphingolipid in hepatitis C virus infection. *J. Virol.* 82, 5715–5724.

Aucoin, M. G., Mena, J. A., and Kamen (2010). Bioprocessing of baculovirus vectors: a review. *Curr. Gene Ther.* 10, 174–186.

Bai, G., Bee, J. S., Biddlecombe, J. G., Chen, Q., and Leach, W. T. (2012). Computational fluid dynamics (CFD) insights into agitation stress methods in biopharmaceutical development. *Int. J. Pharm.* 423, 264–280. doi:10.1016/j.ijpharm.2011.11.044.

Bédard, C., and Kamen, A. (1994). Maximization of recombinant protein yield in the insect cell / baculovirus system by one-time addition of nutrients to high-density batch cultures. *Cytotechnology*, 129–138.

Bédard, C., Perret, S., and Kamen, A. A. (1997). Fed-batch culture of Sf-9 cells supports 3x10 7 cells per ml and improves baculovirus-expressed recombinant protein yields. *Biotechnol. Lett.* 19, 629–632.

Bieniossek, C., Imasaki, T., Takagi, Y., and Berger, I. (2012). MultiBac: expanding the research toolbox for multiprotein complexes. *Trends Biochem. Sci.* 37, 49–57. doi:10.1016/j.tibs.2011.10.005.

Bloch, K. E. (1983). Sterol, Structure and Membrane Function. *Crit. Rev. Biochem. Mol. Biol.* 14, 47–92. doi:10.3109/10409238309102790.

Campbell, S. M., Crowe, S. M., and Mak, J. (2002). Virion-associated cholesterol is critical for the maintenance of HIV-1 structure and infectivity. *AIDS* 16, 2253–2261.

Carinhas, N., Bernal, V., Monteiro, F., Carrondo, M. J. T., Oliveira, R., and Alves, P. M. (2010). Improving baculovirus production at high cell density through manipulation of energy metabolism. *Metab. Eng.* 12, 39–52.

Carinhas, N., Bernal, V., Yokomizo, A. Y., Carrondo, M. J. T., Oliveira, R., and Alves, P. M. (2009). Baculovirus production for gene therapy: the role of cell density, multiplicity of infection and medium exchange. *Appl. Microbiol. Biotechnol.* 81, 1041–9.

Carmo, M., Faria, T. Q., Falk, H., Coroadinha, a. S., Teixeira, M., Merten, O. W., Gény-Fiamma, C., Alves, P. M., Danos, O., Panet, a., et al. (2006). Relationship between retroviral vector membrane and vector stability. *J. Gen. Virol.* 87, 1349–1356. doi:10.1099/vir.0.81302-0.

Cervera, L., Gutiérrez-Granados, S., Martínez, M., Blanco, J., Gòdia, F., and Segura, M. M. (2013). Generation of HIV-1 Gag VLPs by transient transfection of HEK 293 suspension cell cultures using an optimized animal-derived component free medium. *J. Biotechnol.* 166, 152–65.

Chakravarthi, S., Jessop, C. E., and Bulleid, N. J. (2006). The role of glutathione in disulphide bond formation and endoplasmic-reticulum-generated oxidative stress. *EMBO Rep.* 7, 271–5.

Chan, L. C., Greenfield, P. F., and Reid, S. (1998). Optimising fed-batch production of recombinant proteins using the baculovirus expression vector system. *Biotechnol. Bioeng.* 59, 178–188.

Chan, R. B., Tanner, L., and Wenk, M. R. (2010). Implications for lipids during replication of enveloped viruses. *Chem. Phys. Lipids* 163, 449–459. doi:10.1016/j.chemphyslip.2010.03.002.

Chen, B. J., Leser, G. P., Morita, E., and Lamb, R. A. (2007). Influenza virus hemagglutinin and neuraminidase, but not the matrix protein, are required for assembly and budding of plasmid-derived virus-like particles. *J. Virol.* 81, 7111–23.

Chen, Y., Ott, C. J., Townsend, K., Subbaiah, P., Aiyar, A., and Miller, W. M. (2010). Cholesterol Supplementation During Production Increases the Infectivity of Retroviral and Lentiviral Vectors Pseudotyped with the Vesicular Stomatitis Virus Glycoprotein (VSV-G). *Biochem. Eng. J.* 44, 199–207.

Chiou, T.-W., Hsieh, Y.-C., and Ho, C. S. (2000). High density culture of insect cells using rational medium design and feeding strategy. *Bioprocess Eng.* 22, 483–491. doi:10.1007/s004499900091.

Cox, M. M. J., and Hollister, J. R. (2009). FluBlok, a next generation influenza vaccine manufactured in insect cells. *Biologicals* 37, 182–9.

Cruz, P. E., Cunha, A., Peixoto, C. C., Clemente, J., Moreira, J. L., and Carrondo, M. J. (1998). Optimization of the production of virus-like particles in insect cells. *Biotechnol. Bioeng.* 60, 408–418. doi:10.1002/(SICI)1097-0290(19981120)60:4<408::AID-BIT2>3.0.CO;2-Q.

Deroo, T., Jou, W. M., and Fiers, W. (1996). Recombinant neuraminidase vaccine protects against lethal influenza. *Vaccine* 14, 561–9.

Desplanques, A. S., Pontes, M., De Corte, N., Verheyen, N., Nauwynck, H. J., Vercauteren, D., and Favoreel, H. W. (2010). Cholesterol depletion affects infectivity and stability of pseudorabies virus. *Virus Res.* 152, 180–183.

Drugmand, J.-C., Schneider, Y.-J., and Agathos, S. N. (2012). Insect cells as factories for biomanufacturing. *Biotechnol. Adv.* 30, 1140–57. doi:10.1016/j.biotechadv.2011.09.014.

Ferreira, T. B., Ferreira, A. L., Carrondo, M. J. T., and Alves, P. M. (2005). Effect of refeed strategies and non-ammoniagenic medium on adenovirus production at high cell densities. *J. Biotechnol.* 119, 272–280. doi:10.1016/j.jbiotec.2005.03.009.

Goodwin, R. H. (1991). Replacement of vertebrate serum with lipids and other factors in the culture of invertebrate cells, tissues, parasites, and pathogens. *In Vitro Cell. Dev. Biol.* 27A, 470–478. doi:10.1007/BF02631147.

Henry, O., Perrier, M., and Kamen, A. (2005). Metabolic flux analysis of HEK-293 cells in perfusion cultures for the production of adenoviral vectors. *Metab. Eng.* 7, 467–476.

Hu, W., Berdugo, C., and Chalmers, J. J. (2011). The potential of hydrodynamic damage to animal cells of industrial relevance: Current understanding. *Cytotechnology* 63, 445–460. doi:10.1007/s10616-011-9368-3.

Lesch, H. P., Makkonen, K. E., Laitinen, A., Määttä, A. M., Närvänen, O., Airenne, K. J., and Ylä-Herttuala, S. (2011). Requirements for baculoviruses for clinical gene therapy applications. *J. Invertebr. Pathol.* 107. doi:10.1016/j.jip.2011.05.010.

Lim, Y., Wong, N. S. C., Lee, Y. Y., Ku, S. C. Y., Wong, D. C. F., and Yap, M. G. S. (2010). Engineering mammalian cells in bioprocessing - current achievements and future perspectives. *Biotechnol. Appl. Biochem.* 55, 175–89. doi:10.1042/BA20090363.

Liu, F., Wu, X., Li, L., Liu, Z., and Wang, Z. (2013). Use of baculovirus expression system for generation of virus-like particles: successes and challenges. *Protein Expr. Purif.* 90, 104–16. doi:10.1016/j.pep.2013.05.009.

Liu, Y. K., Yang, C. J., Liu, C. L., Shen, C. R., and Shiau, L. D. (2010). Using a fed-batch culture strategy to enhance rAAV production in the baculovirus/insect cell system. *J. Biosci. Bioeng.* 110, 187–193.

Long, G., Pan, X., Kormelink, R., and Vlak, J. M. (2006). Functional entry of baculovirus into insect and mammalian cells is dependent on clathrin-mediated endocytosis. *J. Virol.* 80, 8830–3.

Lowy, D. R., and Schiller, J. T. (2006). Prophylactic human papillomavirus vaccines. *J. Clin. Invest.* 116, 1167–1173.

Lu, H., Chen, Y., and Liu, H. (2012). Baculovirus as a vaccine vector. *Bioengineered*, 271–274.

Maranga, L., Cruz, P. E., Aunins, J. G., and Carrondo, M. J. T. (2002). Production of core and virus-like particles with baculovirus infected insect cells. *Adv. Biochem. Eng. Biotechnol.* 74, 183–206.

Martinez, V., Gerdtzen, Z. P., Andrews, B. A., and Asenjo, J. A. (2010). Viral vectors for the treatment of alcoholism: use of metabolic flux analysis for cell cultivation and vector production. *Metab. Eng.* 12, 129–37. doi:10.1016/j.ymben.2009.09.003.

Mena, J. A., Aucoin, M. G., Montes, J., Chahal, P. S., and Kamen, A. A. (2010). Improving adeno-associated vector yield in high density insect cell cultures. *J. Gene Med.*, 157–167.

Mitta, B., Rimann, M., and Fussenegger, M. (2005). Detailed design and comparative analysis of protocols for optimized production of high-performance HIV-1-derived lentiviral particles. *Metab. Eng.* 7, 426–36.

Monteiro, F., Bernal, V., Saelens, X., Lozano, A. B., Bernal, C., Sevilla, A., Carrondo, M. J. T., and Alves, P. M. (2014). Metabolic profiling of insect cell lines: Unveiling cell line determinants behind system's productivity. *Biotechnol. Bioeng.* 111, 816–28.

Monteiro, F., Carinhas, N., Carrondo, M. J. T., Bernal, V., and Alves, P. M. (2012). Toward system-level understanding of baculovirus-host cell interactions: from molecular fundamental studies to large-scale proteomics approaches. *Front. Microbiol.* 3, 391.

Moran, N. (2012). First gene therapy nears landmark European market authorization. *Nat. Biotechnol.* 30, 807–9. doi:10.1038/nbt0912-807.

Nguyen, B., Jarnagin, K., Williams, S., Chan, H., and Barnett, J. (1993). Fed-batch culture of insect cells: a method to increase the yield of recombinant human nerve growth factor (rhNGF) in the baculovirus expression system. *J. Biotechnol.* 31, 205–217.

Van Oers, M. M., Pijlman, G. P., and Vlak, J. M. (2015). Thirty years of baculovirus-insect cell protein expression: From dark horse to mainstream technology. *J. Gen. Virol.* 96, 6–23. doi:10.1099/vir.0.067108-0.

Orellana, C. a., Marcellin, E., Schulz, B. L., Nouwens, A. S., Gray, P. P., and Nielsen, L. K. (2015). High-Antibody-Producing Chinese Hamster Ovary Cells Up-Regulate Intracellular Protein Transport and Glutathione Synthesis. *J. Proteome Res.* 14, 609–618. doi:10.1021/pr501027c.

Palmberger, D., Klausberger, M., and Grabherr, R. (2013). MultiBac turns sweet. *Bioengineered* 4, 78–83.

Palomares, L. A., López, S., and Ramírez, O. T. (2004). Utilization of oxygen uptake rate to assess the role of glucose and glutamine in the metabolism of infected insect cell cultures. *Biochem. Eng. J.* 19, 87–93.

Palomares, L. A., Mena, J. A., and Ramirez, O. T. (2012). Simultaneous expression of recombinant proteins in the insect cell-baculovirus system: Production of virus-like particles. *Methods* 56, 389–395.

Pillay, S., Meyers, A., Williamson, A. L., and Rybicki, E. P. (2009). Optimization of chimeric HIV-1 virus-like particle production in a baculovirus-insect cell expression system. in *Biotechnology Progress*, 1153–1160.

Raina, A., Tuomi, K., and Mäntyjärvi, R. (1981). Roles of polyamines in the replication of animal viruses. *Med. Biol.* 59, 428–432.

Rodrigues, A. F., Carmo, M., Alves, P. M., and Coroadinha, A. S. (2009). Retroviral vector production under serum deprivation: The role of lipids. *Biotechnol. Bioeng.* 104, 1171–81.

Rodrigues, A. F., Carrondo, M. J. T., Alves, P. M., and Coroadinha, A. S. (2014). Cellular targets for improved manufacturing of virus-based biopharmaceuticals in animal cells. *Trends Biotechnol.* 32, 602–607. doi:10.1016/j.tibtech.2014.09.010.

Rodrigues, A. F., Formas-Oliveira, A. S., Bandeira, V. S., Alves, P. M., Hu, W. S., and Coroadinha, A. S. (2013). Metabolic pathways recruited in the production of a recombinant enveloped virus: mining targets for process and cell engineering. *Metab. Eng.* 20, 131–45.

Roldão, A., Oliveira, R., Carrondo, M. J. T., and Alves, P. M. (2009). Error assessment in recombinant baculovirus titration: evaluation of different methods. *J. Virol. Methods* 159, 69–80.

Seth, G., Charaniya, S., Wlaschin, K. F., and Hu, W. S. (2007). In pursuit of a super producer-alternative paths to high producing recombinant mammalian cells. *Curr. Opin. Biotechnol.* 18, 557–64.

Simons, K., and Ikonen, E. (1997). Functional rafts in cell membranes. *Nature* 387, 569–572.

Taticek, R. A., Choi, C., Phan, S. E., Palomares, L. A., and Shuler, M. L. (2001). Comparison of growth and recombinant protein expression in two different insect cell lines in attached and suspension culture. *Biotechnol. Prog.* 17, 676–84.

Taticek, R. A., and Shuler, M. L. (1997). Effect of elevated oxygen and glutamine levels on foreign protein production at high cell densities using the insect cell-baculovirus expression system. *Biotechnol. Bioeng.* 54, 142–52.

Vieira, H. L. A., Estevao, C., Roldao, A., Peixoto, C. C., Sousa, M. F. Q., Cruz, P. E., Carrondo, M. J. T., and Alves, P. M. (2005). Triple layered rotavirus VLP production: Kinetics of vector replication, mRNA stability and recombinant protein production. *J. Biotechnol.* 120, 72–82.

Wallace, H. M., Fraser, A. V, and Hughes, A. (2003). A perspective of polyamine metabolism. *Biochem. j.* 14, 1–14.

Wang, Y., Oberley, L. W., Howe, D., Jarvis, D. L., Chauhan, G., and Murhammer, D. W. (2004). Effect of expression of manganese superoxide dismutase in baculovirus-infected insect cells. *Appl. Biochem. Biotechnol.* 119, 181–93.

Wang, Y., Oberley, L. W., and Murhammer, D. W. (2001). Evidence of oxidative stress following the viral infection of two lepidopteran insect cell lines. *Free Radic. Biol. Med.* 31, 1448–1455.

Wilde, M., Klausberger, M., Palmberger, D., Ernst, W., and Grabherr, R. (2014). Tnao38, high five and Sf9--evaluation of host-virus interactions in three different insect cell lines: baculovirus production and recombinant protein expression. *Biotechnol. Lett.* 36, 743–9. doi:10.1007/s10529-013-1429-6.

Yang, J., Gecik, P., Collins, A., Czarnecki, S., Hsu, H., Lasdun, A., Sundaram, R., Muthukumar, G., and Silberklangs, M. (1996). Rational Scale-Up of a Baculovirus-Insect Cell Batch Process Based on Medium Nutritional Depth. *Biotechnol. Bioeng.* 52, 696–706.

Ylä-Herttuala, S. (2012). Endgame: Glybera Finally Recommended for Approval as the First Gene Therapy Drug in the European Union. *Mol. Ther.* 20, 1831–1832.

Yuan, M., Huang, Z., Wei, D., Hu, Z., Yang, K., and Pang, Y. (2011). Identification of Autographa californica nucleopolyhedrovirus ac93 as a core gene and its requirement for intranuclear microvesicle formation and nuclear egress of nucleocapsids. *J. Virol.* 85, 11664–74.

Zhang, S. X., Han, Y., and Blissard, G. W. (2003). Palmitoylation of the Autographa californica Multicapsid Nucleopolyhedrovirus Envelope Glycoprotein GP64 : Mapping , Functional Studies , and Lipid Rafts. *J. Virol.* 77, 6265–6273. doi:10.1128/JVI.77.11.6265.

Chapter VII

DISCUSSION

Contents

1. Discussion

The Insect Cell-Baculovirus Expression System (IC-BEVS) has been on the edge of the pharma and biotechnology fields, providing candidates for human and veterinary therapeutics (Felberbaum, 2015). Tales of success enclose the market release of vector-based therapeutics for cancer and metabolic disorders (Moran, 2012; Pasquié et al., 2010) and vaccines for major human infectious diseases (Cox and Hollister, 2009; Lowy and Schiller, 2006). This system bridges together two powerful operational units: the baculovirus, a very potent protein expression vector, and insect cells: robust platforms for complex biopharmaceuticals production. Altogether, this system constitutes a robust platform for the production of complex biopharmaceuticals. The challenges of working with such multifactorial systems arise from the need to fine-tune the infection parameters, in order to maximize infection and protein production kinetics while maintaining an optimal metabolic status of host producer cells. The correlation between cell metabolism and productivity is key, and the pursuit of the finest physiological momentum, as well as its maintenance throughout the bioprocess time frame, is a daunting task. Hyper-productive phenotypes are considered to be the result of the finest rearrangement of a myriad of cellular pathways, which by acting in concert, culminate in such a desired output (Seth et al., 2007). Additionally, viruses can be understood as elegant metabolic engineers (Maynard et al., 2010), having an active role in determining the cellular and metabolic rearrangements that occur following infection. Thus, a thorough analysis of the post-infection scenario, with a main focus on the interactions established between the insect host cell and the baculovirus vector, is strongly encouraged. Deciphering the virus-host interplay will aid in the identification of the hidden constraints that govern productivity. Moreover, it can provide clues on the viral mechanisms that subvert host cell metabolism to support biosynthesis.

This PhD work aimed at improving insect cell-based bioprocesses *via* baculovirus expression for the production of complex biopharmaceuticals, ranging from recombinant proteins to multiprotein complexes as novel vaccine candidates, and

baculovirus vectors with improved titers and quality. A thorough metabolic analysis and characterization of the IC-BEVS system was attained to support the rational bioprocess optimization, focusing on the physiological determinants that contribute to productivity, as well as the target requirements for enhanced product quality.

The thesis work followed three major tasks:

i) characterizing the cellular behavior along the bioprocess time-line, as well as the main metabolic adaptations that followed baculovirus infection;

ii) data contextualization in a metabolic pathway analysis framework for identification of critical pathways in supporting increased productivity phenotypes;

iii) to optimize, in a host cell and target-directed fashion, the IC-BEVS for the generation of improved bioprocesses and delivery of high quality products.

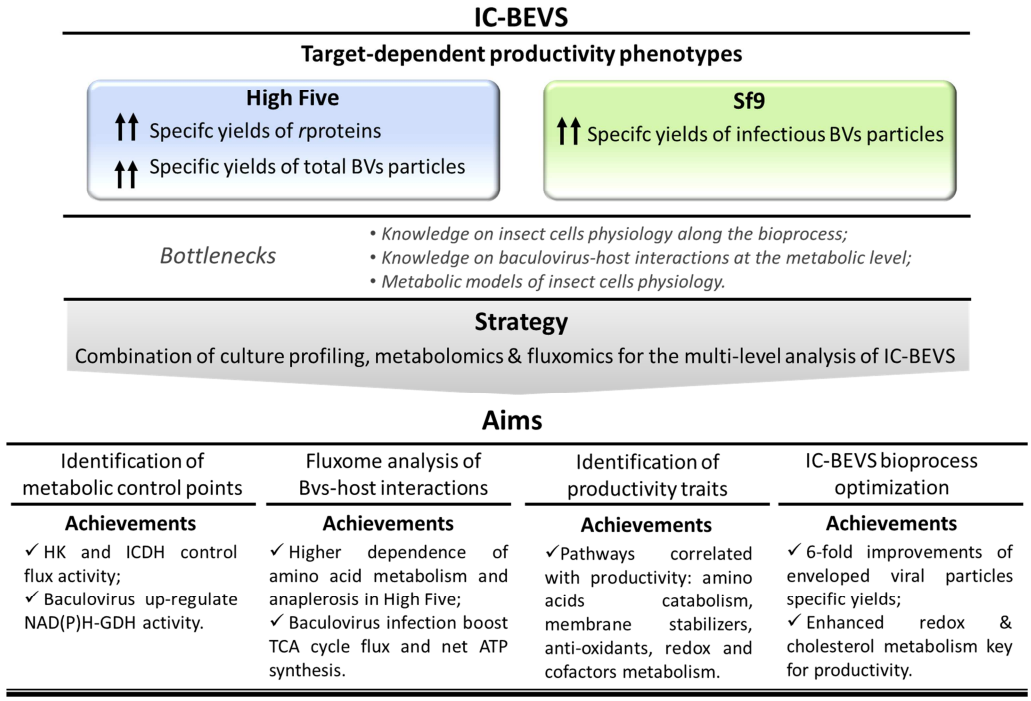

Figure 1. Schematic view of the work developed in this thesis, including initial bottlenecks, specific aims, strategy adopted and main achievements.

Tools for metabolic analysis, including culture profiling, metabolomics, fluxomics, and modeling were complementarily used to better understand and characterize IC-

BEVS based bioprocesses, allowing rational approaches for bioprocess optimization. The specific aims and outcomes of this thesis are summarized in **Figure 1**.

1.1 Metabolic flux analysis of the IC-BEVS: host cell metabolism in bioprocess stringent conditions

Metabolic fluxes represent cell physiology, mirroring the degree of engagement of various pathways in overall cellular function and metabolic processes. With metabolic flux analysis (MFA) the determination of metabolic pathway fluxes is achieved, and a global picture of the cellular fluxome is generated. As a result, a metabolic map representing the estimated distribution of fluxes within the metabolic network is generated, providing an overview of the cellular metabolism. The utility of the generated maps is further increased when the system in subjected to a perturbation (e.g. substrate limitation, viral infection, heterologous protein expression), and the flux shifts between the different conditions can be analyzed. It is through such comparisons that the induced environmental perturbations can be fully assessed and the importance of specific pathways, and reactions within such pathways, accurately described.

Two different insect host cell lines, Sf9 and High Five, which have distinct productivity phenotypes target-dependent, were scrutinized by metabolite profiling techniques to identify the metabolic requirements that preclude productivity. Additionally, the post-infection scenario was carefully examined by subjecting the host cell lines to increasing viral loads, to evaluate the metabolic demand following virus take-over. MFA was performed to characterize the cellular behavior of Sf9 and High Five cells during growth (**Chapter II** and **III**), in the presence of different culture media (**Chapter III**) and after baculovirus infection (**Chapter III** and **IV**). The premise of induced environmental perturbations was respected by analyzing distinct culture states, which enabled the assessment of pivotal pathways in each case scenario. For instance, the culture media used influenced the amount of by-products that accumulated throughout culture time, affecting the metabolic efficiency of High Five

cells (**Chapter III**). Moreover, when comparing Sf9 and High Five cells in the same culture media, we observed that oxidative metabolism was hampered in the latter, which resulted in the accumulation of high amounts of lactate and alanine. High Five cells counterbalanced this situation with higher fluxes through amino acid and anaplerotic metabolic pathways (**Chapter IV**).

Baculovirus imposes a significant biosynthetic demand on their insect host cells, overthrowing cellular resources to sustain their life cycle (Monteiro et al., 2012). Moreover, baculovirus have evolved in the way to manipulate host cell metabolism to fulfill their biosynthetic requirements. Examples are the up-regulation of key metabolic enzymes, such as citrate synthase, pyruvate dehydrogenase and aldehyde dehydrogenase (Carinhas et al., 2011; Iwanaga et al., 2007), or the activation of the PI3K-Akt signaling pathway (Xiao et al., 2009). The infection impact on the metabolism of insect host cells is profound, and should be reflected at the fluxome level. In fact, after baculovirus infection, the metabolic activity of Sf9 and High Five cells was rearranged, and the channeling of glucose towards pyruvate formation and further oxidation at the TCA cycle was much more efficient, as opposed to uninfected High Five cells (**Chapter III** and **IV**). In addition, the glutamate dehydrogenase anaplerotic pathway was activated in Sf9 cells, as observed by the increase in the enzymatic activity of NAD(P)H-dependent glutamate dehydrogenase (**Chapter II**).

The application of MFA to the IC-BEVS aided in the characterization of the metabolic phenotype of cultured Sf9 and High Five cells, shading light on the main implications of baculovirus infection at the fluxome level. Cellular flux activity was seen to be dynamic, and is tuned to address the constraints imposed by the environmental manipulations performed. In addition, it enabled the characterization of nodal flexibility and rigidity, by comparing the changes in α-ketoglutarate and pyruvate branch point flux split ratios. Although extremely valuable for monitoring cell culture dynamics, MFA presents limitations allocated to the degree of redundancy built into calculations. Intracellular fluxes simply calculated from an equal number of algebraic metabolite balances should be regarded with caution as

they depend entirely on the assumed biochemistry and accuracy of extracellular measurements. The incorporation of *in vivo* measurements of pathway activity with MFA calculations, such as the quantification of enzymatic activities, provides physiological relevant data to aid in the overall data interpretation. In this way, the MFA limitations can be by-passed to some extent, and a more accurate analysis of the cellular systems can be performed.

On the other hand, calculated metabolic fluxes that are also consistent with additional quantitative experimental measurements directly dependent upon the fluxes (for instance, the isotopic labelling enrichment of metabolites upon feeding with labeled nutrients) are more reliable measures of the corresponding *in vivo* intracellular fluxes. In this regard, ^{13}C MFA can be considered a more rigorous approach to quantify the metabolic phenotypes by applying isotope tracers to map the flow of carbon through intracellular pathways. Although highly time-consuming and requiring higher computational power in comparison to classical MFA, ^{13}C MFA studies enable the identification of flux reversibility/irreversibility, the quantification of fluxes in parallel pathways and the analysis of intracellular fluxes in different sub-cellular compartments (Wiechert, 2001; Zamboni, 2011). The application of labeling experiments to the IC-BEVS, coupled to MFA modeling, can enlarge our knowledge on key metabolic adaptations that occur in a productive scenario. MFA is an important tool for guiding host cell engineering efforts, as well as media and bioprocess optimization (Boghigian et al., 2010). The application of MFA approaches to industrially relevant expression hosts is a reality (Iwatani et al., 2008), and further work in validating MFA findings as valid metabolic engineering targets for enhanced productivity are strongly recommended.

1.2 Metabolic pathway analysis of baculovirus-host interactions: disclosing cell line determinants behind systems productivity

Although meaningful insights were provided by the fluxome description of Sf9 and High Five cells, such approach is limited to the constraints of MFA-based

modeling previously exposed. Metabolic regulation is the consequence of a cascade of regulatory phenomena: transcriptional, post-transcriptional, post-traductional. All these regulatory layers are highly interconnected and the effects they exert on the amount of active metabolic enzymes or on the concentration of metabolites and cofactors are ultimately determining the cellular phenotype observed. Thus, it is difficult to investigate if the changes in the metabolic fluxes are related to lower enzymatic activities of key regulatory enzymes, or related with perturbations on the intracellular pools of the substrate metabolites that feed those same pathways. Metabolomics is such an enabling technique that aims at the identification and simultaneous quantification of free low weight metabolite pools, allowing monitoring the physiological state of a biological system. In this regard, metabolomics and intracellular metabolite quantification can offer the direct visualization of the main compensatory events that occur along the bioprocess, and highlight the main alterations that follow baculovirus infection on the host cell metabolism.

It is known that fluctuations in the concentrations of specific metabolites can impact the effectiveness of cell cultures towards biopharmaceuticals production (Carinhas et al., 2013; Gilbert et al., 2013). Since metabolism and productivity are connected processes, the quantification of the intracellular metabolite pools during the bioprocess time-frame can provide clues on the metabolic signatures of highly producer states. Taking this into consideration, the metabolome of Sf9 and High Five cells was quantified during growth and following baculovirus infection to identify metabolic determinants precluding productivity.

Infection impact is considerably higher in High Five cells, with a myriad of metabolic pathways being hijacked to support massive production. For example, multivariate analysis identified glutathione metabolism as a determinant feature connected with higher productive High Five cells (**Chapter V**). In addition, MFA calculations indicated an increased carbon oxidation as denoted by higher fluxes throughout the TCA cycle after baculovirus infection (**Chapter IV**). This is in accordance with the higher respiration rates detected in infected cultures, a scenario

also observed by others (Bernal et al., 2009; Kamen et al., 1996; Palomares et al., 2004). Insect cells experience an increased oxidative stress as a consequence of the high biosynthetic demand resulting from baculovirus infection (Wang et al., 2001a). Cellular performance relies on the maintenance of redox homeostasis, challenged by heterologous protein production. The ability to manage the negative effects of reactive oxygen species (ROS) can influence productivity (Saarinen and Murhammer, 2003), and High Five cells are better equipped than Sf9 cells to deal with such stressful conditions, having a more extensive panoply of enzymes dedicated to the scavenging of toxic oxygen species (Wang et al., 2001a, 2001b). Additionally, the role of glutathione in removing ROS has been extensively characterized (Aquilano et al., 2014), and the boost in glutathione biosynthesis and its intracellular availability has been associated recently with significant improvements on the production of recombinant proteins and viral vectors (Orellana et al., 2015; Rodrigues et al., 2013).

Metabolic pathway analysis (MPA) combines the strengths of enrichment analysis with network topology analysis. In this regard, it enables the identification of subtle but meaningful changes that occur following an environmental perturbation, that have an impact on the cellular metabolic activity. Similarly to MFA, by exerting culture perturbations, one can identify which were the pathways affected and, in addition, what are the consequences of altering a specific metabolic pathway in the whole metabolic network. For instance, enrichment analysis retrieved ubiquinone biosynthesis as being significantly affected by baculovirus infection in Sf9 cells. By interpreting only this result, one could assume that ubiquinone biosynthesis is correlated with the infection scenario, being recruited to support the increased biosynthetic activity. However, when looking for the pathway impact value, 0 in this case, a measure given by topology analysis, this means that the effect of the alteration of that specific pathway in the considered metabolic network is residual. The combination of enrichment and topology analysis retrieved amino acid metabolism, redox balancing, taurine and biotin metabolism, and nucleosides biosynthetic pathways as being regulated upon baculovirus infection. At the end

these were the pathways identified as being linked with the increased biosynthetic demand coming from baculovirus infection and, thus, correlated with productivity.

Although powerful, MPA relies on the existence of accurate databases descriptive of the biochemical reactions operating in a cell. MPA has been wildly explored to deal with gene expression data generated from transcriptomic analysis, and several software's and databases have been developed and updated for that aim (Khatri et al., 2012). For metabolomics applications the reality is quite different, and metabolome redundancy can account for the difficulties in addressing if the observed alterations are a cause or a consequence of the environmental perturbation exerted. Regarding insect cells, the lack of sequenced and annotated genomes of the most common used host cells, Sf9 and High Five, impairs the construction of detailed and host specific metabolic maps.

1.3 Tweaking insect cell platforms for the enhanced production of complex biopharmaceuticals *via* BEVS

The recent approval cases of IC-BEVS based biopharmaceuticals for human therapy (Ylä-Herttuala, 2012) shed a new light of interest into this expression system. Coupled with the baculovirus versatility in functioning as vaccine vectors (Lu et al., 2012), the interest in developing high-titer production processes raises.

Growing knowledge about the physiological requirements that sustain biosynthesis turns possible the manipulation and improvement of cell-based bioprocesses (Lim et al., 2010). However, this is only possible when detailed information concerning the metabolic requirements of producing the desired targets exists. Empirical knowledge has been the main driver of bioprocess optimization efforts envisaging the improvement of recombinant proteins produced *via* BEVS (Bédard et al., 1997; Chan et al., 1998; Chiou et al., 2000). Although meaningful, these approaches relied on the interpretation of the culture environment as decision makers to drive bioprocess optimization. Notwithstanding, the application of

bioprocess engineering strategies to the IC-BEVS shows potential and attractiveness, and can profit from a deeper analysis of the system.

The impact of the baculovirus infection on the physiology of High Five and Sf9 host cell lines, with a focus on key cellular features that support higher productivities was performed in greater detail in Chapters IV and V. This information was applied to design tailored supplementation schemes to boost IC-BEVS production yields of three targets with increasing complexity: recombinant influenza neuraminidase (rNeur); enveloped influenza VLPs (iVLP) and the baculovirus itself (BV). Higher rNeur productivities were achieved when supplementing High Five cultures with cholesterol; for Sf9 cells, GSH, antioxidants and polyamines, and cholesterol yielded the best outputs during iVLPs and infectious BVs production (**Chapter VI**). In addition to improved infectious BVs titers, the supplements enhanced the quality of the virus produced by reducing the accumulation of non-infective particles. Baculovirus stock quality (IP *vs* TP) can be influenced by the metabolic state of the producer cell (Aucoin et al., 2010; Carinhas et al., 2010, 2009). Thus, we can postulate that the increased viral infectivity in the above mentioned conditions might be a result of the metabolic state of the producer cell being more compliant with the BV life cycle progression or BV propagation. For the IC-BEVS, the maintenance of redox homeostasis, coupled with an enhanced cholesterol metabolism, are key parameters that should be considered when developing and implementing highly productive bioprocesses.

Although our strategy was based on a deep metabolic characterization of the system, the fold improvements were still modest. Culture manipulation by supplements addition can only result in improved productivities if the metabolic pathways that we are aiming to tackle are active. Thus, if a specific metabolic pathway is down-regulated it cannot be boost by simple supplements addition. In this situation, complementary strategies should be pursued to alleviate the present constrains, and turn the system responsive to the environmental manipulations. Metabolism is the functional output of the transcriptome and the proteome,

however it has a higher degree of redundancy associated. In this regard, by simple metabolic analysis it is difficult to assess if an increased flux of a given metabolic pathway is the direct result of the provoked perturbation. The combination of different layers of cellular information, such as metabolomics and fluxomics, helped in deciphering possible metabolic determinants of highly productive states. In order to precisely identify targets for engineering purposes, the leading causes of superior (or reduced) productive states, further analysis of the IC-BEVS system is encouraged mainly through the combination of functional genomic tools.

2. Final remarks

This PhD thesis contributes to the fields of biotechnology and cell biology by enlarging our knowledge on the physiology and metabolic requirements of insect cell platforms for the production of high-demanding recombinant products, such as VLPs and viral vectors. Moreover, it also provides clues on the baculovirus and infection impact on the insect host cell, adding new insights for the complex study of virus-host interactions and basic virology. Finally, bioengineering principles were applied, improving the state-of-the-art manufacturing of BEVS-driven viral vectors and vaccine candidates.

3. Author contribution

Francisca Monteiro wrote the chapter.

4. References

Aquilano, K., Baldelli, S., Ciriolo, M.R., 2014. Glutathione: new roles in redox signaling for an old antioxidant. Front. Pharmacol. 5, 1–12. doi:10.3389/fphar.2014.00196

Aucoin, M.G., Mena, J.A., Kamen, 2010. Bioprocessing of baculovirus vectors: a review. Curr. Gene Ther. 10, 174–186.

Bédard, C., Perret, S., Kamen, A.A., 1997. Fed-batch culture of Sf-9 cells supports 3x10 7 cells per ml and improves baculovirus-expressed recombinant protein yields. Biotechnol. Lett. 19, 629–632.

Bernal, V., Carinhas, N., Yokomizo, A.Y., Carrondo, M.J.T., Alves, P.M., 2009. Cell density effect in the baculovirus-insect cells system: a quantitative analysis of energetic metabolism. Biotechnol. Bioeng. 104, 162–80.

Boghigian, B.A., Seth, G., Kiss, R., Pfeifer, B.A., 2010. Metabolic flux analysis and pharmaceutical production. Metab. Eng. 12, 81–95.

Carinhas, N., Bernal, V., Monteiro, F., Carrondo, M.J.T., Oliveira, R., Alves, P.M., 2010. Improving baculovirus production at high cell density through manipulation of energy metabolism. Metab. Eng. 12, 39–52.

Carinhas, N., Bernal, V., Yokomizo, A.Y., Carrondo, M.J.T., Oliveira, R., Alves, P.M., 2009. Baculovirus production for gene therapy: the role of cell density, multiplicity of infection and medium exchange. Appl. Microbiol. Biotechnol. 81, 1041–9.

Carinhas, N., Duarte, T.M., Barreiro, L.C., Carrondo, M.J.T., Alves, P.M., Teixeira, A.P., 2013. Metabolic signatures of GS-CHO cell clones associated with butyrate treatment and culture phase transition. Biotechnol. Bioeng. 110, 3244–3257. doi:10.1002/bit.24983

Carinhas, N., Robitaille, A.M., Moes, S., Carrondo, M.J.T., Jenoe, P., Oliveira, R., Alves, P.M., 2011. Quantitative proteomics of Spodoptera frugiperda cells during growth and baculovirus infection. PLoS One 6, e26444.

Chan, L.C., Greenfield, P.F., Reid, S., 1998. Optimising fed-batch production of recombinant proteins using the baculovirus expression vector system. Biotechnol. Bioeng. 59, 178–188.

Chiou, T.-W., Hsieh, Y.-C., Ho, C.S., 2000. High density culture of insect cells using rational medium design and feeding strategy. Bioprocess Eng. 22, 483–491. doi:10.1007/s004499900091

Cox, M.M.J., Hollister, J.R., 2009. FluBlok, a next generation influenza vaccine manufactured in insect cells. Biologicals 37, 182–9.

Felberbaum, R.S., 2015. The baculovirus expression vector system: A commercial manufacturing platform for viral vaccines and gene therapy vectors. Biotechnol. J. 10, 702–714. doi:10.1002/biot.201400438

Gilbert, A., Mcelearney, K., Kshirsagar, R., Sinacore, M.S., Ryll, T., 2013. Investigation of metabolic variability observed in extended fed batch cell culture. Biotechnol. Prog. 29, 1519–1527.

Iwanaga, M., Shimada, T., Kobayashi, M., Kang, W., 2007. Identification of differentially expressed host genes in Bombyx mori nucleopolyhedrovirus infected cells by using subtractive hybridization. Appl. Entomol. Zool. 42, 151–159.

Iwatani, S., Yamada, Y., Usuda, Y., 2008. Metabolic flux analysis in biotechnology processes. Biotechnol. Lett. 30, 791–9.

Kamen, a a, Bédard, C., Tom, R., Perret, S., Jardin, B., 1996. On-line monitoring of respiration in recombinant-baculovirus infected and uninfected insect cell bioreactor cultures. Biotechnol. Bioeng. 50, 36–48.

Khatri, P., Sirota, M., Butte, A.J., 2012. Ten years of pathway analysis: Current approaches and outstanding challenges. PLoS Comput. Biol.

Lim, Y., Wong, N.S.C., Lee, Y.Y., Ku, S.C.Y., Wong, D.C.F., Yap, M.G.S., 2010. Engineering mammalian cells in bioprocessing - current achievements and future perspectives. Biotechnol. Appl. Biochem. 55, 175–89. doi:10.1042/BA20090363

Lowy, D.R., Schiller, J.T., 2006. Prophylactic human papillomavirus vaccines. J. Clin. Invest. 116, 1167–1173.

Lu, H., Chen, Y., Liu, H., 2012. Baculovirus as a vaccine vector. Bioengineered 271–274.

Maynard, N.D., Gutschow, M. V, Birch, E.W., Covert, M.W., 2010. The virus as metabolic engineer. Biotechnol. J. 5, 686–94.

Monteiro, F., Carinhas, N., Carrondo, M.J.T., Bernal, V., Alves, P.M., 2012. Toward system-level understanding of baculovirus-host cell interactions: from molecular fundamental studies to large-scale proteomics approaches. Front. Microbiol. 3, 391.

Moran, N., 2012. First gene therapy nears landmark European market authorization. Nat. Biotechnol. 30, 807–9. doi:10.1038/nbt0912-807

Orellana, C. a., Marcellin, E., Schulz, B.L., Nouwens, A.S., Gray, P.P., Nielsen, L.K., 2015. High-Antibody-Producing Chinese Hamster Ovary Cells Up-Regulate Intracellular Protein Transport and Glutathione Synthesis. J. Proteome Res. 14, 609–618. doi:10.1021/pr501027c

Palomares, L.A., López, S., Ramírez, O.T., 2004. Utilization of oxygen uptake rate to assess the role of glucose and glutamine in the metabolism of infected insect cell cultures. Biochem. Eng. J. 19, 87–93.

Pasquié, J., Scavée, C., Bordachar, P., Clémenty, J., Haïssaguerre, M., 2010. Sipuleucel-T Immunotherapy for Castration-Resistant Prostate Cancer. N. Engl. J. Med. 363, 2373–2383. doi:10.1056/NEJMoa1407764

Rodrigues, A.F., Formas-Oliveira, A.S., Bandeira, V.S., Alves, P.M., Hu, W.S., Coroadinha, A.S., 2013. Metabolic pathways recruited in the production of a recombinant enveloped virus: mining targets for process and cell engineering. Metab. Eng. 20, 131–45.

Saarinen, M. a, Murhammer, D.W., 2003. The response of virally infected insect cells to dissolved oxygen concentration: recombinant protein production and oxidative damage. Biotechnol. Bioeng. 81, 106–14.

Seth, G., Charaniya, S., Wlaschin, K.F., Hu, W.S., 2007. In pursuit of a super producer-alternative paths to high producing recombinant mammalian cells. Curr. Opin. Biotechnol. 18, 557–64.

Wang, Y., Oberley, L.W., Murhammer, D.W., 2001a. Evidence of oxidative stress following the viral infection of two lepidopteran insect cell lines. Free Radic. Biol. Med. 31, 1448–1455.

Wang, Y., Oberley, L.W., Murhammer, D.W., 2001b. Antioxidant defense systems of two lipidopteran insect cell lines. Free Radic. Biol. Med. 30, 1254–1262.

Wiechert, W., 2001. 13C metabolic flux analysis. Metab. Eng. 3, 195–206.

Xiao, W., Yang, Y., Weng, Q., Lin, T., Yuan, M., Yang, K., Pang, Y., 2009. The role of the PI3K-Akt signal transduction pathway in Autographa californica multiple nucleopolyhedrovirus infection of Spodoptera frugiperda cells. Virology 391, 83–9.

Ylä-Herttuala, S., 2012. Endgame: Glybera Finally Recommended for Approval as the First Gene Therapy Drug in the European Union. Mol. Ther.

Zamboni, N., 2011. 13C metabolic flux analysis in complex systems. Curr. Opin. Biotechnol. 22, 103–8.

Appendix

Contents

1. Appendix I. List of biochemical reactions considered in Sf9 and High Five metabolic models.

Table I-1. List of cellular metabolic reactions of Sf9 and High Five cells

#	Reversibility	Reaction
		Glycolysis
1	0	Glc + ATP = G6P + ADP
2	0	G6P = F6P
3	0	F6P + ATP = 2 GAP
4	0	GAP + NAD + ADP = PEP + NADH + ATP
5	-1	PEP + ADP = Pyr + ATP
		Pentose Phosphate Pathway
6	0	3 G6P + 6 NADP = 3 CO_2+ 3 R5P + 6 NADPH
		TCA Cycle
7	0	Pyr + NAD = ACoA + CO_2 + NADH
8	0	ACoA + OAA = Cit
9	0	Cit + NAD = CO_2 + AKG + NADH
10	0	AKG + NAD = CO_2 + SuCoA + NADH
11	0	SuCoA + ADP = Succ + ATP
12	0	Succ + FAD = Fum + $FADH_2$
13	0	Fum = Mal
14	0	Mal + NAD = OAA + NADH
		Anaplerotic Reaction
15	0	Mal = Pyr + CO_2
		Pyruvate Reactions
16	-1	Pyr + NADH = Lac + NAD
17	-1	Pyr + Glu = Ala + AKG
		Amino Acids Metabolism
18	-1	Glu + NAD = AKG + Amm + NADH
19	-1	Ser=Pyr+Amm
20	-1	Glu + OAA = AKG + Asp
21	0	Ser + Met + NAD + ATP = SuCoA + Amm + Cys + NADH + 2 ADP
22	0	Cys = Pyr + Amm
23	-1	2 Gly + NAD = CO_2 + Amm+ Ser + NADH
24	0	2 AKG + Lys + 4 NAD + NADPH + FAD = 2 CO_2 + 2Glu + 2AcCoA + 4 NADH + NADP + $FADH_2$
25	0	AKG + Leu + NAD + ATP + FAD = CO_2 + Glu + 2AcCoA + NADH + ADP + $FADH_2$ + mevalonate
26	0	AKG + Ile + 2 NAD + ATP + FAD = CO_2 + Glu + AcCoA + SuCoA + 2 NADH + ADP + $FADH_2$
27		AKG + Arg + NAD = 2 Glu + NADH + urea
28	0	Thr + NAD = AcCoA + Gly + NADH
29	0	AKG + Val + 3 NAD + ATP + FAD = CO_2 + Glu + SuCoA + 3 NADH + ADP + $FADH_2$
30	0	Phe + NADH + O_2 = Tyr + NAD
31	0	AKG + Tyr + O_2 = CO_2 + Glu + AcCoA + Fum
32	0	His = Glu + Amm
33	-1	Asn = Amm + Asp
34	-1	Pro + NADP + 0.5 O_2 = Glu + NADPH

Energy Production (Respiration and Futile Cycles)		
35	-1	NADH + 2.5 ADP + 0.5 O2 = NAD + 2.5 ATP
36	-1	1.5 ADP + FADH2 + 0.5 O2 = 2.5 ATP + FAD
37	-1	NAD + NADPH = NADH + NADP
38	-1	ATP = Energy
Biomass Synthesis		
39	0	1000 Protein + 219.8 FA + 177.3 DNA + 445 RNA = 1 Biomass
40	0	0.758 Ala + 0.276 Glu + 0.347 Gln + 0.931 Gly + 0.537 Ser + 0.38 Lys + 0.506 Leu + 0.263 Ile + 0.279 Arg + 0.289 Asp + 0.394 Thr + 0.421 Val + 0.119 Met + 0.158 Phe + 0.117 Tyr + 0.114 His + 0.374 Pro + 0.273 Asn + 10.014 ATP + 0.189 Cys = 1 Protein + 10.014 ADP
41	0	0.5 CO2 + 1 R5P + 1.9 Gln + 1.3 Ser + 1.3 Asp + 0.7 NAD + 1 NADPH + 9 ATP = 1.9 Glu + 0.8 Fum + 0.8 Gly + 1 DNA + 0.7 NADH + 1 NADP + 9 ADP
42	0	1 CO2 + 1 R5P + 1.9 Gln + 1 Ser + 1.3 Asp + 1 NAD + 1 ATP = 1 Glu + 0.8 Fum + 0.5 Gly + 1 RNA + 1 NADH + 1 ADP
43	0	9 ACoA + 10 NADH + 7 NADPH + 26 ATP + 1 O2 = 1 FA + 10 NAD + 7 NADP + 26 ADP
Transport Reactions		
44	0	$Glc_e = Glc_i$
45	-1	$Lac_i = Lac_e$
46	-1	$Ala_i = Ala_e$
47	-1	$Amm_i = Amm_e$
48	0	$CO_{2i} = CO_{2e}$
49	0	$O_{2e} = O_{2i}$
50	-1	Glu_e + 1 ATP = Glu_i + 1 ADP
51	-1	Asp_e + 1ATP = Asp_i + 1ADP
52	-1	Gln_e + 0.33 ATP = Gln_i + 0.33 ADP
53	-1	Ser_e + 0.33 ATP = Ser_i + 0.33 ADP
54	-1	Gly_e + 0.33 ATP = Gly_i + 0.33 ADP
55	0	Thr_e + 0.33 ATP = Thr_i + 0.33 ADP
56	0	Met_e + 0.33 ATP = Met_i + 0.33 ADP
57	-1	Pro_e + 0.33 ATP = Pro_i + 0.33 ADP
58	-1	Asn_e + 0.33 ATP = Asn_i + 0.33 ADP
59	0	Leu_e + 0.33 ATP = Leu_i + 0.33 ADP
60	0	Ile_e + 0.33 ATP = Ile_i + 0.33 ADP
61	0	Val_e + 0.33 ATP = Val_i + 0.33 ADP
62	0	Phe_e + 0.33 ATP = Phe_i + 0.33 ADP
63	-1	Tyr_e + 0.33 ATP = Tyr_i + 0.33 ADP
64	0	His_e + 0.33 ATP = His_i + 0.33 ADP
65	0	Lys_e + 0.33 ATP = Lys_i + 0.33 ADP
66	-1	Arg_e + 0.33 ATP = Arg_i + 0.33 ADP
67	-1	Cys_e + 0.33 ATP = Cys_i + 0.33 ADP
68	0	= rBiomass
69*	0	AKG + Gln + NADH = 2 Glu + NAD

*Reaction only present in Sf9 cells.

Table I-2. List of baculovirus and rNeuraminidase biosynthesis reactions considered in Sf9 and High Five metabolic models.

#	Reversibility	Reaction
Baculovirus biomass synthesis		
70	0	0.000435bacDNA+0.001bacProt=1Bac : 0.000435 bacDNA + 0.001 bacProt = 1 Bac
71	0	0.0039 Ala + 0.0047 Glu + 0.0023 Gln + 0.0058 Gly + 0.0072 Ser + 0.0016 Lys + 0.0036 Leu + 0.0036 Ile + 0.0077 Arg + 0.0074 Asp + 0.0045 Thr + 0.0026 Val + 0.0011 Met + 0.0023 Phe + 0.0024 Tyr + 0.0006 His + 0.0039 Pro + 0.0034 Asn + 0.0006 Cys = 1 bacProt
72	0	0.5 CO2 + 1 R5P + 1.9 Gln + 1.3 Ser + 1.3 Asp + 0.7 NAD + 1 NADPH + 9 ATP = 1.9 Glu + 0.8 Fum + 0.8 Gly + 0.7 NADH + 1 NADP + 9 ADP + 1 bacDNA
73	0	= rBac
rNeuraminidase synthesis		
74	0	0.00016 Ala + 0.00012 Arg + 0.00015 Asn + 0.00021 Asp + 0.00015 Cys + 0.00005 Gln + 0.00011 Glu + 0.00053 Gly + 0.00004 His + 0.00021 Ile + 0.00013 Leu + 0.00014 Lys + 0.00005 Met + 0.0001 Phe + 0.00019 Pro + 0.0004 Ser + 0.00019 Thr + 0.00007 Trp + 0.00007 Tyr + 0.00021 Val = 1 Neur
75	0	= rNeur

1.1 Detailed description of the biomass equations used Sf9 and High Five metabolic models

The cells biomass equation was calculated on the basis of composition data found in the literature (Ferrance et al., 1993). The considered cell composition, 72,9% Protein + 13.5% Fatty Acids + 1.4 % DNA + 3.8% RNA (w/w), was used to estimate the requirements of each component in the biomass equation. The amino acid composition of insect cell proteins was retrieved form the literature (Ferrance et al., 1993; Xie and Wang, 1994), and used to calculate the contribution of each amino acid to protein synthesis. Regarding nucleic acids synthesis, the GC content of lepidopteran cell lines (%GC 40) was considered.

The molar requirements of each component of cellular biomass were calculated on the basis of the cell dry weight determined at exponential growth phase (1123 pg.cell^{-1}) and after infection (1410 pg.cell^{-1}). The contributions of each component for cellular biomass synthesis are shown in Table I-3.

Table I-3. Cellular biomass composition and molar coefficients

			nmol.10^{-6} cells			
Biomass component	***% w/w***	***MW (g/mol)***	***Hi5 growth***	***Hi5 infected***	***Sf9 growth***	***Sf9 infected***
Ala	8.25	89.1	758.1	951.9	221.4	339.6
Arg	5.93	174.2	278.7	349.9	81.4	124.8
Asn	4.4	132.1	272.6	342.3	79.6	122.1
Asp	4.69	133.1	288.5	362.2	84.3	129.2
Cys	2.8	121.2	189.2	237.5	55.3	84.7
Gln	6.2	146.1	347.3	436.1	101.4	155.6
Glu	4.96	147.1	276.0	346.5	80.6	123.6
Gly	8.54	75.1	931.4	1169.4	272.0	417.2
His	2.16	155.2	114.0	143.1	33.3	51.0
Ile	4.22	131.2	263.4	330.7	76.9	118.0
Leu	8.11	131.2	506.2	635.5	147.8	226.7
Lys	6.79	146.2	380.2	477.4	111.1	170.3
Met	2.17	149.2	119.1	149.5	34.8	53.3
Phe	3.19	165.2	158.1	198.5	46.2	70.8
Pro	5.26	115.1	374.0	469.6	109.2	167.5
Ser	6.89	105.1	536.7	673.9	156.8	240.4
Thr	5.73	119.1	393.8	494.4	115.0	176.4
Trp	1.1	204.2	44.1	55.4	12.9	19.8
Tyr	2.59	181.2	117.0	146.9	34.2	52.4
Val	6.02	117.2	420.7	528.2	122.9	188.4
dAMP	0.42	347.2	0.2	0.2	0.1	0.1
dCMP	0.28	307.2	0.1	0.2	0.0	0.1
dGMP	0.28	347.2	0.1	0.2	0.0	0.1
dTMP	0.42	322.2	0.2	0.3	0.1	0.1
AMPRN	1.14	347.2	1.4	1.8	0.4	0.6
CMPRN	0.76	307.2	1.1	1.3	0.3	0.5
GMPRN	0.76	347.2	0.9	1.2	0.3	0.4
UMPRN	1.14	322.2	1.5	1.9	0.4	0.7
FA	13.5	750.0	202.1	253.8	59.0	90.5

The biosynthesis reactions for baculovirus were estimated from the literature (Bergold and Wellington, 1953), taking into account their amino acid and DNA composition (76% Protein + 8% DNA, w/w). Molar percentages of amino acids in

insect viruses were taken as the average values from (Wellington, 1954). Each viral particle was considered to weight $1.07x10^{-17}$ g and has a circular genome of 262000 deoxyribonucleotides. Recombinant Neuraminidase (rNeur) synthesis was calculated taking into account the amino acid composition of the protein detailed in the Protein Data Bank (PDB) website (http://www.rcsb.org/pdb/home/home.do). The molar weight of rNeur considered was 240 KDa. The contributions of each component for baculovirus and rNeuraminidase syntheses are described in Table II and III, respectively.

Table I-4. Baculovirus biomass composition and molar coefficients

Biomass component	*% w/w*	*MW (g/mol)*	*pmol.10^{-6} virions*
Ala	4.3	89.1	0.0039
Arg	16.4	174.2	0.0077
Asn		132.1	0.0034
Asp	12.1	133.1	0.0074
Cys	0.8	121.2	0.0006
Gln		146.1	0.0023
Glu	8.5	147.1	0.0047
Gly	5.3	75.1	0.0058
His	1.1	155.2	0.0006
Ile	5.8	131.2	0.0036
Leu	5.8	131.2	0.0036
Lys	2.9	146.2	0.0016
Met	2.1	149.2	0.0011
Phe	4.7	165.2	0.0023
Pro	5.5	115.1	0.0039
Ser	9.3	105.1	0.0072
Thr	6.6	119.1	0.0045
Tyr	5.2	181.2	0.0024
Val	3.7	117.2	0.0026
dAMP	2.4	347.2	0.0006
dCMP	1.6	307.2	0.0004
dGMP	1.6	347.2	0.0004
dTMP	2.4	322.2	0.0006

Table I-5. rNeuraminidase biomass composition and molar coefficients

Amino acid (a.a.)	*nr a.a./rNeur*	*% a.a/rNeur*	*MW (g/mol)*	*pmol.rNeur^{-1}*
Ala	14	3.7	89.1	0.00016
Arg	20	5.3	174.2	0.00012
Asn	19	5.0	132.1	0.00015
Asp	27	7.1	133.1	0.00021
Cys	17	4.5	121.2	0.00015
Gln	7	1.8	146.1	0.00005
Glu	16	4.2	147.1	0.00011
Gly	38	10.0	75.1	0.00053
His	6	1.6	155.2	0.00004
Ile	26	6.8	131.2	0.00021
Leu	16	4.2	131.2	0.00013
Lys	19	5.0	146.2	0.00014
Met	7	1.8	149.2	0.00005
Phe	16	4.2	165.2	0.00010
Pro	21	5.5	115.1	0.00019
Ser	40	10.5	105.1	0.00040
Thr	22	5.8	119.1	0.00019
Trp	14	3.7	204.2	0.00007
Tyr	12	3.2	181.2	0.00007
Val	23	6.1	117.2	0.00021

2. Appendix II. Metabolic partitioning coefficients at the pyruvate and α-ketoglutarate nodes

Metabolic partitioning coefficients are defined as carbon flux channeled through a given branch of a metabolic node, normalized by the total fluxes into that node (Vallino and Stephanopoulos, 2000). Coefficients were determined considering the fluxes calculated with FluxAnalyzer software (Klamt et al., 2003).

Pyruvate Node

To analyze flux partitioning at this node, two main pathways yielding pyruvate are considered (glycolysis and pyruvate recycling) and three metabolic fates (lactate, alanine, and acetyl-CoA).

Incoming fluxes		
PEP	*Pyruvate kinase* (PK)	$\frac{v_{PK}}{v_{PK}+v_{ME}+v_{other}}$
Malate	*Malic enzyme* (ME)	$\frac{v_{ME}}{v_{PK}+v_{ME}+v_{other}}$
Outgoing fluxes		
Lactate	*Lactate dehydrogenase* (LDH)	$\frac{v_{LDH}}{v_{LDH}+v_{AlaAT}+v_{PDH}+v_{other}}$
Alanine	*Alanine aminotransferase* (AlaAT)	$\frac{v_{AlaAT}}{v_{LDH}+v_{AlaAT}+v_{PDH}+v_{other}}$
ACoA	*Pyruvate dehydrogenase* (PDH)	$\frac{v_{PDH}}{v_{LDH}+v_{AlaAT}+v_{PDH}+v_{other}}$

α-ketoglutarate Node

To analyze flux partitioning at this node, four main pathways yielding a-ketoglutarate (the TCA cycle, vOAA; the alanine and aspartate transaminase pathways, vAspAT and vAlaAT; glutamate dehydrogenase, vGDH) and two main metabolic fates (TCA cycle vSucCoA, and glutamate synthase, vGOGAT) are considered.

Incoming fluxes		
Isocitrate	*Isocitrate dehydrogenase* (ICDH)	$\frac{v_{Isocit}}{v_{ICDH}+v_{AlaAT}+v_{other}}$
Alanine	*Alanine aminotransferase* (AlaAT)	$\frac{v_{AlaAT}}{v_{ICDH}+v_{AlaAT}+v_{other}}$
Outgoing fluxes		
Glutamate	*Glutamate dehydrogenase* (GDH)	$\frac{v_{GDH}}{v_{GDH}+v_{aKGDH}+v_{GOGAT}+v_{other}}$
Succinyl-CoA	*α-Ketoglutarate dehydrogenase* (αKGDH)	$\frac{v_{aKGDH}}{v_{GDH}+v_{aKGDH}+v_{GOGAT}+v_{other}}$
Glutamate	*Glutamate synthase* (GOGAT)	$\frac{v_{GOGAT}}{v_{GDH}+v_{aKGDH}+v_{GOGAT}+v_{other}}$

3. Appendix III. Metabolic fluxes of Sf9 and High Five cells

Table III-1. Absolute fluxes of High 5 and Sf9 cells during growth

			Hi5	Sf9
	Acronym	**Reaction**	**Flux ± SE**	**Flux ± SE**
Glycolysis	**HK**	Glc + ATP = G6P + ADP	114.5 ± 5.2	58.6 ± 3.9
	PGI	G6P = F6P	97.1 ± 6.6	52.4 ± 4.7
	F6P-2GAP	F6P + ATP = 2 GAP	97.1 ± 6.6	52.4 ± 4.7
	GAP-PEP	GAP + NAD + ADP = PEP + NADH + ATP	194.1 ± 13.3	104.9 ± 9.5
	PEP-Pyr	PEP + ADP = Pyr + ATP	194.1 ± 13.3	104.9 ± 9.5
	LDH	Pyr + NADH = Lac + NAD	54.3 ± 10.0	2.1 ± 0.5
	AlaAT	Pyr + Glu = Ala + AKG	164.6 ± 4.8	23.1 ± 3.4
	PPP	3 G6P + 6 NADP = 3 CO_2+ 3 R5P + 6 NADPH	5.8 ± 0.6	2.1 ± 0.4
TCA & Anaplerosis	**PDH**	Pyr + NAD = ACoA + CO_2 + NADH	131.2 ± 14.5	101.7 ± 9.7
	CS	ACoA + OAA = Cit	81.3 ± 20.7	87.0 ± 16.1
	AkgDH	AKG + NAD = CO_2 + SuCoA + NADH	143.7 ± 21.7	107.2 ± 13.4
	SucCoAs	SuCoA + ADP = Succ + ATP	155.5 ± 31.3	113.9 ± 10.1
	SucDH	Succ + FAD = Fum + $FADH_2$	155.5 ± 31.3	113.9 ± 10.1
	Fum	Fum = Mal	175.5 ± 37.3	121.0 ± 8.8
	MDH	Mal + NAD = OAA + NADH	-34.2 ± 7.7	93.4 ± 16.2
	ME	Mal = Pyr + CO_2	196.4 ± 17.1	27.6 ± 8.0
A.A. Metab	**AlaAT**	Pyr + Glu = Ala + AKG	164.6 ± 4.8	23.1 ± 3.4
	GOGAT	Gln + AKG + NADH = 2 Glu + NAD	*N.A.*	2.9 ± 1.2
	GDH	Glu + NAD = AKG + Amm + NADH	50.7 ± 1.7	4.4 ± 0.4
	SerDeg	Ser=Pyr+Amm	-42.1 ± 7.1	-2.6 ± 0.0
	AspAT	Glu + OAA = AKG + Asp	-102.2 ± 0.0	6.4 ± 0.1
	MetDeg	Ser + Met + NAD + ATP = SuCoA + Amm + Cys + NADH + 2 ADP	2.1 ± 0.4	1.4 ± 0.0
	AsnDeg	Glu + Asn = Asp + Gln	134.2 ± 1.4	1.7 ± 1.7
	CysDeg	Cys = Pyr + Amm	-2.8 ± 0.2	2.2 ± 0.2
Macro. synt.	**Prot**	Protein synthesis	28.0 ± 3.1	34.0 ± 5.8
	DNA	DNA synthesis	5.0 ± 0.6	1.8 ± 0.3
	RNA	RNA synthesis	12.5 ± 1.4	4.4 ± 0.8
	FA	Fatty Acid synthesis	6.2 ± 0.7	2.2 ± 0.4
E rx	**O2**	Respiration	337.2 ± 77.1	303.9 ± 39.8
	NADH	Net NADH	478.4 ± 95.4	480.5 ± 70.3
	ATP	Net ATP synthesis	1130.4 ± 237.9	1124.6 ± 288.6

Cultures were performed as described in Materials and Methods, and a single exponential growth phase was considered. Fluxes were computed with the FluxAnalyzer software, and are expressed in nmol.(10^6.cells.h)$^{-1}$ as the mean average value of three independent replicates (n=3). N.A. stands for Not Applicable.

Table III-2. Absolute fluxes of High Five and Sf9 cells after baculovirus infection

			Hi5	Sf9
			CCI 1	
			MOI 0.2	
	Acronym	Reaction	Flux ± SE	Flux ± SE
Glycolysis	HK	Glc + ATP = G6P + ADP	143.3 ± 5.4	54.8 ± 5.1
	PGI	G6P = F6P	130.7 ± 5.9	51.5 ± 4.6
	F6P-2GAP	F6P + ATP = 2 GAP	130.7 ± 5.9	51.5 ± 4.6
	GAP-PEP	GAP + NAD + ADP = PEP + NADH + ATP	261.4 ± 11.8	103.0 ± 9.2
	PEP-Pyr	PEP + ADP = Pyr + ATP	261.4 ± 11.8	103.0 ± 9.2
	LDH	Pyr + NADH = Lac + NAD	34.1 ± 10.2	0.6 ± 0.3
	AlaAT	Pyr + Glu = Ala + AKG	95.5 ± 9.6	39.9 ± 4.6
	PPP	3 G6P + 6 NADP = 3 CO_2+ 3 R5P + 6 NADPH	4.2 ± 0.5	1.1 ± 0.2
TCA & Anaplerosis	PDH	Pyr + NAD = ACoA + CO_2 + NADH	227.9 ± 9.2	110.1 ± 9.6
	CS	ACoA + OAA = Cit	208.5 ± 18.6	116.7 ± 7.5
	AkgDH	AKG + NAD = CO_2 + SuCoA + NADH	232.8 ± 23.4	127.1 ± 12.6
	SucCoAs	SuCoA + ADP = Succ + ATP	241.6 ± 29.2	137.5 ± 13.7
	SucDH	Succ + FAD = Fum + $FADH_2$	241.6 ± 29.2	137.5 ± 13.7
	Fum	Fum = Mal	256.7 ± 31.9	147.0 ± 14.4
	MDH	Mal + NAD = OAA + NADH	137.3 ± 23.6	109.7 ± 7.3
	ME	Mal = Pyr + CO_2	119.4 ± 8.9	37.3 ± 7.3
A.A. Metab	AlaAT	Pyr + Glu = Ala + AKG	95.5 ± 9.6	39.9 ± 4.6
	GOGAT	Gln + AKG + NADH = 2 Glu + NAD	*N.A.*	-6.5 ± 2.1
	GDH	Glu + NAD = AKG + Amm + NADH	20.7 ± 4.4	-6.7 ± 1.2
	SerDeg	Ser=Pyr+Amm	-28.0 ± 6.2	-3.5 ± 0.4
	AspAT	Glu + OAA = AKG + Asp	-71.2 ± 5.1	-7.0 ± 0.9
	MetDeg	Ser + Met + NAD + ATP = SuCoA + Amm + Cys + NADH + 2 ADP	6.3 ± 0.4	5.0 ± 1.0
	AsnDeg	Glu + Asn = Asp + Gln	81.7 ± 8.8	2.3 ± 1.5
	CysDeg	Cys = Pyr + Amm	4.6 ± 1.5	10.7 ± 1.7
Macro. synt.	Prot	Protein synthesis	16.1 ± 1.8	11.6 ± 1.9
	DNA	DNA synthesis	3.6 ± 0.4	0.9 ± 0.1
	RNA	RNA synthesis	9.0 ± 1.0	2.3 ± 0.4
	FA	Fatty Acid synthesis	4.4 ± 0.5	1.1 ± 0.2
E rx	O2	Respiration	657.8 ± 75.4	381.2 ± 35.4
	NADH	Net NADH	1036.6 ± 103.5	582.2 ± 49.3
	ATP	Net ATP synthesis	3034.4 ± 341.5	1701.2 ± 140.1

Cultures were performed as described in Materials and Methods, and a single phase post-infection was considered. Fluxes were computed with the FluxAnalyzer software, and are expressed in nmol.(10^6.cells.h)$^{-1}$ as the mean average value of three independent replicates (n=3). N.A. stands for Not Applicable.

4. Appendix IV. Supplementary material for metabolomics and pathway analysis (Chapter V).

Detailed protocol for the metabolomic analysis of insect cells

(i) Quenching: Cells were harvested and placed in ice-cold quenching solution (60% (vol/vol) methanol/water with 0.85% ammonium bicarbonate). Afterwards, cells were pelleted by centrifugation (400 x g, 5 min, -12ºC), frozen in liquid nitrogen and kept at -85ºC until extraction. The supernatant was kept for subsequent analysis to check for potential leaking.

(ii) Extraction: Metabolite extraction was based on the work of (Lazzarino et al., 2003). Samples and standard mixtures were resuspended in 2 mL of extraction solution (acetonitrile + 10mM KH_2PO_4 (3:1 v/v) at pH 7.4) and homogenized for 30 minutes at 4ºC, and centrifuged at 15,000 x g for 20 min at 4ºC. The supernatant was added to 4 mL of chloroform and centrifuged again at 15,000 x g for 5 min yielding a biphasic system, from which the aqueous phase was harvested and filtered through a sterile 0.2 µm filter. Extracts were prepared at the time of analysis to avoid degradation.

(iii) Metabolite Analysis: Previous to the quantification process, unequivocal identification of the metabolites was performed using the retention time and relative intensities of the diagnostic ions of a pool of samples. The utilized diagnostic ions and their relative intensities are summarized in Table IV-1. Due to the limitations of a single quadrupole regarding isobaric compounds, which cannot be unequivocally identified with the previous method, their chromatographic separation was confirmed. Measurements for quantification were conducted using single ion monitoring (SIM). The measured metabolites and the SIM ions used for quantification are detailed in Table VI-1. LC-MS experiments were performed on a 1200 series HPLC instrument (Agilent Technologies; California, USA) coupled to an Agilent 6120 single quadrupole mass spectrometer with orthogonal ESI source. The separation was performed using two different methods based on the chemical classes of the analyzed metabolites. For amino acids and co-enzymes the method previously described in (Preinerstorfer et al., 2010) was applied. Briefly, an injection volume of 10 µl was used with a ZIC-HILIC stationary phase, 150 mm x 4.6 mm internal diameter, and 5 µm particle size, provided with a guard column, 20 x 2.1 mm, 5 µm (Merck SeQuant, Marl, Germany) operated at 25ºC. For metabolite elution, a gradient method was applied with a flow rate of 0.5 ml/min. Mobile phases were 20 mM ammonium acetate (adjusted to pH 7.5 with NH_4OH) in H_2O (solvent A) and 20

mM ammonium acetate in AcN (solvent B). Gradient elution was performed, starting with 0% A and increasing to 80% A for 30 minutes, then back to starting conditions (80-0% A) for 1 minute followed by a re-equilibration period (0% A) of 14 minutes. The mass spectrometer was operated in the positive ESI mode, using the SIM mode for the m/z of each compound. The ion spray voltage was set at 4000 V. Nitrogen with a flux of 12 l/min was used as the sheath gas (35 psi) and the auxiliary gas. The ion transfer capillary was heated to 300ºC. The fragmentation voltage was set at 100 V. For organic acids, an injection volume of 10 µl was used with a Aminex-HPX-87H cation exchanger column, 300 x 7.8 mm internal diameter and 9 µm particle size (BioRad Labs, Hercules, USA), at 40ºC. For elution, an isocratic method was applied with a flow rate of 0.5 ml/min, with formic acid 0.1% as a mobile phase. The mass spectrometer was operated in the negative ESI mode, using the SIM mode for the m/z of each compound (see Supplemental Table 1). The ion spray voltage was set at 3500 V. Nitrogen with a flux of 12 l/min was used as the sheath gas (40 psi) and the auxiliary gas. The ion transfer capillary was heated to 350 ºC. The fragmentation voltage was set at 70 V. Data were acquired using the Agilent Chemstation software package, and EasyLCMS was used for automated quantification (Fructuoso et al., 2012).

(iv) ***Quality control:*** The quality of the results was assessed by: checking the extraction method with standard mixtures, internal standard (IS); and quality control samples (QC). The extraction method was validated by comparing the concentration of standard mixtures with and without the extraction process. Recoveries were higher than 85% in all of the analyzed metabolites (results not shown). Three deuterated compounds were added as IS, reaching a final concentration of 50 µM in each analyzed sample, and the analysis was monitored by controlling that the internal standard areas and retention times were always within an acceptable range. Acceptable coefficient of variation was set at 20% for the peak area and 2% for retention time. With respect to quality control samples, two types of QCs were incorporated in the analysis: a pool of samples and a pool of standards. QC analysis was performed for all of the analyzed metabolites in the standard pool samples, and in all of those in which concentration was over the quantification limits in the sample pools. This was carried out by comparing the corrected areas. For the standard pool, the theoretical corrected area was calculated for the measured concentration. Regarding the pool of samples, the corrected areas were compared among all of the samples. An acceptable coefficient of variation was set at 20% for the peak area and 2% for retention time.

Table IV-1. LC-ESI-MS analytical parameters and method performance for compound standards of the quantified metabolites.

Metabolite	Abbreviation	Parent ion formula	Diagnostic ions (relative abundance)	RT (min)	SIM ion	LOD[a] (nmol/mL)	LOQ[b] (nmol/mL)	R^2	Intraday[c] RSD (%)	Interday[c] RSD (%)
Glycine	Gly	$C_2H_6NO_2^+$	76 (82), 98 (8), 150 (52)	15.0 [e]	76	4.71	15.71	0.9782	8.75	12.21
Pyruvic acid	Pyr	$C_3H_3O_3^-$	81 (1), 83 (3), 87 (100)	10.0 [h]	87	3.59	11.96	0.9954	7.72	6.50
Lactic acid	Lac	$C_3H_5O_3^-$	89 (100), 90(4), 91 (5)	16.0 [h]	89	5.99	19.96	0.9945	1.37	10.65
L-Alanine	Ala	$C_3H_8NO_2^+$	90 (100), 112 (13), 134 (5)	14.3 [e]	90	4.81	16.03	0.9944	1.94	8.40
L-Serine	Ser	$C_3H_8NO_3^+$	88 (20), 106 (100),128 (10)	13.2 [e]	106	0.02	0.05	0.9826	1.50	9.35
Fumaric acid	Fum	$C_4H_3O_4^-$	98 (10), 115 (100), 116 (10)	19.0 [h]	115	1.11	3.73	0.9993	4.43	5.86
L-Proline	Pro	$C_5H_{10}NO_2^+$	70 (2), 116 (100),138 (10)	25.8 [e]	116	0.90	3.00	0.9905	1.38	18.24
Succinic acid	Succ	$C_4H_5O_4^-$	95 (4), 117 (100), 118 (5)	16.0 [h]	117	1.12	3.74	0.9941	7.45	15.8
L-Valine	Val	$C_5H_{12}NO_2^+$	72 (5), 118 (80), 140 (15)	12.6 [e]	118	0.83	2.77	0.9935	1.14	11.56
L-Threonine	Thr	$C_4H_8NO_3^+$	74 (5), 120 (100), 142 (10)	10.0 [e]	120 [d]	0.91	3.03	0.9824	28.85	6.58
L-Homoserine	HomoSer	$C_4H_{10}NO^+$	74 (5), 120 (100),142 (8)	14.2 [e]	120 [d]	0.28	0.94	0.9981	0.79	15.24
Taurine	Taurine	$C_2H_6NO_3S^+$	126 (100), 146 (10), 148 (12), 251 (15)	12.1 [e]	126	3.11	10.36	0.9950	2.40	5.86
Thymine	Thymine	$C_5H_7N_2O_2^+$	127 (100), 149 (10), 171 (10)	4.0 [g]	127	0.07	0.22	0.9991	0.45	13.75
L-Hydroxyproline	HydroxyPro	$C_5H_9NO_3^+$	86 (10), 132 (100),154 (20)	14.1 [e]	132 [d]	1.73	5.77	0.9947	13.41	18.65
L-Isoleucine	Ileu	$C_6H_{14}NO_2^+$	86 (50), 132 (100),154 (10)	10.7 [e]	132 [d]	0.45	1.50	0.9899	0.33	5.20
L-Leucine	Leu	$C_6H_{14}NO_2^+$	86 (50), 132 (100),154 (10)	11.7 [e]	132 [d]	0.07	0.25	0.9926	1.22	16.74
L-Asparagine	Asn	$C_4H_9N_2O_3^+$	87 (10), 133 (100),155 (10)	14.5 [e]	133 [d]	1.10	3.66	0.9834	1.31	0.93
L-Ornithine	Orn	$C_5H_{13}N_2O_2^+$	115 (25), 133 (100),155 (10)	26.5 [e]	133 [d]	0.43	1.43	0.9902	0.44	2.55
L-Malic acid	Mal	$C_4H_5O_5^-$	115 (8), 133 (100), 134 (5)	13.0 [h]	133	0.78	2.62	0.9899	7.32	0.87
L-Aspartic acid	Asp	$C_4H_6NO_4^+$	121 (20), 134 (100), 200 (75)	15.2 [e]	134	6.28	20.93	0.9837	2.78	4.98
L-Homocysteine	HomoCys	$C_4H_{10}NO_2S^+$	90 (10), 136 (100), 158 (10)	12.4 [e]	136	1.14	3.82	0.9859	0.37	6.79
Hypoxanthine	Hypoxan	$C_5H_5N_4O^+$	137 (70), 159 (100), 175 (10)	11.0 [g]	137	0.23	0.77	0.9986	2.52	10.27
Oxoglutaric acid	OxoGlut	$C_5H_5O_5^-$	110 (33), 145 (100), 146 (5)	9.6 [h]	145	0.01	0.04	0.9993	0.42	5.60
L-Lysine	Lys	$C_6H_{15}N_2O_2^+$	84 (8), 130 (30), 147 (100), 169 (8)	25.9 [e]	147 [d]	0.10	0.35	0.9892	1.10	12.60
L-Glutamine	Gln	$C_5H_{11}N_2O_3^+$	130 (50), 147 (100), 169 (67)	14.7 [e]	147 [d]	0.73	2.45	0.9901	3.91	9.97
L-Glutamic acid	Glu	$C_5H_{10}NO_4^+$	102 (60), 148 (100), 170 (30),	14.9 [e]	148	0.37	1.23	0.9882	0.64	5.00
L-Histidine	His	$C_6H_{10}N_3O_2^+$	137 (25), 156 (100), 178 (5)	15.0 [e]	156	0.24	0.79	0.9801	7.08	21.55
L-Carnitine	Carnitine	$C_7H_{16}NO_3^+$	149 (1), 162 (100), 184 (5)	15.7 [e]	162	0.02	0.08	0.9899	4.04	7.96
L-Phenylalanine	Phe	$C_9H_{12}NO_2^+$	137 (35), 166 (100), 188 (20)	9.9 [e]	166	0.74	2.47	0.9987	2.08	12.53
Dihydroxyacetone phosphate	DHAP	$C_3H_6O_6P^-$	89 (10), 169 (100), 170 (10)	8.0 [h]	169	0.92	3.08	0.9988	8.54	10.6
L-Arginine	Arg	$C_6H_{13}N_4O_2^+$	140 (5), 175 (100), 197 (2)	24.5 [e]	175	0.02	0.08	0.9950	1.47	16.47
L-Citrulline	CIR	$C_6H_{12}N_3O_3^+$	159 (19), 176 (100), 198 (18)	15.3 [e]	176	0.38	1.26	0.9846	26.65	14.25
L-Tyrosine	Tyr	$C_9H_{12}NO_3^+$	163 (15), 182 (100), 204 (5)	12.1 [e]	182	0.76	2.55	0.9892	0.97	6.40
Citric acid	CitAc	$C_6H_7O_8^-$	111 (2), 191 (100), 192 (5)	11.0 [h]	191	0.20	0.67	0.9991	10.25	9.74
L-Tryptophan	Trp	$C_{11}H_{13}N_2O_2^+$	177 (10), 205 (100), 227 (30)	10.1 [e]	205	2.99	9.97	0.9897	5.13	2.44
L-Cystine	Cystin	$C_6H_{12}N_2O_4S_2^+$	156 (100), 241 (30), 263 (18)	17.0 [e]	241	12.07	40.24	0.9577	3.97	0.87
Thymidine	Thymidine	$C_{10}H_{13}N_2O_5^+$	243 (38), 265 (100), 281 (38)	4.2 [g]	243	0.17	0.57	0.9949	0.19	1.46

Biotin	Biotin	$C_{10}H_{17}N_2O_3S^+$	245 (43),267 (30), 527 (55)	10.8 [g]	245	1.52	5.07	0.9974	4.87	16.17
L-Glutathione	GSH	$C_{10}H_{18}N_3O_6S^+$	308 (100), 330 (10), 618 (10)	14.6 [e]	308	5.64	18.82	0.9864	0.30	6.44
5-Thymidlic acid	TMP	$C_{10}H_{16}N_2O_8P^+$	207 (25), 323 (100), 345 (50)	14.4 [g]	323	15.8	52.40	0.9799	4.10	0.80
Cytidine monophosphate	CMP	$C_9H_{15}N_3O_8P^+$	112 (20), 266 (10), 324 (100)	16.0 [g]	324	1.25	4.18	0.9881	5.07	0.96
Uridine 5'-monophosphate	UMP	$C_9H_{14}N_2O_9P^+$	172 (90), 325 (100), 342 (25)	15.0 [g]	325	26.55	88.51	0.9820	3.53	10.67
Fructose 1,6-bisphosphate	F16P	$C_6H_{13}O_{12}P_2^-$	197 (10), 339 (100), 361 (15)	7.8 [h]	339	0.03	0.10	0.9990	1.57	8.60
Thiamine monophosphate	ThiaMP	$C_{12}H_{18}N_4O_4PS^+$	122 (25), 345 (100), 367 (15)	20.5 [g]	345	2.30	7.60	0.9812	12.4	14.66
Adenosine monophosphate	AMP	$C_{10}H_{11}N_5O_6P^+$	268 (15), 348 (100), 370 (10)	14.7 [g]	348	0.64	2.15	0.9910	2.04	18.44
Inosinic acid	IMP	$C_{10}H_{14}N_4O_8P^+$	138 (50), 349 (100), 371 (41)	15.4 [g]	349	93.71	312.39	0.9810	11.13	23.16
Xanthylic acid	XMP	$C_{10}H_{14}N_4O_9P^+$	157 (50), 365 (100), 387 (27)	15.7 [g]	365	17.85	59.49	0.9945	2.57	5.00
S-Adenosyl-Homocyscteine	SAH	$C_{14}H_{21}N_6O_5S^+$	317 (45), 385 (100), 407 (10)	13.6 [g]	385	0.01	0.04	0.9967	11.79	9.50
S-Adenosyl-Methionine	SAM	$C_{15}H_{23}N_6O_5S^+$	298 (3), 399 (100), 416 (3)	21.0 [g]	399	1.33	4.44	0.9715	2.98	10.60
Cytidine diphosphate	CDP	$C_9H_{14}N_3O_{11}P_2^+$	381 (40), 404 (100),426 (48)	16.0 [g]	404	2.32	7.74	0.9822	5.48	8.82
Uridine 5'-diphosphate	UDP	$C_9H_{13}N_2O_{12}P_2^+$	301 (95), 405 (100), 427 (60)	15.4 [g]	405	73.50	350.02	0.9949	2.42	0.93
Adenosine diphosphate	ADP	$C_{10}H_{14}N_5O_{10}P_2^+$	348 (40), 428 (100), 450 (20)	15.7 [g]	428	1.95	5.50	0.9941	2.07	9.41
Flavin Mononucleotide	FMN	$C_{17}H_{20}N_4O_9P^+$	399 (30), 457 (100), 479 (30)	13.6 [g]	457	2.33	7.76	0.9942	2.17	11.57
Cytidine triphosphate	CTP	$C_9H_{15}N_3O_{14}P_3^+$	177 (43), 484 (100), 506 (60)	16.7 [g]	484	0.62	2.08	0.9501	12.17	8.47
Uridine triphosphate	UTP	$C_9H_{14}N_2O_{15}P_3^+$	485 (100), 507 (50), 589 (20)	15.9 [g]	485	2.25	7.49	0.9961	5.56	13.76
Citicoline	CDP-choline	$C_{14}H_{27}N_4O_{11}P_2^+$	112 (20), 489 (100), 511 (80)	17.0 [g]	489	9.41	31.38	0.9949	5.70	4.66
Adenosine triphosphate	ATP	$C_{10}H_{15}N_5O_{13}P_3^+$	410 (15), 508 (100), 530 (20)	15.6 [g]	508	7.68	25.62	0.9877	1.74	12.51
L-Glutathione oxidised form	GSSG	$C_{20}H_{33}N_6O_{12}S_2^+$	307 (100), 613 (100), 635 (50)	16.5 [e]	613	4.09	13.63	0.9913	4.84	5.44
Nicotinamide adenine dinucleotide oxidised form	NAD	$C_{21}H_{26}N_7O_{14}P_2^+$	123 (20), 333 (30), 664 (100), 686 (50)	15.2 [g]	664	3.44	11.46	0.9943	3.08	6.74
Nicotinamide adenine dinucleotide reduced form	NADH	$C_{21}H_{28}N_7O_{14}P_2^+$	334 (70), 666 (80), 688 (50)	16.0 [g]	666	49.24	164.15	0.9834	4.51	7.81
Coenzyme A	CoA	$C_{21}H_{37}N_7O_{16}P_3S^+$	385 (60),768 (100), 790 (25)	14.8 [g]	768	18.65	62.18	0.9913	6.79	9.74
Acetyl-CoA	AcCoA	$C_{23}H_{39}N_7O_{17}P_3S^+$	406 (100),810 (95), 832 (25)	14.1 [g]	810	16.38	54.60	0.9881	2.89	1.42

[a] LOD calculated from standard deviation of memory peak areas of blank runs: 3 x standard deviation of memory peak area (n=6)/slope of calibration function with neat standard solutions;

[b] LOQ calculated from standard deviation of memory peak areas of blank runs: 10 x standard deviation of memory peak area (n=6)/slope of calibration function with neat standard solutions;

[c] The intra- and inter-day precision were determined by analyzing six replicates of the standards at the same concentration level and calculated as the relative standard deviation (RSD) defined as the ratio of the standard deviation to the mean response factor of each metabolite;

[d] Chromatographically separated;

[e] Analytical Method 1 using L-Phenyl-d5-alanine as internal standard;

[g] Analytical Method 1 using Thymine-d_4 (methyl-d_3,6-d_1) as internal standard;

[h] Analytical Method 2 using Succinic acid-2,2,3,3-d_4 as internal standard.

Table IV-2. Metabolic Pathway Analysis of baculovirus infected Sf9 cells.

Metabolic pathways	Total Compounds	Hits	Raw p	-log (p)	Holm adjust	FDR	Impact
Nitrogen metabolism	7	3	5.2E-06	12.2	2.3E-04	9.5E-05	0
Valine, leucine and isoleucine biosynthesis	13	5	5.5E-06	12.1	2.3E-04	9.5E-05	1
Glycine, serine and threonine metabolism	25	4	9.7E-06	11.5	4.1E-04	9.5E-05	0.6
D-Glutamine and D-glutamate metabolism	5	3	1.0E-05	11.5	4.2E-04	9.5E-05	1
Alanine, aspartate and glutamate metabolism	23	9	1.2E-05	11.3	4.9E-04	9.5E-05	0.7
Aminoacyl-tRNA biosynthesis	67	18	1.3E-05	11.2	5.2E-04	9.5E-05	0.1
Methane metabolism	9	2	1.7E-05	11.0	6.6E-04	9.5E-05	0.4
Cyanoamino acid metabolism	6	2	1.7E-05	11.0	6.6E-04	9.5E-05	0
Cysteine and methionine metabolism	25	5	2.1E-05	10.8	7.5E-04	1.0E-04	0.3
Histidine metabolism	7	1	2.7E-05	10.5	9.4E-04	1.1E-04	1
Porphyrin and chlorophyll metabolism	23	2	2.7E-05	10.5	9.4E-04	1.1E-04	0
Sphingolipid metabolism	18	1	3.2E-05	10.3	1.1E-03	1.2E-04	0
Pantothenate and CoA biosynthesis	12	1	4.8E-05	10.0	1.5E-03	1.6E-04	0
Ubiquinone and other terpenoid-quinone biosynthesis	3	1	8.5E-05	9.4	2.6E-03	2.4E-04	0
Phenylalanine, tyrosine and tryptophan biosynthesis	4	2	8.5E-05	9.4	2.6E-03	2.4E-04	1
Phenylalanine metabolism	10	2	8.5E-05	9.4	2.6E-03	2.4E-04	0.7
Valine, leucine and isoleucine degradation	35	4	1.2E-04	9.0	3.3E-03	3.1E-04	0
Tyrosine metabolism	30	2	1.3E-04	9.0	3.4E-03	3.1E-04	0.2
Glycerophospholipid metabolism	27	2	6.4E-04	7.4	1.7E-02	1.5E-03	0
Riboflavin metabolism	7	1	1.5E-03	6.5	3.8E-02	3.4E-03	0.3
Arginine and proline metabolism	37	10	2.4E-03	6.0	5.7E-02	5.0E-03	0.5
Glutathione metabolism	26	5	6.0E-03	5.1	1.4E-01	1.2E-02	0.5
Pyrimidine metabolism	41	9	6.8E-03	5.0	1.5E-01	1.3E-02	0.3
Fatty acid metabolism	38	2	7.9E-03	4.8	1.7E-01	1.5E-02	0.3
Nicotinate and nicotinamide metabolism	9	1	9.3E-03	4.7	1.9E-01	1.6E-02	0.3
Biotin metabolism	5	1	9.4E-03	4.7	1.9E-01	1.6E-02	0
Butanoate metabolism	21	5	1.2E-02	4.4	2.1E-01	1.9E-02	0
Citrate cycle (TCA cycle)	20	7	1.7E-02	4.1	2.9E-01	2.6E-02	0.3

Pyruvate metabolism	24	4	2.0E-02	3.9	3.3E-01	3.1E-02	0.4
Glycolysis or Gluconeogenesis	25	4	2.2E-02	3.8	3.3E-01	3.2E-02	0.1
Purine metabolism	64	7	3.0E-02	3.5	4.3E-01	4.3E-02	0.3
One carbon pool by folate	8	1	8.7E-02	2.4	1.0E+00	1.2E-01	0.2
Folate biosynthesis	16	1	8.7E-02	2.4	1.0E+00	1.2E-01	0
Lysine degradation	17	2	3.6E-01	1.0	1.0E+00	4.7E-01	0
Glyoxylate and dicarboxylate metabolism	16	3	3.9E-01	0.9	1.0E+00	4.9E-01	0.3
Fatty acid elongation in mitochondria	27	1	5.5E-01	0.6	1.0E+00	6.2E-01	0.3
Fatty acid biosynthesis	38	1	5.5E-01	0.6	1.0E+00	6.2E-01	0
Synthesis and degradation of ketone bodies	5	1	5.5E-01	0.6	1.0E+00	6.2E-01	0
Terpenoid backbone biosynthesis	13	1	5.5E-01	0.6	1.0E+00	6.2E-01	0
Fructose and mannose metabolism	18	1	5.6E-01	0.6	1.0E+00	6.2E-01	0
Tryptophan metabolism	23	2	5.8E-01	0.5	1.0E+00	6.2E-01	0.4
Inositol phosphate metabolism	24	2	6.4E-01	0.4	1.0E+00	6.7E-01	0
Propanoate metabolism	18	2	6.9E-01	0.4	1.0E+00	7.0E-01	0
beta-Alanine metabolism	13	1	8.1E-01	0.2	1.0E+00	8.1E-01	0

Total compounds correspond to the total number of compounds in the pathway; the Hits is the actually matched number from the intracellular quantifications data; the Raw p is the original p value calculated from the enrichment analysis; the Holm p is the p value adjusted by Holm-Bonferroni method; the FDR p is the p value adjusted using False Discovery Rate; the Impact is the pathway impact value calculated from pathway topology analysis.

Table IV-3. Metabolic Pathway Analysis of baculovirus infected High Five cells.

Metabolic pathways	Total Compounds	Hits	Raw p	-log (p)	Holm adjust	FDR	Impact
Biotin metabolism	5	2	1.1E-10	22.9	4.9E-09	4.9E-09	0.4
Glycolysis or Gluconeogenesis	25	4	3.6E-05	10.2	1.6E-03	5.8E-04	0.1
Pyruvate metabolism	24	4	3.9E-05	10.2	1.7E-03	5.8E-04	0.4
Taurine and hypotaurine metabolism	6	1	6.9E-05	9.6	2.9E-03	6.0E-04	0.5
Valine, leucine and isoleucine biosynthesis	13	5	7.2E-05	9.5	2.9E-03	6.0E-04	1
Butanoate metabolism	21	5	8.0E-05	9.4	3.2E-03	6.0E-04	0
Ubiquinone and other terpenoid-quinone biosynthesis	3	1	1.5E-04	8.8	5.9E-03	9.5E-04	0
Citrate cycle (TCA cycle)	20	7	1.8E-04	8.6	6.7E-03	9.5E-04	0.3
Glycine, serine and threonine metabolism	25	4	1.9E-04	8.6	7.1E-03	9.5E-04	0.6
Alanine, aspartate and glutamate metabolism	23	9	2.9E-04	8.1	1.1E-02	1.2E-03	0.7
Valine, leucine and isoleucine degradation	35	4	3.0E-04	8.1	1.1E-02	1.2E-03	0
Tyrosine metabolism	30	2	3.1E-04	8.1	1.1E-02	1.2E-03	0.2
Phenylalanine, tyrosine and tryptophan biosynthesis	4	2	4.9E-04	7.6	1.6E-02	1.5E-03	1
Phenylalanine metabolism	10	2	4.9E-04	7.6	1.6E-02	1.5E-03	0.7
Pyrimidine metabolism	41	10	5.0E-04	7.6	1.6E-02	1.5E-03	0.3
Histidine metabolism	7	1	7.4E-04	7.2	2.2E-02	2.0E-03	1
Tryptophan metabolism	23	2	8.4E-04	7.1	2.4E-02	2.0E-03	0.4
Glyoxylate and dicarboxylate metabolism	16	3	8.9E-04	7.0	2.5E-02	2.0E-03	0.3
Lysine degradation	17	2	9.2E-04	7.0	2.5E-02	2.0E-03	0
Propanoate metabolism	18	2	9.6E-04	7.0	2.5E-02	2.0E-03	0
Glutathione metabolism	26	5	9.9E-04	6.9	2.5E-02	2.0E-03	0.5
Fatty acid elongation in mitochondria	27	1	1.1E-03	6.8	2.7E-02	2.0E-03	0.3
Fatty acid biosynthesis	38	1	1.1E-03	6.8	2.7E-02	2.0E-03	0
Synthesis and degradation of ketone bodies	5	1	1.1E-03	6.8	2.7E-02	2.0E-03	0
Terpenoid backbone biosynthesis	13	1	1.1E-03	6.8	2.7E-02	2.0E-03	0
Cysteine and methionine metabolism	25	5	1.2E-03	6.7	2.7E-02	2.1E-03	0.3
Pantothenate and CoA biosynthesis	12	1	1.3E-03	6.6	2.7E-02	2.2E-03	0
Inositol phosphate metabolism	24	2	1.4E-03	6.6	2.7E-02	2.3E-03	0
Nicotinate and nicotinamide metabolism	9	1	1.6E-03	6.4	2.7E-02	2.5E-03	0.3
Aminoacyl-tRNA biosynthesis	67	18	2.2E-03	6.1	3.5E-02	3.3E-03	0.1
beta-Alanine metabolism	13	1	3.2E-03	5.7	4.9E-02	4.7E-03	0

Arginine and proline metabolism	37	10	4.2E-03	5.5	5.9E-02	5.9E-03	0.5
D-Glutamine and D-glutamate metabolism	5	3	9.9E-03	4.6	1.3E-01	1.3E-02	1
Nitrogen metabolism	7	3	1.1E-02	4.5	1.3E-01	1.4E-02	0
Porphyrin and chlorophyll metabolism	23	2	1.2E-02	4.4	1.3E-01	1.6E-02	0
Sphingolipid metabolism	18	1	2.4E-02	3.7	2.4E-01	3.0E-02	0
Purine metabolism	64	7	2.5E-02	3.7	2.4E-01	3.1E-02	0.3
Methane metabolism	9	2	4.3E-02	3.1	3.5E-01	5.0E-02	0.4
Cyanoamino acid metabolism	6	2	4.3E-02	3.1	3.5E-01	5.0E-02	0
Glycerophospholipid metabolism	27	2	1.0E-01	2.3	6.2E-01	1.2E-01	0
Fatty acid metabolism	38	2	1.5E-01	1.9	7.6E-01	1.7E-01	0.3
Riboflavin metabolism	7	1	2.3E-01	1.5	9.1E-01	2.4E-01	0.3
Fructose and mannose metabolism	18	1	2.5E-01	1.4	9.1E-01	2.6E-01	0
One carbon pool by folate	8	1	3.6E-01	1.0	9.1E-01	3.6E-01	0.2
Folate biosynthesis	16	1	3.6E-01	1.0	9.1E-01	3.6E-01	0

Total compounds correspond to the total number of compounds in the pathway; the Hits is the actually matched number from the intracellular quantifications data; the Raw p is the original p value calculated from the enrichment analysis; the Holm p is the p value adjusted by Holm-Bonferroni method; the FDR p is the p value adjusted using False Discovery Rate; the Impact is the pathway impact value calculated from pathway topology analysis.

5. Appendix V. Supplementary material for IC-BEVS bioprocess optimization (Chapter VI).

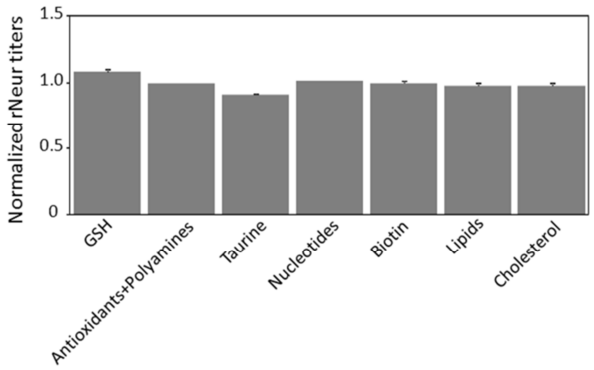

Supplementary Figure V-1. Stability test of rNeuraminidase in the presence of media supplements. The titers of rNeur were normalized with the volumetric titers of the non-supplemented control.

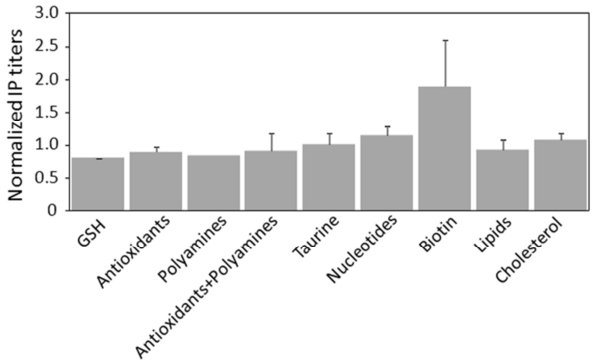

Supplementary Figure V-2. Stability test of infectious baculovirus in the presence of media supplements. The IP titers were normalized with the volumetric titers of the non-supplemented control.

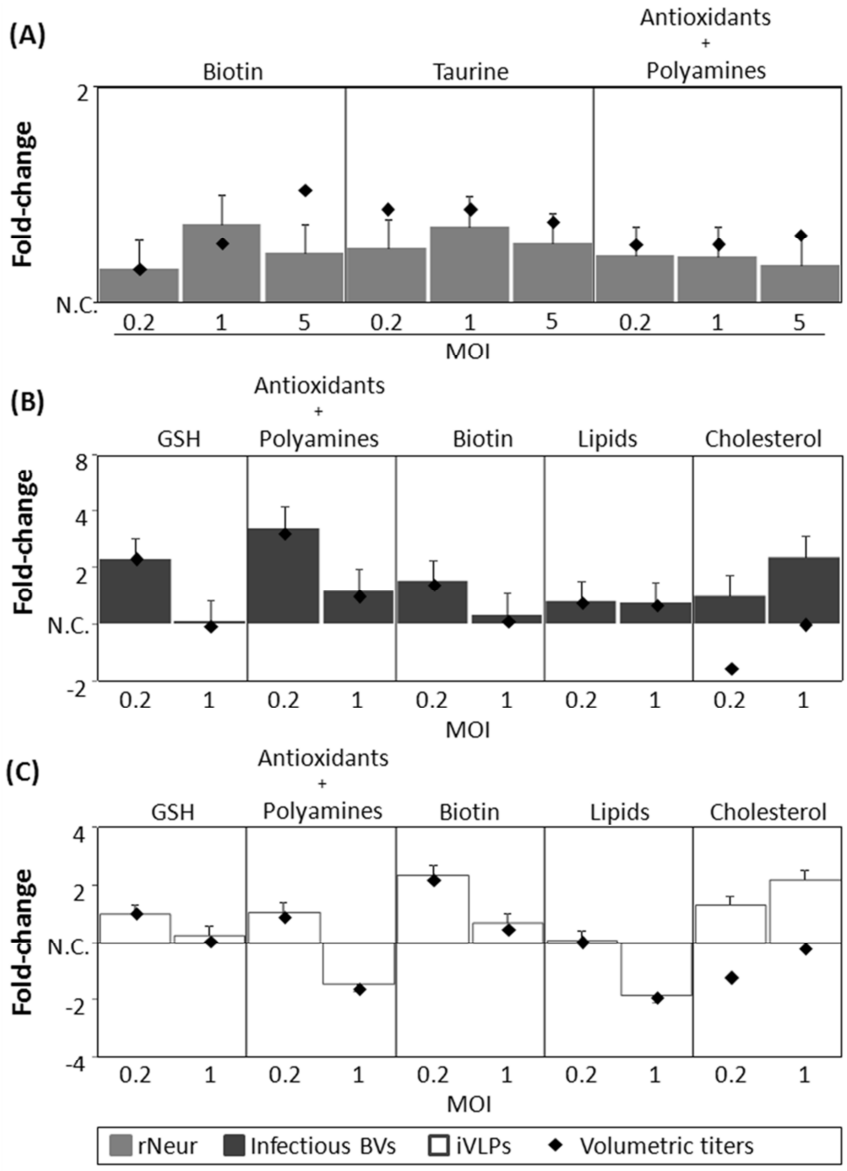

Supplementary Figure V-3. Preliminary screening of the impact of culture supplements on the specific yields of Sf9 cells. (A) Recombinant neuraminidase, rNeur (light bars); **(B)** Infectious baculovirus, BVs (dark bars); **(C)** Influenza VLPs, Inf-VLPs (white bars). The results are presented as fold-change in the specific yields of supplemented *versus* control (non-supplemented) cultures. Dots indicate the fold-change in the volumetric titers of the target products analyzed. Cultures were performed in the Ambr system, as described in the M&M section. Infections were performed at a CCI of $1x10^6$ cells.mL^{-1} varying the MOI as indicated. The data corresponds to 48 hpi; error bars correspond to 30% of inter-assay variability for infectious BVs and 10% for rNeur and Inf-VLPs quantification. Error bars for volumetric titers were ommitted for simplicity reasons. N.C. stands for - No change observed.

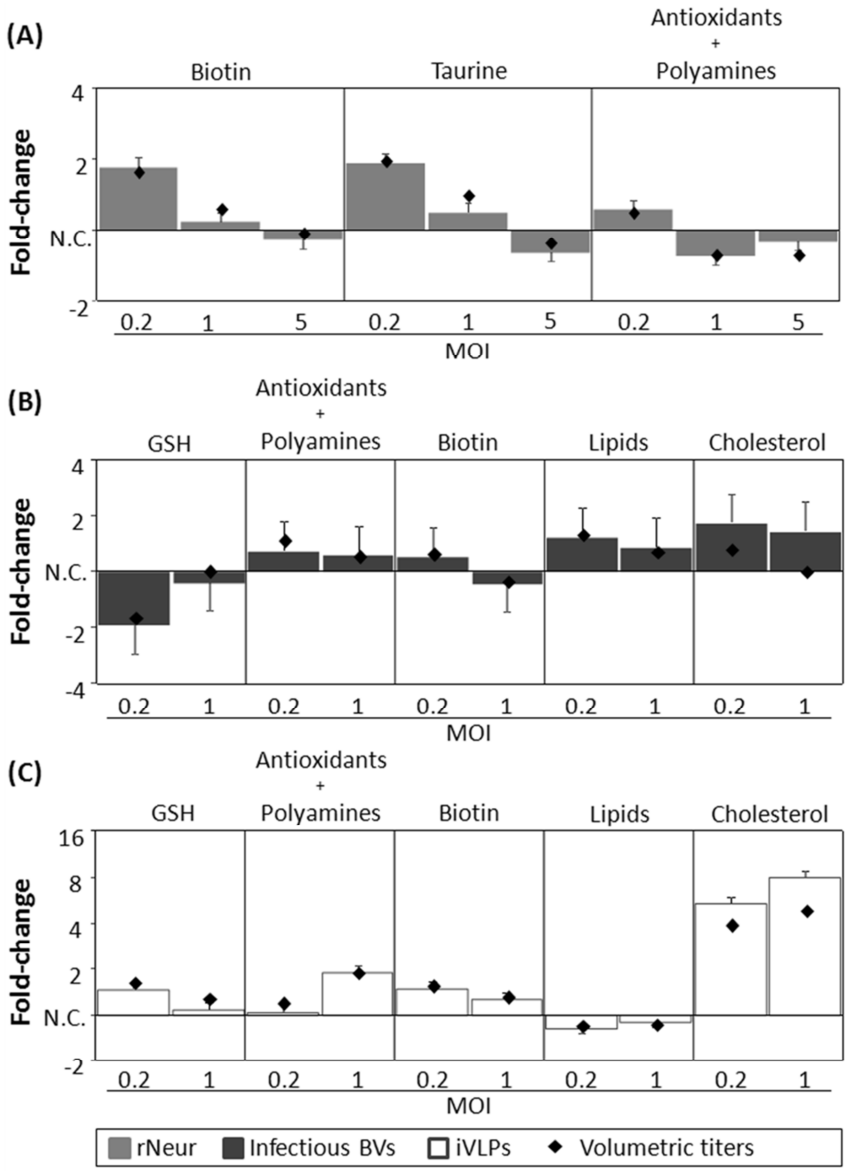

Supplementary Figure V-4 Preliminary screening of the impact of culture supplements on the specific yields of High Five cells. (A) Recombinant neuraminidase, rNeur (light bars); **(B)** Infectious baculovirus, BVs (dark bars); **(C)** Influenza VLPs, Inf-VLPs (white bars). The results are presented as fold-change in the specific yields of supplemented *versus* control (non-supplemented) cultures. Dots indicate the fold-change in the volumetric titers of the target products analyzed. Cultures were performed in the Ambr system, as described in the M&M section. Infections were performed at a CCI of $1x10^6$ cells.mL^{-1} varying the MOI as indicated. The data corresponds to 48 hpi; error bars correspond to 30% of inter-assay variability for infectious BVs and 10% for rNeur and Inf-VLPs quantification. Error bars for volumetric titers were ommitted for simplicity reasons. N.C. stands for - No change observed.

6. References

Bergold, G.H., Wellington, E.F., 1953. Isolation and chemical composition of the membranes of an insect virus and their relation to the virus and polyhedral bodies. J. Bacteriol. 210–216.

Ferrance, J.P., Goel, A., Ataai, M.M., 1993. Utilization of glucose and amino acids in insect cell cultures: Quantifying the metabolic flows within the primary pathways and medium development. Biotechnol. Bioeng. 42, 697–707.

Fructuoso, S., Sevilla, A., Bernal, C., Lozano, A.B., Iborra, J.L., Cánovas, M., 2012. EasyLCMS: an asynchronous web application for the automated quantification of LC-MS data. BMC Res. Notes 5, 428.

Klamt, S., Stelling, J., Ginkel, M., Gilles, E.D., 2003. FluxAnalyzer: exploring structure, pathways, and flux distributions in metabolic networks on interactive flux maps. Bioinformatics 19, 261–269.

Lazzarino, G., Amorini, A., Fazzina, G., Vagnozzi, R., Signoretti, S., Donzelli, S., Di Stasio, E., Giardina, B., Tavazzi, B., 2003. Single-sample preparation for simultaneous cellular redox and energy state determination. Anal. Biochem. 322, 51–59.

Preinerstorfer, B., Schiesel, S., Lämmerhofer, M., Lindner, W., 2010. Metabolic profiling of intracellular metabolites in fermentation broths from beta-lactam antibiotics production by liquid chromatography-tandem mass spectrometry methods. J. Chromatogr. A 1217, 312–28.

Vallino, J.J., Stephanopoulos, G., 2000. Metabolic flux distributions in Corynebacterium glutamicum during growth and lysine overproduction. Reprinted from Biotechnology and Bioengineering, Vol. 41, Pp 633-646 (1993). Biotechnol. Bioeng. 67, 872–885.

Wellington, E.F., 1954. The amino acid composition of some insect viruses and their characteristic inclusion-body proteins. Biochem. J. 57, 334–338.

Xie, L., Wang, D.I., 1994. Applications of improved stoichiometric model in medium design and fed-batch cultivation of animal cells in bioreactor. Cytotechnology 15, 17–29.